

# Targeting GPVI

Citation for published version (APA):

Jooss, N. J. (2023). *Targeting GPVI: impact of modulating platelet-collagen interactions on receptor signaling and thrombus formation*. [Doctoral Thesis, Maastricht University, University of Birmingham]. Maastricht University. <https://doi.org/10.26481/dis.20230216nj>

## Document status and date:

Published: 01/01/2023

## DOI:

[10.26481/dis.20230216nj](https://doi.org/10.26481/dis.20230216nj)

## Document Version:

Publisher's PDF, also known as Version of record

## Please check the document version of this publication:

- A submitted manuscript is the version of the article upon submission and before peer-review. There can be important differences between the submitted version and the official published version of record. People interested in the research are advised to contact the author for the final version of the publication, or visit the DOI to the publisher's website.
- The final author version and the galley proof are versions of the publication after peer review.
- The final published version features the final layout of the paper including the volume, issue and page numbers.

[Link to publication](#)

## General rights

Copyright and moral rights for the publications made accessible in the public portal are retained by the authors and/or other copyright owners and it is a condition of accessing publications that users recognise and abide by the legal requirements associated with these rights.

- Users may download and print one copy of any publication from the public portal for the purpose of private study or research.
- You may not further distribute the material or use it for any profit-making activity or commercial gain
- You may freely distribute the URL identifying the publication in the public portal.

If the publication is distributed under the terms of Article 25fa of the Dutch Copyright Act, indicated by the "Taverne" license above, please follow below link for the End User Agreement:

[www.umlib.nl/taverne-license](http://www.umlib.nl/taverne-license)

## Take down policy

If you believe that this document breaches copyright please contact us at:

[repository@maastrichtuniversity.nl](mailto:repository@maastrichtuniversity.nl)

providing details and we will investigate your claim.

The background of the slide is filled with numerous outlines of platelets, each rendered in a different color. The colors include shades of purple, green, yellow, cyan, blue, and red. The platelets are scattered across the entire page, with some appearing larger and more detailed than others. The outlines represent the complex, irregular shape of a platelet, showing various protrusions and indentations.

Natalie J. Jooss

# Targeting GPVI:

impact of modulating platelet-collagen interactions on receptor signaling and thrombus formation



**Targeting GPVI:  
impact of modulating platelet-collagen  
interactions on receptor signaling and  
thrombus formation**

Natalie J. Jooss

Ph.D. Thesis manuscript submitted to the assessment committee for Maastricht University

The research in the thesis was supported by funding from the European Union's Horizon 2020 research and innovation program under the Marie Skłodowska-Curie grant agreement No. 766118 (TAPAS). This thesis is the result of the joint doctorate program of Natalie Jooss at the Universities of Maastricht and Birmingham.

**Targeting GPVI: impact of modulating platelet-collagen interactions on receptor signaling and thrombus formation**

PhD thesis: Maastricht University

ISBN: 978-94-6469-172-6

Production: ProefschriftMaken

© Natalie Jooss, Maastricht 2022

Cover design: Charlie Palleis

**Targeting GPVI:  
impact of modulating platelet-collagen interactions on  
receptor signaling and thrombus formation**

DISSERTATION

To obtain the degree of Doctor at Maastricht University and  
Doctor of Philosophy at the University of Birmingham,  
on the authority of the Rector Magnificus,  
Prof. Dr. Pamela Habibović  
in accordance with the decision of  
the Board of Deans,  
to be defended in public  
on

Thursday, 16 February 2023 at 10:00 hours

by

Natalie Jasmin Jooss

Born in Heidenheim an der Brenz, 20 October 1989

**Promotors**

Prof. Dr. J.W.M. Heemskerk, Maastricht University  
Prof. Dr. S. P. Watson, University of Birmingham, UK  
Prof. Dr. Y.M.C. Henskens, Maastricht University

**Co-promotors**

Dr. N.S. Poulter, University of Birmingham, UK

**Assessment Committee**

Prof. Dr. E.M.A. Beckers (Chair), Maastricht University  
Dr. I. Dumitriu (University of Birmingham, UK)  
Dr. C.C.F.M.J. Baaten, Maastricht University  
Prof. Dr. Ph.G. de Groot (University of Utrecht)  
Prof. Dr. N. Morgan (University of Birmingham, UK)  
Prof. Dr. A.W. Poole (University of Bristol, UK)

Financial support for publication of this thesis by Stichting Hart Onderzoek Nederland ([www.hartonderzoek.nu](http://www.hartonderzoek.nu)) is gratefully acknowledged.





# Contents

Chapter 1	General Introduction	1
Chapter 2	A large-scale histological investigation gives insight into the structure of ischemic stroke thrombi	37
Chapter 3	Comparative analysis of pharmacological drugs interfering with collagen induced thrombus formation	47
Chapter 4	Anti-GPVI nanobody blocks collagen- and atherosclerotic plaque-induced GPVI clustering, signaling and thrombus formation	83
Chapter 5	Platelet GPVI cluster size is related to thrombus formation and phosphatidylserine exposure in collagen-adherent platelets under arterial shear stress	125
Chapter 6	Platelet glycoprotein VI and tyrosine kinase Syk in thrombus formation on collagen-like surfaces	145
Chapter 7	Modulating roles of platelet PECAM1 and ITIM linked PTPN11 in collagen- and glycoprotein VI-induced thrombus formation	183
Chapter 8	General discussion	223
Chapter 9	Samenvatting	245
	Summary	
	Zusammenfassung	
	Impact	
	Curriculum Vitae	
	Publications	
	Acknowledgement	



# Chapter 1

## General Introduction

## **1.1 Platelet functions, thrombosis and hemostasis**

Cardiovascular diseases and related complications are still leading causes of death worldwide <sup>1,2</sup>. In the most common pathology of non-fatal or fatal arterial thrombosis (myocardial infarction, stroke), platelets play a key role by assembling into a thrombus occluding the affected artery <sup>3</sup>. When the underlying cause is rupture or erosion of an atherosclerotic plaque, this process is referred to as atherothrombosis <sup>4</sup>. On the other hand, in physiological hemostasis, platelets are also essential to stop bleeding after vascular injury by adhering to the site of injury and forming a thrombus that halts loss blood <sup>5,6</sup>.

First described as small blood components in 1873 by Osler, platelets are nowadays recognized as anucleated cell fragments, derived from megakaryocytes resident in the bone marrow <sup>7</sup>. For a long time, platelets were known to have functions in thrombosis and hemostasis, but it has become clear that they play additional roles in processes such as vascular repair, infection, inflammation, and cancer metastasis <sup>8,9</sup>. The formation of platelets is in two stages: polyploid megakaryocytes first shed so-called proplatelets, after which they divide into discoid platelets <sup>7</sup>. Once formed, platelets remain in the circulation for 7-10 days, before being cleared in the liver and spleen <sup>10</sup>. Below, I will briefly introduce the functional responses of platelets, especially in relation to collagens, hemostasis, and thrombosis, as far as appropriate for this thesis.

### **Platelets in thrombus formation**

Platelets are activated by multiple agonists due to their broad receptor repertoire. Current omics analyses predict the presence of >2,500 platelet membrane receptors and channels, the vast majority with still unclear roles <sup>11</sup>. Multiple overviews are available discussing the best known receptors, which can be divided into adhesive receptors (e.g., integrins), ITAM-linked receptors

(with an immunoreceptor tyrosine-based activation motif), and ITIM-linked receptors (with an immunoreceptor tyrosine-based inhibitory motif)<sup>12,13</sup>. Some of the adhesive, ITAM-linked and ITIM-linked receptors are important in flow-dependent platelet activation and thrombus formation<sup>9</sup>, as summarized in **Table 1**. An extended description of the receptors relevant for this thesis is given in Section 3.

**Table 1 – Key platelet adhesive and tyrosine kinase signaling receptors and their ligands.** G-protein coupled receptors and agonists are not included. Data are taken from Refs.<sup>14-22</sup>.

Receptor	Estimated copy number/platelet	Ligands	Effect on platelets
<i>GP1b-IX-V</i>	30,000-50,000	VWF, thrombin	Plt tethering to VWF
<i>GPVI (ITAM)</i>	4,000-6,000	Collagens, fibrin(ogen)	Collagen-, fibrin- and CRP-induced Plt activation
<i>CLEC-2 (hem-ITAM)</i>	1,500	Podoplanin, rhodocytin	Plt activation
<i>FcγRIIA (ITAM)</i>	1,000	IgG antibodies	Plt activation
<i>PECAM1 (ITIM)</i>	5,000–20,000	PECAM1	Negative regulator of Plt activation
<i>G6b-B (ITIM)</i>	14,000	Heparin (sulfate)	Complex negative regulator of Plt activation
<i>Integrin α2β1</i>	2,000-4,000	Collagens	Plt adhesion to collagens
<i>Integrin α1bβ3</i>	80,000-100,000	Fibrin(ogen), VWF	Plt adhesion to VWF, Plt aggregation
<i>Integrin αvβ3</i>	500	Vitronectin, osteontin	Plt adhesion to ligands
<i>Integrin α5β1</i>	1,000	Fibronectin	Plt adhesion to fibronectin
<i>Integrin α6β1</i>	1,000	Laminins	Plt adhesion to laminins, activation

VWF, von Willebrand factor; plt, platelet; CRP, collagen-related peptide.

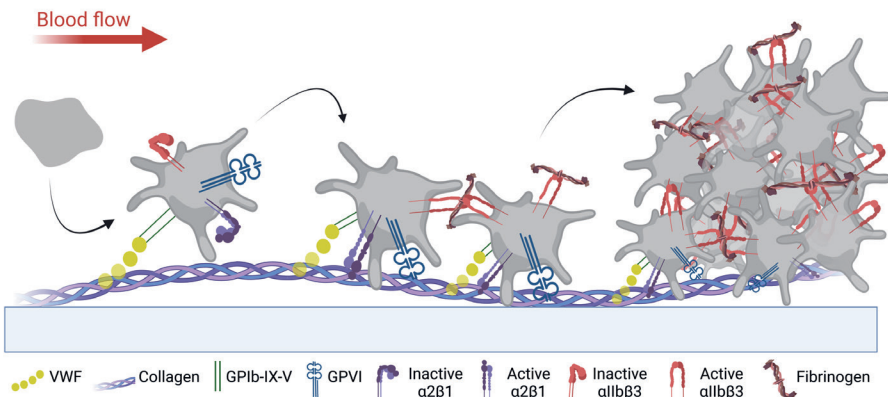


**Figure 1 – Initial stages of platelet activation in thrombus formation.** Flowed platelets transiently adhere to exposed collagen fibers, covered with von Willebrand factor (VWF), via the GPIb-IX-V complex. Stable platelet adhesion occurs by engagement of the collagen receptors, integrin  $\alpha2\beta1$  and glycoprotein VI (GPVI). Enhanced by autocrine mediators (ADP, thromboxane  $A_2$ ), integrin  $\alpha11\beta3$  becomes activated, and adjacent platelets connect by fibrinogen binding, resulting in platelet aggregation. Modified after Ref.<sup>9</sup>. Created with BioRender.com.

The tethering of platelets to collagen-bound von Willebrand factor (VWF) via the glycoprotein Ib-IX-V (GPIb-IX-V) complex is considered as an initial event in thrombus formation<sup>6,23</sup>. In addition, under flow conditions, two platelet collagen receptors are engaged, glycoprotein VI (GPVI) and integrin  $\alpha2\beta1$  (**Figure 1**), establishing stable adhesion and initial activation of platelets<sup>24-27</sup>. Subsequent platelet responses include shape change, granule secretion, thromboxane  $A_2$  release, integrin  $\alpha11\beta3$  activation, platelet aggregation and development of procoagulant activity (**Figure 2**)<sup>9,28</sup>.

Under high-shear flow conditions, the activation processes jointly lead to the formation of a thrombus composed of aggregated and contracted platelets<sup>6,29</sup>. The thrombus-forming process also involves positive feedback loops, to trap flowing platelets from the blood stream via the release of ADP and thromboxane  $A_2$  (TXA<sub>2</sub>) from adhered platelets. The platelet secretion

process involves two types of storage granules, namely  $\alpha$ - and  $\delta$ - granules, containing protein compounds (fibrinogen, VWF) and non-protein compounds (ADP, ATP, polyphosphates), respectively<sup>30,31</sup>. Upon stimulation with a strong agonist like thrombin, secretion also includes content of lysosomes, which contain a variety of protein-degrading enzymes<sup>32</sup>.

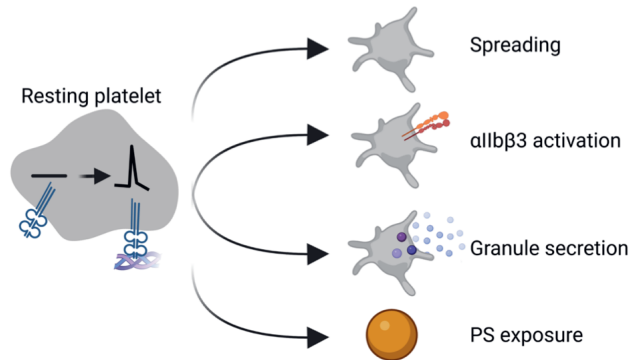


**Figure 2 – Diversity of platelet responses in collagen-dependent thrombus formation.**

Upon adhesion to collagen/VWF, platelets undergo a rise in cytosolic  $\text{Ca}^{2+}$ , leading to shape change and spreading of the cells, alteration of integrin  $\alpha\text{IIb}\beta 3$  into its active conformation, secretion of granules as well as exposure of phosphatidylserine (PS) to form procoagulant platelets. These responses are also measured in common platelet activation tests. Original drawing, created with BioRender.com.

Important positive feedback loops in platelet activation are provided by the group of G protein-coupled receptors (GPCR), the majority of which have soluble agonists as ligands<sup>9,13</sup>. Of these, ADP activates via binding to the  $\text{P2Y}_1$  receptors (coupled to the  $\text{Gq}\alpha$  protein) and  $\text{P2Y}_{12}$  receptors (coupled to the  $\text{Gi}\alpha$  protein), while  $\text{TXA}_2$  engages the thromboxane receptor (coupled to  $\text{Gq}\alpha$ ).

In addition, tissue factor-triggered initiation of the coagulation process leads to initial thrombin generation, a process that is greatly enhanced by the formation of procoagulant platelets, exposing phosphatidylserine<sup>6</sup>. The formed thrombin cleaves fibrinogen into fibrin and, furthermore, activates

platelets via protease-activated receptors (PARs), of which the isoforms PAR1 and PAR4 are expressed on human platelets (both coupled to Gq $\alpha$ ).

For the signaling pathways, induced by these receptors, I refer to an excellent review <sup>12</sup>. The same paper also explains key pathways of platelet inhibition via prostacyclin and nitric oxide.

### Platelet adhesion and spreading

Resting platelets are maintained in a discoid shape via the actin-myosin and tubulin cytoskeletons. Upon activation of the platelets, the cytoskeletons quickly reorganize, resulting in a cellular shape change from discoid to rounded; and in case of adhered platelets, from discoid to spreading <sup>33</sup>. In the adhered and spreading platelets, the actin filaments polymerize, supporting the formation of filopodial protrusions which later extend to form broader lamellipodia (**Figure 3**).

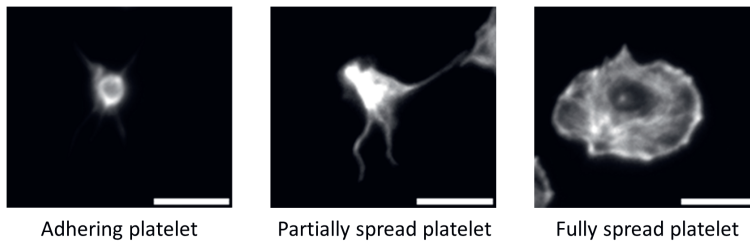


**Figure 3 – Stages of spreading platelets.** Upon adhesion to collagen or fibrinogen, platelets undergo a sequence of shape changes. They first form filopodia (adhering platelet) that develop into lamellipodia (partial spreading), resulting in a ‘fried egg’ type of shape (full spreading). Shown are fluorescence micrographs of platelets, where actin filaments were labeled with phalloidin- Alexa Fluor 488. Scale bars, 3  $\mu$ m. Original images from the author.

At a final stage of spreading this results in cell flattening and acquiring a ‘fried egg’ phenotype. Herein, the actin filaments are organized into large stress fibers, of which the distal regions are sheet-like, and the central domains connect the cellular organelles and granules <sup>34</sup>. In addition, the

microtubule (tubulin cytoskeleton) becomes depolymerized, which removes other structural restraints for shape change and spreading<sup>35</sup>. Several other processes support the spreading of platelets, in particular fibrinogen secretion, GPIIb/IIIa activation and integrin  $\alpha$ IIb $\beta$ 3 or  $\alpha$ 6 $\beta$ 1 binding, integrins act via so-called outside-in signaling reactions<sup>36-38</sup>.

## Platelet-dependent coagulation

The coagulation process is commonly separated into extrinsic and intrinsic coagulation cascades, which are triggered by tissue factor (TF) and factor (F)XIIa, respectively<sup>39</sup>. Both pathways have in common that, once triggered, coagulation factors consecutively cleave one another to produce the active protein form. Both pathways converge into the common pathway.

In the extrinsic pathway, TF interacts with FVII(a)<sup>40</sup>, which complex induces initial activation of FIX and FX<sup>41</sup>. In the intrinsic (or contact activation) pathway, FXII becomes activated by kallikrein, after which FXIIa induces the formation of FXIa and the consecutive cleavage of FIX into FIXa<sup>6,42</sup>. In the common pathway, more FX and thrombin are generated in a phospholipid (phosphatidylserine) dependent way through the tenase and prothrombinase complexes<sup>43</sup>. Cofactors in these complexes are (thrombin cleaved) FVIIIa and FVa, respectively. The generated thrombin cleaves fibrinogen into fibrin, and furthermore activates several coagulation factors (FV, FVIII) and stimulates platelets via the PAR receptors<sup>6,44</sup>.

Platelets are important for accelerating and steering the coagulation process, by both providing a procoagulant surface and binding to and contracting fibrin fibers<sup>29,44</sup>. A population of strongly activated platelets – often referred to as collagen-and-thrombin activated (COAT) platelets – provides the phosphatidylserine surface that is required for tenase and prothrombinase activities<sup>45</sup>. The phosphatidylserine exposure is achieved in platelets stimulated by strong agonists, for example collagen plus thrombin, causing a



high and sustained rise in  $[Ca^{2+}]_i$ . This high  $Ca^{2+}$  response activates the  $Ca^{2+}$ -dependent anoectamin-6 protein in the plasma membrane, which mediate the scrambling of phosphatidylserine as well as the swelling of platelets into balloon-formed structures<sup>44,46</sup>. Phosphatidylserine-exposing platelets strongly support the common coagulation cascade, as they provide a surface for the assembly of Gla-containing coagulation factors<sup>6,43</sup>. The formed thrombin produces fibrin fibers, which consolidate a thrombus and trap red blood cells (**Figure 4**).

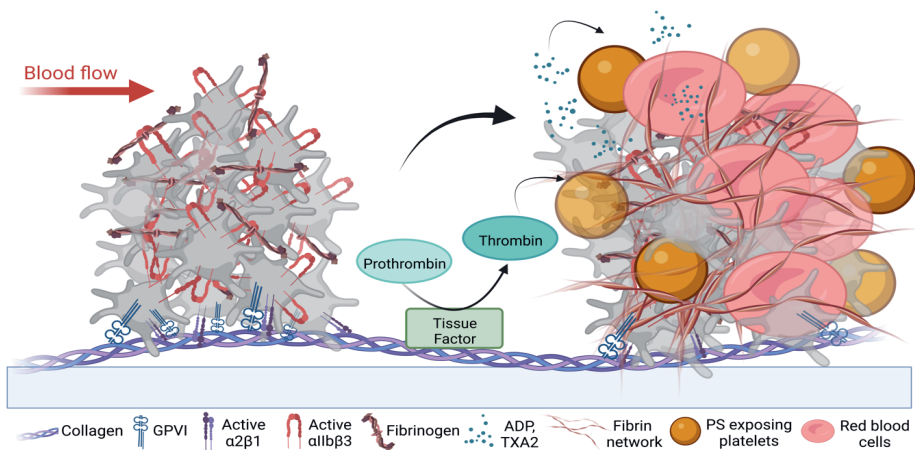


**Figure 4 – Formation of a stabilized arterial thrombus by phosphatidylserine-exposing platelets.** Vascular tissue factor (TF) triggers initial thrombin formation, which induces phosphatidylserine (PS) exposure of collagen-adhered platelets. The PS-exposing, ballooned platelets enhance further thrombin generation, required for the formation of fibrin fibers and the trapping of red blood cells. Note that secondary mediators such as ADP and  $TXA_2$  enhance the thrombus growth. Modified after Ref. <sup>6</sup>. Created with BioRender.com.

## Heterogeneous thrombus structure

According to the conventional Virchow model, a ‘red’ venous thrombus arises upon blood stasis or at a hyperactive state of the blood, whilst a ‘white’ thrombus forms under high-shear condition, such as in inflamed and atherosclerotic arteries<sup>47</sup>. However, intermediate and mixed types of thrombi

can also be formed. Moreover, it has become clear that the structure and composition of an intravascular thrombus is often heterogenous. This concerns the overall architecture and is often independent of the site of thrombus formation (arterial or venous, macro- or microcirculation) <sup>48</sup>. Knowledge about the precise thrombus (clot) composition can help to improve the treatment and the chances of a positive outcome for patients undergoing thrombectomy <sup>49</sup>. As it has been demonstrated that thrombi that are richer in red blood cells can easier be mechanically removed by the surgical procedures <sup>50</sup>. Also, the quantity and quality of fibrin fibers can be of clinical impact <sup>51-53</sup>. However, more knowledge of the mechanism of heterogeneous thrombus formation is needed.

Regarding platelets, evidence for thrombus heterogeneity has also been reported in mouse *in vivo* models. Work by Stalker *et al.* shows that the thrombi generated in injured arterioles of mice consist of a layered structure, with a dense thrombus core of contracted platelets and a loose outer shell of partly discoid platelets <sup>54</sup>. Later studies of this group confirmed the presence of a similar structure in the thrombi formed in larger arterial vessels <sup>55</sup>. In comparison, *in vitro* collagen-based flow studies with human whole blood have pointed to the formation of patches within formed thrombi, in which platelets differently undergo responses like spreading, secretion, aggregation, phosphatidylserine exposure and deposition of fibrin <sup>6,56</sup>. It is considered that GPVI has a central role in this heterogeneity, but its precise role herein *in vivo* or *in vitro* is still unclear.

## **1.2 Platelets and collagens**

Triple-helical collagens make up an abundant and important component of the human body. The overall function of collagens is to provide a stable extracellular structure for cells, tissues and organs. Twenty different types of collagens can be identified, which in part concentrate in different locations of

the body <sup>57,58</sup>. In the intact vessel wall, contact of collagens with the blood stream is prevented by a confluent layer of endothelial cells. Upon vascular injury or atherosclerotic plaque rupture, these collagens become exposed to the blood, thereby inducing their thrombogenic functions <sup>58</sup>. Below, I provide a short overview of the collagens in a vessel wall, in atherosclerotic plaques, and of the synthetic collagen-related peptides.

### **Collagens in the vessel wall**

Collagens in the vessel wall serve to ensure tissue stability and to provide a scaffold for resident cells, including endothelial cells and smooth muscle cells <sup>58</sup>. In a given vessel wall, up to nine collagen types can be identified, accounting for up to 40% of the extracellular matrix weight <sup>57</sup>. The predominant forms are collagens of types I, III, IV and VI <sup>59,60</sup>.

Common to these collagen types is a triple helical structure with three winded peptide chains, which have repeated GXX' sequences <sup>61</sup>. Per collagen type, the precise amino acid sequence determines how cells can interact with their collagen receptors <sup>58</sup>. In the thicker, fibrillar collagens (types I, III, VI), the triple helices assemble into fibrils, which can bundle to macroscopic fiber forms <sup>62</sup>. Differently from the fibrous collagens, collagen type IV adopts a sheet-like network without fibrils <sup>58,63</sup>. The vascular collagens are all considered to bind VWF, initiate platelet adhesion and subsequent platelet activation under flow. However, to what extent the various collagen types induce and contribute to these processes is still not completely understood.

### **Collagens in atherosclerotic plaques**

Atherosclerotic lesions or plaques are formed in the larger arterial vessels of all aged humans. The lesion development is driven by inflammation and local lipid deposition and is accountable for the onset of cardiovascular disease <sup>64,65</sup>. Upon progression of an atherosclerotic plaque, the lumen of the affected artery is drastically reduced <sup>66</sup>. However, problematic become plaques that

present as unstable (often lipid-rich) are prone to rupture or erosion, which triggers thrombotic events, followed by heart infarction, transient ischemic attack, or stroke <sup>64,67</sup>. Next to coagulation factors <sup>68</sup>, several platelet-activating substances have been identified in atherosclerotic plaque tissue. These include the weak platelet agonists, lysophosphatidic acid <sup>69</sup>, sphingosine-1 phosphate <sup>70</sup>, fibronectin and fibrin(ogen) <sup>71</sup>. Yet, the main platelet-activating substances are most likely collagens because collagenase treatment of plaque material strongly reduces platelet activation <sup>72</sup>. On the other hand, plaque tissue also contains tissue factor, which via thrombin can enhance collagen-mediated platelet activation <sup>73</sup>.

Collagens in a plaque are mostly of vascular origin <sup>74</sup> but may in part be secreted by plaque-resident cells, in particular collagen-I and -III <sup>59</sup>. These collagens are often distributed differently within a plaque, with collagen-I enriched in the fibrous cap and collagen-III more present in the lipid core <sup>74,75</sup>. Interestingly, *in vitro* studies indicate that the plaque collagens interact with platelets by engagement of GPVI, rather than integrin  $\alpha 2\beta 1$  <sup>72,75,76</sup>. On the other hand, it is considered that platelet adhesion to the majority of (vascular) collagen types I-VIII relies on integrin  $\alpha 2\beta 1$  <sup>77</sup>, with especially adhesion to collagen type IV dependent on this integrin <sup>63</sup>. The precise role of  $\alpha 2\beta 1$  in plaque-induced thrombus formation is hence unclear.

### **Collagen-related peptides**

The majority of vascular collagens bind VWF and platelets <sup>58,78,79</sup>. However, the complex, triple-helical structure of collagens has hampered identification of the recognition sites for VWF and platelet receptors. To overcome this limitation, a library of synthesized peptides of overlapping sequences of collagens-II and -III – which contain three different helices - was developed by the Farndale lab, which was then used as a collagen peptide toolkit for identification of the binding motifs for VWF, GPVI or integrin  $\alpha 2\beta 1$  <sup>61,80</sup>. Use of

the toolkit showed that peptides enriched in the triplet glycine-proline-hydroxyproline (GPO) preferentially served as GPVI-binding sites <sup>61,81</sup> (**Figure 5**). Thus, the synthesis of triple-helical polypeptide (GPO)<sub>10</sub>, also known as collagen-related-peptide (CRP), acts as a strong GPVI agonist, once cross-linked to form CRP-XL <sup>58,82</sup>. On the other hand, collagen sequences similar to glycine-phenylalanine-hydroxyproline-glycine-glutamic acid-arginine (GFOGER) were found to bind to integrin  $\alpha 2\beta 1$  <sup>83</sup>. Similarly, a VWF-binding sequence was identified, leading to the synthesis of a VWF-binding peptide (VWF-BP) <sup>84</sup>, which support platelet tethering via the GPIb-IX-V complex <sup>85</sup>. *In vitro* work further indicated that the combination of various collagen-like peptides and the VWF-BP can mimic the effect of whole collagens for the establishment of thrombus formation under flow <sup>19,82,86</sup>.

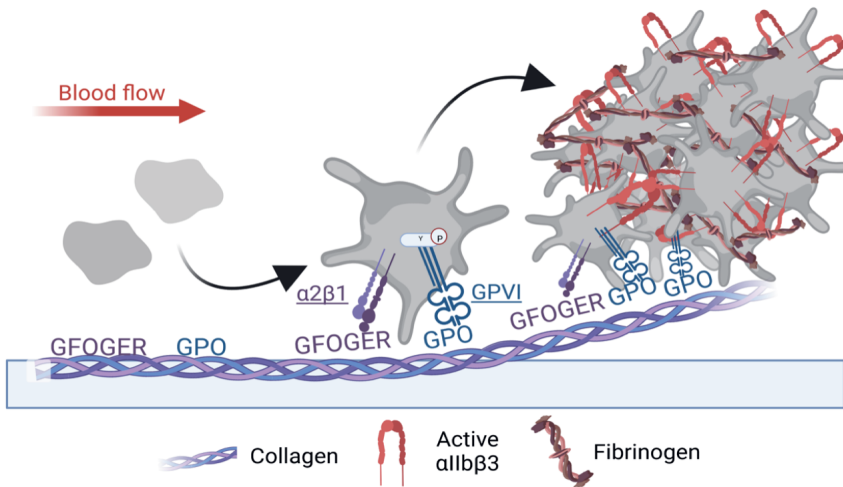


**Figure 5 – The platelet receptors binding to specific collagen motifs required for thrombus formation.** In the triple helical collagens, (GPO)<sub>n</sub> motifs bind to GPVI, initiating platelet activation. In addition, GFOGER or similar motifs interact with integrin  $\alpha 2\beta 1$  to stabilize the platelet-collagen interaction. Under flow conditions, both receptors contribute to formation of a platelet thrombus. The additional presence of VWF under shear conditions is not indicated. Modified after Refs. <sup>61,80</sup>. Created with BioRender.com.

In the context of this thesis, it is worth to mention that common platelet function tests in the research and diagnostic laboratories rely on the use of another modified collagen form *i.e.*, equine Horn collagen, enriched in collagen-I fibrils<sup>58,87</sup>. Better knowledge of the platelet-activating mechanisms of native vascular collagens is needed to determine their possible use for diagnostic purposes.

### **1.3 Tyrosine kinase-linked receptors and signaling**

As general background for this thesis, I introduce below the ITAM-linked receptors involved in platelet interaction with collagens and their key signaling pathways.

#### **Immunoreceptor tyrosine-based activation motif (ITAM) receptors**

Three platelets (hemi-)ITAM receptors have been studied in greater detail, namely GPVI, C-type lectin-like receptor-2 (CLEC-2) and FcγRIIA receptors (**Table 1**). Overall, CLEC-2 and FcγRIIA share a large part of their signaling with GPVI<sup>17,27</sup>. In the following section I will only focus on GPVI. As a glycoprotein specifically expressed on megakaryocytes and platelets, GPVI forms a transmembrane receptor, consisting of two Ig domains on the extracellular face<sup>27</sup>.

For signaling responses, GPVI requires complex formation with the ITAM-containing co-receptor, the FcR γ-chain (**Figure 6**). Ligand binding to GPVI leads to a tyrosine phosphorylation cascade, which involves assembly of a targeted signalosome of the transmembrane protein LAT<sup>17,27</sup>. In brief, upon receptor activation, the Src-family kinases Lyn and Fyn phosphorylate the ITAM-motif, which allows recruitment there of the tyrosine kinase Syk<sup>88</sup>. In turn, Syk phosphorylates multiple signaling proteins, including adaptor molecules (LAT, SLP-76 and other), protein tyrosine kinases (Btk) and the effector signaling enzyme phospholipase C<sub>γ</sub>2 (PLC<sub>γ</sub>2). The signal

transduction is enhanced via phosphoinositide 3-kinase (PI3K), which is included in the signalosome. The latter converts phosphoinositide bisphosphate into phosphoinositide trisphosphate. In contrast, PLC $\gamma$ 2 cleaves phosphoinositide bisphosphate into inositol trisphosphate (InsP $_3$ ) and 1,2-diacylglycerol (DAG), which mobilizes intracellular Ca $^{2+}$  and activates protein kinase C (PKC), respectively <sup>13,17,27</sup>.

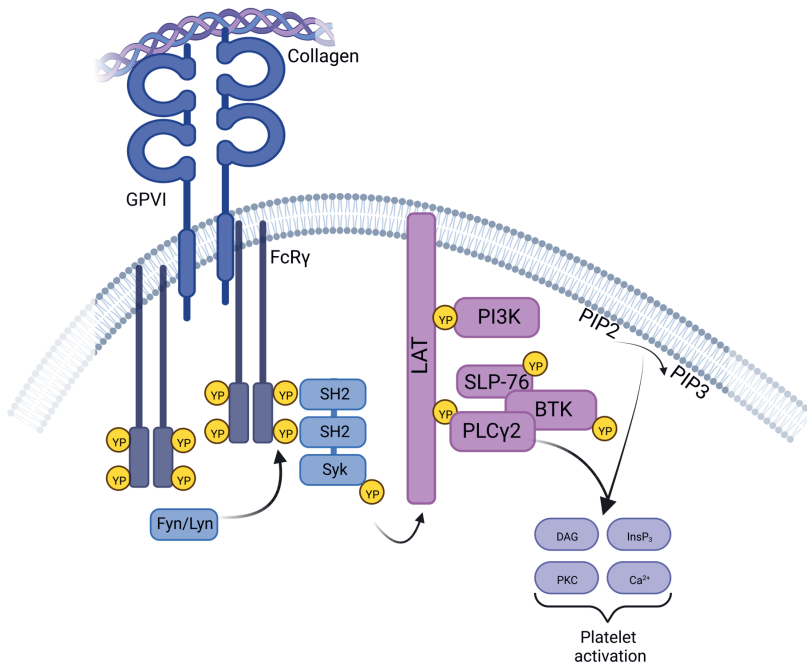


**Figure 6 – GPVI signalosome and early signaling cascade.** Upon collagen binding, GPVI in association with its co-receptor, FcR $\gamma$ , dimerizes, and the ITAM motif becomes phosphorylated by tyrosine kinases Fyn and Lyn. This induces tyrosine phosphorylation and activation of Syk, followed by assembly of a signalosome around the adaptor molecule LAT. The signaling ensues via activated PLC $\gamma$ 2, mobilization of intracellular Ca $^{2+}$ , and activation of broad-spectrum Ser/Thr kinase PKC isoforms. For further explanation, see text. Modified after Refs.<sup>97-99</sup>. Created with BioRender.com.

Jointly, the routes of tyrosine kinases, PI3K and PKC lead to multiple downstream platelet responses, including cytoskeletal changes, granule secretion, integrin  $\alpha\text{IIb}\beta\text{3}$  activation, platelet aggregation and procoagulant activity <sup>6,9</sup>. In recent years, GPVI was found to be a receptor not only for collagens <sup>89</sup>, but also for laminins <sup>36</sup>, fibrin and fibrinogen <sup>37,90-94</sup>. Some other identified ligands for GPVI are CD147 <sup>95</sup> and galectin-9 <sup>96</sup>. The signaling via these other ligands is only partly understood <sup>94</sup>.

### **Glycoprotein VI and ITAM receptor clustering**

The clustering of receptors may regulate signaling responses, because this can increase receptor avidity (functional affinity), suppress negative regulators, and bring together downstream signaling molecules <sup>100</sup>. There is some knowledge of receptor clustering in immune cells which – similarly to GPVI – also operate via ITAMs. The clustering of T-cell receptors was found to be crucial in the interplay between antigen recognition and signaling strength <sup>101</sup>. On B-cells, artificial crosslinking can result in super-clusters of the Fc $\gamma$ RIIB1 receptor <sup>102</sup>. This increased negative signaling by engagement of isoforms of the protein tyrosine phosphatases SHP and SHIP. In general, receptor clustering can be achieved by (multivalent) receptor-agonist interactions or by bivalent antibodies <sup>103</sup>.

Regarding platelets, recent advances in single molecule super-resolution microscopy allow to probe the distribution and clustering of plasma membrane receptors on nanoscale <sup>104</sup>. It was hypothesized that GPVI clustering via ITAM in the FcR  $\gamma$ -chain can also enhance the signal duration and strength. Some evidence for this was found in studies showing that GPVI clusters in platelets adhering to collagen macro-fibers <sup>105</sup>, and that this enhances the co-localization of signaling molecules <sup>106</sup>. Surprisingly, inhibition of the GPVI signalosome <sup>106</sup> or of signaling pathways <sup>107</sup> did not appear to



affect the clusters once these had been formed. A limitation of these studies is that these were confined to observation on washed platelets.

### **Glycoprotein VI receptor shedding**

Proteolytic cleavage of the extracellular domain of GPVI can act as a mechanism to halt platelet activation. Shedding of the GPVI on activated platelets is predominantly mediated by the protease ADAM10 (a disintegrin and metalloproteinase) <sup>108</sup>. Triggers for inducing ADAM10 are high shear rates, strong platelet activation as well as apoptosis <sup>109,110</sup>. For the regulation of ADAM activity, which is less central in this thesis, I would like to refer to the cited literature <sup>108-110</sup>.

### **Glycoprotein VI receptor antagonism**

Platelets not only become activated by a broad spectrum of stimuli but are also sensitive to several inhibitory mechanisms. The latter serve to prevent unwanted platelet activation at an intact vessel wall, or to restrict thrombus build-up to the site of vascular injury. Endothelial cells play an important role in preventing platelet activation by releasing soluble inhibitory molecules such as prostacyclin and nitric oxide <sup>111,112</sup>.

In addition, platelets possess a repertoire of inhibitory receptors that are linked to protein tyrosine phosphatases. For this thesis the ITIM-containing receptors G6b-B (gene *MPIG6B*) <sup>14,113</sup> and endothelial cell adhesion molecule 1 (PECAM1, also known as CD31) are relevant <sup>114,115</sup>. The ITIM residues of these receptors in part, but not always <sup>116</sup>, negatively modulate the activity of ITAM receptors via the tyrosine phosphatases isoforms SHP1/2 and SHIP1/2 (**Figure 7**) <sup>117-119</sup>. In mouse platelets, PECAM1 was found to have an inhibitory role in tyrosine kinase-dependent activation, but to enhance integrin  $\alpha\text{IIb}\beta\text{3}$  activation <sup>120</sup>. In human platelets, PECAM1 expression levels appeared to be negatively correlated to the strength of CRP- and ADP-mediated platelet

activation<sup>12,115</sup>. For these and other reasons, it has been commented that ITIM receptors are more than just inhibitors of platelet activation<sup>18</sup>. However, the precise roles of such ITIM receptors in platelet physiology are still under debate.

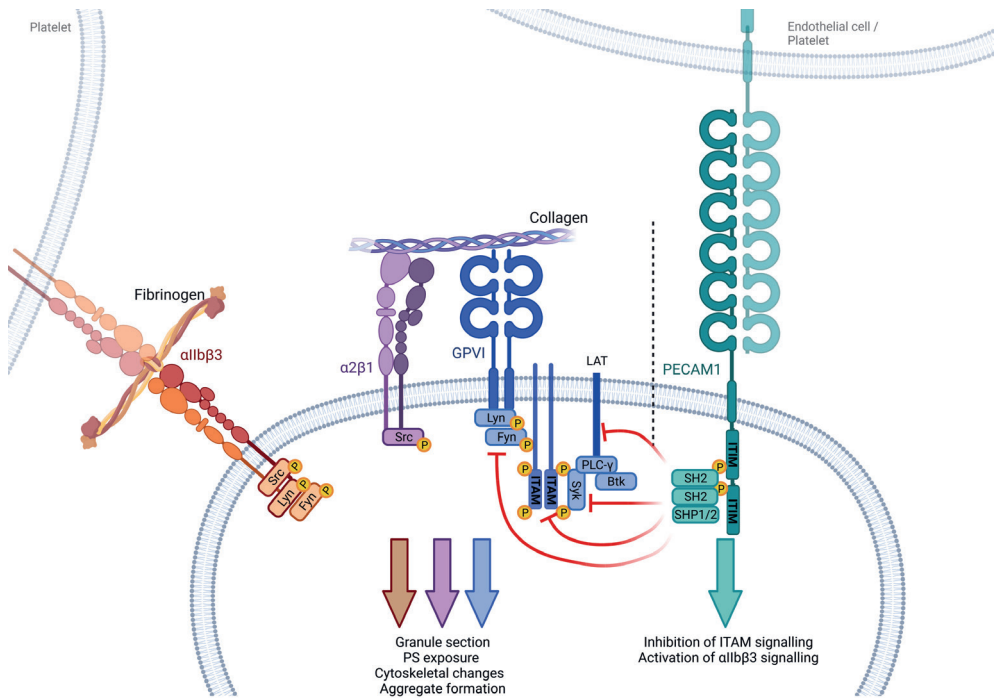


**Figure 7 – Cartooned overview of ITAM- and ITIM-dependent signaling in platelets.** Upon collagen binding to GPVI, the ITAM-dependent signaling become activated. Phosphorylation of downstream proteins results in mobilization of intracellular  $\text{Ca}^{2+}$  and further platelet responses, such as granule secretion, PS exposure,  $\alpha\text{IIb}\beta\text{3}$  activation, platelet spreading and aggregate formation. Negative signal modulation via PECAM1 and other ITIM-linked receptors can suppress phosphorylations in the GPVI signalosome. Modified after Ref. <sup>18</sup>. Created with BioRender.com.

## 1.4 Platelet integrins and signaling

Integrins of platelets and other cells are composed of an  $\alpha$  and  $\beta$  chain. On resting platelets, integrins are present in an inactive state with a low ligand affinity, while upon platelet activation the extracellular parts undergo a change in conformation (active conformation), resulting in an increased ligand affinity<sup>121,122</sup>. For the  $\beta 1$  subunit platelets express integrins  $\alpha 2\beta 1$ ,  $\alpha 5\beta 1$  and  $\alpha 6\beta 1$ ; while for the  $\beta 3$  subunit, platelets express  $\alpha 11\beta 3$  and  $\alpha v\beta 3$  (**Table 1**). Below I will only discuss the integrins  $\alpha 11\beta 3$  and  $\alpha 2\beta 1$ .

Integrin  $\alpha 11\beta 3$  is expressed on platelets with the highest copy number and mediates platelet aggregation by binding the bivalent ligand fibrinogen<sup>6, 122</sup>. In addition,  $\alpha 11\beta 3$  can interact with fibrin, VWF, fibronectin and thrombospondin<sup>122, 123</sup>. Synthetic peptides containing an RGD sequence intervene in the ligand binding<sup>124</sup>. The (inside-out) signaling pathway towards  $\alpha 11\beta 3$  activation has partly been elucidated, with a major role of PI3K isoforms and small G-protein regulators leading to Rap1b activation and establishing cytoskeletal links to talin-1 and kindlin-3, both of which function in establishing the active integrin conformation<sup>38,122</sup>. In addition, activated integrin  $\alpha 11\beta 3$  can signal itself (outside-in signaling), which process supports platelet spreading and clot retraction<sup>121</sup>.

Less prevalent but with a central role in collagen-dependent platelet activation is the integrin  $\alpha 2\beta 1$ . Its activation is achieved through a GPVI-dependent platelet mechanism<sup>81</sup>, can however, also be induced through other pathways, as for instance via P2Y<sub>12</sub><sup>28</sup>. In addition, it is able to bind GFOGER-like motifs on collagens without pre-activation<sup>125</sup>. Overall, integrin  $\alpha 2\beta 1$  and GPVI show a partial redundancy in the binding of collagens, in which one receptor takes over if the other receptor is inhibited<sup>28</sup>. In terms of signaling, it is commonly accepted that the role of  $\alpha 2\beta 1$  is to facilitate the activation via

other receptors, in particular GPVI. An interesting observation is the suggested minor role of  $\alpha 2\beta 1$  in plaque-induced thrombus formation<sup>72,75,76</sup>.

## 1.5 Anti-platelet drugs

In agreement with the major role of platelets in atherothrombosis, antiplatelet drugs provide a first-line therapy for secondary prevention against occlusive arterial thrombus formation. Current antiplatelet therapies are effective in the majority of patients, but these are accompanied by significant number of unwanted bleeding side effects<sup>126-128</sup>. Current targets are, alone or in combination: *i*) the cyclooxygenase and thromboxane synthase complex (aspirin), *ii*) the ADP receptor P2Y<sub>12</sub> (clopidogrel, prasugrel, ticagrelor), *iii*) integrin  $\alpha \text{IIb}\beta 3$  (intravenous abciximab, tirofiban or eptifibatide, and *iv*) the thrombin receptor PAR1 (vorapaxar)<sup>9,129,130</sup>. In addition, there are also several initiatives to target platelet GPVI, which are discussed below.

### **Drugs developed to target GPVI**

Because of its confined expression to platelets and megakaryocytes, GPVI is considered to be a promising anti-thrombotic target. Prior studies in mouse models have shown that defects in GPVI lead to a protection against experimental thrombosis, while only causing minor bleeding events<sup>17,131</sup>. Also in humans, defective expression of GPVI is not accompanied with a major bleeding phenotype<sup>132,133</sup>. Several approaches are being undertaken to clinically interfere with the GPVI-collagen interaction.

### **Recombinant fusion protein Revacept**

Revacept is developed as a recombinant dimeric GPVI fusion protein, which interferes in the collagen mediated platelet activation<sup>129</sup>. Its intended mode of action is to mask GPO motifs of vascular-exposed collagens and thereby antagonize GPVI-dependent adhesion (**Figure 8**). Initial investigations in man and mouse showed that Revacept had promising inhibitory effects on platelet

activation and whole blood thrombus formation, without prolonging the tail bleeding time in mice <sup>134-137</sup>. Murine models furthermore revealed: *i*) in experimental stroke a smaller infarct size and a declined risk for intracranial hemorrhage <sup>138</sup>, and *ii*) upon coronary ligation a smaller myocardial infarct size and better left ventricular ejection fraction <sup>139</sup>.

A human phase I study (NCT01042964) showed safety and a good tolerability of applied Revacept. *In vitro* experiments conducted with platelets from the study participants showed a lower collagen-induced aggregation persisting for up to 48 hours <sup>140</sup>. A subsequent phase II study (ISAR-PLASTER, NCT03312855) investigated intravenously administered Revacept on top of standard dual antiplatelet therapy in patients undergoing treatment for narrowed coronary arteries (percutaneous coronary intervention) <sup>141</sup>. For the primary endpoint of myocardial injury, the trial data showed no significant difference between the treatment groups (two doses of Revacept or placebo), but there were fewer bleeding events in the Revacept arms <sup>142</sup>.

## **9O12 Fab and Glenzocimab**

An alternative approach for blocking platelet-collagen interaction is provided by antibodies against platelet GPVI (**Figure 8**). Firstly, described as 9O12.2, a murine monoclonal antibody Fab fragment against human GPVI was tested with positive outcome in non-human primates <sup>143</sup>. Later it was humanized for use with human blood <sup>144</sup>. Subsequent studies were started with a version under the name ACT017, later changed to Glenzocimab. Both 9O12 Fab and Glenzocimab display high affinity towards GPVI and show strong platelet-inhibiting effects in human blood *in vitro* studies <sup>143,145-147</sup>. The first human trial demonstrated ACT017 to be a safe and tolerable reagent, with no effect on platelet count or platelet GPVI expression; yet with a long plasma half-life and an effective inhibition of collagen-induced platelet activation <sup>148</sup>. With promising results *in vitro* <sup>28,37,94,149</sup>, Glenzocimab moved to a phase II clinical

study, from which preliminary data indicated that the *ex vivo* platelet aggregation with collagen was reduced in most study participants up to 12 hours after administration<sup>150</sup>. The drug is now being assessed in patients with acute ischemic stroke (NCT03803007) and a transition to phase III (ACTISAVE, NCT05070260). In another phase II trial, the drug is tested in COVID-19 positive patients with acute respiratory distress syndrome (GARDEN, NCT04659109).

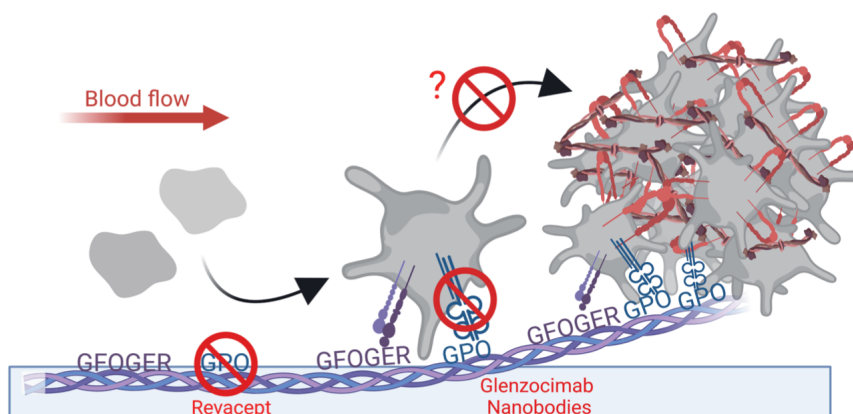


**Figure 8 – Mode of actions of GPVI-directed interventions.** The dimeric GPVI fusion protein Revacept masks the GPVI-binding motifs on exposed collagens. On the other hand, 9O12 Fab, Glenzocimab and anti-GPVI nanobodies bind to GPVI, and can thereby block signaling. Studies with Revacept and Glenzocimab have shown their potency in suppressing thrombus formation *in vitro* and *in vivo*. Nanobodies may become promising tools as well. Original drawing, created with BioRender.com.

### Anti-GPVI nanobodies

Still in their infancy, but promising, are the newly raised nanobodies against GPVI that were introduced and characterized in 2021<sup>151</sup>. The nanobodies consist of only the variable region of cameloid antibodies and are unique not only for their small size (around 15kDa), but also their high affinity and low immunogenicity. Nanobody libraries are relatively easy to generate and maintain; and nanobodies can be expressed in large quantities, making them

more cost-effective than antibodies<sup>152,153</sup>. A drawback can be their short half-life in the circulation. Some other nanobodies have been approved or are currently tested in clinical trials. Relevant for the platelet field is the anti-VWF nanobody Caplacizumab<sup>154,155</sup>, which was approved in 2018 for treatment of acquired thrombotic thrombocytopenic purpura by the European Medicines Agency (EMA)<sup>156,157</sup>. The characterization of anti-GPVI nanobodies considering their potential as anti-thrombotic tools are examined in this thesis.

## **1.6 Platelet function testing by microfluidics**

Microfluidic set-ups have evolved over the years for the assessment of qualitative and quantitative platelet traits in whole blood under flow to approximate (patho)physiological conditions<sup>158</sup>. The Maastricht chamber allows quantitative measurement of multiple platelet and thrombus parameters at the same time using small volumes of blood<sup>159</sup>. Flow setups are beneficial, because *i*) studies can be conducted with whole blood in a point-of-care setting, *ii*) different shear rates can be applied, and *iii*) results obtained with isolated mouse blood can be compared with those from *in vivo* thrombosis models<sup>160</sup>. Accordingly, it has been shown that whole blood microfluidic tests can correctly phenotype the changed platelet functions in multiple genetically modified mice<sup>160,161</sup>, as well as in patients with a bleeding or thrombosis tendency<sup>162-165</sup>.

To date, blood samples from patients have mostly been investigated to answer scientific research questions. However, efforts are being made to move microfluidic testing from research to routine diagnostic laboratories. Preliminary studies indicate that this method, e.g., using collagen type of microspots, may help to characterize patients presenting with a bleeding tendency<sup>19,158</sup>. It can be anticipated that the use of microfluidic chambers may allow clinicians to monitor patients taking anti-thrombotics<sup>166-169</sup>, or patients on other therapies potentially affecting platelets<sup>170,171</sup>. In this thesis, it is

considered how manipulation of the collagen surface can help to better assess platelet activation properties under flow conditions.

## **1.7 Hypothesis and aims**

In this thesis, I investigate how the two main platelet collagen receptors, glycoprotein VI (GPVI) and integrin  $\alpha 2\beta 1$  determine, stimulate and restrict the adhesion as well as activation of platelets via vascular- or plaque-derived collagens. **Chapter 1** details on collagens present in the vessel wall, and it presents GPVI as key signaling receptor for collagen and fibrin(ogen) on platelets with good potential as an antithrombotic target. **Chapter 2** extensively comments on a study investigating the heterogeneity of thrombus structures, and the relevance of such heterogeneity for a successful removal of massive clots in patients who experienced stroke or other thrombotic diseases. In **Chapter 3**, two stage-II pharmaceuticals are examined that target the collagen-GPVI interaction, and thereby the GPVI-induced platelet activation, namely the 9O12 Fab fragment against GPVI (as a proxy of Glencocimab) and the dimeric recombinant GPVI construct Revacept. Their inhibitory patterns are compared, using a variety of collagens and collagen-like substrates. Further, the efficacy of the GPVI intervention is compared to the blockade of GPVI downstream signaling via Syk tyrosine kinase or the blockage of integrin  $\alpha 2\beta 1$  as a backup collagen receptor. In **Chapter 4**, novel anti-GPVI nanobodies (Nb) are introduced as additional tools to interfere in collagen-induced platelet activation and furthermore to visualize the clustering of GPVI on platelets. The chapter focusses on investigating the underlying mechanism of GPVI inhibition exhibited by Nb2. Also, a novel GPVI imaging tool is introduced, allowing first time visualization of the GPVI clustering in whole blood thrombus formation using the fluorescently labeled, non-inhibitory nanobody Nb28. This nanobody is also utilized in **Chapter 5** in order to establish whether the GPVI cluster size correlates to the collagen-dependent



thrombus size under flow conditions. As a readout of the GPVI-induced platelet activation, the exposure of procoagulant phosphatidylserine is taken. Considering that the GPVI-induced platelet activation is abrogated by inhibition of the tyrosine kinase Syk, we have examined how the GPVI clustering depends on this tyrosine kinase signaling pathway. In **Chapter 6**, the effects of Syk inhibition are studied in more detail in thrombus formation using as substrates various fibrillar collagens, non-fibrillar collagens and triple helical collagen-related peptides. In addition, the collagen-induced intracellular  $\text{Ca}^{2+}$  signaling is investigated in detail, and the results are used to generate a model for the GPVI dependency of the signal induced by different collagen preparations. **Chapter 7** explores to which extent the tyrosine phosphatase SHP2 (gene *PTPN11*) is able to counteract the platelet activation and thrombus formation induced by GPVI. This chapter also considers the postulated redundant roles of GPVI and integrin  $\alpha 2\beta 1$  in platelet adhesion and ensued signaling. As a tyrosine phosphatase-dependent negatively modulator of GPVI, involvement of the receptor PECAM1 (CD31) is investigated, which upon activation can suppress collagen-induced platelet activation processes. The final **Chapter 8** discusses key findings of this thesis and places these in context with the literature.

## **1.8 References**

1. Wendelboe AM, Raskob GE. Global burden of thrombosis: epidemiologic aspects. *Circ Res.* 2016;118:1340-1347.
2. World Health Organization. Cardiovascular diseases(CVD). <https://www.who.int/health-topics/cardiovascular-diseases>. Accessed 2022.
3. Koupenova M, Kehrel BE, Corkrey HA, Freedman JE. Thrombosis and platelets: an update. *Eur Heart J.* 2017;38:785-791.
4. Viles-Gonzalez JF, Fuster V, Badimon JJ. Atherothrombosis: a widespread disease with unpredictable and life-threatening consequences. *Eur Heart J.* 2004;25:1197-1207.
5. Periyah MH, Halim AS, Mat Saad AZ. Mechanism action of platelets and crucial blood coagulation pathways in hemostasis. *Int J Hematol Oncol Stem Cell Res.*2017;11:319-327.

6. Versteeg HH, Heemskerk JW, Levi M, Reitsma PH. New fundamentals in hemostasis. *Physiol Rev.* 2013;93:327-358.
7. Patel SR, Hartwig JH, Italiano JE. The biogenesis of platelets from megakaryocyte proplatelets. *J Clin Invest.* 2005;115:3348-3354.
8. Smyth SS, McEver RP, Weyrich AS, *et al.* Platelet functions beyond hemostasis. *J Thromb Haemost.* 2009;7:1759-1766.
9. Van der Meijden PE, Heemskerk JW. Platelet biology and functions: new concepts and future clinical perspectives *Nat Rev Cardiol.* 2019;16:166-179.
10. Quach ME, Chen W, Li R. Mechanisms of platelet clearance and translation to improve platelet storage. *Blood.* 2018;131:1512-1521.
11. Huang J, Swieringa F, Solari FA, *et al.* Assessment of a complete and classified platelet proteome from genome-wide transcripts of human platelets and megakaryocytes covering platelet functions. *Sci Rep.* 2021;11:12358.
12. Bye AP, Unsworth AJ, Gibbins JM. Platelet signaling: a complex interplay between inhibitory and activatory networks. *J Thromb Haemost.* 2016;14:918-930.
13. Fernandez DI, Kuijpers MJ, Heemskerk JW. Platelet calcium signalling by G-protein coupled and ITAM-linked receptors regulating anoctamin-6 and procoagulant activity. *Platelets.* 2021;32:863-871.
14. Newland SA, Macaulay IC, Floto AR, *et al.* The novel inhibitory receptor G6B is expressed on the surface of platelets and attenuates platelet function in vitro. *Blood.* 2007;109:4806-4809.
15. Saboor M, Ayub Q, Ilyas S, Moinuddin. Platelet receptors: an instrumental of platelet physiology. *Pak J Med Sci.* 2013;29:891-896.
16. Schaff M, Tang C, Maurer E, *et al.* Integrin  $\alpha 6 \beta 1$  is the main receptor for vascular laminins and plays a role in platelet adhesion, activation, and arterial thrombosis. *Circulation.* 2013;128:541-552.
17. Stegner D, Haining EJ, Nieswandt B. Targeting glycoprotein VI and the immunoreceptor tyrosine-based activation motif signaling pathway. *Arterioscler Thromb Vasc Biol.* 2014;34:1615-1620.
18. Coxon CH, Geer MJ, Senis YA. ITIM receptors: more than just inhibitors of platelet activation. *Blood.* 2017;129:3407-3418.
19. De Witt SM, Swieringa F, Cavill R, *et al.* Identification of platelet function defects by multi-parameter assessment of thrombus formation. *Nat Commun.* 2014;5:4257.
20. Poddar MK, Banerjee S. Molecular aspects of pathophysiology of platelet receptors. In: *Platelets* (Kerrigan SW, ed.). Intech Open, 2020.
21. Soriano Jerez EM, Gibbins JM, Hughes CE. Targeting platelet inhibition receptors for novel therapies: PECAM-1 and G6b-B. *Platelets.* 2021;32:761-769.

22. Janus-Bell E, Yakusheva A, Scandola C, *et al.* Characterization of the role of integrin  $\alpha 5\beta 1$  in platelet function, hemostasis, and experimental thrombosis. *Thromb Haemost.* 2022;122:767-776.
23. Clemetson KJ, Clemetson JM. Platelet GPIb-V-IX complex: structure, function, physiology, and pathology. *Semin Thromb Hemost.* 1995;21:130-136.
24. Santoro SA. Identification of a 160,000 dalton platelet membrane protein that mediates the initial divalent cation-dependent adhesion of platelets to collagen. *Cell.* 1986;46:913-920.
25. Moroi M, Jung SM, Okuma M, Shinmyozu K. A patient with platelets deficient in glycoprotein VI that lack both collagen-induced aggregation and adhesion. *J Clin Invest.* 1989;84:1440-1445.
26. Kehrel B, Wierwille S, Clemetson KJ, *et al.* Glycoprotein VI is a major collagen receptor for platelet activation: it recognizes the platelet-activating quaternary structure of collagen, whereas CD36, glycoprotein IIb/IIIa, and von Willebrand factor do not. *Blood.* 1998;91:491-499.
27. Watson SP, Herbert JM, Pollitt AY. GPVI and CLEC-2 in hemostasis and vascular integrity. *J Thromb Haemost.* 2010;8:1456-1467.
28. Lecut C, Schoolmeester A, Kuijpers MJ, *et al.* Principal role of glycoprotein VI in  $\alpha 2\beta 1$  and  $\alpha 11\beta 3$  activation during collagen-induced thrombus formation. *Arterioscler Thromb Vasc Biol.* 2004;24:1727-1733.
29. Monroe DM, Hoffman M, Roberts HR. Platelets and thrombin generation. *Arterioscler Thromb Vasc Biol.* 2002;22:1381-1389.
30. Sharda A, Flaumenhaft R. The life cycle of platelet granules. *F1000 Res.* 2018;7:236.
31. Smith CW. Release of  $\alpha$ -granule contents during platelet activation. *Platelets.* 2022;33:491-502.
32. Rendu F, Brohard-Bohn B. The platelet release reaction: granules' constituents, secretion and functions. *Platelets.* 2001;12:261-273.
33. Bearer EL, Prakash JM, Li Z. Actin dynamics in platelets. *Int Rev Cytol.* 2002;217:137-182.
34. Sorrentino S, Studt JD, Horev MB, Medalia O, Sapra KT. Toward correlating structure and mechanics of platelets. *Cell Adh Migr.* 2016;10:568-575.
35. Diagouraga B, Grichine A, Fertin A, *et al.* Motor-driven marginal band coiling promotes cell shape change during platelet activation. *J Cell Biol.* 2014;204:177-185.
36. Inoue O, Suzuki-Inoue K, McCarty OJ, *et al.* Laminin stimulates spreading of platelets through integrin  $\alpha 6\beta 1$ -dependent activation of GPVI. *Blood.* 2006;107:1405-1412.
37. Mangin PH, Onselaer MB, Receveur N, *et al.* Immobilized fibrinogen activates human platelets through glycoprotein VI. *Haematologica.* 2018;103:898-907.

38. Huang J, Li X, Shi X, *et al.* Platelet integrin  $\alpha\text{IIb}\beta\text{3}$ : signal transduction, regulation, and its therapeutic targeting. *J Hematol Oncol.* 2019;12:26.
39. Smith SA, Travers RJ, Morrissey JH. How it all starts: initiation of the clotting cascade. *Crit Rev Biochem Mol Biol.* 2015;50:326-336.
40. Morrissey JH, Macik BG, Neuenschwander PF, Comp PC. Quantitation of activated factor VII levels in plasma using a tissue factor mutant selectively deficient in promoting factor VII activation. *Blood.* 1993;81:734-744.
41. Bom VJ, Bertina RM. The contributions of  $\text{Ca}^{2+}$ , phospholipids and tissue-factor apoprotein to the activation of human blood-coagulation factor X by activated factor VII. *Biochem J.* 1990;265:327-336.
42. Furie B, Furie BC. The molecular basis of blood coagulation. *Cell.* 1988;53:505-518.
43. Zwaal RF, Schroit AJ. Pathophysiologic implications of membrane phospholipid asymmetry in blood cells. *Blood.* 1997;89:1121-1132.
44. Swieringa F, Spronk HM, Heemskerk JW, van der Meijden PE. Integrating platelet and coagulation activation in fibrin clot formation. *Res PractThrombHaemost.* 2018;2:450-460.
45. Heemskerk JW, Matheij NJ, Cosemans JM. Platelet-based coagulation: different populations, different functions. *J Thromb Haemost.* 2013;11:2-16.
46. Matheij NJ, Braun A, van Kruchten R, *et al.* Survival protein anoctamin-6 controls multiple platelet responses including phospholipid scrambling, swelling, and protein cleavage. *FASEB J.* 2016;30:727-737.
47. Rumbaut RE, Thiagarajan P. Platelet adhesion to vascular walls. In: *Platelet-vessel wall interactions in hemostasis and thrombosis (e-Book)*. Morgan & Claypool Life Sciences, San Rafael (CA, USA), 2010: Chapter 3.
48. Chernysh IN, Nagaswami C, Kosolapova S, *et al.* The distinctive structure and composition of arterial and venous thrombi and pulmonary emboli. *Sci Rep.* 2020;10:5112.
49. Vidale S, Agostoni EC. Organizing healthcare for optimal acute ischemic stroke treatment. *J Clin Neurol.* 2020;16:183-190.
50. Mengozzi L, Widimsky P. The potential value of histological analysis of thrombi extracted through mechanical thrombectomy during acute ischemic stroke treatment. *Anatol J Cardiol.* 2020;23:254-259.
51. Ryan EA, Mockros LF, Weisel JW, Lorand L. Structural origins of fibrin clot rheology. *Biophys J.* 1999;77:2813-2826.
52. Longstaff C, Varjú I, Sótonyi P, *et al.* Mechanical stability and fibrinolytic resistance of clots containing fibrin, DNA, and histones. *J Biol Chem.* 2013;288:6946-6956.
53. Miszta A, Pelkmans L, Lindhout T, *et al.* Thrombin-dependent incorporation of von Willebrand factor into a fibrin network. *J Biol Chem.* 2014;289:35979-35986.

54. Stalker TJ, Welsh JD, Brass LF. Shaping the platelet response to vascular injury. *Curr Opin Hematol*. 2014;21:410-417.
55. Welsh JD, Poventud-Fuentes I, Sampietro S, *et al*. Hierarchical organization of the hemostatic response to penetrating injuries in the mouse macrovasculature. *J Thromb Haemost*. 2017;15:526-537.
56. Mattheij NJ, Swieringa F, Mastenbroek TG, *et al*. Coated platelets function in platelet-dependent fibrin formation via integrin  $\alpha\text{IIb}\beta\text{3}$  and transglutaminase factor XIII. *Haematologica*. 2016;101:427-436.
57. Kehrel B. Platelet-collagen interactions. *Semin Thromb Hemost*. 1995;21:123-129
58. Farndale RW, Sixma JJ, Barnes MJ, de Groot PG. The role of collagen in thrombosis and hemostasis. *J Thromb Haemost*. 2004;2:561-573.
59. Barnes MJ, Farndale RW. Collagens and atherosclerosis. *ExpGerontol*.1999;34:513-525.
60. Jacob MP, Badier-Commander C, Fontaine V, *et al*. Extracellular matrix remodeling in the vascular wall. *Pathol Biol (Paris)*. 2001;49:326-332.
61. Farndale RW, Lisman T, Bihan D, *et al*. Cell-collagen interactions: the use of peptide toolkits to investigate collagen-receptor interactions. *BiochemSocTrans*.2008;36:241-250.
62. Birk DE, Southern JF, Zycband EI, Fallon JT, Trelstad RL. Collagen fibril bundles: a branching assembly unit in tendon morphogenesis. *Development*. 1989;107:437-443.
63. Van Zanten HG, Saelman EU, Schut-Hese KM, *et al*. Platelet adhesion to collagen type IV under flow conditions. *Blood*. 1996;88:3862-3871.
64. Virmani R, Kolodgie FD, Burke AP, *et al*. Atherosclerotic plaque progression and vulnerability to rupture: angiogenesis as a source of intraplaque hemorrhage. *Arterioscler Thromb Vasc Biol*. 2005;25:2054-2061.
65. Gui Y, Zheng H, Cao RY. Foam cells in atherosclerosis: novel insights into the origins, consequences, and molecular mechanisms. *Front Cardiovasc Med*. 2022;9:845942.
66. Fishbein MC, Siegel RJ. How big are coronary atherosclerotic plaques that rupture? *Circulation*. 1996;94:2662-2666.
67. Lutgens E, van Suylen RJ, Faber BC, *et al*. Atherosclerotic plaque rupture: local or systemic process? *Arterioscler Thromb Vasc Biol*. 2003;23:2123-2130.
68. Borissoff JI, Heeneman S, Kiliç E, *et al*. Early atherosclerosis exhibits an enhanced procoagulant state. *Circulation*. 2010;122:821-830.
69. Siess W, Zangl KJ, Essler M, *et al*. Lysophosphatidic acid mediates the rapid activation of platelets and endothelial cells by mildly oxidized low density lipoprotein and accumulates in human atherosclerotic lesions. *ProcNatlAcadSciUSA*.1999;96:6931-6936.

70. Siess W. Athero- and thrombogenic actions of lysophosphatidic acid and sphingosine-1-phosphate. *Biochim Biophys Acta*. 2002;1582:204-215.
71. Van Zanten GH, de Graaf S, Slootweg PJ, *et al*. Increased platelet deposition on atherosclerotic coronary arteries. *J Clin Invest*. 1994;93:615-632.
72. Penz S, Reininger AJ, Brandl R, *et al*. Human atheromatous plaques stimulate thrombus formation by activating platelet glycoprotein VI. *FASEB J*. 2005;19:898-909.
73. Cosemans JM, Kuijpers MJ, Lecut C, *et al*. Contribution of platelet glycoprotein VI to the thrombogenic effect of collagens in fibrous atherosclerotic lesions. *Atherosclerosis*. 2005;181:19-27.
74. Shekhonin BV, Domogatsky SP, Idelson GL, Koteliansky VE, Rukosuev VS. Relative distribution of fibronectin and type I, III, IV, V collagens in normal and atherosclerotic intima of human arteries. *Atherosclerosis*. 1987;67:9-16.
75. Schulz C, Penz S, Hoffmann C, *et al*. Platelet GPVI binds to collagenous structures in the core region of human atheromatous plaque and is critical for atheroprogession in vivo. *Basic Res Cardiol*. 2008;103:356-367.
76. Busygina K, Jamasbi J, Seiler T, *et al*. Oral Bruton tyrosine kinase inhibitors selectively block atherosclerotic plaque-triggered thrombus formation in humans. *Blood*. 2018;131:2605-2616.
77. Saelman EU, Nieuwenhuis HK, Hese KM, *et al*. Platelet adhesion to collagen types I through VIII under conditions of stasis and flow is mediated by GPIa/IIa ( $\alpha 2\beta 1$ -integrin). *Blood*. 1994;83:1244-1250.
78. Wu YP, van Breugel HH, Lankhof H, *et al*. Platelet adhesion to multimeric and dimeric von Willebrand factor and to collagen type III preincubated with von Willebrand factor. *Arterioscler Thromb Vasc Biol*. 1996;16:611-620.
79. Verkleij MW, Morton LF, Knight CG, *et al*. Simple collagen-like peptides support platelet adhesion under static but not under flow conditions: interaction via  $\alpha 2\beta 1$  and von Willebrand factor with specific sequences in native collagen is a requirement to resist shear forces. *Blood*. 1998;91:3808-3816.
80. Hamaia S, Farndale RW. Integrin recognition motifs in the human collagens. *Adv Exp Med Biol*. 2014;819:127-142.
81. Herr AB, Farndale RW. Structural insights into the interactions between platelet receptors and fibrillar collagen. *J Biol Chem*. 2009;284:19781-19785.
82. Munnix IC, Gilio K, Siljander PR, *et al*. Collagen-mimetic peptides mediate flow-dependent thrombus formation by high- or low-affinity binding of integrin  $\alpha 2\beta 1$  and glycoprotein VI. *J Thromb Haemost*. 2008;6:2132-2142.
83. Knight CG, Morton LF, Peachey AR, *et al*. The collagen-binding A-domains of integrins  $\alpha 1\beta 1$  and  $\alpha 2\beta 1$  recognize the same specific amino acid sequence, GFOGER, in native (triple-helical) collagens. *J Biol Chem*. 2000;275:35-40.

84. Romijn RA, Bouma B, Wuyster W, *et al.* Identification of the collagen-binding site of the von Willebrand factor A3-domain. *J Biol Chem.* 2001;276:9985-9991.
85. Lisman T, Raynal N, Groeneveld D, *et al.* A single high-affinity binding site for von Willebrand factor in collagen III, identified using synthetic triple-helical peptides. *Blood.* 2006;108:3753-3756.
86. Pugh N, Maddox BD, Bihan D, *et al.* Differential integrin activity mediated by platelet collagen receptor engagement under flow conditions. *Thromb Haemost.* 2017;117:1588-1600.
87. Heemskerk JW, Sakariassen KS, Zwaginga JJ, *et al.* Collagen surfaces to measure thrombus formation under flow: possibilities for standardization. *J Thromb Haemost.* 2011;9:856-858.
88. Suzuki-Inoue K, Tulasne D, Shen Y, *et al.* Association of Fyn and Lyn with the proline-rich domain of glycoprotein VI regulates intracellular signaling. *J Biol Chem.* 2002;277:21561-21566.
89. Nieswandt B, Watson SP. Platelet-collagen interaction: is GPVI the central receptor? *Blood.* 2003;102:449-461.
90. Alshehri OM, Hughes CE, Montague S, *et al.* Fibrin activates GPVI in human and mouse platelets. *Blood.* 2015;126:1601-1608.
91. Onselaer MB, Hardy AT, Wilson C, *et al.* Fibrin and D-dimer bind to monomeric GPVI. *Blood Adv.* 2017;1:1495-1504.
92. Induruwa I, Moroi M, Bonna A, *et al.* Platelet collagen receptor glycoprotein VI-dimer recognizes fibrinogen and fibrin through their D-domains, contributing to platelet adhesion and activation during thrombus formation. *J Thromb Haemost.* 2018;16:389-404.
93. Mammadova-Bach E, Ollivier V, Loyau S, *et al.* Platelet glycoprotein VI binds to polymerized fibrin and promotes thrombin generation. *Blood.* 2015;126:683-691.
94. Perrella G, Huang J, Provenzale I, *et al.* Nonredundant roles of platelet glycoprotein VI and integrin  $\alpha$ IIb $\beta$ 3 in fibrin-mediated microthrombus formation. *Arterioscler Thromb Vasc Biol.* 2021;41:e97-e111.
95. Schulz C, von Brühl ML, Barocke V, *et al.* EMMPRIN (CD147/basigin) mediates platelet-monocyte interactions in vivo and augments monocyte recruitment to the vascular wall. *J Thromb Haemost.* 2011;9:1007-1019.
96. Zhi Z, Jooss NJ, Sun Y, *et al.* Galectin-9 activates platelet ITAM receptors glycoprotein VI and C-type lectin-like receptor-2. *J Thromb Haemost.* 2022;20:936-950.
97. Watson SP, Auger JM, McCarty OJ, Pearce AC. GPVI and integrin  $\alpha$ IIb $\beta$ 3 signaling in platelets. *J Thromb Haemost.* 2005;3:1752-1762.
98. Rayes J, Watson SP, Nieswandt B. Functional significance of the platelet immune receptors GPVI and CLEC-2. *J Clin Invest.* 2019;129:12-23.

99. Bergmeier W, Stefanini L. Platelet ITAM signaling. *Curr Opin Hematol.* 2013;20:445-450
100. Bethani I, Skånland SS, Dikic I, Acker-Palmer A. Spatial organization of transmembrane receptor signalling. *EMBO J.* 2010;29:2677-2688.
101. Pigeon SV, Tabarin T, Yamamoto Y, *et al.* Functional role of T-cell receptor nanoclusters in signal initiation and antigen discrimination. *Proc Natl Acad Sci USA.* 2016;113:e5454-5463.
102. Sato K, Ochi A. Superclustering of B cell receptor and FcγRIIB1 activates Src homology 2-containing protein tyrosine phosphatase-1. *J Immunol.* 1998;161:2716-2722.
103. Hartman NC, Groves JT. Signaling clusters in the cell membrane. *Curr Opin Cell Biol.* 2011;23:370-376.
104. Montague SJ, Lim YJ, Lee WM, Gardiner EE. Imaging platelet processes and function-current and emerging approaches for imaging in vitro and in vivo. *Front Immunol.* 2020;11:78.
105. Poulter NS, Pollitt AY, Owen DM, *et al.* Clustering of glycoprotein VI dimers upon adhesion to collagen as a mechanism to regulate GPVI signaling in platelets. *J Thromb Haemost.* 2017;15:549-564.
106. Pallini C, Pike JA, O'Shea C, *et al.* Immobilized collagen prevents shedding and induces sustained GPVI clustering and signaling in platelets. *Platelets.* 2021;32:59-73.
107. Clark JC, Kavanagh DM, Watson S, *et al.* Adenosine and forskolin inhibit platelet aggregation by collagen but not the proximal signalling events. *Thromb Haemost.* 2019;119:1124-1137.
108. Andrews RK, Karunakaran D, Gardiner EE, Berndt MC. Platelet receptor proteolysis: a mechanism for downregulating platelet reactivity. *Arterioscler Thromb Vasc Biol.* 2007;27:1511-1120.
109. Andrews RK, Gardiner EE. Basic mechanisms of platelet receptor shedding. *Platelets.* 2017;28:319-324.
110. Baaten CC, Swieringa F, Misztal T, *et al.* Platelet heterogeneity in activation-induced glycoprotein shedding: functional effects. *Blood Adv.* 2018;2:2320-2331.
111. Mellion BT, Ignarro LJ, Ohlstein EH, *et al.* Evidence for the inhibitory role of guanosine 3', 5'-monophosphate in ADP-induced human platelet aggregation in the presence of nitric oxide and related vasodilators. *Blood.* 1981;57:946-955.
112. Swieringa F, Kuijpers MJ, Heemskerk JW, van der Meijden PE. Targeting platelet receptor function in thrombus formation: the risk of bleeding. *Blood Rev.* 2014;28:9-21.
113. Mori J, Pearce AC, Spalton JC, *et al.* G6b-B inhibits constitutive and agonist-induced signaling by glycoprotein VI and CLEC-2. *J Biol Chem.* 2008;283:35419-35427.



114. Cicmil M, Thomas JM, Leduc M, Bon C, Gibbins JM. Platelet endothelial cell adhesion molecule-1 signaling inhibits the activation of human platelets. *Blood*. 2002;99:137-144.
115. Jones CI, Garner SF, Moraes LA, *et al*. PECAM-1 expression and activity negatively regulate multiple platelet signaling pathways. *FEBS Lett*. 2009;583:3618-3624.
116. Heemskerk JW. More than reverting tyrosine kinases. *Blood*. 2022;140:939-941.
117. Kharitonov A, Chen Z, Sures I, *et al*. A family of proteins that inhibit signalling through tyrosine kinase receptors. *Nature*. 1997;386:181-186.
118. Bruhns P, Vely F, Malbec O, *et al*. Molecular basis of the recruitment of the SH2 domain-containing inositol 5-phosphatases SHIP1 and SHIP2 by Fc $\gamma$ RIIB. *J Biol Chem*. 2000;275:37357-37364.
119. Moraes LA, Barrett NE, Jones CI, *et al*. Platelet endothelial cell adhesion molecule-1 regulates collagen-stimulated platelet function by modulating the association of phosphatidylinositol 3-kinase with Grb-2-associated binding protein-1 and linker for activation of T cells. *J Thromb Haemost*. 2010;8:2530-2541.
120. Wee JL, Jackson DE. The Ig-ITIM superfamily member PECAM-1 regulates the outside-in signaling properties of integrin  $\alpha$ IIb $\beta$ 3 in platelets. *Blood*. 2005;106:3816-3823.
121. Kasirer-Friede A, Kahn ML, Shattil SJ. Platelet integrins and immunoreceptors. *Immunol Rev*. 2007;218:247-264.
122. Nieswandt B, Varga-Szabo D, Elvers M. Integrins in platelet activation. *J Thromb Haemost*. 2009;7 Suppl 1:206-209.
123. Plow EF, McEver RP, Collier BS, *et al*. Related binding mechanisms for fibrinogen, fibronectin, von Willebrand factor, and thrombospondin on thrombin-stimulated human platelets. *Blood*. 1985;66:724-727.
124. Ruoslahti E. Integrins. *J Clin Invest*. 1991;87:1-5.
125. Siljander PR, Hamaia S, Peachey AR, *et al*. Integrin activation state determines selectivity for novel recognition sites in fibrillar collagens. *J Biol Chem*. 2004;279:47763-47772.
126. Sørensen R, Hansen ML, Abildstrom SZ, *et al*. Risk of bleeding in patients with acute myocardial infarction treated with different combinations of aspirin, clopidogrel, and vitamin K antagonists in Denmark: a retrospective analysis of nationwide registry data. *Lancet*. 2009;374:1967-1974.
127. Lamberts M, Olesen JB, Ruwald MH, *et al*. Bleeding after initiation of multiple antithrombotic drugs, including triple therapy, in atrial fibrillation patients following myocardial infarction and coronary intervention: a nationwide cohort study. *Circulation*. 2012;126:1185-1193.

128. Vries MJ, van der Meijden PE, Henskens YM, ten Cate-Hoek AJ, ten Cate H. Assessment of bleeding risk in patients with coronary artery disease on dual antiplatelet therapy. A systematic review. *Thromb Haemost.* 2016;115:7-24.
129. Andrews RK, Arthur JF, Gardiner EE. Targeting GPVI as a novel antithrombotic strategy. *J Blood Med.* 2014;5:59-68.
130. Gremmel T, Michelson AD, Frelinger AL, Bhatt DL. Novel aspects of antiplatelet therapy in cardiovascular disease. *Res Pract Thromb Haemost.* 2018;2:439-449.
131. Lockyer S, Okuyama K, Begum S, *et al.* GPVI-deficient mice lack collagen responses and are protected against experimentally induced pulmonary thromboembolism. *Thromb Res.* 2006;118:371-380.
132. Arai M, Yamamoto N, Moroi M, *et al.* Platelets with 10% of the normal amount of glycoprotein VI have an impaired response to collagen that results in a mild bleeding tendency. *Br J Haematol.* 1995;89:124-130.
133. Nurden AT. Clinical significance of altered collagen-receptor functioning in platelets with emphasis on glycoprotein VI. *Blood Rev.* 2019;38:100592.
134. Bültmann A, Herdeg C, Li Z, *et al.* Local delivery of soluble platelet collagen receptor glycoprotein VI inhibits thrombus formation in vivo. *Thromb Haemost.* 2006;95:763-6.
135. Jamasbi J, Megens RT, Bianchini M, *et al.* Differential inhibition of human atherosclerotic plaque-induced platelet activation by dimeric GPVI-Fc and anti-GPVI antibodies: functional and imaging studies. *J Am Coll Cardiol.* 2015;65:2404-2415.
136. Mojica Muñoz AK, Jamasbi J, Uhland K, *et al.* Recombinant GPVI-Fc added to single or dual antiplatelet therapy in vitro prevents plaque-induced platelet thrombus formation. *Thromb Haemost.* 2017;117:1651-1659.
137. Ungerer M, Li Z, Baumgartner C, *et al.* The GPVI-Fc fusion protein revacept reduces thrombus formation and improves vascular dysfunction in atherosclerosis without any impact on bleeding times. *Plos One.* 2013;8:e71193.
138. Goebel S, Li Z, Vogelmann J, *et al.* The GPVI-Fc fusion protein revacept improves cerebral infarct volume and functional outcome in stroke. *PLoS One.* 2013;8:e66960.
139. Schönberger T, Ziegler M, Borst O, *et al.* The dimeric platelet collagen receptor GPVI-Fc reduces platelet adhesion to activated endothelium and preserves myocardial function after transient ischemia in mice. *Am J Physiol.* 2012;303:C757-766.
140. Ungerer M, Rosport K, Bültmann A, *et al.* Novel antiplatelet drug revacept (dimeric glycoprotein VI-Fc) specifically and efficiently inhibited collagen-induced platelet aggregation without affecting general hemostasis in humans. *Circulation.* 2011;123:1891-1899.

141. Schüpke S, Hein-Rothweiler R, Mayer K, *et al.* Revacept, a novel inhibitor of platelet adhesion, in patients undergoing elective PCI - design and rationale of the randomized ISAR-PLASTER trial. *Thromb Haemost.* 2019;119:1539-1545.
142. Mayer K, Hein-Rothweiler R, Schüpke S, *et al.* Efficacy and safety of revacept, a novel lesion-directed competitive antagonist to platelet glycoprotein VI, in patients undergoing elective percutaneous coronary intervention for stable ischemic heart disease: the randomized, double-blind, placebo-controlled ISAR-PLASTER phase 2 trial. *JAMA Cardiol.* 2021;6:753-761.
143. Ohlmann P, Hechler B, Ravanat C, *et al.* Ex vivo inhibition of thrombus formation by an anti-glycoprotein VI Fab fragment in non-human primates without modification of glycoprotein VI expression. *J Thromb Haemost.* 2008;6:1003-1011.
144. Muzard J, Bouabdelli M, Zahid M, *et al.* Design and humanization of a murine scFv that blocks human platelet glycoprotein VI in vitro. *FEBS J.* 2009;276:4207-4222.
145. Lecut C, Feeney LA, Kingsbury G, *et al.* Human platelet glycoprotein VI function is antagonized by monoclonal antibody-derived Fab fragments. *J Thromb Haemost.* 2003;1:2653-2662.
146. Mangin PH, Tang C, Bourdon C, *et al.* A humanized glycoprotein VI (GPVI) mouse model to assess the antithrombotic efficacies of anti-GPVI agents. *J Pharmacol Exp Ther.* 2012;341:156-163.
147. Lebozec K, Jandrot-Perrus M, Avenard G, Favre-Bulle O, Billiald P. Design, development and characterization of ACT017, a humanized Fab that blocks platelet's glycoprotein VI function without causing bleeding risks. *MAbs.* 2017;9:945-958.
148. Voors-Pette C, Lebozec K, Dogterom P, *et al.* Safety and tolerability, pharmacokinetics, and pharmacodynamics of ACT017, an antiplatelet GPVI (glycoprotein VI) Fab. *Arterioscler Thromb Vasc Biol.* 2019;39:956-964.
149. Lecut C, Feijge MA, Cosemans JM, Jandrot-Perrus M, Heemskerk JW. Fibrillar type I collagens enhance platelet-dependent thrombin generation via glycoprotein VI with direct support of  $\alpha 2\beta 1$  but not  $\alpha 11\beta 3$  integrin. *Thromb Haemost.* 2005;94:107-114.
150. Renaud L, Lebozec K, Voors-Pette C, *et al.* Population pharmacokinetic/pharmacodynamic modeling of glenzocimab (ACT017), a glycoprotein VI inhibitor of collagen-induced platelet aggregation. *J Clin Pharmacol.* 2020;60:1198-1208.
151. Slater A, Di Y, Clark JC, *et al.* Structural characterization of a novel GPVI-nanobody complex reveals a biologically active domain-swapped GPVI dimer. *Blood.* 2021; 137:3443-3453.
152. Hamers-Casterman C, Atarhouch T, Muyldermans S, *et al.* Naturally occurring antibodies devoid of light chains. *Nature.* 1993;363:446-448.

153. Steeland S, Vandenbroucke RE, Libert C. Nanobodies as therapeutics: big opportunities for small antibodies. *Drug Discov Today*. 2016;21:1076-1113.
154. Ulrichs H, Silence K, Schoolmeester A, *et al*. Antithrombotic drug candidate ALX-0081 shows superior preclinical efficacy and safety compared with currently marketed antiplatelet drugs. *Blood*. 2011;118:757-765.
155. Duggan S. Caplacizumab: first global approval. *Drugs*. 2018;78:1639-1642.
156. EMA. <https://www.ema.europa.eu/en/medicines/human/EPAR/cablivi>. 2022.
157. FDA US Food and Drug Administration. Drug trials snapshots: cablivi. 2019. <https://www.fda.gov/drugs/drug-trials-snapshots-cablivi>.
158. Schoeman RM, Lehmann M, Neeves KB. Flow chamber and microfluidic approaches for measuring thrombus formation in genetic bleeding disorders. *Platelets*. 2017;28:463-471.
159. Van Kruchten R, Cosemans JM, Heemskerk JW. Measurement of whole blood thrombus formation using parallel-plate flow chambers: practical guide. *Platelets*. 2012;23:229-242.
160. Nagy M, van Geffen JP, Stegner D, *et al*. Comparative analysis of microfluidics thrombus formation in multiple genetically modified mice: link to thrombosis and hemostasis. *Front Cardiovasc Med*. 2019;6:99.
161. Baaten CC, Meacham S, de Witt SM, *et al*. A synthesis approach of mouse studies to identify genes and proteins in arterial thrombosis and bleeding. *Blood*. 2018;132:e35-e46.
162. Colace TV, Fogarty PF, Panckeri KA, Li R, Diamond SL. Microfluidic assay of hemophilic blood clotting: distinct deficits in platelet and fibrin deposition at low factor levels. *J Thromb Haemost*. 2014;12:147-158.
163. Lehmann M, Ashworth K, Manco-Johnson M, *et al*. Evaluation of a microfluidic flow assay to screen for von Willebrand disease and low von Willebrand factor levels. *J Thromb Haemost*. 2018;16:104-115.
164. Brouns SL, Tullemans BM, Bulato C, *et al*. Protein C or protein S deficiency associates with paradoxically impaired platelet-dependent thrombus and fibrin formation under flow. *Res Pract Thromb Haemost*. 2022;6:e12678.
165. Heubel-Moenen FC, Brouns SL, Herfs L, *et al*. Multiparameter platelet function analysis of bleeding patients with a prolonged platelet function analyser closure time. *Br J Haematol*. 2022;196:1388-1400.
166. Baaten CC, Veenstra LF, Wetzels R, *et al*. Gradual increase in thrombogenicity of juvenile platelets formed upon offset of prasugrel medication. *Haematologica*. 2015;100:1131-1138.
167. Herfs L, Swieringa F, Jooss N, *et al*. Multiparameter microfluidics assay of thrombus formation reveals increased sensitivity to contraction and antiplatelet agents at physiological temperature. *Thromb Res*. 2021;203:46-56.
168. Jose B, McCluskey P, Gilmartin N, *et al*. Self-powered microfluidic device for rapid assay of antiplatelet drugs. *Langmuir*. 2016;32:2820-2828.

169. Li R, Grosser T, Diamond SL. Microfluidic whole blood testing of platelet response to pharmacological agents. *Platelets*. 2017;28:457-462.
170. Sabrkhany S, Griffioen AW, Pineda S, *et al*. Sunitinib uptake inhibits platelet function in cancer patients. *Eur J Cancer*. 2016;66:47-54.
171. Tullemans BM, Veninga A, Fernandez DI, *et al*. Multiparameter evaluation of the platelet-inhibitory effects of tyrosine kinase inhibitors used for cancer treatment. *Int J Mol Sci*. 2021;22:11199.
172. Staessens S, De Meyer SF. Thrombus heterogeneity in ischemic stroke. *Platelets*. 2021;32:331-339.



# Chapter 2

**A large-scale histological investigation gives insight into the structure of ischemic stroke thrombi**

Natalie J. Jooss and Natalie S. Poulter

Contributions: NJJ wrote the manuscript and prepared figures  
Published: Platelets, 2021, Vol 32, Pages 147-150

Worldwide, 15 million people suffer a stroke every year <sup>1</sup>, it is therefore a significant global health and financial burden. In Europe alone, there were more than 600,000 people who endured a stroke in 2015 and this is estimated to increase to over 800,000 by 2035, equating to a massive financial burden of 45 billion Euros <sup>2</sup>. The majority of strokes (85%) are ischemic, triggered by a thrombus occluding a blood vessel, decreasing oxygen supply to the affected area and resulting in tissue damage. The remaining 15% of strokes are hemorrhagic and caused by rupture of a major vessel <sup>3,4</sup>. The severity of stroke can vary; in Europe it is the second most common cause of death <sup>5</sup> but even if the patient recovers, rehabilitation can take many months, or even years, and some individuals have to learn to live with permanent disabilities as a result of the stroke <sup>2</sup>. The best outcome for the patient is achieved if the blood flow is restored as promptly as possible <sup>6</sup>. European guidelines indicate that treatment for ischemic stroke should occur within the first 4.5 hours of the onset of symptoms <sup>3</sup>. At present there are two approved treatment strategies for stroke. Most patients are treated with intravenous administration of recombinant tissue plasminogen activator (rtPA) <sup>2</sup>, an enzyme that catalyzes the conversion of plasminogen to plasmin, which induces thrombolysis (clot breakdown) <sup>3</sup>. A more recently employed technique is thrombectomy, where the clot is retrieved mechanically <sup>7,8</sup>. In many cases, these treatments are not sufficient to remove the occluding thrombus and restore blood flow. The underlying reason for this is still not fully understood. It is thought that this may be related to the great heterogeneity that is present in the stroke-causing thrombi that could make a clot more, or less, susceptible to degradation by rtPA or affect the likelihood of successful retrieval. Understanding the thrombus composition and structure could lead to more targeted and effective treatments for stroke <sup>6</sup>.

The recent work of Staessens *et al.* <sup>9</sup> has made further advances in addressing the question of thrombus composition. In this paper the authors

interrogated the structure of 177 thrombi from acute ischemic stroke patients isolated by thrombectomy and have made further steps towards deciphering the cellular components involved <sup>9</sup>. To our knowledge, this is the first study to use such a large number of samples to systematically characterize thrombus structure utilizing histological stains and immunofluorescence labeling for red blood cells (RBC), platelets, fibrin(ogen), von Willebrand factor (VWF) and DNA.

In the present study <sup>9</sup>, thrombi were retrieved and analyzed from ischemic stroke patients, regardless of prior rtPA treatment. However, the authors did not correlate the results with the treatment to determine if there was any effect of the rtPA on thrombus structure. Further, they also acknowledge that findings may potentially be biased, as only retrievable thrombi were interrogated. In fact, there is evidence that RBC-rich thrombi are more easily removed by thrombectomy <sup>10</sup>. Nevertheless, all 177 thrombi in this study were subjected to the full range of analyses, with authors able to show that thrombi contain RBC-rich as well as platelet-rich areas. Regardless of the above-mentioned limitations, they elegantly demonstrate the continuum observed in the makeup of thrombi and the proportion of RBC-rich and platelet-rich areas, summarized in **Figure 1**.

Within the different zones, Staessens *et al.* <sup>9</sup> showed that RBC-rich areas were composed of densely packed RBCs with a fine fibrin meshwork throughout. Nucleated cells, VWF and platelets were rarely seen in these areas. This relatively simple structure is in contrast to the platelet-rich areas where fibrin and VWF often colocalized, and leukocytes and an abundance of extracellular DNA were observed. The extracellular DNA was hypothesized to be the result of neutrophil extracellular traps (NETs) formation which has been shown to not only interact with platelets <sup>11</sup> but also to play a role in venous thrombosis <sup>12,13</sup>.



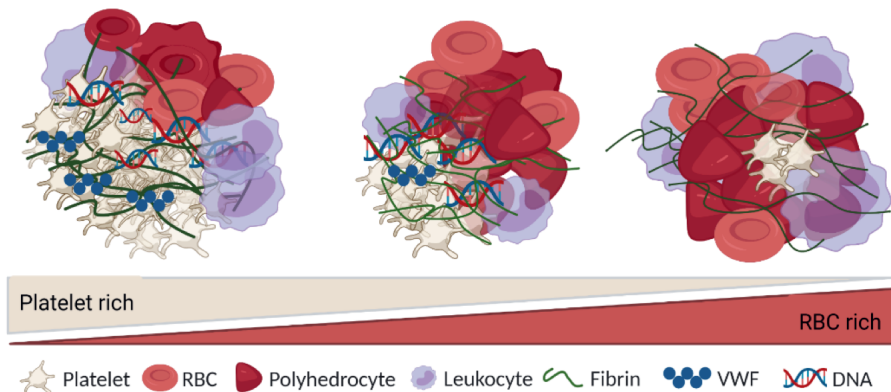


**Figure 1 – Different thrombus morphology as observed by Staessens *et al.***<sup>9</sup>. Thrombi from stroke patients extracted by mechanical removal (thrombectomy) were found to be composed of a platelet-rich areas containing thick fibrin fibers, seemingly crosslinked with VWF and DNA. Red blood cell (RBC)-rich areas, with a loose fibrin network and some leukocytes were also present. Interestingly, leukocytes and DNA were shown to colocalize at the border between platelet- and RBC-rich areas. The 177 thrombi analyzed showed a full range of compositions from predominantly platelet-rich to almost entirely RBC-rich. Figure created with BioRender.com.

However, further staining for citrullinated histone h3<sup>14</sup> and myeloperoxidase was not performed<sup>15</sup>. More specific staining for NETosis can confirm that the detected DNA is in fact neutrophil-derived and not induced by cell death or necrosis; additionally, it also makes it possible to narrow down the specific pathway of the neutrophil activation and subsequent NET formation<sup>16</sup>.

Putting these observations into the context of other studies the authors speculate that the rtPA resistance of platelet-rich thrombi could be due to DNA modification of the fibrin structure<sup>17,18</sup>. They also suggest that covalent cross-linking of VWF and fibrin by Factor XIII may contribute to the rtPA resistance<sup>19-23</sup>. Factor XIII is a transglutaminase which circulates in the blood as an inactive zymogen. Once activated by thrombin (to become FXIIIa), it can

crosslink fibrin via isopeptide bonds which increases clot stability and makes it more resistant to fibrinolysis. FXIIIa has also been shown to crosslink VWF to fibrin<sup>21</sup>. As both fibrin and VWF have been observed to colocalize in the thrombus it would be interesting to probe the sections for factor XIII to see if it was also present to support this hypothesis. This could explain why less than half of the patients that receive rtPA treatment to induce thrombolysis have a positive outcome<sup>24,8</sup>. The present work, therefore, strongly suggests DNase and/or ADAMTS13 (a plasma metalloproteinase that cleaves VWF) may increase thrombolysis. These interesting findings warrant more in-depth study of rtPA alone or in combination with DNase1/ADAMTS13. In fact, Denorme *et al.*<sup>22</sup> have shown the presence of VWF in 36 ischemic stroke thrombi, but also that tPA treatment was more efficient after pre-infusion of ADAMTS13 in a murine stroke model<sup>22</sup>. Very recent work by Ahmed *et al.*<sup>25</sup> has shown that the platelet collagen and fibrin(ogen) receptor GPVI might be involved in stabilizing thrombi. Hence, an anti-GPVI agent could be used in combination with rtPA to promote disaggregation of platelet-rich thrombi<sup>25</sup>. This again provides further evidence that understanding thrombus structure could offer enhanced treatment strategies. It will be interesting to see whether the results of these mouse model and in vitro studies hold true in-patient studies to see if such combination therapies could be used in the future to increase the success of stroke treatment and patient outcomes.

Although the conclusions of Staessens *et al.*<sup>9</sup> are based on a large dataset, detailed quantification of the data obtained by immunohistochemistry for VWF, platelets, fibrin(ogen) and leukocytes are missing. Quantification of the impressive number of thrombi investigated could potentially provide not only numerical data in order to compare different thrombi, but also present the opportunity to interrogate the heterogeneity within an individual thrombus. A machine-learning approach to quantify labeled thrombus sections has been used previously<sup>26,27</sup> and the work by Staessens *et al.*<sup>9</sup> would benefit from a

similar approach and therefore presents an opportunity for further exploitation of their large dataset.

This study is an important addition to a whole body of work that could significantly improve outcomes for stroke patients by improving treatment strategies. Similar studies state various patient parameters such as gender, age, pre-existing conditions, stroke etiology or even occlusion site <sup>28,29</sup>. Connecting them to thrombus morphology could be key in determining patient-specific therapeutic approaches. Therefore, follow-up studies should be pursued that investigate the correlation between thrombus structure and patient parameters, as well as plasma samples, to give more information on how different factors influence stroke severity, as well as patient outcome. Boeckh-Behrens *et al.* <sup>30</sup> investigated whether the underlying cause for ischemic stroke in 145 patients was due to a cardioembolic event. By combining semi-quantitative analysis of the thrombi with clinical data they concluded that most strokes were of cardioembolic origin <sup>30</sup>. More information about thrombus structure poses the potential to expand the choice and manner of treatment strategies thereby improving outcomes for ischemic stroke patients. In fact, there is evidence that in coronary thrombi fibrin content increases, while the presence of platelets decreases the ischemic time (duration from onset of symptoms to the primary percutaneous intervention) <sup>31</sup>.

Whilst this is a well-executed study, the conclusions are based upon observations and further experimental work is required. For example, laser capture microdissection could be utilized to not only visualize areas of interest, but also enable incorporation of other experimental measures such as proteomics, transcriptomics, or genomics to investigate regions/cells <sup>32</sup>. This type of approach would complement existing data obtained from mass spectrometry on stroke thrombi where Munoz *et al.* <sup>33</sup> identified 339 proteins commonly detected in the four patients investigated <sup>33</sup>. Further, as there is

evidence that the composition of the thrombus plays an important role in the efficacy of thrombolytic treatment, it would be of interest to know what the underlying mechanism is for the formation of the two thrombi subpopulations (RBC- or platelet-rich). For example, different shear rates may influence the composition of the thrombus<sup>34</sup> and this could be something to further interrogate. Also, changes in the vessel wall, which can be picked up by noninvasive imaging techniques such as CT (computed tomography) or MRI (magnetic resonance imaging), have been correlated to an increased amount of RBC in the thrombus<sup>35</sup>.

In summary, the authors are in the possession of a large treasure trove of samples. Other studies conducted on comparable specimens with similar methodologies did so with far fewer samples<sup>36,37</sup> or did not carry out such in-depth investigations<sup>30</sup>. The present study elegantly offers validation for textbook knowledge in a large cohort of patients, thereby laying the foundation for more in-depth investigations to improve treatment options for ischemic stroke patients.

**Acknowledgments and Funding** NJJ is funded by a European Union's Horizon 2020 research and innovation program under Marie Skłodowska-Curie grant agreement No. 766118. NSP is supported by the British Heart Foundation through the Chair award (CH0/03/003) to Steve P. Watson. We thank Christopher W. Smith for critical reading of the manuscript.

**Conflicts of Interest** The authors declare no competing financial interests.

## References

1. WHO. The atlas of heart disease and stroke, deaths from stroke. [https://www.who.int/cardiovascular\\_diseases/en/cvd\\_atlas\\_15\\_burden\\_stroke.pdf](https://www.who.int/cardiovascular_diseases/en/cvd_atlas_15_burden_stroke.pdf). Accessed 09.11.2020.

2. Stevens E. MC, Emmett E., Wolfe C., Wang Y. The burden of stroke in Europe: challenges for policy makers. <https://strokeeurope.eu/media/download/> Stroke Alliance for Europe 2017. Accessed 05.09.2020.
3. Mahmood SS, Levy D, Vasan RS, Wang TJ. The Framingham heart study and the epidemiology of cardiovascular disease: a historical perspective. *Lancet*.2014;383:999-1008.
4. Tadi P, Lui F. Acute stroke. BTI – StatPearls; Internet publication June 28, 2022.
5. Timmis A, Townsend N, Gale C, *et al*. European society of cardiology: cardiovascular disease statistics 2017. *Eur Heart J*. 2018; 39:508-579.
6. Vidale. S, Agostoni. EC. Organizing healthcare for optimal acute ischemic stroke treatment. *J Clin Neurol*. 2020; 16:183-190.
7. Prabhakaran S, Ruff I, Bernstein RA. Acute stroke intervention: a systematic review. *JAMA*. 2015; 313:1451-1462.
8. Vanacker P, Lambrou D, Eskandari A, *et al*. Improving the prediction of spontaneous and post-thrombolytic recanalization in ischemic stroke patients. *J Stroke Cerebrovasc Dis*. 2015; 24:1781-1786.
9. Staessens S, Denorme F, Francois O, *et al*. Structural analysis of ischemic stroke thrombi: histological indications for therapy resistance. *Haematologica*.2020;105:498-507.
10. Mengozzi L, Widimsky P. The potential value of histological analysis of thrombi extracted through mechanical thrombectomy during acute ischemic stroke treatment. *Anatol J Cardiol*. 2020; 254-259.
11. Fuchs TA, Brill A, Duerschmied D, Schatzberg D, *et al*. Extracellular DNA traps promote thrombosis. *Proc Natl Acad Sci USA*. 2010; 107:15880-15885.
12. Martinod K, Wagner DD. Thrombosis: tangled up in NETs. *Blood*. 2014; 123:2768-2776.
13. Brill A, Fuchs TA, Savchenko AS, *et al*. Neutrophil extracellular traps promote deep vein thrombosis in mice. *J Thromb Haemost*. 2012; 10:136-144.
14. Leshner M, Wang S, Lewis C, *et al*. PAD4 mediated histone hypercitrullination induces heterochromatin decondensation and chromatin unfolding to form neutrophil extracellular trap-like structures. *Frontiers Immunol*. 2012; 3.
15. Brinjikji W, Duffy S, Burrows A, *et al*. Correlation of imaging and histopathology of thrombi in acute ischemic stroke with etiology and outcome: a systematic review. *J Neurointerv Surg*. 2017; 9:529-534.
16. Masuda S, Nakazawa D, Shida H, *et al*. NETosis markers: Quest for specific, objective, and quantitative markers. *Clin Chim Acta*. 2016; 89-93.
17. Longstaff C, Varjú I, Sótonyi P, Szabó L, *et al*. Mechanical stability and fibrinolytic resistance of clots containing fibrin, DNA, and histones. *J Biol Chem*. 2013; 288:6946-56.
18. Ryan EA, Mockros L, Weisel JW, Lorand L. Structural origins of fibrin clot rheology. *Biophys J*.1999; 772813-77226.

19. Miszta A, Pelkmans L, Lindhout T, *et al.* Thrombin-dependent incorporation of von Willebrand factor into a fibrin network. *J Biol Chem.* 2014; 289:35979-35986.
20. Keuren JF, Baruch D, Legendre P, Denis CV, *et al.* von Willebrand factor C1C2 domain is involved in platelet adhesion to polymerized fibrin at high shear rate. *Blood.* 2004; 103:1741-1746.
21. Hada M, Kaminski M, Bockenstedt P, McDonagh J. Covalent crosslinking of von Willebrand factor to fibrin. *Blood.* 1986; 68:95-101.
22. Denorme F, Langhauser F, Desender L, *et al.* ADAMTS13-mediated thrombolysis of t-PA-resistant occlusions in ischemic stroke in mice. *Blood.* 2016; 127:2337-2345.
23. Martinez de Lizarrondo S, Gakuba C, Herbig BA, *et al.* Potent thrombolytic effect of N-acetylcysteine on arterial thrombi. *Circulation.* 2017; 136:646-660.
24. Prabhakaran S, Ruff I, Bernstein RA. Acute stroke intervention: a systematic review. *JAMA.* 2015; 313:1451-1462.
25. Ahmed MU, Kaneva V, Loyau S, *et al.* Pharmacological blockade of glycoprotein VI promotes thrombus disaggregation in the absence of thrombin. *Arterioscler Thromb Vasc Biol.* 2020; 40:2127-2142.
26. Douglas A, Fitzgerald S, Mereuta OM, *et al.* Platelet-rich emboli are associated with von Willebrand factor levels and have poorer revascularization outcomes. *J Neurointerv Surg.* 2020; 12:557.
27. Bankhead P, Loughrey MB, Fernández JA, *et al.* QuPath: open source software for digital pathology image analysis. *Sci Rep.* 2017; 7:16878.
28. Maekawa K, Shibata M, Nakajima H, *et al.* Erythrocyte-rich thrombus is associated with reduced number of maneuvers and procedure time in patients with acute ischemic stroke undergoing mechanical thrombectomy. *Cerebrovasc Dis Extra.* 2018; 8:39-49.
29. Riegger J, Byrne RA, Joner M, *et al.* Histopathological evaluation of thrombus in patients presenting with stent thrombosis. A multicenter European study: a report of the prevention of late stent thrombosis by an interdisciplinary global European effort consortium. *Eur Heart J.* 2015; 37:1538-1549.
30. Boeckh-Behrens T, Kleine JF, Zimmer C, *et al.* Thrombus histology suggests cardioembolic cause in cryptogenic stroke. *Stroke.* 2016; 47:1864-1871.
31. Silvain J, Collet JP, Nagaswami C, *et al.* Composition of coronary thrombus in acute myocardial infarction. *J Am Coll Cardiol.* 2011; 57:1359-1367.
32. Leica. Laser microdissection LMD. <https://www.leica-microsystems.com/solutions/life-science/laser-microdissection/>. 2020. Accessed 16.10.2020.
33. Muñoz R, Santamaría EA-O, Rubio I, *et al.* Mass spectrometry-based proteomic profiling of thrombotic material obtained by endovascular thrombectomy in patients with ischemic stroke. *Int J Mol Sci.* 2018; 19:498.

34. Mehta BP, Nogueira RG. Should clot composition affect choice of endovascular therapy? *Neurology*. 2012; 79:S63-67.
35. Liebeskind DS, Sanossian N, Yong WH, Starkman S, *et al*. CT and MRI early vessel signs reflect clot composition in acute stroke. *Stroke*. 2011; 42:1237-1243.
36. Marder VJ, Chute Dj, Starkman S, Abolian AM, *et al*. Analysis of thrombi retrieved from cerebral arteries of patients with acute ischemic stroke. *Stroke*. 2006; 37:2086-2093.
37. Niesten JM, van der Schaaf IC, van Dam L, *et al*. Histopathologic composition of cerebral thrombi of acute stroke patients is correlated with stroke subtype and thrombus attenuation. *Plos One*. 2014; 9:e88882.



# Chapter 3

## **Comparative analysis of pharmacological drugs interfering with collagen induced thrombus formation**

Natalie J. Jooss, Yvonne M.C. Henskens, Steve P. Watson, Richard W. Farndale, Meinrad P. Gawaz, Martine Jandrot-Perrus, Natalie S. Poulter and Johan W. M. Heemskerk

Contributions: NJJ designed and performed experiments,  
analyzed data, prepared figures and wrote the manuscript  
Under revision: Thrombosis and Haemostatis, 2022



**Abstract** In secondary cardiovascular disease prevention, treatments blocking platelet-derived secondary mediators pose a risk of bleeding. Pharmacological interference of the interaction of platelets with exposed vascular collagens is an attractive alternative, with clinical trials ongoing. Reported antagonists of the collagen receptors, glycoprotein VI (GPVI) and integrin  $\alpha 2\beta 1$ , include recombinant GPVI-Fc dimer Revacept, 9O12 mAb-based GPVI-blocking immunoreagent Glenzocimab, Syk tyrosine kinase inhibitor PRT-060318, and anti-  $\alpha 2\beta 1$  mAb 6F1. No direct comparison has been made of the antithrombotic potential of these drugs. Using a multiparameter whole blood microfluidic assay, we compared the intervention effects of Revacept, 9O12 Fab, PRT-060318 and 6F1 mAb for a range of vascular collagens and collagen-like substrates, with varying stimulation of GPVI and  $\alpha 2\beta 1$ . To inform on GPVI localization, we used fluorescent-labeled anti-GPVI nanobody 28. In this first comparison of four inhibitors of platelet-collagen interactions with antithrombotic potential we find that at arterial shear rate: *i*) the thrombus-inhibiting effect of Revacept was restricted to highly GPVI-activating surfaces; *ii*) 9O12 Fab consistently but partly inhibited thrombus size on all surfaces; *iii*) effects that were surpassed by Syk inhibition and *iv*) 6F1 mAb intervention was most suppressing on those collagens with limited effects of 9O12 Fab or Revacept. Our data hence reveal a distinct pharmacological profile for GPVI binding competition (Revacept), GPVI receptor blockage (9O12 Fab), GPVI signaling (PRT-060318) and  $\alpha 2\beta 1$ -directed intervention (6F1 mAb) on thrombus formation depending on the type of collagen substrate. This work thus points to additive antithrombotic action mechanisms of the investigated drugs.

### 3.1 Introduction

The interaction of platelets with the various collagens in the vessel wall, exposed upon injury, is critical for hemostasis, where a tightly regulated formation of thrombi limits blood loss. In atherothrombosis, in denuded or ruptured plaques, platelets interact with subendothelial collagens leading to the formation of thrombi that now cause vascular occlusion, leading to ischemia <sup>1</sup>. In both processes, collagens of various types become exposed to the circulating blood, most of which bind von Willebrand factor (VWF) and ligate, to a variable extent, the platelet receptors glycoprotein VI (GPVI) and integrin  $\alpha 2\beta 1$ . In arterial thrombus formation, GPVI as an ITAM-linked receptor for collagen and fibrin, is known to play a central signaling role <sup>2</sup>. In addition, platelet GPVI regulates the maintenance of vascular integrity upon thromboinflammation <sup>3,4</sup>. On the other hand, this receptor is considered to have an only minor role in normal hemostasis <sup>5</sup>. Thus, subjects lacking expression of GPVI on megakaryocytes and platelets present with a no more than minor bleeding phenotype <sup>6,7</sup>.

The platelet GPVI signaling pathway involves phosphorylation of the co-receptor FcR $\gamma$  chain via Src-family kinases, followed by phosphorylation and activation of Syk kinase, formation of the LAT signalosome, and culminating in activation of phospholipase C (PLC) $\gamma 2$  <sup>8</sup>. This pathway results in a continued rise in cytosolic Ca<sup>2+</sup> level, and a prolonged priming of platelets for additional stimulation <sup>9</sup>. Platelet responses evoked by collagens and GPVI include granular secretion, aggregate formation, platelet ballooning, and surface exposure of procoagulant phosphatidylserine <sup>10</sup>. However, recent reports indicate that not all GPVI ligands induce the same extent of platelet activation. For instance, several vascular collagens and fibrin evoke a relatively mild GPVI signal <sup>11,12</sup>, whereas fibrillar collagen type I and triple-

helical (GPO)<sub>n</sub>-containing collagen-related peptides (cross-linked collagen-related peptide CRP-XL and GFOGER-GPO) are potent GPVI agonists <sup>13</sup>.

Similarly, integrin  $\alpha 2\beta 1$  (glycoprotein Ia/IIa), of which the  $\alpha 2$  chain is selectively expressed on platelets and endothelial cells, act as a receptor for collagens. In 1985 a patient with bleeding symptoms (temporarily) lacking  $\alpha 2\beta 1$  was reported <sup>14</sup>, its role hemostasis was later confirmed in mice as well. <sup>15</sup> The integrin enhances collagen dependent platelet adhesion and supports the activation via GPVI as well as Gq $\alpha$ -coupled receptors <sup>16,17</sup>. Under flow conditions, a crosstalk mechanism of GPVI and integrin  $\alpha 2\beta 1$  was identified, which also included the GPIb-V-IX receptor for VWF <sup>18,19</sup>.

In the past decade, GPVI has been identified as a promising target for new antithrombotic drugs. Currently, two GPVI-directed inhibitors are being investigated in clinical trials, namely Revacept and Glenzocimab (ACT017). Revacept is a recombinant dimeric fusion protein of the extracellular domain of human GPVI and the Fc fragment. It competitively interferes with collagen-induced platelet aggregation <sup>20</sup> and in whole blood flow assays it suppresses thrombus formation on collagen containing atherosclerotic plaques on top of aspirin or ticagrelor <sup>21</sup>. A similar Revacept-like GPVI construct has antithrombotic activity in mouse in vivo <sup>22</sup>. The ISAR-PLASTER phase-2 trial, investigating the effect of Revacept infusion during percutaneous coronary intervention, points to a small but significant reduction in collagen-induced platelet aggregation in subjects of the treatment arm <sup>23</sup>. Revacept on top of standard antithrombotic treatment is well tolerated, but no difference is seen so far in the endpoints of early death and myocardial infarction <sup>24</sup>.

The agent Glenzocimab (ACT017) is a clinical-grade humanized antibody fragment derived from the blocking anti-human GPVI Fab 9O12. In a phase-1 study, Glenzocimab was found to be well tolerated without effect on bleeding time <sup>25</sup>. In an animal study, Glenzocimab did not impact the GPVI-

dependent inflammatory hemostasis <sup>26</sup>. Current clinical trials focus on monitoring its effects during ischemic stroke intervention and upon SARS-CoV-2 induced acute respiratory distress syndrome <sup>27</sup>. Several in vitro studies indicated that the 9O12 Fab, as well as its derived from ACT017, suppresses collagen- and fibrin induced platelet aggregation and thrombus formation under flow <sup>12,28,29</sup>. Herein, 9O12 Fab also interfered with GPVI-induced platelet activation responses, including surface expression of P-selectin and phosphatidylserine <sup>28</sup>. Another means to suppress collagen-induced platelet activation is by targeting the protein tyrosine kinase downstream of GPVI, *e.g.*, with utilizing the Syk-kinase inhibitor PRT-060318 <sup>11</sup>. In the past, blocking of integrin  $\alpha 2\beta 1$  with mAb 6F1 has been proposed as a possible antithrombotic strategy too, <sup>30</sup> but so far, the antibody has not been evaluated in (pre)clinical trials.

Surprisingly the thrombus-inhibiting potential of Revacept, 9O12 Fab (to proxy Glenzocimab), PRT-060318 and 6F1 mAb have not directly been compared. For the present paper, we used a previously validated multiparameter microfluidic assay of whole blood thrombus formation at high shear rate <sup>31</sup>, to determine how the drugs affect platelet adhesion, activation and aggregation under flow using a broad panel of vascular-derived collagens and collagen-like peptides, ranging from low to high GPVI and  $\alpha 2\beta 1$  reactivity. We thereby aimed to characterize the relative inhibitory profile and potency provide of these four drugs targeting platelet-collagen interactions.

## **3.2 Materials and Methods**

### **Materials**

Collagen-related triple-helical peptides were obtained as C-terminal amides, as described <sup>32,33</sup>: cross-linked Collagen-Related Peptide, GCO(GPO)<sub>10</sub>GCO-NH<sub>2</sub>, (CRP-XL); GPC(GPO)<sub>3</sub>GFOGER(GPO)<sub>3</sub>GPC-NH<sub>2</sub> (GFOGER-GPO); collagen type III derived VWF-binding peptide, GPC(GPP)<sub>5</sub>GPRGQO

GVMGFO(GPP)<sub>5</sub>GPC-NH<sub>2</sub> (VWF-BP) (CambCol, Cambridge, UK). Fibrillar collagen type I Horm was from Nycomed (Hoofddorp, The Netherlands); human collagen-I (C7774) and human collagen-IV (C7521) were from (Sigma-Aldrich (Zwijndrecht, The Netherlands); human collagen-III (1230-01S) was supplied by Southern Biotechnology (Birmingham, AL, USA) and D-Phe-Pro-Arg chloromethyl ketone (PPACK) was from Merck Millipore (Amsterdam, The Netherlands). Blocking anti-GPVI 9O12 Fab was supplied by Dr. M. Jandrot-Perrus (INSERM, University Paris Cité, Paris, France). Revacept was supplied by Dr. M.P. Gawaz (Tübingen, Germany). The batch was checked for inhibiting CRP-XL-induced platelet aggregation. The blocking mAb 6F1 against integrin  $\alpha 2\beta 1$  was kindly provided by Dr. B.S. Coller (New York, USA). PRT-060318 was from BioConnect (Huissen, the Netherlands). Used for fluorescent staining were AlexaFluor(AF) 647 labeled anti-human CD62P mAb (304918, Biologend, London, United Kingdom); FITC-labeled anti-fibrinogen antibody (F0111, Dako, Amstelveen, The Netherlands); AF568 labeled annexin A5 (A13202, ThermoFisher, Eindhoven, The Netherlands). Other materials were from sources described before<sup>34</sup>. The non-blocking anti-GPVI nanobody 28 (Nb28) was expressed and characterized, as described elsewhere<sup>35</sup>. AF488 labeling of the nanobody was according to the manufacturer's instructions (ThermoFisher)<sup>44</sup>.

### **Preparation of blood**

Blood was obtained from healthy volunteers by antecubital venepuncture. Subjects had not received anti-platelet medication for at least two weeks and gave full informed consent according to the declaration of Helsinki. Studies were approved by the local Medical Ethics Committee. Blood collection was into 3.2% trisodium citrate (Vacuette tubes, Greiner Bio-One, Alphen a/d Rijn, The Netherlands). All donors had platelet counts within the reference range, measured with a Sysmex XN-9000 analyzer (Sysmex, Cho-ku, Kobe, Japan)

<sup>34</sup>.

## Microfluidics thrombus formation

Selected collagen-like peptides and collagens were microspotted on glass coverslips, as detailed elsewhere<sup>36</sup>. Coding of the six microspots (M1-6) is depicted in **Table 1**. In brief, washed coverslips were coated with 3 different microspots, in which the most active microspot was always located downstream, thereby preventing cross-activation between microspots. Coated coverslips were incubated overnight and blocked with HEPES buffer pH 7.45 containing 1% BSA, before mounting into the flow chamber.

**Table 1 – Overview of microspots used (M1-6) and relevant platelet receptors in high-shear thrombus formation.** Information on relative increase in strength of roles of GPIb-V-IX, GPVI and integrin  $\alpha 2\beta 1$  (o, +, ++, +++), see references<sup>11,13,37</sup>. Also listed are analyzed parameters (P1-8) from brightfield and fluorescence microscopic images, as well as scaling factors in heatmaps. \*, Plasma-derived VWF binding to collagen.

		Platelet receptors		
<i>Microspot</i>		GPVI	$\alpha 2\beta 1$	GPIb
<i>M1</i>	Collagen-H (VWF*)	++	++	+
<i>M2</i>	GFOGER-GPO + VWF-BP	+++	+	+
<i>M3</i>	CRP-XL + VWF-BP	+++	o	+
<i>M4</i>	Collagen-I (VWF*)	+	+	+
<i>M5</i>	Collagen-IV (VWF*)	n.d.	n.d.	+
<i>M6</i>	Collagen-III (VWF*)	+	+	+
<i>Parameter</i>		range	scaled	
<i>Brightfield</i>				
<i>P1</i>	Platelet deposition (% SAC)	0 - 79	0 - 10	
<i>P2</i>	Platelet aggregate coverage (% SAC)	0 - 16	0 - 10	
<i>P3</i>	Thrombus morphological score	0 - 4	0 - 10	
<i>P4</i>	Thrombus multilayer score	0 - 2	0 - 10	
<i>P5</i>	Thrombus contraction score	0 - 3	0 - 10	
<i>Fluorescence images</i>				
<i>P6</i>	P-selectin expression (AF647 $\alpha$ -CD62P mAb, % SAC)	0 - 65	0 - 10	
<i>P7</i>	Integrin $\alpha$ Ib $\beta$ 3 activation (FITC $\alpha$ -fibrinogen Ab, % SAC)	0 - 21	0 - 10	
<i>P8</i>	PS exposure (AF568 annexin A5, % SAC)	0 - 25	0 - 10	

N.d., not determined.

Whole blood flow perfusion assays were performed according to standard procedures, as described <sup>11,31</sup>. In brief, 500  $\mu$ l samples of citrated whole blood were supplemented with PPACK (40  $\mu$ M, f.c.), recalcified (3.75 mM MgCl<sub>2</sub> and 7.5 mM CaCl<sub>2</sub>), and then perfused through the microspot-containing flow chamber for 3.5 minutes at wall shear rate of 1000/s. Where indicated, blood samples were preincubated with relevant vehicle or inhibitor for 10 minutes <sup>11</sup>. After 3.5 minutes of blood flow, tricolor staining was started by post-perfusion of labels in HEPES buffer pH 7.45 containing 2 mM CaCl<sub>2</sub> and 1 U/ml heparin, during which two brightfield microscopic images were taken per microspot <sup>31</sup>. After labeling for two minutes and rinsing, three 3-color fluorescence images were captured. The following labels were used: AF647 anti-CD62P mAb for CD62P expression, FITC anti-fibrinogen antibody for integrin  $\alpha$ IIb $\beta$ 3 activation, and AF568 annexin A5 for phosphatidylserine exposure.

### **Microscopy and image analysis**

Brightfield and fluorescence images were taken with an EVOS-FL microscope (Life Technologies, Bleiswijk, The Netherlands), equipped with Cy5, RFP and GFP LEDs, an Olympus UPLSAPO 60x oil-immersion objective, and a sensitive 1360 $\times$ 1024 pixel CCD camera. Standardized image analysis was performed using semi-automated scripts operated in Fiji (ImageJ). Parameters obtained from brightfield (P1-5) and from fluorescence (P6-8) images, were as explained in **Table 1**.

### **Data handling and statistics**

Statistical analysis was performed with GraphPad Prism 8 (San Diego, CA, USA). Heatmaps were generated with the program R V.3.5.2 (R-graph-gallery.com). For heatmap representation, parameter values were univariate normalized at a scale of 0-10 <sup>31</sup>. Thrombus values of flow runs (vehicle, inhibitor) from the same blood donor were averaged to obtain one parameter set per microspot and donor. Mean values of control and inhibitor runs were

then compared per blood sample, using paired Student t-test, as previously described <sup>11</sup>. Statistical significance was set at P-values below 0.05.

### **3.3 Results**

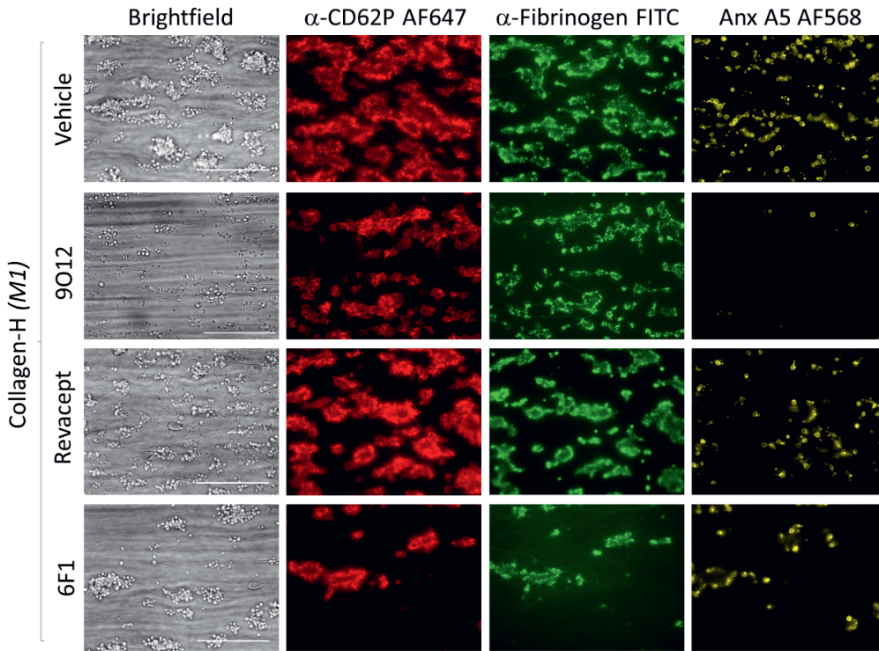
#### **Differential effects of antagonists on whole blood thrombus formation with fibrillar collagens**

To quantitatively compare the antithrombotic potential of clinically promising inhibitors of platelet receptor-collagen interactions, we performed a set of high-shear (1000/s) experiments, in which whole blood was flowed over microspots of different collagens or collagen-like surfaces. Blood samples from the same donor were pre-treated with one of the antagonists of interest, *i.e.*, GPVI-blocking 9O12 Fab (50 µg/ml), the GPVI-Fc fusion protein Revacept (50 µg/ml), Syk inhibitor PRT-060318 (20 µM) or integrin  $\alpha 2\beta 1$ -blocking mAb 6F1 (20 µg/ml). The antagonist concentrations were chosen, as to block near maximally GPVI- or  $\alpha 2\beta 1$ -dependent platelet adhesion to the reference collagen-H or to plaque material <sup>11,21</sup>.

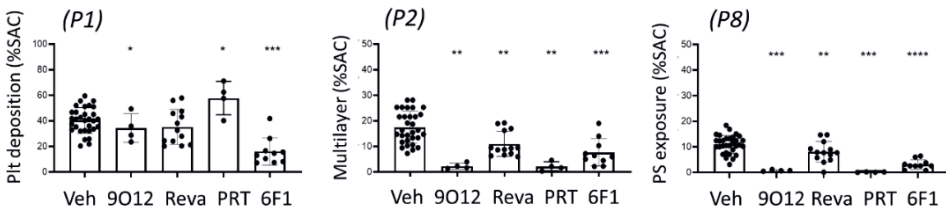
Considering that the equine-derived, fibrillar collagen-H is used as a standard platelet agonist in the diagnostic and research laboratories, we first evaluated antagonist effects on thrombus formation parameters for microspots of collagen-H (M1). Microscopic image recording was performed of brightfield images and, after post-staining with AF647  $\alpha$ -CD62P mAb, FITC  $\alpha$ -fibrinogen antibody and AF568 annexin A5, of triple fluorescent images <sup>31</sup>. Quantitative and qualitative image analysis provided information on eight parameters: platelet deposition (P1), thrombus phenotype (P2-5) and platelet activation (P6-8), such as indicated in **Table 1**.



**A**



**B**



**C**

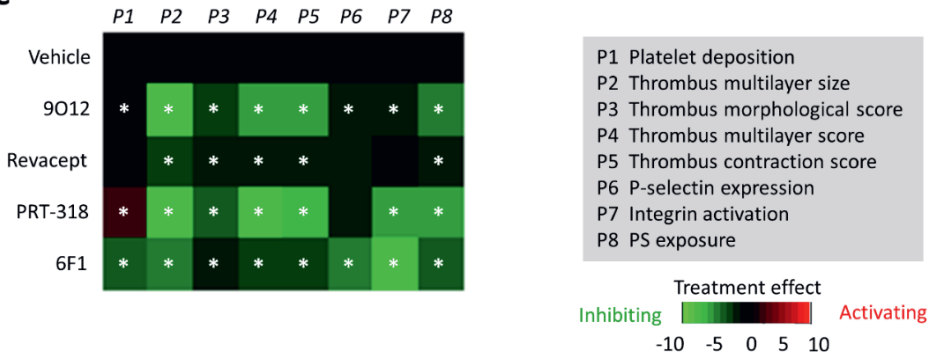


**Figure 1 (previous page) – Effects of collagen-interfering antagonists on thrombus formation with standard collagen-H.** Whole blood was perfused at 1000/s for 3.5 minutes over surface of collagen-H (microspot M1); pre-treatment was with vehicle or with indicated inhibitory agents, i.e. GPVI-blocking 9O12 Fab (50 µg/ml), GPVI-FC fusion protein Revacept (50 µg/ml), Syk kinase PRT-060318 (PRT, 20 µM), or integrin  $\alpha 2\beta 1$ -blocking 6F1 mAb (20 µg/ml), at previously optimized concentrations. Post-staining was performed according to protocol with AF647  $\alpha$ -CD62P mAb (for P-selectin expression), FITC  $\alpha$ -fibrinogen Ab (for  $\alpha$ IIb $\beta$ 3 activation) and AF568 annexin A5 (for phosphatidylserine exposure). (A) Representative brightfield and fluorescence microscopic images at end point. Scale bars = 50 µm. (B) Quantification of surface area covered by: all platelets (P1), platelets in multilayers (P2), and platelets with phosphatidylserine exposure (P8). Data are means  $\pm$  SD (n=5-7); \*p <0.05, \*\*p <0.01, \*\*\*p <0.001 with paired t-test. (C) Subtraction heatmap of parameter values univariately scaled over all surfaces, indicating treatment effects on collagen-H. Green color indicates decrease and red color increase of the respective parameter due to treatment. Significance (p <0.05) indicated by \*. For other raw data see Supplementary Figure 1B, for scaling factors see Table 1.

Using untreated control blood samples, perfusion over collagen-H led to the formation of large thrombi of aggregated platelets, staining highly positively for P-selectin expression, integrin  $\alpha$ IIb $\beta$ 3 activation and phosphatidylserine exposure, the latter as a proxy measurement of GPVI activity<sup>7</sup>. Treatment of the blood with 9O12 Fab (**Figure 1A**) or PRT-060318 (**Supplementary Figure 1A**) resulted in major reductions in aggregate size, accompanied by a strongly decreased staining for activation markers, including phosphatidylserine exposure. Blood treatment with Revacept resulted in less clear effects, while with 6F1 mAb present only few large aggregates were formed (**Figure 1A**). Image quantification of the three most distinct output markers - platelet deposition (P1), thrombus multilayer size (P2) and phosphatidylserine exposure (P8) showed that 9O12 Fab and 6F1 mAb significantly suppressed P1, while all four inhibitors caused reductions in P2 and P8 (**Figure 1B**). Complete raw data of P1-8 are given in **Supplementary Figure 1**. The subtraction heatmap of intervention effects for all eight

parameters (univariately scaled 0-10) indicated consistent and significant reductions by 9O12 Fab, PRT-060318 and 6F1 mAb. Revacept, although less effective, it still significantly reduced 5 out of 8 parameters (**Figure 1C**). Overall, these data indicate that the drugs intervening at the receptors GPVI or  $\alpha 2\beta 1$  or in downstream signaling cause a quantitatively different pattern of inhibition of platelet aggregation and thrombus formation on the highly thrombogenic, standard collagen-H.

### **Antagonist effects on whole blood thrombus formation on collagen-like peptides**

Given that collagen-based peptides also support thrombus formation, we investigated the drug effects on such collagen-like peptides with high (GPO) triplet content and hence high GPVI dependency, i.e., the triple helical peptides GFOGER-GPO (microspot M2) and CRP-XL (M3)<sup>13,37</sup>. The GFOGER motif ensured platelet adhesion via integrin  $\alpha 2\beta 1$  (**Table 1**). Both peptides were microspotted together with VWF-binding peptide (VWF-BP), which captures plasma-derived VWF and thus allowed GPIIb-dependent platelet adhesion under flow. For both microspots M2 and M3, 9O12 Fab and Revacept greatly affected platelet deposition, aggregate formation, and platelet activation (including the high phosphatidylserine exposure, pointing to high GPVI activity) (**Figure 2A,B**). Integrin  $\alpha 2\beta 1$  blockage with 6F1 mAb reduced platelet deposition only on M2.

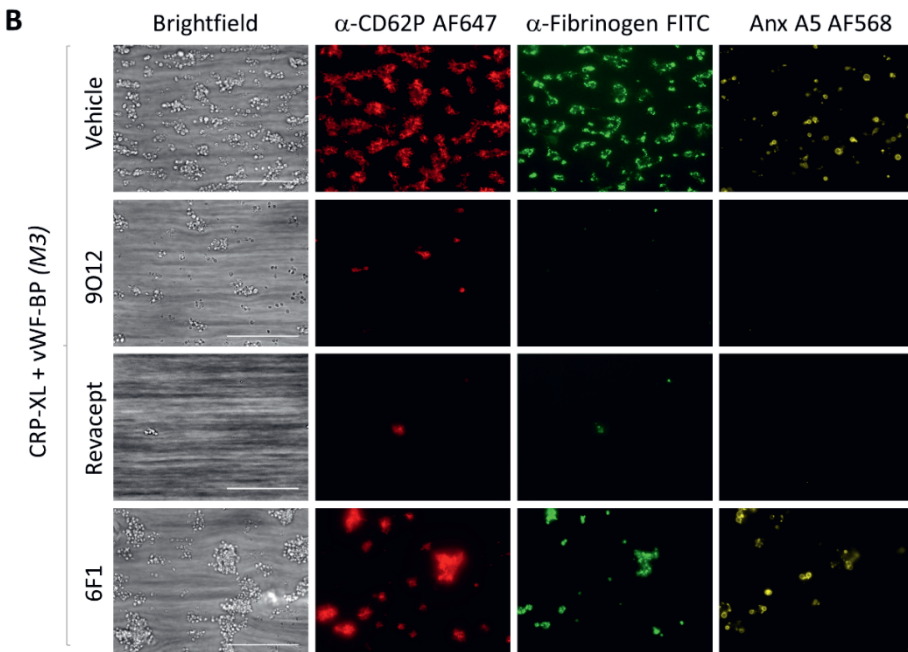
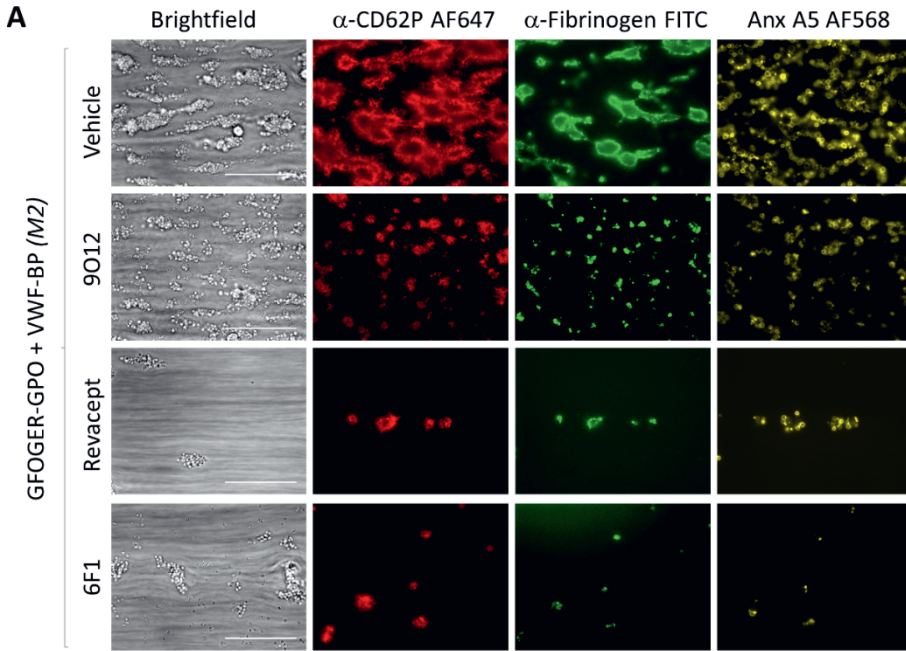
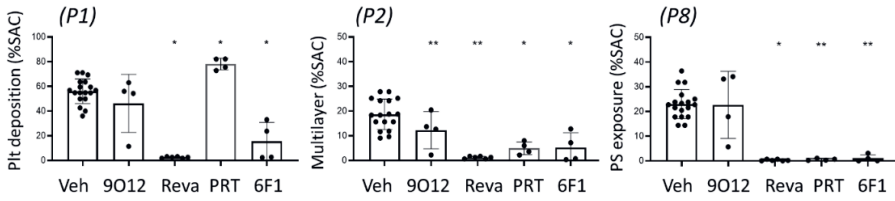


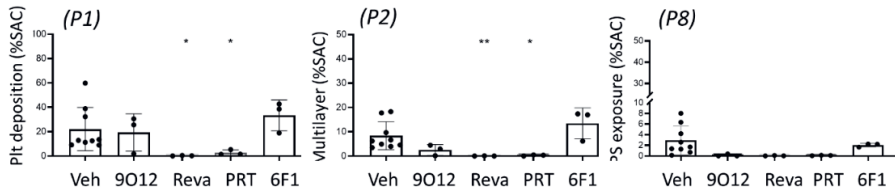
**Figure 2 (previous page) – Effects of collagen-interfering antagonists on thrombus formation with GPO-rich, high GPVI-activating peptides.** Whole blood was perfused at 1000/s for 3.5 minutes over surfaces with collagen-like peptides: GFOGER-GPO + VWF-BP (microspot M2) or CRP-XL + VWF-BP (M3). Pre-treatment was with vehicle medium or inhibitory agents, 9O12 Fab, Revacept, PRT-060318 (PRT) or 6F1 mAb (see Figure 1). Post-staining was performed with AF647  $\alpha$ -CD62P mAb (for P-selectin expression), FITC  $\alpha$ -fibrinogen Ab (for integrin  $\alpha$ IIb $\beta$ 3 activation) and AF568 annexin A5 (for phosphatidylserine exposure). Representative brightfield and fluorescence microscopic images at end stage for M2 (A) and M3 (B). Scale bars represent 50  $\mu$ m, n = 3-4.

Quantitative comparison of the parameters P1, P2 and P8 pointed to more profound effects of Revacept and PRT-060318 than of 9O12 Fab for microspot M3 (**Figure 3A,B**). Interestingly, 9O12 Fab was without effect on adhesion and activation parameters for the  $\alpha$ 2 $\beta$ 1-adhesive surface M2, suggesting a compensating role of the integrin in platelet adhesion but not aggregation. As expected, the 6F1 mAb suppressed the various parameters only on the GFOGER-containing,  $\alpha$ 2 $\beta$ 1-adhesive surface of M2. All GPVI-directed drugs (Revacept, 9O12 Fab, PRT-050318) suppressed the formation of platelet aggregates on M2 and M3 (**Figure 3, Supplementary Figure 2A**). Quantitation of all eight parameters indicated that Revacept and PRT-060318 most strongly reduced the formation of contracted multilayers of thrombi (**Supplementary Figure 2B**). The subtraction heatmap generated for all scaled parameters pointed to the following intervention effects (**Figure 3C**): *i*) a moderate and partly significant reduction of 9O12 Fab on some parameters for M2-3; *ii*) a strong inhibitory pattern of Revacept for M2 and M3 (6 and 5 parameters, respectively); *iii*) an overall inhibition effect of PRT-060318 resembling that of Revacept, but with a slightly increased platelet activation (P6-7) for M2; *iv*) and a selective suppression by 6F1 mAb of the majority of parameters for M2 only. In summary, on GPO-rich collagen-like peptides were the GPVI construct Revacept and the Syk kinase inhibitor PRT-060318 most effective.

**A** GFOGER-GPO + VWF-BP (M2)



**B** CRP-XL + VWF-BP (M3)



**C**

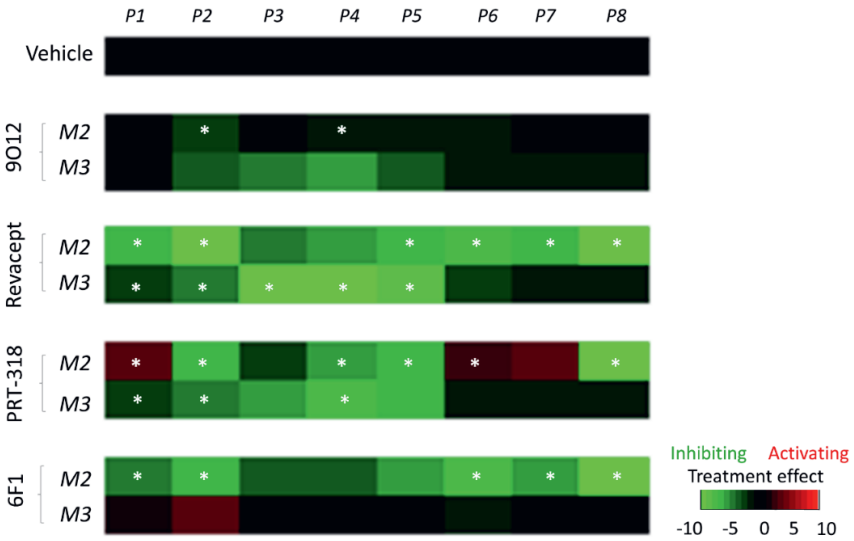


**Figure 3 (previous page) – Quantitative effects of collagen-interfering antagonists on thrombus formation with high GPVI-activating peptides.** Experiments performed as in Figure 2. Quantitation of thrombi formed on GFOGER-GPO + VWF-BP (A) and CRP-XL + VWF-BP (B). Data are given of surface area covered by all platelets (P1), platelets in multilayers (P2), and platelets with phosphatidylserine exposure (P3). Data are means  $\pm$  SD (n=3-4); \*p <0.05, \*\*p <0.01, \*\*\*p <0.001. For additional images and raw data, see Supplementary Figure 1. (C) Subtraction heatmap of scaled parameters versus vehicle control condition for P1-8. Color code represents decrease (green) or increase (red) in comparison to vehicle. Means  $\pm$  SD (n=3-4), \*p <0.05 (t-test).

### **Antagonist effects on whole blood thrombus formation on vascular collagens**

Early studies have provided evidence that human, vascular-type collagens (collagen-I, -III, -IV), exposed upon vascular injury, support flow-dependent platelet adhesion<sup>38-40</sup>. To examine how the antagonists of GPVI and  $\alpha 2\beta 1$  affected thrombus formation at such collagens, we microspotted the fibrillar collagen types I and III, and the non-fibrillar network-forming collagen-IV. All collagens also contained binding sites for plasma VWF<sup>38,40-42</sup>.

Blood perfusion over human collagen-I only moderately supported platelet adhesion (**Supplementary Figure 3**). Likewise, blood perfusion over collagen-IV (M5) led to the formation of small-sized thrombi. Representative images demonstrated that the adhered platelets still responded by P-selectin expression and integrin  $\alpha \text{IIb}\beta 3$  activation, although phosphatidylserine exposure was minimal, pointing to a limited extent of GPVI activation (**Figure 4A**). Using collagen-III (M6), somewhat larger thrombi were formed, containing higher platelet activation profiles (**Figure 4B**).

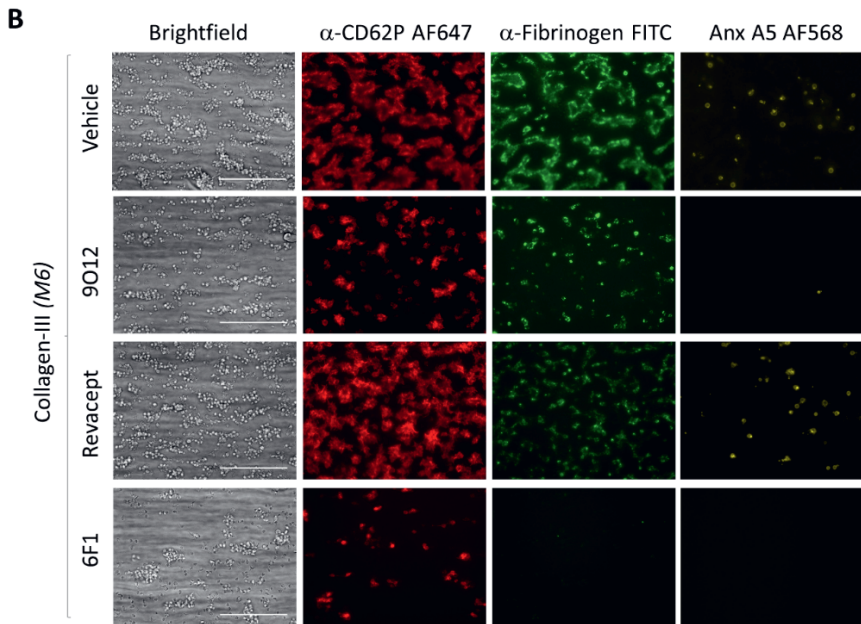
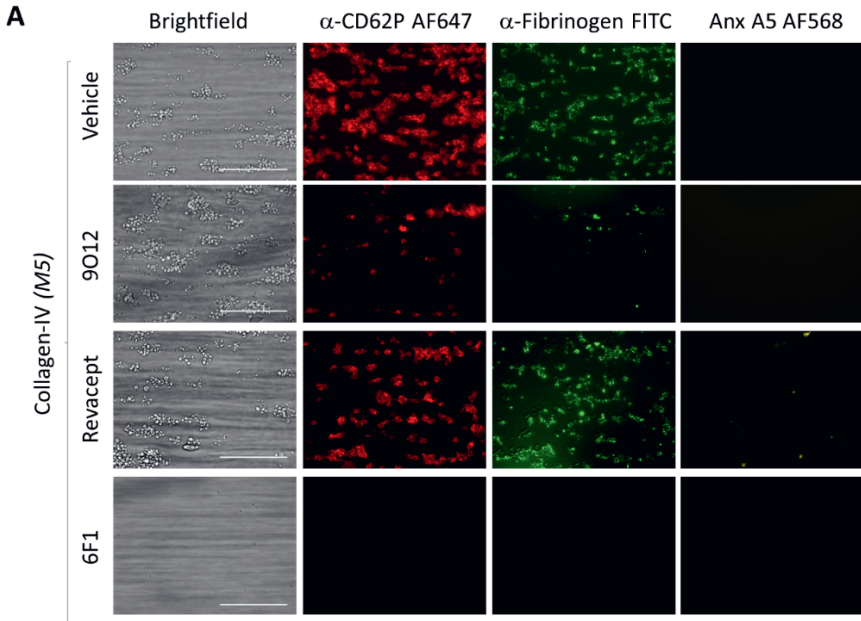
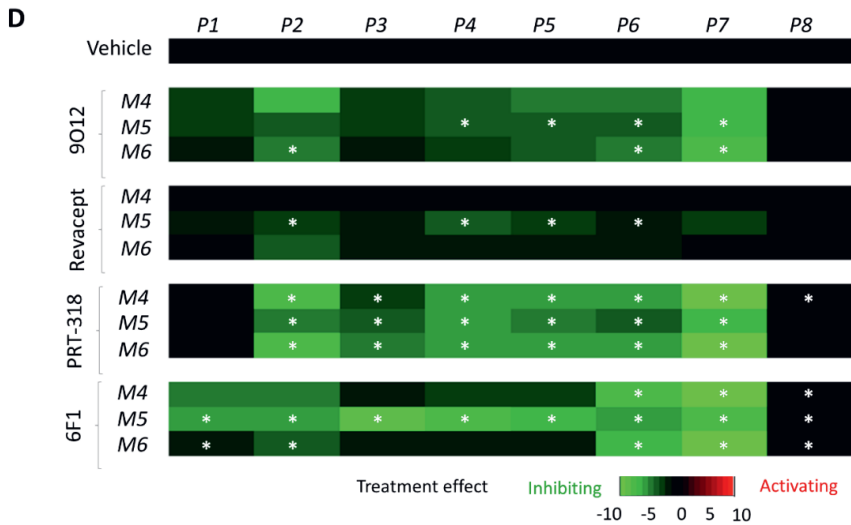
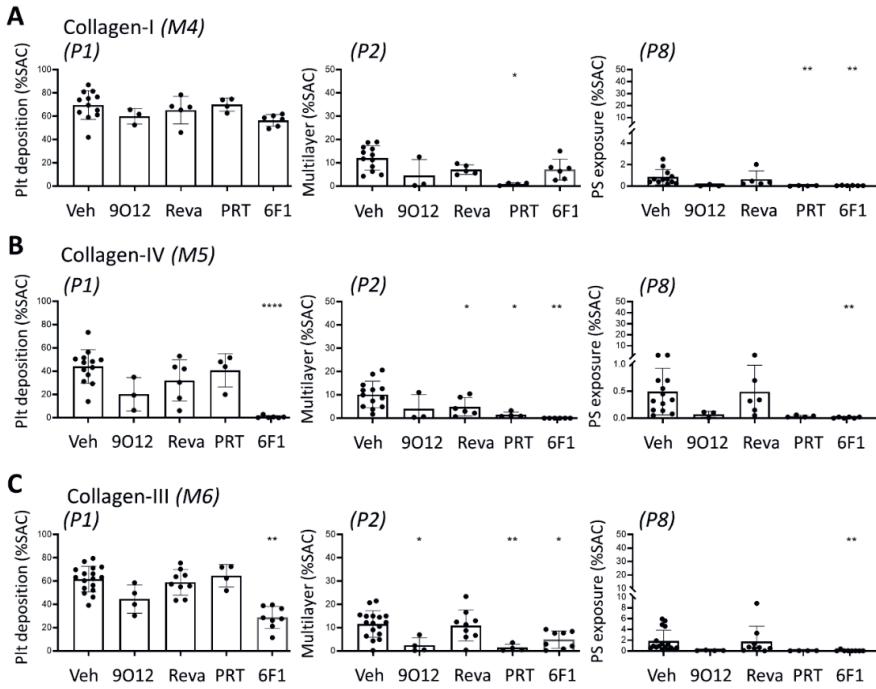




**Figure 4 (previous page) – Effects of interfering antagonists on thrombus formation with vascular-derived collagens.** Whole blood was perfused at 1000/s for 3.5 minutes over surfaces of the vascular-derived collagen preparations: collagen-I (M4), collagen-IV (M5) and collagen-III (M6). Pre-treatment was with vehicle or with inhibitory agents, 9O12 Fab, Revacept, PRT-060318 or 6F1 mAb (see Fig. 1). Multicolor post-staining was performed for P-selectin expression, integrin  $\alpha\text{IIb}\beta\text{3}$  activation and phosphatidylserine exposure. Shown are representative brightfield and fluorescence images at end stage for M5 (A) and M6 (B). Scale bars represent 50  $\mu\text{m}$ , n = 3-9. Complementary images for M4 are shown in Supplementary Figure 3.

Quantitative analysis indicated that on collagen-I and collagen-IV (M4-5), platelet deposition (P1) was only partially affected by each of the four interventions, while the thrombus characteristics (P2) and the already low phosphatidylserine exposure (P8) tended to be lowered by 9O12 Fab, Revacept, PRT-060318 and 6F1 mAb (**Figure 5A,B**). Collagen-IV (M5) was most susceptible towards  $\alpha\text{2}\beta\text{1}$  inhibition with 6F1 mAb, which essentially abolished platelet adhesion and subsequent parameters. Noteworthy, only Revacept marginally reduced phosphatidylserine exposure on M5. Regarding the slightly more active surface collagen-III (M6), a similar pattern of inhibition was observed, in which 9O12 Fab, PRT-060318 and 6F1 mAb were more effective inhibitors for platelet aggregation (P2) than Revacept (**Figure 5C**).



3

**Figure 5 (previous page) – Quantitative antagonist effects on thrombus formation with vascular-derived collagens.** Pre-treated whole blood was perfused over collagen-I (M4), collagen-IV (M5) and collagen-III (M6), as for Figure 4. End-stage images were analyzed for parameters P1-8. Shown are for M4 (A), M5 (B) and M6 (C), quantified values of surface area covered by all platelets (P1), platelets in multilayers (P2), and platelets with phosphatidylserine exposure (P8). Data are means  $\pm$  SD (n=3-9), \*p <0.05, \*\*p <0.01, \*\*\*p <0.001 (paired t-test). Values of other parameters are given in Supplementary Figure 5. (D) Subtraction heatmap of scaled parameters versus vehicle control condition for P1-8. Color code represents decrease (green) or increase (red) in comparison to vehicle. Means  $\pm$  SD (n=3-9), \*p <0.05 (t-test).

On all three surfaces M4-6, inhibition of Syk with PRT-060318 completely abolished the limited platelet aggregation (**Supplementary Figure 4**), thereby showing a similar inhibition pattern as 9O12 Fab, although with stronger effect size. This was also apparent from analysis of the additional parameter values (**Supplementary Figure 5**). Subtraction heatmap presentation of the eight scaled parameters indicated that, for the three vascular-derived collagens, PRT-060318 and 6F1 mAb were most effective in thrombus suppression, followed by 9O12 Fab and Revacept (**Figure 5D**). Still, on collagen-IV (M5), 9O12 Fab and Revacept significantly decreased 4 out of 8 parameters, in particular the thrombus characteristics. On the other hand, PRT-060318 and 6F1 mAb decreased 7 and 8 parameters, respectively. Taken together, these data point to a most effective suppression of thrombus formation on vascular-derived collagens by inhibition of Syk or  $\alpha 2\beta 1$ , surpassing the effect of blockage of the GPVI-collagen interaction.

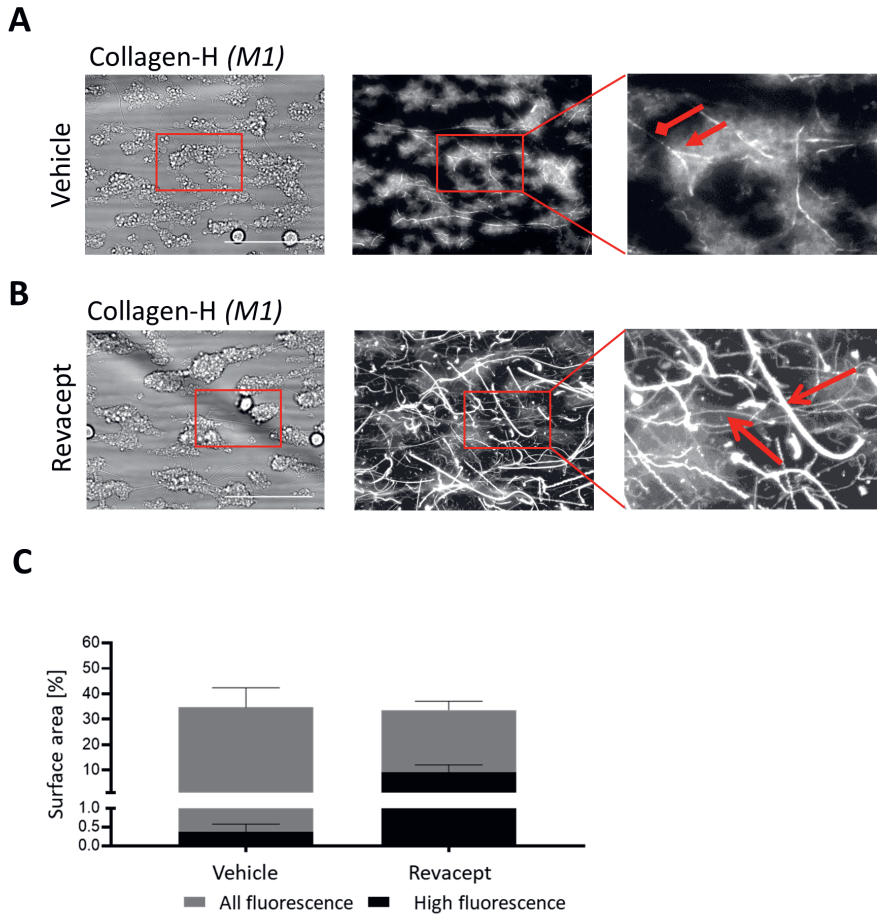


**Figure 6 – Establishing of platelet GPVI Revacept distribution profiles on platelets and standard collagen.** Whole blood was preincubated for 10 minutes with vehicle or 50  $\mu\text{g/ml}$  Revacept and perfused over collagen-H at 1000/s in the presence of non-inhibitory GPVI-binding Nb28 AF488 (100 nM). Shown are representative brightfield and fluorescence microscopic images with enlargements. Scale bars = 50  $\mu\text{m}$ . Data are from 4 donors. (A) For control condition, closed headed arrow indicates labeled GPVI clusters along collagen-H fibers; diamond headed arrow indicates absence of labeling where fibers, but no platelets are present. (B) With Revacept present, labeled Nb28 stains Revacept bound to collagen-H fibers (open headed arrows), regardless of the localization of platelet aggregates. (C) Quantification of overall Nb28 AF488 labeling (indicative of GPVI presence) and high labeling (indicative of clustered GPVI or Revacept).

## Visualization of collagen bound GPVI

The clustering of GPVI along collagen-H fibers has been considered as a mechanism to steer GPVI signaling in platelets <sup>43</sup>. To find out whether the incomplete inhibitory effects of Revacept with collagen-H could be explained by reversible binding to the fibers, we used a newly AF488-labeled anti-GPVI nanobody 28 (Nb28 AF488), which binds to GPVI with high affinity, but does not interfere with GPVI-induced platelet activation <sup>35</sup>. This labeled nanobody is suitable for the imaging of GPVI on adhered platelets <sup>44</sup>. After whole blood perfusion, platelets that adhered to collagen-H showed a high Nb28 AF488 signal. The fluorescence was strongly concentrated at contact sites of the platelets with collagen (**Figure 6A**), hence pointing towards clustering of GPVI receptor molecules along the collagen fibers. In the presence of Revacept, however, the Nb28 AF488 fluorescence was mostly localized at the collagen fibers, regardless of the local presence of platelets, thus indicating that the GPVI-Fc dimer Revacept effectively bound to the collagen fibers (**Figure 6B,C**). Given that with Revacept present still residual thrombi with phosphatidylserine-positive platelets were formed (**Figure 1**), this suggests that either the Revacept binding was not saturated or that it was partly replaced by platelet GPVI.

## 3.4 Discussion

This study provides a first in vitro quantitative comparison of four pharmacological antagonists, used in the laboratory or in clinical studies, that target platelet-collagen interactions in flowed human whole blood. For the study, we used a range of collagens and collagen-like peptides as substrates with a different platelet-activating potential, as apparent from the thrombus sizes and platelet activation markers. By collecting and analyzing brightfield and tricolor fluorescence microscopic images from microspots in a standardized way, we were able to provide a high-throughput, multi-parameter

quantification of the thrombus-forming process; this included parameters of platelet deposition, thrombus size and contraction and platelet P-selectin expression, integrin  $\alpha\text{IIb}\beta\text{3}$  activation and phosphatidylserine exposure<sup>31</sup>. The last marker of platelet procoagulant activity provided an accepted measure of the GPVI-induced signaling strength<sup>7,37</sup>.

Overall our data reveal that in flowed whole blood: *i)* the thrombus-inhibiting effect of Revacept was predominant for highly GPVI-activating collagen-like peptides and collagens; *ii)* the anti-GPVI 9O12 Fab caused a consistent partial inhibition of platelet activation and thrombus size extending to all collagen-like surfaces; *iii)* the Syk inhibitor PRT-060318 provided the most powerful antithrombotic effects exceeding that of GPVI blockage or GPVI competition, regardless of the collagen type; and *iv)* the 6F1 mAb intervention was most effective on those collagens (collagen-H,-IV, GFOGER-GPO) where 9O12 Fab was less effective. Regarding the human collagens-I, -III and -IV, at the concentrations applied, 9O12 Fab was acting better than Revacept on most parameters. These results are consistent with the infrequent presence of GPO triplets in such vascular-derived collagens<sup>40</sup>.

Jointly, these data point to a different, collagen-type dependent action mechanism of the drugs with 9O12 partly acting in comparison to the stronger Syk inhibition; while Revacept and  $\alpha\text{2}\beta\text{1}$  blockage act on distinct sets of collagens. Given that the damaged or plaque ruptured vessel wall causes exposure of multiple collagen types to the circulating platelets, this work thus suggests that the antithrombotic action mechanisms of the investigated drugs are at least in part additive. In other words, a combined intervention may result in a stronger antithrombotic potential, although a risk of bleeding cannot be excluded beforehand.

The 6F1 mAb was universally potent as an inhibitor of platelet adhesion to the vascular-derived collagens and subsequent thrombus build-

up, but it did not abrogate the activation parameters of residual adhered platelets. On the other hand, at the CRP-XL surface, lacking integrin  $\alpha 2\beta 1$ -adhesive elements, the addition of 6F1 mAb did not affect any of the thrombus-forming parameters. These findings are potentially relevant for the clinic, since 6F1 targets the platelet-specific  $\alpha 2$  subunit of  $\alpha 2\beta 1$ , and since the absence of  $\alpha 2$  in mice did not lead to a major bleeding tendency<sup>45</sup>. In addition, integrin  $\alpha 2\beta 1$  has been shown to be of importance in thrombus formation after vascular injury<sup>46</sup>. Of relevance, a pharmacological integrin  $\alpha 2$  inhibitor has been tested for treatment of patients with advanced malignancies<sup>52</sup>. On the other hand, concerning plaque rupture-induced atherothrombosis,  $\alpha 2\beta 1$ -directed intervention may not be a good treatment option, given the publications that platelet activation mediated by human atherosclerotic plaque material in vitro is more driven by GPVI than by integrin  $\alpha 2\beta 1$ <sup>30,47</sup>. Hence, while collagens are the primary platelet agonist in vascular injury as well as atherosclerotic plaque rupture, blockage of GPV seems to be the most effective scenario.

Our findings furthermore add to efforts undertaken to repurpose drugs, which are already approved for the treatment of different diseases, for antiplatelet medication. For example, it has been established a sub-therapeutic dose of Btk inhibitors can inhibit GPVI-mediated platelet activation, suggesting that these provide an alternative approach to treat plaque rupture-induced thrombosis<sup>48,49</sup>. This inhibition appears to be most obvious for the first generation of Btk inhibitors, possibly indicating off-target effects (e.g., on Syk)<sup>48</sup>. As in the present study strong effects were observed by the Syk inhibitor PRT-060318, this protein kinase may prove to be an even more interesting target. In this respect, the Syk inhibitor, Fostamatinib, is already being used as a therapeutic for chronic immune thrombocytopenia<sup>50</sup>. On the other hand, it should be mentioned that PF4-Cre mice, lacking Syk in

platelets and megakaryocytes, present with a bleeding phenotype, in contrast to GPVI-deficient mice <sup>5</sup>.

Under the present flow conditions, the dimeric GPVI-Fc construct Revacept had the most potent antithrombotic potential with GPO-rich collagen-like surfaces, extending to collagen-H and-IV. By utilizing a directly labeled nanobody against GPVI, we found a prominent binding of Revacept to the collagen fibers. In case of collagen-H, even though Revacept efficiently bound to the collagen fibers, therefore masking GPVI binding motifs, the lack of complete blockage of thrombus formation is explained by the engagement of integrin  $\alpha 2\beta 1$ . Several in vitro studies have shown that atherosclerotic plaque-mediated platelet activation is more driven by GPVI than by  $\alpha 2\beta 1$  <sup>47</sup>. Although the extent of GPO sites has not been determined for such plaque material, the high GPVI-dependency suggest that Revacept can act as an efficient antithrombotic drug in this setting. However, the nature of the collagen (or fibrin) GPVI substrates after pathological plaque rupture or erosion is still unknown.

Besides masking GPVI binding motifs, the 9O12 Fab fragment was capable of reducing, but in an incomplete way, platelet activation and thrombus formation on multiple collagen types in our microfluidics assay. There is preclinical evidence about the in vivo efficiency and safety of Glencocimab, the clinical grade humanized version of the 9O12 Fab, supporting its development as a therapeutic <sup>25,51</sup>. Currently there is still an unmet need for more targeted antithrombotic therapy, as most current approaches still pose a significant risk for bleeding. Taken together, this first-time comparison, showing differential anti-thrombus-formation action spectra of the investigated antagonists to intervene in collagen dependent platelet activation, poses the potential of an effective combined use of these agents.



**Author Contributions** NJJ designed and performed experiments, analyzed data, prepared figures and wrote the manuscript. MPG provided Revacept and revised the manuscript. MJP supplied 9O12 Fab and revised the manuscript. YH, NSP and SPW contributed by funding and supervision, and revised the manuscript. JWMH designed experiments, provided supervision and funding, and wrote the manuscript. All authors have read and approved the manuscript.

**Acknowledgments and Funding** This work has received funding from the European Union's Horizon 2020 research and innovation program under the Marie Skłodowska-Curie grant agreement No. 766118 (TAPAS). This project was supported by the Deutsche Forschungsgemeinschaft (DFG, German Research Foundation) – project number 374031971 – TRR 240 (MPG). N.J.J. is enrolled in a joint PhD program of the Universities of Maastricht and Birmingham (UK). We thank Dr. B. S. Coller, Rockefeller University, New York (USAS) for supplying 6F1 antibody.

**Conflicts of Interest** MPG is co-inventor of Revacept. For Nb28, NSP and SPW have a patent WO2022/136457. MJP is a founder and scientific adviser for Acticor Biotech. RWF is Chief Scientific Officer of CambCol Laboratories Ltd, Ely, UK.

### **3.5 References**

1. Van der Meijden PE, Heemskerk JW. Platelet biology and functions: new concepts and future clinical perspectives. *Nat Rev Cardiol.* 2019; 16:166-179.
2. Borst O, Gawaz M. Glycoprotein VI: novel target in antiplatelet medication. *Pharmacol Ther.* 2021; 217:107630.
3. Boulaftali Y, Mawhin MA, Jandrot-Perrus M, Ho-Tin-Noé B. Glycoprotein VI in securing vascular integrity in inflamed vessels. *Res Pract Thromb Haemost.* 2018; 2:228-239.
4. Rayes J, Watson SP, Nieswandt B. Functional significance of the platelet immune receptors GPVI and CLEC-2. *J Clin Invest.* 2019; 129:12-23.

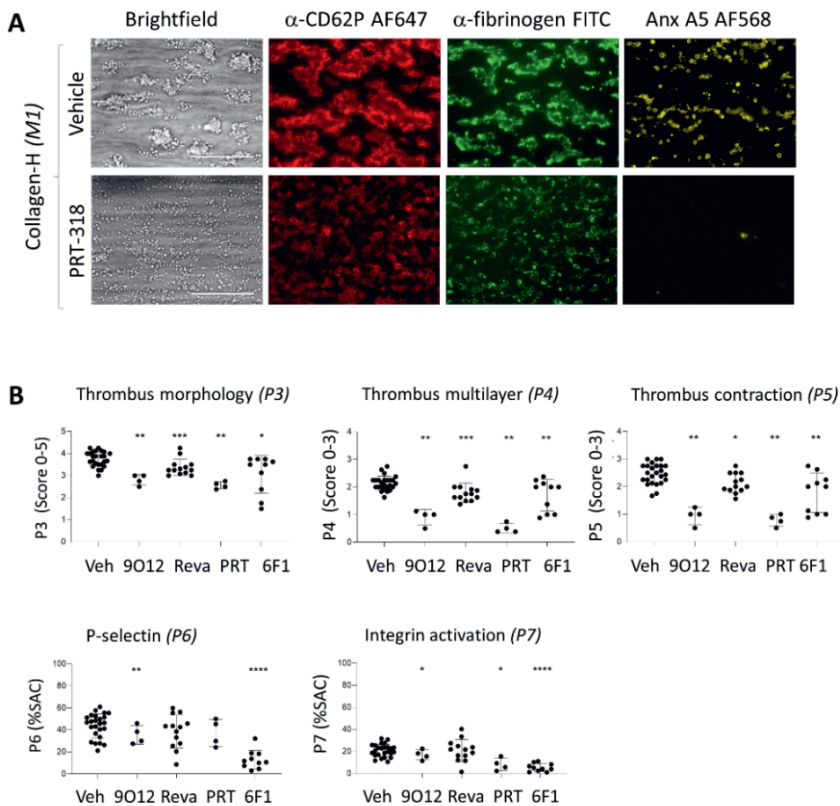
5. Baaten CC, Meacham S, de Witt SM, *et al.* A synthesis approach of mouse studies to identify genes and proteins in arterial thrombosis and bleeding. *Blood*. 2018; 132:e35-46
6. Jandrot-Perrus M, Hermans C, Mezzano D. Platelet glycoprotein VI genetic quantitative and qualitative defects. *Platelets*. 2019; 30:708-713.
7. Nagy M, Perrella G, Dalby A, *et al.* Flow studies on human GPVI-deficient blood under coagulating and non-coagulating conditions. *Blood Adv*. 2020; 4:2953-2961.
8. Nieswandt B, Watson SP. Platelet-collagen interaction: is GPVI the central receptor? *Blood*. 2003; 102:449-461.
9. Zou J, Wu J, Roest M, Heemkerk JWM. Long-term platelet priming after glycoprotein VI stimulation in comparison to protease-activating receptor (PAR) stimulation. *Plos One*. 2021; 16:e0247425.
10. Agbani EO, van den Bosch MT, Brown E, *et al.* Coordinated membrane ballooning and procoagulant spreading in human platelets. *Circulation*. 2015; 132:1414-1424.
11. Jooss NJ, De Simone I, Provenzale I, *et al.* Role of platelet glycoprotein VI and tyrosine kinase Syk in thrombus formation on collagen-like surfaces. *Int J Mol Sci*. 2019; 20:e2788
12. Perrella G, Huang J, Provenzale I, *et al.* Non-redundant roles of platelet glycoprotein VI and integrin  $\alpha$ IIb $\beta$ 3 in fibrin-mediated microthrombus formation. *Arterioscler Thromb Vasc Biol*. 2021; 41:e97-e111.
13. Pugh N, Simpson AM, Smethurst PA, *et al.* Synergism between platelet collagen receptors defined using receptor-specific collagen-mimetic peptide substrata in flowing blood. *Blood*. 2010; 115:5069-5079.
14. Nieuwenhuis HK, Akkerman JW, Houdijk WP, Sixma JJ. Human blood platelets showing no response to collagen fail to express surface glycoprotein Ia. *Nature*. 1985; 318:470-472.
15. Holtkötter O, Nieswandt B, Smyth N, *et al.* Integrin  $\alpha$ 2-deficient mice develop normally, are fertile, but display partially defective platelet interaction with collagen. *J Biol Chem*. 2002; 277:10789-10794.
16. Auger JM, Kuijpers MJ, Senis YA, Watson SP, Heemskerk JW. Adhesion of human and mouse platelets to collagen under shear: a unifying model. *FASEB J*. 2005; 19:825-827.
17. Sarratt KL, Chen HH, Zutter MM, *et al.* GPVI and  $\alpha$ 2 $\beta$ 1 play independent critical roles during platelet adhesion and aggregate formation to collagen under flow. *Blood*. 2005; 106:1268-1277.
18. Lecut C, Schoolmeester A, Kuijpers MJ, *et al.* Principal role of glycoprotein VI in  $\alpha$ 2 $\beta$ 1 and  $\alpha$ IIb $\beta$ 3 activation during collagen-induced thrombus formation. *Arterioscler Thromb Vasc Biol*. 2004; 24:1727-1733.

19. Pugh N, Maddox BD, Bihan D, *et al.* Differential integrin activity mediated by platelet collagen receptor engagement under flow conditions. *Thromb Haemost.* 2017; 117:1588-1600.
20. Jamashi J, Megens RT, Bionchini M, *et al.* Cross-linking GPVI-Fc by anti-Fc antibodies potentiates its inhibition of atherosclerotic plaque- and collagen-induced platelet activation. *JACC Basic Transl Sci.* 2016; 1:131-142.
21. Mojica Munoz AK, Jamasbi J, Uhland K, *et al.* Recombinant GPVI-Fc added to single or dual antiplatelet therapy in vitro prevents plaque-induced platelet thrombus formation. *Thromb Haemost.* 2017; 117:1651-1659.
22. Massberg S, Konrad I, Bültmann A, *et al.* Soluble glycoprotein VI dimer inhibits platelet adhesion and aggregation to the injured vessel wall in vivo. *FASEB J.* 2004; 18:397-399
23. Gröschel K, Uphaus T, Loftus I, *et al.* Revacept, an inhibitor of platelet adhesion in symptomatic carotid artery stenosis: design and rationale of a randomized phase II clinical trial. *TH Open.* 2020; 4:e393-e399.
24. Mayer K, Hein-Rothweiler R, Schüpke S, *et al.* Efficacy and safety of revacept, a novel lesion-directed competitive antagonist to platelet glycoprotein VI, in patients undergoing elective percutaneous coronary intervention for stable ischemic heart disease: the randomized, double-blind, placebo-controlled ISAR-PLASTER phase 2 trial. *JAMA Cardiol.* 2021; 6:753-761.
25. Voors-Pette C, Lebozec K, Dogterom P, *et al.* Safety and tolerability, pharmacokinetics, and pharmacodynamics of ACT017, an antiplatelet GPVI (glycoprotein VI) Fab. *Arterioscler Thromb Vasc Biol.* 2019; 39:956-964.
26. Jadoui S, Le Chapelain O, Ollivier V, *et al.* Glencocimab does not impact glycoprotein VI-dependent inflammatory haemostasis. *Haematologica.* 2021; 106:2000-2003.
27. <https://clinicaltrials.gov/ct2>. 2022.
28. Mangin PH, Onselaer MB, Receveur N, *et al.* Immobilized fibrinogen activates human platelets through glycoprotein VI. *Haematologica.* 2018; 103:898-907.
29. Alenazy FO, Harbi MH, Kavanagh DP, *et al.* GPVI inhibition by glencocimab synergistically inhibits atherosclerotic plaque-induced platelet activation when combined with conventional dual antiplatelet therapy. *Eur Heart J.* 2021; 42.
30. Penz S, Reininger AJ, Brandl R, *et al.* Human atheromatous plaques stimulate thrombus formation by activating platelet glycoprotein VI. *FASEB J.* 2005; 19:898-909.
31. Van Geffen JP, Brouns S, Batista J, *et al.* High-throughput elucidation of thrombus formation reveals sources of platelet function variability. *Haematologica.* 2019; 104:1256-1267.
32. Smethurst PA, Joutsu-Korhonen L, O'Connor MN, *et al.* Identification of the primary collagen-binding surface on human glycoprotein VI by site-directed mutagenesis and by a blocking phage antibody. *Blood.* 2004; 103:903-911.

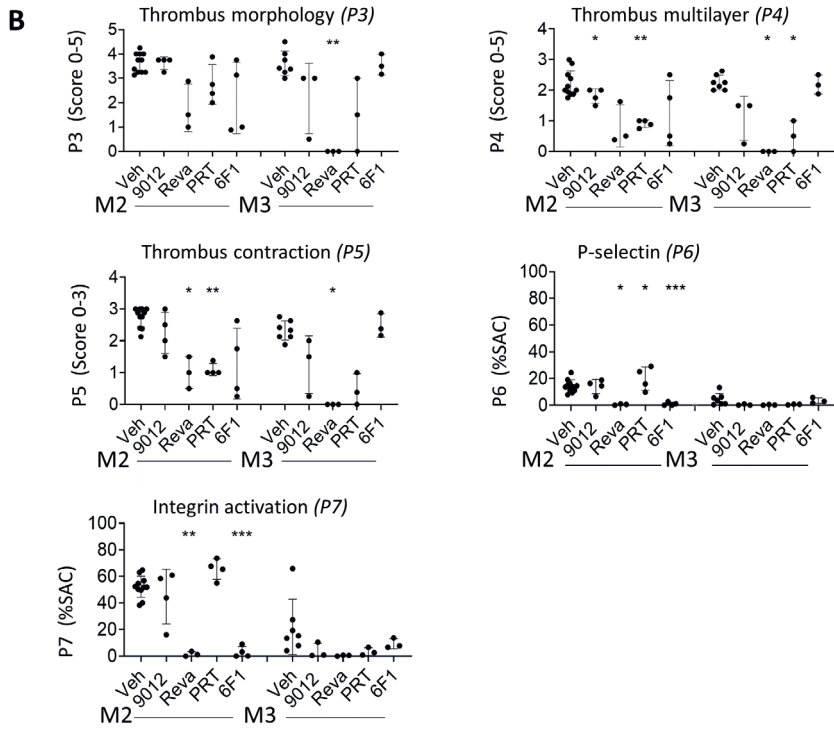
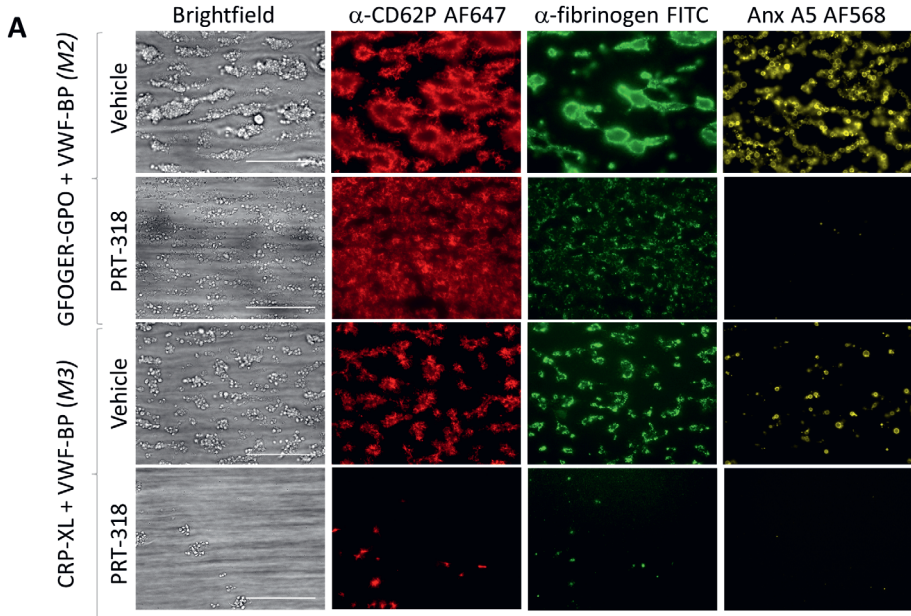
33. De Witt S, Swieringa F, Cosemans JM, Heemkerk JW. Thrombus formation on microspotted arrays of thrombogenic surfaces. *Nat Protocol Exchange*. 2014; 2014:3309.
34. Gilio K, Harper MT, Cosemans JM, *et al*. Functional divergence of platelet protein kinase C (PKC) isoforms in thrombus formation on collagen. *JBiolChem*.2010;285:23410-23419.
35. Slater A, Di Y, Clark JC, *et al*. Structural characterization of a novel GPVI-nanobody complex reveals a biologically active domain-swapped GPVI dimer. *Blood*. 2021; 137:3443-3453.
36. De Witt SM, Swieringa F, Cavill R, *et al*. Identification of platelet function defects by multi-parameter assessment of thrombus formation. *Nat Commun*. 2014; 5:4257.
37. Munnix IC, Gilio K, Siljander PR, *et al*. Collagen-mimetic peptides mediate flow-dependent thrombus formation by high- or low-affinity binding of integrin  $\alpha 2\beta 1$  and glycoprotein VI. *J Thromb Haemost*. 2008; 6:2132-2142.
38. Van Zanten GH, Saelman EU, Schut-Hese KM, *et al*. Platelet adhesion to collagen type IV under flow conditions. *Blood*. 1996; 88:3862-3871.
39. Morton LF, Peachey AR, Knight CG, Farndale RW, Barnes MJ. The platelet reactivity of synthetic peptides based on the collagen III fragment  $\alpha 1(\text{III})\text{CB4}$ : evidence for an integrin  $\alpha 2\beta 1$  recognition site involving residues 522-528 of the  $\alpha 1(\text{III})$  collagen chain. *J Biol Chem*. 1997; 272:11044-11048.
40. Farndale RW, Sixma JJ, Barnes MJ, de Groot PG. The role of collagen in thrombosis and haemostasis. *J Thromb Haemost*. 2004; 2:561-573.
41. Savage B, Almus-Jacobs F, Ruggeri ZM. Specific synergy of multiple substrate-receptor interactions in platelet thrombus formation under flow. *Cell*. 1998; 94:657-666.
42. Jung SM, Takemura Y, Imamura Y, *et al*. Collagen-type specificity of glycoprotein VI as a determinant of platelet adhesion. *Platelets*. 2008; 19:32-42.
43. Poulter NS, Pollitt AY, Owen DM, *et al*. Clustering of glycoprotein VI (GPVI) dimers upon adhesion to collagen as a mechanism to regulate GPVI signaling in platelets. *J Thromb Haemost*. 2017; 15:549-564.
44. Jooss NJ, Smith CW, Slater A, *et al*. Anti-GPVI nanobody blocks collagen- and atherosclerotic plaque-induced GPVI clustering, signaling and thrombus formation. *J Thromb Haemost*. 2022, in press.
45. Nieswandt B, Brakebusch C, Bergmeier W, *et al*. Glycoprotein VI but not  $\alpha 2\beta 1$  integrin is essential for platelet interaction with collagen. *EMBO J*. 2001; 20:2120-2130.
46. He L, Pappan LK, Grenache DG, *et al*. The contributions of the  $\alpha 2\beta 1$  integrin to vascular thrombosis in vivo. *Blood*. 2003; 102:3652-3657.

47. Schulz C, Penz S, Hoffmann C, *et al.* Platelet GPVI binds to collagenous structures in the core region of human atheromatous plaque and is critical for atheroprogession in vivo. *Basic Res Cardiol.* 2008; 103:356-367.
48. Busygina K, Jamasbi J, Seiler T, *et al.* Oral Bruton tyrosine kinase inhibitors selectively block atherosclerotic plaque-triggered thrombus formation in humans. *Blood.* 2018; 131:2605-2616.
49. Harbi MH, Smith CW, Nicolson PLR, Watson SP, Thomas MR. Novel antiplatelet strategies targeting GPVI, CLEC-2 and tyrosine kinases. *Platelets.* 2021; 32:29-41.
50. Hughes DM, Toste C, Nelson C, *et al.* Transitioning from thrombopoietin agonists to the novel Syk inhibitor fostamatinib: a multicenter, real-world case series. *J Adv Pract Oncol.* 2021; 12:508-517.
51. Renaud L, Lebozec K, Voors-Pette C, *et al.* Population pharmacokinetic/pharmacodynamic modeling of glenzocimab (ACT017), a glycoprotein VI inhibitor of collagen-induced platelet aggregation. *J Clin Pharmacol.* 2020; 60:1198-1208.
52. Mita M, Kelly KR, Mita A, *et al.* Phase I study of E7820, an oral inhibitor of integrin  $\alpha 2$  expression with antiangiogenic properties, in patients with advanced malignancies. *Clin Cancer Res.* 2011; 17:193-200.

### 3.6 Supplementary Figures

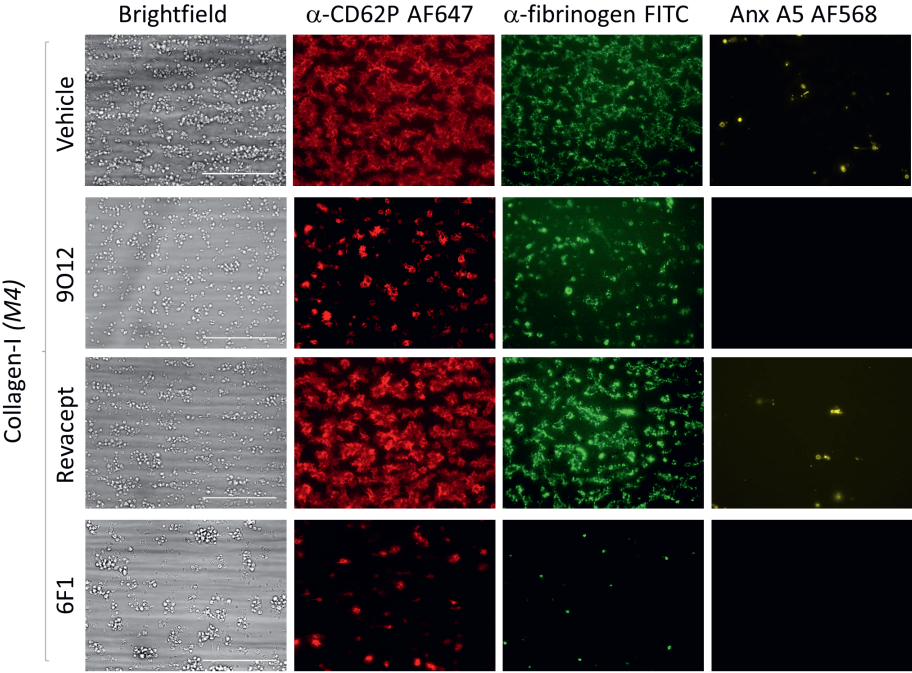


**Supplementary Figure 1 – Effects of collagen-interfering antagonists on thrombus formation with standard collagen-H.** Whole blood was perfused at 1000/s for 3.5 minutes over surface of collagen-H (microspot M1); pre-treatment was with vehicle or with indicated inhibitory agents, i.e. GPVI-blocking 9O12 Fab (50  $\mu$ g/ml), GPVI-FC fusion protein Revacept (50  $\mu$ g/ml), Syk kinase PRT-060318 (PRT, 20  $\mu$ M), or integrin  $\alpha$ 2 $\beta$ 1-blocking 6F1 mAb (20  $\mu$ g/ml), at previously optimized concentrations. Post-staining was performed according to protocol with AF647  $\alpha$ -CD62P mAb (for P-selectin expression), FITC  $\alpha$ -fibrinogen Ab (for  $\alpha$ IIb $\beta$ 3 activation) and AF568 annexin A5 (for phosphatidylserine exposure). (A) Representative brightfield and fluorescence microscopic images at end point in the presence and absence of PRT-060318. Scale bars represent 50  $\mu$ m. (B) Assessment of formed aggregates regarding their: overall size (P3), approximate height (P4) and density (P5) as well as quantification of surface area covered by: P-selectin expressing aggregates (P6) and fibrinogen bound  $\alpha$ IIb $\beta$ 3 (P7). Data are means  $\pm$  SD (n=5-7); \*p < 0.05, \*\*p < 0.01, \*\*\*p < 0.001 with paired t-tests.

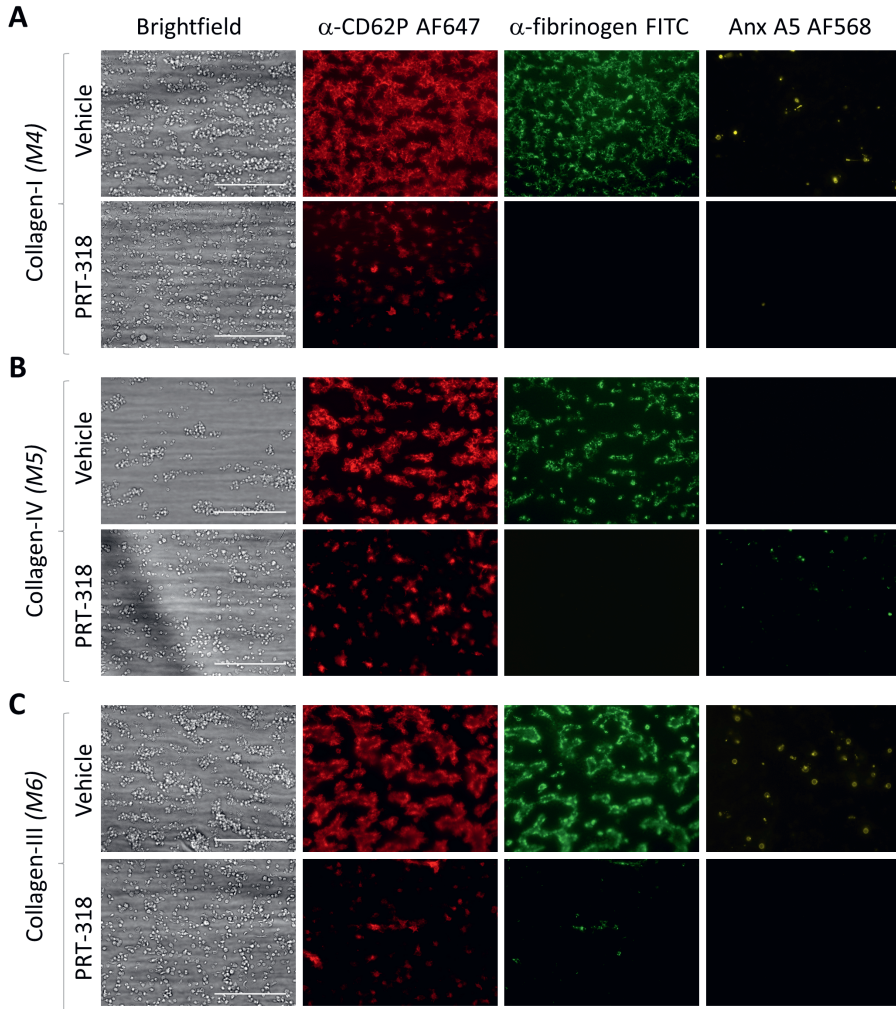


**Supplementary Figure 2 (previous page) – Effects of collagen-interfering antagonists on thrombus formation with GPO-rich, high GPVI-activating peptides.** Whole blood was perfused at 1000/s for 3.5 minutes over surfaces with collagen-like peptides: GFOGER-GPO + VWF-BP (microspot M2) or CRP-XL + VWF-BP (M3). Pre-treatment was with vehicle or inhibitory agents, 9O12 Fab, Revacept, PRT-060318 (PRT) or 6F1 mAb. Post-staining was performed with AF647  $\alpha$ -CD62P mAb (for P-selectin expression), FITC  $\alpha$ -fibrinogen Ab (for integrin  $\alpha$ IIb $\beta$ 3 activation) and AF568 annexin A5 (for phosphatidylserine exposure). (A) Representative brightfield and fluorescence microscopic images at end stage in the presence or absence of PRT-060318. Scale bars = 50  $\mu$ m. (B) Assessment of formed aggregates, between both substrates and all treatments, regarding their: overall size (P3), approximate height (P4) and density (P5) as well as quantification of surface area covered by: P-selectin expressing aggregates (P6) and fibrinogen bound  $\alpha$ IIb $\beta$ 3 (P7). Data are means  $\pm$  SD (n=3-4); \*p <0.05, \*\*p <0.01, \*\*\*p <0.001.



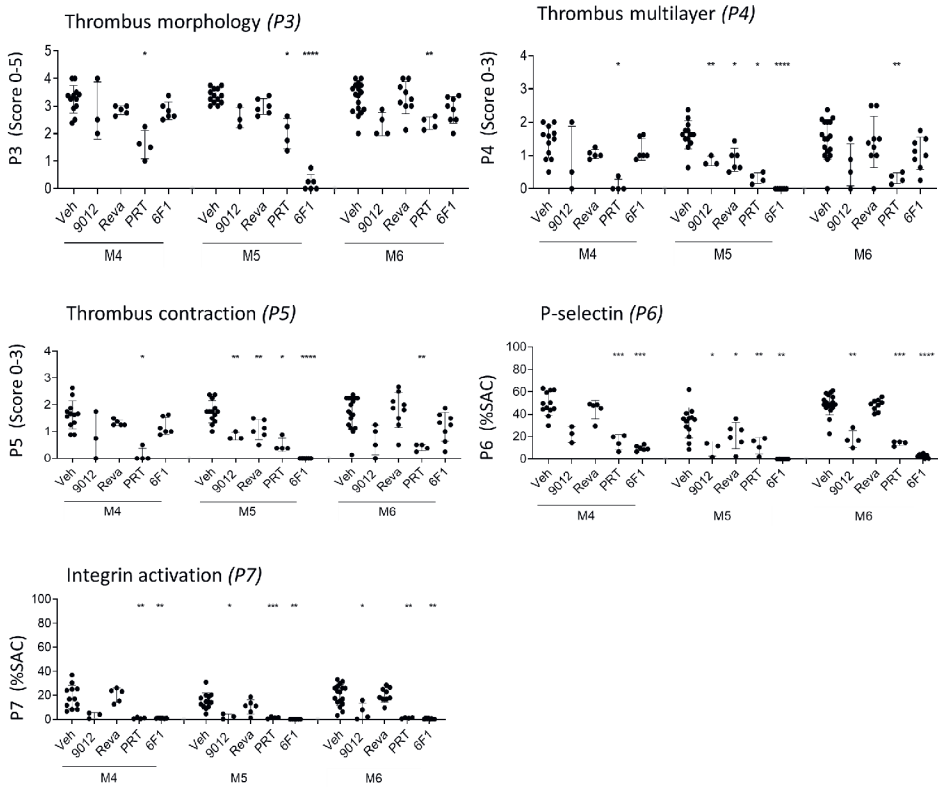


**Supplementary Figure 3 – Effects of interfering antagonists on thrombus formation with vascular-derived collagens.** Whole blood was perfused at 1000/s for 3.5 minutes over collagen-I (M4). Pre-treatment was with vehicle or with inhibitory agents, 9O12 Fab, Revacept, PRT-060318 or 6F1 mAb. Multicolor post-staining was performed for P-selectin expression, integrin  $\alpha$ IIb $\beta$ 3 activation and phosphatidylserine exposure. Shown are representative brightfield and fluorescence images at end stage. Scale bars = 50  $\mu$ m, n = 3-9.



**Supplementary Figure 4 – Effects of Syk-inhibition with PRT-060318 interfering on thrombus formation with vascular-derived collagens.** Whole blood was perfused at 1000/s for 3.5 minutes over surfaces of the vascular-derived collagen preparations: collagen-I (M4), collagen-IV (M5) and collagen-III (M6). Multicolor post-staining was performed for P-selectin expression, integrin  $\alpha\text{IIb}\beta\text{3}$  activation and phosphatidylserine exposure. Shown are representative brightfield and fluorescence images at end stage for M4 (A), M5 (B) and M6 (C). Scale bars represent 50  $\mu\text{m}$  n = 4.

3



**Supplementary Figure 5 – Quantitative antagonist effects on thrombus formation with vascular-derived collagens.** Pre-treated whole blood was perfused over collagen-I (M4), collagen-IV (M5) and collagen-III (M6). End-stage images were analyzed for parameters P1-8. Shown are assessment of formed aggregates, between all three substrates and all treatments, regarding their: overall size (P3), approximate height (P4) and density (P5) as well as quantification of surface area covered by: P-selectin expressing aggregates (P6) and fibrinogen bound  $\alpha$ IIb $\beta$ 3 (P7). Data are means  $\pm$  SD (n=3-9), \*p < 0.05, \*\*p < 0.01, \*\*\*p < 0.001, paired t-test.



# Chapter 4

## **Anti-GPVI nanobody blocks collagen- and atherosclerotic plaque-induced GPVI clustering, signaling and thrombus formation**

Natalie J. Jooss, Christopher W. Smith, Alexandre Slater, Samantha J. Montague, Ying Di, Christopher O'Shea, Mark R. Thomas, Yvonne M. C. Henskens, Johan W. M. Heemskerk, Steve P. Watson, and Natalie S. Poulter

Contributions: NJJ designed and performed experiments, analyzed data, prepared figures and wrote the manuscript  
Published: Journal of Thrombosis and Haemostasis, 2022, in press

**Abstract** The collagen receptor glycoprotein-VI (GPVI) is an attractive antiplatelet target due to its critical role in thrombosis but minor implication in hemostasis. To investigate GPVI receptor involvement in platelet activation by collagen-I and atherosclerotic plaque using novel blocking and non-blocking anti-GPVI nanobodies (Nbs). Nb effects on GPVI-mediated signaling and function were assessed by western blot and whole blood thrombus formation under flow. GPVI clustering was visualized in thrombi using fluorescently labeled Nb28. Under arterial shear, inhibitory Nb2 blocks thrombus formation and platelet activation on collagen and plaque, but only reduces adhesion on plaque. In contrast, adhesion on collagen, but not plaque, is decreased by blocking integrin  $\alpha 2\beta 1$ . Adhesion on plaque is maintained despite inhibition of integrins  $\alpha v\beta 3$ ,  $\alpha 5\beta 1$ ,  $\alpha 6\beta 1$  and  $\alpha IIb\beta 3$ . Only combined  $\alpha IIb\beta 3$  and  $\alpha 2\beta 1$  blockade inhibits adhesion and thrombus formation to the same extent as Nb2 alone. Nb2 prevents GPVI signaling, with loss of Syk, Lat and PLC $\gamma 2$  phosphorylation, especially to plaque stimulation. Non-blocking fluorescently labeled Nb28 reveals distinct GPVI distribution patterns on collagen and plaque, with GPVI clustering clearly apparent on collagen fibers and less frequent on plaque. Clustering on collagen fibers is lost in the presence of Nb2. This work emphasizes the critical difference in GPVI-mediated platelet activation by plaque and collagen; it highlights the importance of GPVI clustering for downstream signaling and thrombus formation. Labeled Nb28 is a novel tool for providing mechanistic insight into this process and the data suggest Nb2 warrants further investigation as a potential anti-thrombotic agent.

## 4.1 Introduction

Cardiovascular diseases (CVD) associated with thrombosis, including acute coronary syndromes and stroke, are among the world's leading causes of death, with 17.9 million deaths in 2019 <sup>1</sup>. Improved anti-thrombotic therapies with reduced bleeding side effects are required to increase survival, improve patients' quality of life, and ease the financial burden of CVD. Platelets are small highly reactive anucleate blood cells, known for their major contribution to hemostasis, but also play a central role in thrombotic events, as well as in a myriad of other (patho)physiological processes <sup>2</sup>.

Platelets become activated by extracellular matrix proteins exposed upon vessel damage, as well as by atherosclerotic plaque components uncovered by plaque rupture or erosion <sup>3</sup>. The formation and progression of atherosclerotic plaques is caused by an inflammatory process within the vessel wall, mediated by macrophage incorporation, vascular cell proliferation and lipid deposition. The lipid-rich necrotic core of an atherosclerotic plaque is sealed with a collagen-rich cap <sup>4</sup>. Rupture of the fibrous cap induces platelet activation. Weak platelet agonists present are, lysophosphatidic acid <sup>5</sup>, sphingosine-1-phosphate <sup>6</sup>, fibronectin and fibrin(ogen) <sup>3</sup>. However, plaque-mediated platelet activation has been shown to be predominantly induced by collagens <sup>7</sup>. Intriguingly, these collagens, mostly of types I and III <sup>3, 7-9</sup>, have been observed to mediate platelet activation via GPVI but not integrin  $\alpha 2\beta 1$ , in contrast to in vitro studies on immobilized collagens where both receptors play a role <sup>7, 8, 10, 11</sup>.

GPVI is a platelet and megakaryocyte-specific ~62 kDa immunoglobulin-like transmembrane receptor. It is expressed at the platelet surface in complex with the immunoreceptor tyrosine-based activation motif (ITAM)-containing Fc receptor  $\gamma$ -chain (FcR $\gamma$ ) <sup>12</sup> and is considered to be the main signaling receptor in platelets <sup>13, 14</sup>. Its primary ligand is collagen, but it

has been shown to act as a multi-ligand receptor, binding to substrates including fibrin, fibrinogen or laminin <sup>15</sup>. Upon ligand binding, the GPVI-FcRγ complex initiates intracellular signaling by phosphorylation of several downstream molecules, including Syk, LAT and PLCγ2, inducing Ca<sup>2+</sup> mobilization and resulting in platelet activation and thrombus formation <sup>16, 17</sup>. Signaling strength and duration is amplified by clustering of GPVI, induced by platelet attachment to collagen fibers <sup>18-21</sup>. The restricted expression of GPVI to platelets and megakaryocytes and its minor role in hemostasis <sup>16, 22, 23</sup> make GPVI a target for novel anti-atherothrombotic therapies <sup>24</sup>.

We have recently described a series of novel anti-GPVI nanobodies (Nbs), several of which are potent GPVI inhibitors <sup>25</sup>. Cameloid-derived Nbs contain only a single chain of the variable region of full-size antibodies, making them smaller than antibody F(ab) fragments (15 kDa versus 50 kDa), whilst maintaining high binding affinities and antigen specificity <sup>26</sup>. Nbs display several beneficial features, such as stability, tissue penetration and a low immunogenic impact, making them suitable for multiple applications including imaging <sup>27</sup> and as therapeutic agents <sup>28, 29</sup>.

In this study we have compared the activation potential of atherosclerotic plaque homogenate to fibrillar collagen type I. We used plaque homogenate as a physiological ligand to evaluate the effectiveness of the novel anti-GPVI Nb2 in inhibiting whole blood thrombus formation. In addition, we introduce a fluorescently labeled non-inhibitory anti-GPVI Nb (Nb28), allowing for the first-time investigation of GPVI localization and clustering in platelets forming thrombi under flow, and assess the effect of GPVI inhibitors on this. We show Nb2 is a potent inhibitor of collagen-induced platelet activation, which results in a strong reduction of GPVI downstream signaling and subsequent thrombus formation. Further, we propose that this inhibitory mechanism is mediated by

complete disruption of GPVI receptor clustering. These findings support the suitability of Nb2 as an anti-thrombotic agent, especially in atherothrombosis.

## **4.2 Materials and Methods**

### **Antibodies and reagents**

Nanobodies raised against the extracellular domain of GPVI were expressed as previously described<sup>25</sup>. Nb28 was labeled using AlexaFluor 647 NHS ester (ThermoFisher Scientific). Fibrillar collagen-I (Horm) was from Nycomed, P11 from TOCRIS, eptifibatide from GSK, JBS5 from Santa Cruz, GoH3 from Invitrogen and 6F1 mAb was a gift from Barry Coller (Rockefeller University).

### **Histology of human atherosclerotic plaque and generation of pooled homogenates**

10 patients undergoing carotid endarterectomy at the Queen Elizabeth Hospital in Birmingham gave informed consent (ethical approval: North West – Haydock Research Ethics Committee 20/NW/0001) and donated their extracted plaque material, which was snap frozen in liquid nitrogen and stored at -80°C. Before use, the samples were divided in half, one half was used for histological analysis and the other half was utilized to generate a pooled plaque homogenate.

Histological staining to assess plaque composition was conducted on OCT (Sakura) embedded, cryo-sectioned (6 µm) samples, co-stained for Ca<sup>2+</sup> and global collagen content with von Kossa (Merck) and van Gieson (Atom Scientific) respectively. Further sections were investigated for either lipid content with OilRedO (Sigma Aldrich) or with hematoxylin and eosin (Atom Scientific) for tissue orientation. All stains were used in accordance with the respective manufacturer's instructions, before being mounted (DPX, Merck) and imaged at 20x magnification with an Axio Slide scanner (Zeiss).



In order to generate plaque homogenate, frozen plaque samples were mechanically pulverized with a glass mortar and pestle in liquid nitrogen to generate a fine powder. This was pooled and dissolved in PBS, solubilized by sonification (5x10 seconds), and a short centrifugation step to remove debris. The supernatant was aliquoted and stored at -80°C. Protein concentration was determined using a standard Bradford protein assay and demonstrated to be 14 mg/ml. The plaque homogenate was tested at various concentrations between 0.5 mg/ml up to 5 mg/ml (in line with the literature <sup>10, 11</sup>) in whole blood microfluidics, and the lowest concentration that gave maximal thrombus formation and platelet activation was used, 500 µg/ml.

### **Platelet isolation**

Blood was collected into 4% sodium citrate, after informed consent, from drug-free healthy volunteers in accordance with the Declaration of Helsinki and ethical approval granted by University of Birmingham internal ethical review (ERN-11-0175). Washed platelets were isolated as previously described <sup>30</sup>. Briefly, acid citrate dextrose (ACD, 1:10 v/v) was added to blood then platelet-rich plasma (PRP) was obtained by centrifugation at 200 g for 20 minutes at room temperature (RT). Washed platelets were isolated by centrifugation of the PRP in the presence of 0.2 µg/ml prostacyclin (1000 g, 10 minutes, RT), then washed in modified Tyrode's buffer (129 mM NaCl, 0.34 mM Na<sub>2</sub>HPO<sub>4</sub>, 2.9 mM KCl, 12 mM NaHCO<sub>3</sub>, 20 mM HEPES, 5 mM glucose, 1 mM MgCl<sub>2</sub>; pH 7.3) supplemented with ACD, centrifuged again in the presence of 0.2 µg/ml prostacyclin (1000 g, 10 minutes, RT), then the platelet pellet was resuspended in modified Tyrode's-HEPES buffer and left to rest for 30 minutes before being used in experiments.

### **Platelet spreading**

Glass coverslips were coated with 10 µg/ml fibrillar collagen-I or 500 µg/ml plaque homogenate (overnight, 4°C) then blocked with 5 mg/ml BSA (1 hour,

room temperature). Platelets were preincubated with PBS or 500 nM Nb2, spread for 45 minutes (37°C), fixed, permeabilized and labeled with phalloidin-Alexa Fluor 488. Spreading analysis was as described in Pike *et al.*<sup>31</sup>.

### **Cytosolic Ca<sup>2+</sup> mobilization in live spread platelets**

Glass bottom dishes (MatTek Corp) were coated and blocked, as above. Washed platelets were loaded with 1 μM Oregon Green-488 BAPTA-1-AM (ThermoFisher Scientific) and spread for 45 minutes. Pre- and post-treatment videos were captured and platelet Ca<sup>2+</sup> mobilization analyzed as detailed in supporting information.

### **Western blotting**

Washed platelets preincubated with PBS, 500 nM Nb2 or Nb53, were stimulated with 10 μg/ml fibrillar collagen-I or 500 μg/ml pooled plaque homogenate under stirring conditions as previously described. Whole cell lysates were then probed for total phosphotyrosine (4G10, Millipore), PLCγ2-pY<sup>1217</sup> (Cell Signaling, 3871S), LAT-pY<sup>200</sup> (Abcam, ab68139), Syk-pY<sup>525/526</sup> (Cell Signaling, 2710S) and total Syk (4D10, Santa Cruz)<sup>30</sup>. Bands were visualized using autoradiography film, and Odyssey Fc System (LI-COR Biosciences) and quantified in Image studio lite v5.2.

### **Light transmission aggregometry**

Platelet aggregation was assessed using a light transmission aggregometer (Model 700, ChronoLog; 37°C, 1200 rpm), washed platelets (2x10<sup>8</sup>/ml) were stimulated with 10 μg/ml fibrillar collagen-I following vehicle, 500 nM Nb2, Nb53 or Nb28 preincubation.

### **Competition assays**

For flow cytometry, washed platelets were preincubated with 500 nM Nb2 or PBS, followed by addition of 100 nM Nb28 AF647 and immediate fixation (4% paraformaldehyde). 50,000 events acquired (BD Accuri C6 flow cytometer)

and plotted in FlowJo (BD). For ELISA, Nb28 and Nb21 binding to immobilized GPVI-Fc in the presence of Nb2 was assessed as previously described<sup>25</sup>.

### **GPVI shedding assay**

Washed platelets ( $2 \times 10^8/\text{ml}$ ) were recalcified with calcium chloride (1 mM) before treatment with 500 nM Nb2 or Nb53 for 2 hours, under static conditions at room temperature. Platelets were also stimulated with 5 mM N-ethylmaleimide (NEM), as a positive control for GPVI shedding. After treatment, platelets were incubated with PE-conjugated anti-GPVI antibody (HY101, BD Biosciences) for 30 minutes before dilution in PBS and GPVI surface expression (median fluorescence intensity; MFI) measured by flow cytometry (10,000 events acquired, BD Accuri C6 flow cytometer, plotted in FlowJo). Reduction in platelet GPVI MFI compared to resting controls represented GPVI shedding.

### **Whole blood microfluidics**

Citrated whole blood was preincubated with vehicle, 500 nM Nb, or 20  $\mu\text{g}/\text{ml}$  6F1, thrombin-inhibited (40  $\mu\text{M}$  PPACK) and recalcified (3.75 mM  $\text{MgCl}_2$  and 7.5 mM  $\text{CaCl}_2$ ) then perfused over plaque and collagen microspots in a Maastricht flow chamber at 1000/s, as described<sup>32</sup>. Platelets were labeled for activation markers: AF568 annexin A5 (for phosphatidylserine exposure, procoagulant platelets, ThermoFisher), AF647 anti-CD62P mAb (for CD62P expression,  $\alpha$ -granule secretion, BioLegend), and anti-fibrinogen FITC Ab (for fibrinogen binding, integrin  $\alpha\text{IIb}\beta_3$  activation, DAKO) and endpoint images obtained on an EVOS AMF4300 microscope (Life Technologies). Thrombus formation and platelet activation was quantified. See supporting information for full details of image capture and analysis.

## Visualization of GPVI clustering

Flow adhesion was performed as above, with GPVI visualized by addition of 100 nM Nb28 AF647 prior to flow.

## Statistical analysis

Data is shown as mean  $\pm$  standard deviation (SD). Statistical tests are indicated in figure legends and were performed in GraphPad Prism V7.

## 4.3 Results

### Atherosclerotic plaque homogenate activates platelets under static and flow conditions

Human atherosclerotic plaque has been previously described as a heterogeneous substrate, rich in collagen type I and III<sup>3, 7, 11</sup>. Histology on sections of the plaques used in this study highlighted their collagen rich nature but demonstrated differences in composition and structure of individual plaques (**Supplementary Figure 1**). Hence, we pooled 10 atherosclerotic plaques and assessed the platelet activatory potential of the pooled homogenate compared to standard fibrillary collagen-I in platelet activation assays. Plaque homogenate supported platelet spreading to a similar extent as fibrillar collagen-I (**Figure 1A**). Next, we investigated Ca<sup>2+</sup> mobilization, as it represents the latter stages of the GPVI signaling pathway. We performed live-cell fluorescence imaging of Ca<sup>2+</sup> mobilization in individual platelets on the two substrates using the Ca<sup>2+</sup> indicator dye Oregon Green 488 BAPTA-1 (**Supplementary Video 1**). No significant difference in percentage of Ca<sup>2+</sup> spiking platelets, or spike duration or amplitude between plaque and collagen-I was observed (**Figure 1B**).

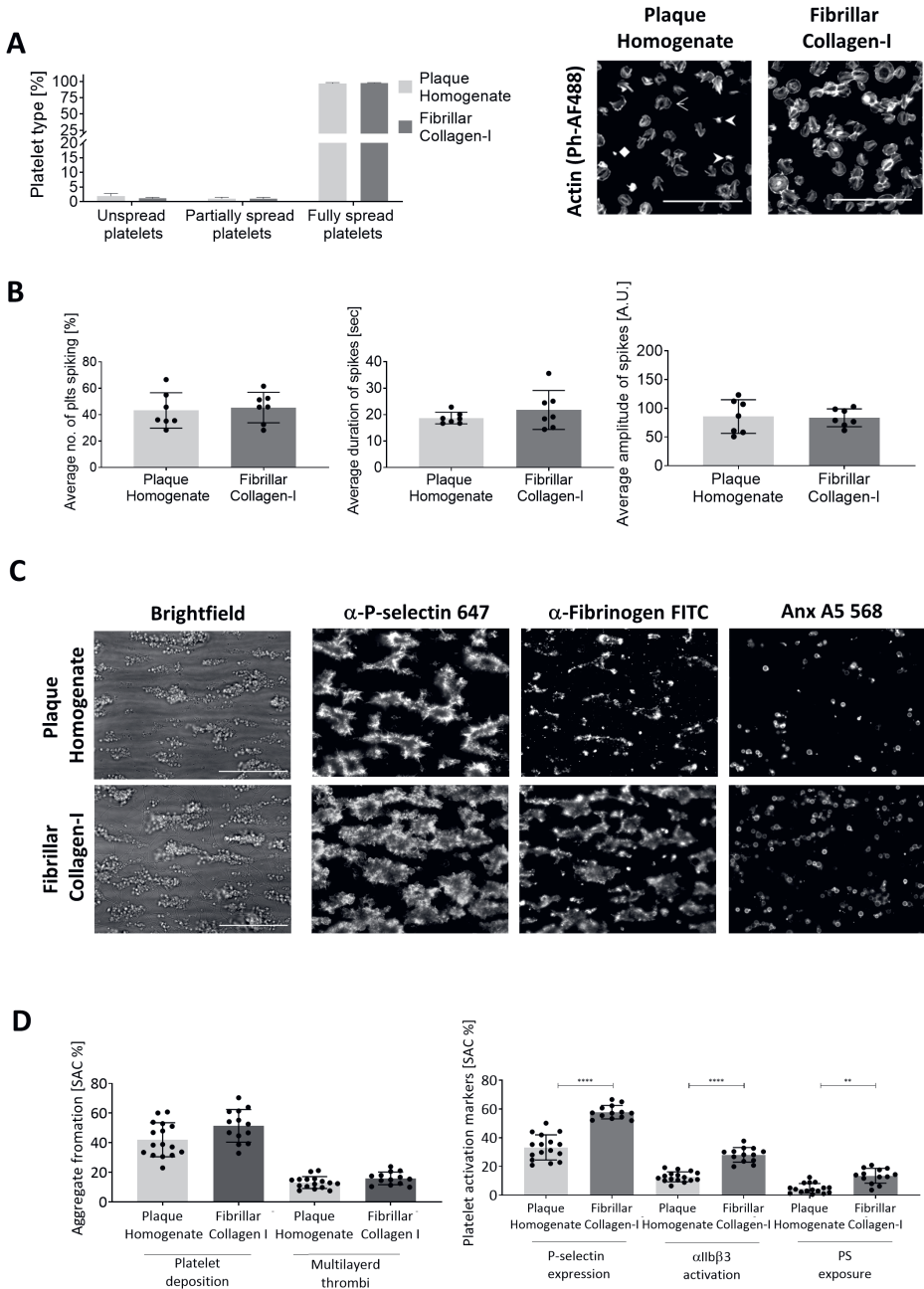


**Figure 1 (previous page) – Plaque homogenate supports platelet activation under static and flow conditions.** (A) Platelets were spread on fibrillar collagen-I (10 µg/ml) and plaque homogenate (500 µg/ml) and percentage of non-spread, partially spread or fully spread platelets quantified. Spreading states are indicated on the plaque representative image with diamond, non-spread; stealth, partially spread or open arrow, fully spread. 6 fields of view containing a total of 900-1200 platelets per condition per experiment were analyzed (n=3). (B) Ca<sup>2+</sup> spiking of spreading platelets loaded with 1 µM BAPTA-Oregon Green Ca<sup>2+</sup> indicator dye. Percentage of platelets exhibiting spikes, spike duration and amplitude were assessed. (n=7, unpaired t-test). (C) Representative images of aggregate formation and platelet activation on fibrillar collagen-I and plaque homogenate microspots in the Maastricht flow chamber perfused with thrombin-inhibited whole blood at 1000/s. (D) Quantitation of aggregate formation and platelet activation. Means ± SD (n=14-16), \*p <0.05, \*\* p <0.005, \*\*\*p <0.0005, \*\*\*\*p <0.0001 (one-way ANOVA). Scale bars = 50 µm, SAC = surface area coverage.

The ability of the plaque homogenate to stimulate platelet adhesion, activation and thrombus formation under flow at arterial shear (1000/s) was also assessed in comparison to collagen-I (**Figure 1C,D**). Platelet adhesion (deposition) and thrombus size (multilayer) on plaque was not significantly different from collagen-I. Plaque induced platelet α-granule release (P-selectin), integrin αIIbβ3 activation (fibrinogen binding) and phosphatidylserine (PS) exposure (Annexin A5) (**Figure 1C,D**). However, collagen-I induced significantly more (~50%) platelet activation in these 3 measured parameters (**Figure 1C,D**). Taken together, these results indicate that plaque homogenate supports platelet spreading, Ca<sup>2+</sup> mobilization and thrombus formation. However, collagen-I is a more potent ligand, stimulating greater platelet activation during thrombus formation than plaque. Nevertheless, plaque is a more physiological ligand and can therefore be used to assess the effect of our recently generated anti-GPVI Nb2<sup>25</sup> in platelet activation.

## Platelet activation by plaque homogenate under flow is integrin independent

Platelet activation by plaque has previously been shown to be primarily mediated through GPVI, and independent of the collagen binding integrin  $\alpha 2\beta 1$  <sup>7, 8, 10, 11</sup>. However, platelets express multiple integrin receptors and plaque contains several integrin substrates. Therefore, we investigated the potential involvement of other platelet integrins in thrombus formation under arterial shear using blocking reagents to  $\alpha 5\beta 1$  (fibronectin; JBS5),  $\alpha 6\beta 1$  (laminin; G0H3),  $\alpha v\beta 3$  (vitronectin; P11),  $\alpha IIb\beta 3$  (fibrinogen; eptifibatide) and  $\alpha 2\beta 1$  (collagen; 6F1). Representative images and subtraction heatmaps, showing only significant differences from controls, are shown in **Figure 2**. Our results confirmed inhibiting  $\alpha 2\beta 1$  had no effect on thrombus formation on plaque, however it reduced platelet deposition and activation markers on collagen-I (**Figure 2B, Supplementary Figure 2**). Integrin  $\alpha IIb\beta 3$  inhibition blocked thrombus propagation (multilayer) on both substrates, as expected (**Figure 2A,B**). However, other platelet activation parameters (P-selectin expression, integrin activation, PS exposure) were not affected on either substrate (**Figure 2B, Supplementary Figure 2**). Inhibition of the other individual integrins did not affect thrombus formation parameters on either substrate (**Supplementary Figure 3**). Combined blockade of integrins  $\alpha 2\beta 1$  and  $\alpha IIb\beta 3$  had a greater effect than blocking either alone, and resulted in significant inhibition of platelet adhesion, thrombus formation and platelet activation on both plaque and collagen-I (**Figure 2, Supplementary Figure 2**). To investigate this further, we inhibited all integrins by removing free ions with EDTA. Thrombus formation on plaque and collagen-I was not affected by 2 mM EDTA <sup>33,34</sup>, however at higher concentrations (9 mM) <sup>35</sup> a significant decrease in thrombus formation and platelet activation markers were observed on collagen-I. On plaque a slight, but not significant, reduction was

noted with 9mM EDTA (**Figure 2A, Supplementary Figure 2**). These results indicate that plaque-induced platelet adhesion and activation is largely independent of individual integrin activation.

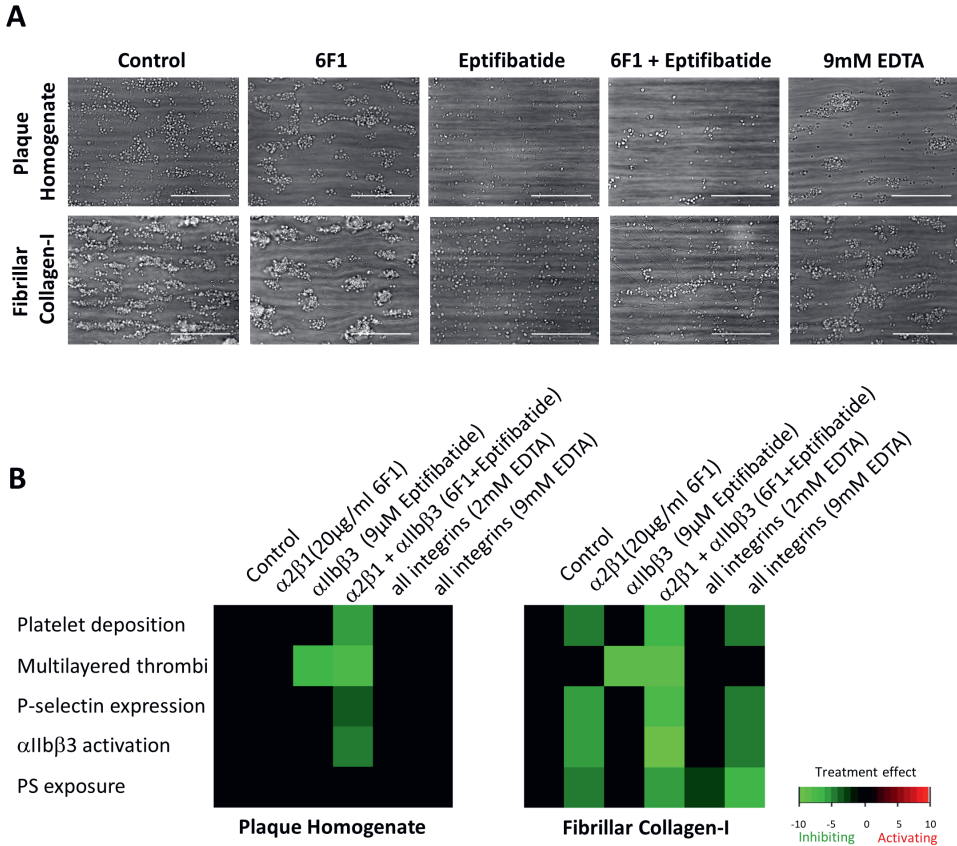


**Figure 2 – Platelet activation induced by plaque homogenate is integrin independent.** (A) Representative brightfield images of thrombi formed on plaque homogenate and fibrillar collagen-I in the presence of vehicle (PBS) or integrin inhibitors. Scale bars = 50  $\mu$ m. (B) Heatmaps summarizing significant effects of the indicated treatments. For each parameter, raw data across all surfaces and donors was univariately scaled (0-10), and control values, then subtracted from treatment values with only significant ( $p < 0.05$ ) changes displayed. Green indicates significant reduction. N=3-5, one-way ANOVA. For raw data see Supplementary Figure 5.



## **Nb2 effectively blocks atherosclerotic plaque-induced platelet activation and thrombus formation**

Of the 54 novel anti-GPVI Nbs we recently generated <sup>25</sup>, three have been used in this study: Nb2 a potent inhibitor of GPVI-collagen interactions; Nb53, a weak GPVI-binder that is non-inhibitory and was used as an isotype, negative, control in all experiments; Nb28, a non-inhibitory Nb that strongly binds GPVI and has been used to label and visualize GPVI for microscopy. The non-inhibitory nature of Nb53 and Nb28 was confirmed by platelet aggregation in response to collagen **Supplementary Figure 4**. To further characterize the potential anti-thrombotic properties of Nb2 we tested its effect on plaque-mediated platelet activation under flow. Blood was pre-treated with 500 nM Nb, a concentration previously shown to completely block collagen-induced platelet aggregation <sup>25</sup>, before being perfused over plaque (**Figure 3A**) and collagen-I (**Figure 3B**) microspots at arterial shear (1000/s) and thrombus formation and platelet activation assessed. Significant effects on thrombus formation and platelet activation were summarized into subtraction heatmaps, where bright green indicates strong, statistically significant, inhibition (**Figure 3C, Supplementary Figure 5**). On plaque, Nb2 inhibited platelet adhesion and thrombus formation, as well as reduced platelet  $\alpha$ -granule secretion, integrin  $\alpha$ IIb $\beta$ 3 activation and PS exposure. On collagen-I, Nb2 reduced thrombus formation and platelet activation markers, but did not affect platelet adhesion. On both agonists, the negative control Nb53 had no effect. These results demonstrate that Nb2 is a potent inhibitor of platelet activation by both plaque and collagen-I, but plaque exhibits more selective dependency on GPVI for thrombus formation.

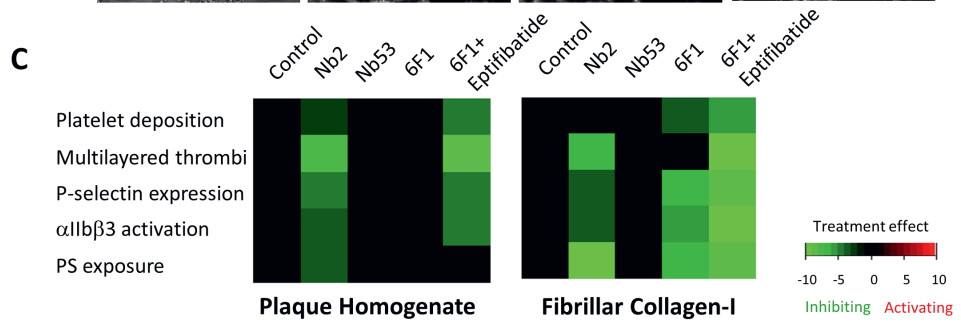
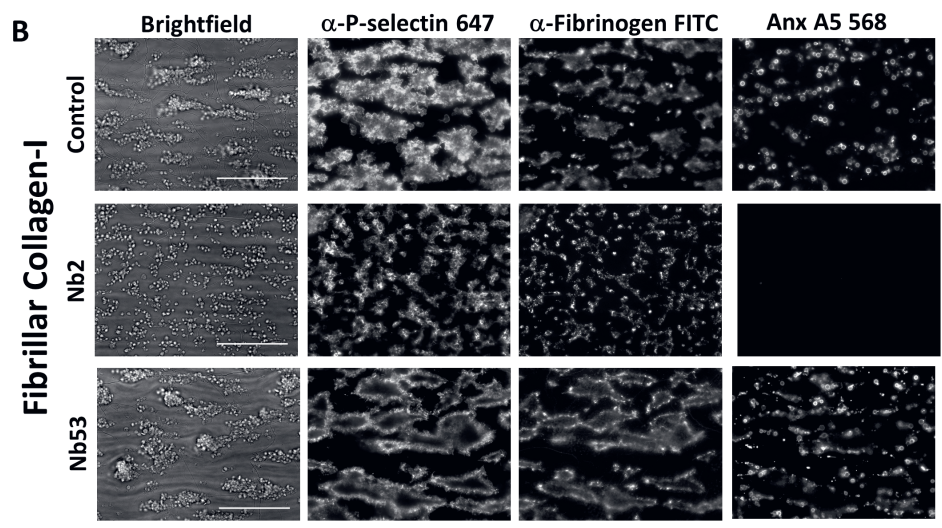
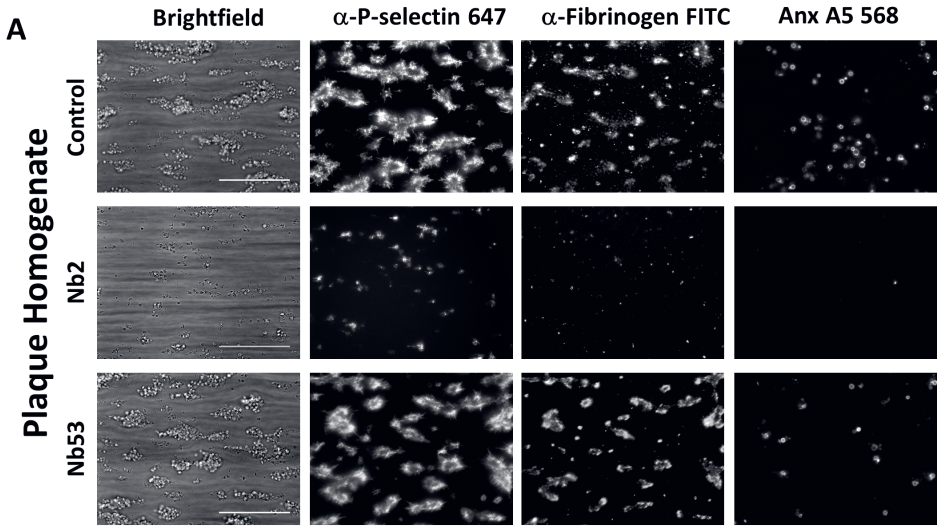


**Figure 3 (previous page) – Anti-GPVI Nb 2 inhibits platelet activation at arterial shear rates.** Blood was preincubated with either vehicle (PBS), 500 nM Nb2 or negative control Nb53 for 10 minutes and then perfused at 1000/s over (A) plaque homogenate or (B) fibrillar collagen-I. Brightfield images give information about thrombus size and morphology, while  $\alpha$ -P-selectin is used to assess  $\alpha$ -granule secretion,  $\alpha$ -fibrinogen to indicate  $\alpha$ IIb $\beta$ 3 activation and annexin A5 to approximate procoagulant activity by PS exposure. Scale bars = 50  $\mu$ m. (C) Heatmaps, generated by subtracting the univariately scaled values of the vehicle from the scaled values of the respective treatment for each parameter with only significant ( $p < 0.05$ ) changes indicated. Green indicates significant reduction. N=5-8, one-way ANOVA. For raw data see Supplementary Figure 5.

### **Nb2 strongly inhibits collagen- and atherosclerotic plaque-induced GPVI signaling**

To investigate the effect of Nb2 on GPVI signaling we used western blot to examine downstream phosphorylation following stimulation with plaque or collagen-I. Both substrates induced strong tyrosine phosphorylation in platelets (**Figure 4A**). Nb2 addition caused a visible reduction in platelet global tyrosine phosphorylation to plaque stimulation, and strongly inhibited phosphorylation of GPVI downstream signaling proteins Syk Y<sup>525/526</sup>, LAT Y<sup>200</sup> and PLC $\gamma$ 2 Y<sup>1217</sup> in both plaque and collagen-I stimulated platelets (**Figure 4A**). Nb53 had no effect. Quantitation (**Figure 4B**) revealed strong and consistent reduction of phosphorylation by Nb2 in response to plaque, whereas a slightly weaker and more variable response was observed to collagen-I, probably reflecting the involvement of other platelet receptors<sup>36</sup>.

To assess Ca<sup>2+</sup> signaling, washed platelets loaded with the Ca<sup>2+</sup> indicator dye were preincubated with Nb2 and spread on collagen-I or plaque. However, no platelets adhered under these conditions. We therefore spread platelets onto collagen-I or plaque before adding Nb2. Ca<sup>2+</sup> mobilization was quantified both pre- and post-Nb2 addition (**Figure 4C**). Nb2 significantly reduced the percentage of Ca<sup>2+</sup> spiking platelets on collagen-I, but had no

effect on those spreading on plaque. Nb2 had no effect on spike duration or amplitude on either substrate. The negative control Nb53 had no effect on any parameter (data not shown). Taken together these results show that Nb2 effectively inhibited GPVI-mediated signaling in response to both collagen-I and plaque but was unable to reverse plaque-mediated  $Ca^{2+}$  signaling in adhered platelets.

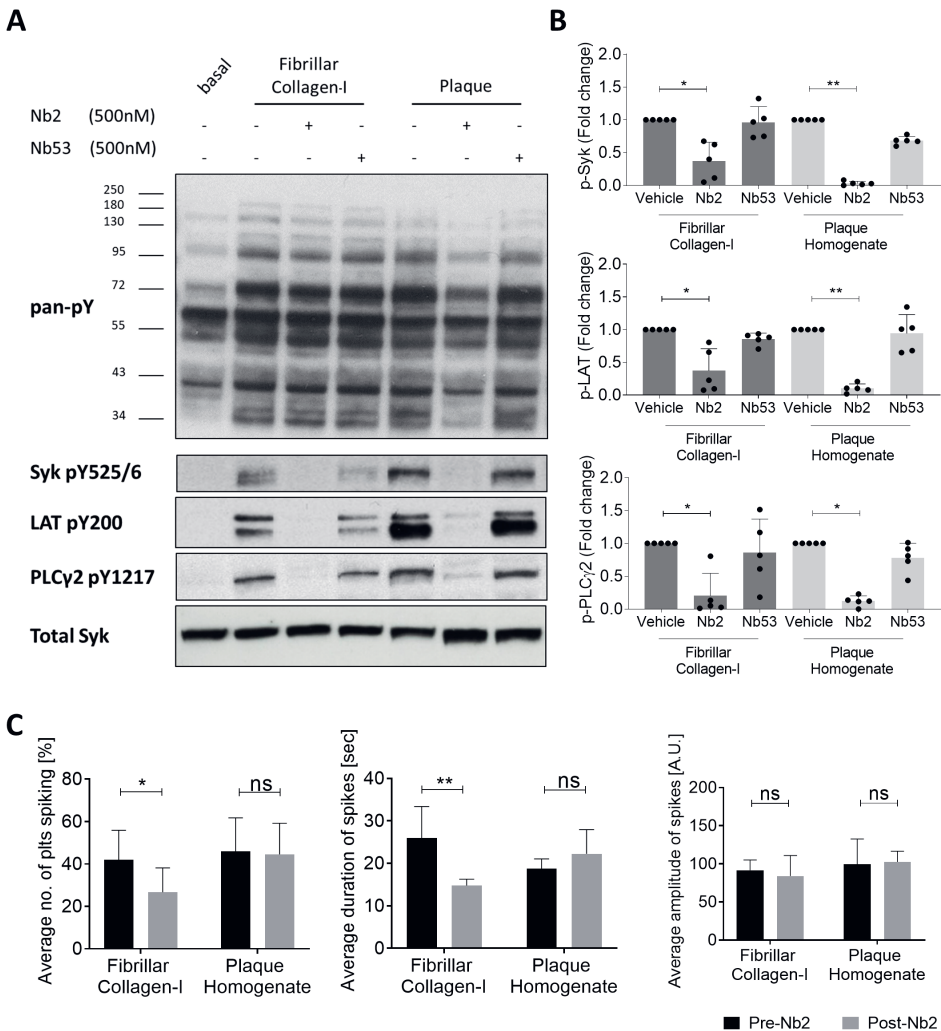


**Figure 4 (previous page)– Nb2 strongly inhibits collagen- and atherosclerotic plaque induced GPVI signaling.** (A) Representative western blots and (B) quantification of phosphorylation of GPVI downstream signaling proteins following stimulation of washed platelets with fibrillar collagen I or plaque for 180 seconds in the presence or absence of Nb2 or negative control Nb53 (n=5, one-way AVOVA). (C) Ca<sup>2+</sup> spiking of spreading platelets loaded with 1  $\mu$ M BAPTA-Oregon Green Ca<sup>2+</sup> indicator were assessed for percentages of platelets exhibiting spikes, as well as spike duration and amplitude, before and after addition of 500 nM Nb2 or Nb53. Means  $\pm$  SD (n=4), ns: not significant, \*p <0.05, \*\*p <0.005 (one-way ANOVA).

### **Non-inhibitory Nb28 and inhibitory Nb2 have distinct binding sites on GPVI**

In order to visualize the effect of Nb2 on GPVI localization we required a non-inhibitory anti-GPVI Nb that could be used in imaging studies. Nb28 strongly binds GPVI but does not inhibit GPVI-collagen interactions <sup>25</sup> (**Supplementary Figure 4**). To further test the validity of using Nb28 in imaging studies we confirmed that it did not inhibit thrombus formation (**Figure 5A**) and subsequent expression of platelet activation markers on collagen-I under flow (**Figure 5B**). To verify that Nb28 binds a distinct site and does not interfere with Nb2 GPVI binding a competition ELISA was used (**Figure 5C**). Nb21, another inhibitory Nb known to bind to a similar epitope in GPVI as Nb2, was used as a control. Nb21 signal decreased due to competition with Nb2 whereas Nb28 signal did not change, suggesting a distinct binding site from Nb2. We fluorescently labeled Nb28 with AlexaFluor 647 (Nb28 AF647) and assessed binding to platelets, as well as competitive binding with inhibitory Nb2, using flow cytometry (**Figure 5D**). Quantification of flow cytometry experiments revealed no significant difference between platelets labeled with Nb28 AF647 alone or those preincubated with unlabeled Nb2 (**Figure 5E**), confirming distinct epitopes on GPVI and making Nb28 AF647 suitable for imaging of GPVI in experiments where Nb2 is also present.

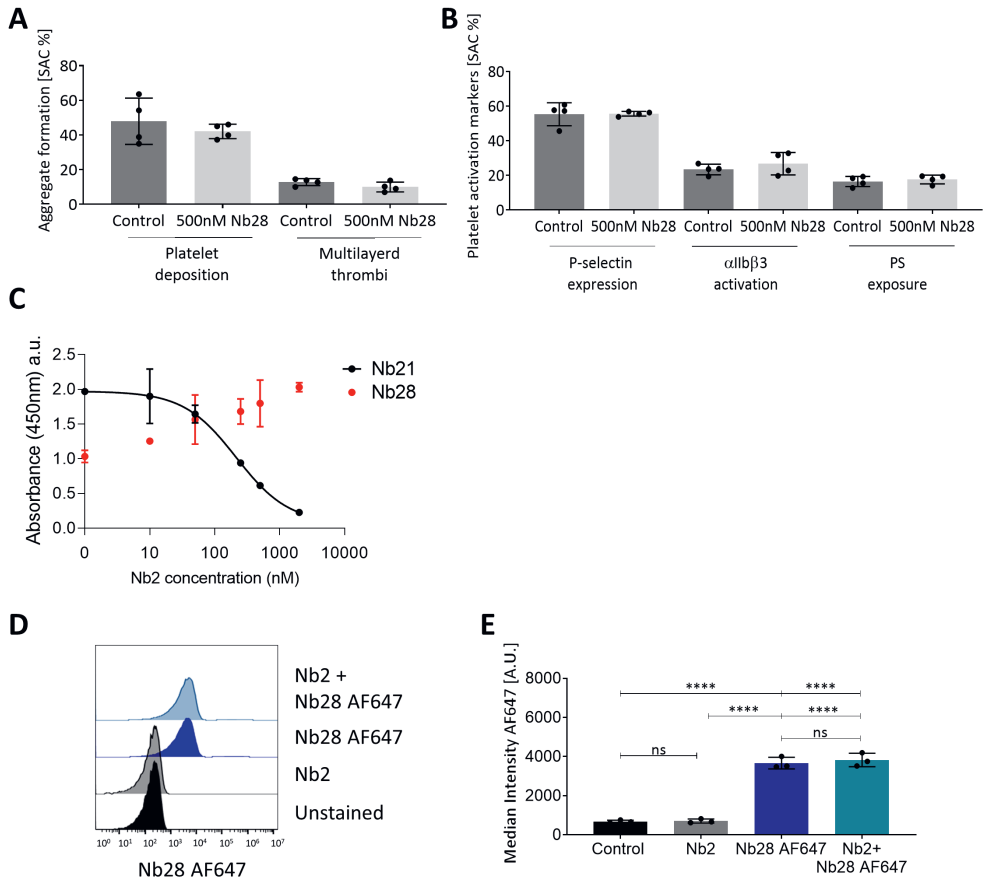


**Figure 5 – Nb28 does not affect adhesion and activation under flow or compete with Nb2 binding.** Thrombin inhibited whole blood was preincubated with either vehicle (PBS) or 500 nM of unlabeled Nb28 and then flowed over fibrillar collagen-I utilizing the Maastricht flow chamber at 1000/s and assessed for (A) platelet deposition and multilayer thrombi formation and (B) platelet activation markers: PS exposure, P-selectin expression and integrin  $\alpha$ IIb $\beta$ 3 activation. Each data point represents one donor (n=4), one-way ANOVA. SAC = surface area coverage. (C) A solid-phase binding assay measuring Nb28 and Nb21 binding to recombinant GPVI in the presence of increasing concentrations of Nb2. Competition between Nb2 and labeled Nb28 AF647 binding on platelets was assessed by flow cytometry. Washed platelets were preincubated with 500 nM Nb2 or vehicle (PBS) for 10 minutes, then labeled with 100 nM Nb28 AF647 and 50,000 events acquired. (D) Representative histograms and (E) quantitative analysis of median fluorescence intensity. Means  $\pm$  SD (n=3), ns: not significant, \*\*\*\*p < 0.0001 (two-way ANOVA).

## Nb2 disrupts GPVI clustering

We have previously shown that GPVI clustering contributes to sustained GPVI signaling in spread platelets on collagen-I<sup>19</sup>. To see if GPVI clustering occurs in platelets forming thrombi under flow we preincubated blood with Nb28 AF647, before perfusing it over collagen-I and taking fluorescent images. GPVI was clearly seen to be enriched at visible collagen fibers, forming long bright clusters in all thrombi (**Figure 6A**). As platelet activation by plaque was also highly GPVI-dependent we investigated GPVI distribution on platelets adhering and forming thrombi on plaque. No collagen fibers were visible in the brightfield image of the plaque, however in some areas GPVI was seen to form brighter clusters that ran across several platelets in a thrombus, reminiscent of those seen in collagen-I (**Figure 6B**). To investigate the effect of Nb2 on GPVI localization we preincubated blood with Nb2 and Nb28 AF647 before flow. As very few platelets adhered to plaque in the presence of Nb2 we only investigated GPVI distribution in platelets perfused over collagen-I, where clustering was also easily visualized (**Figure 6C**). Under control conditions, GPVI clustered along the collagen fibers. However, pre-treatment with Nb2 disrupted the GPVI localization and no organized clustering along collagen fibers was seen. Control Nb53 and 6F1 (integrin  $\alpha 2\beta 1$  inhibitor) had no effect on GPVI localization or clustering in the platelets that adhered and formed thrombi on collagen-I. GPVI is known to be shed from the platelet surface under certain conditions<sup>37</sup>. In order to investigate whether the Nbs had an effect on GPVI shedding, which could cause loss of clusters, GPVI surface expression was measured using flow cytometry after preincubation of platelets with the Nbs. The thiol-modifying compound NEM, which activates metalloproteinases and causes strong shedding of GPVI<sup>38</sup> was used as a positive control. **Figure 6D** and **E** show no effect of either Nb2 or Nb53 on GPVI surface expression, whereas NEM caused complete loss of the receptor. These results show that Nb2 did not cause receptor shedding but

effectively disrupted GPVI clustering along collagen fibers as well as prevented thrombus formation, demonstrating that clustering is important for thrombus formation under flow.

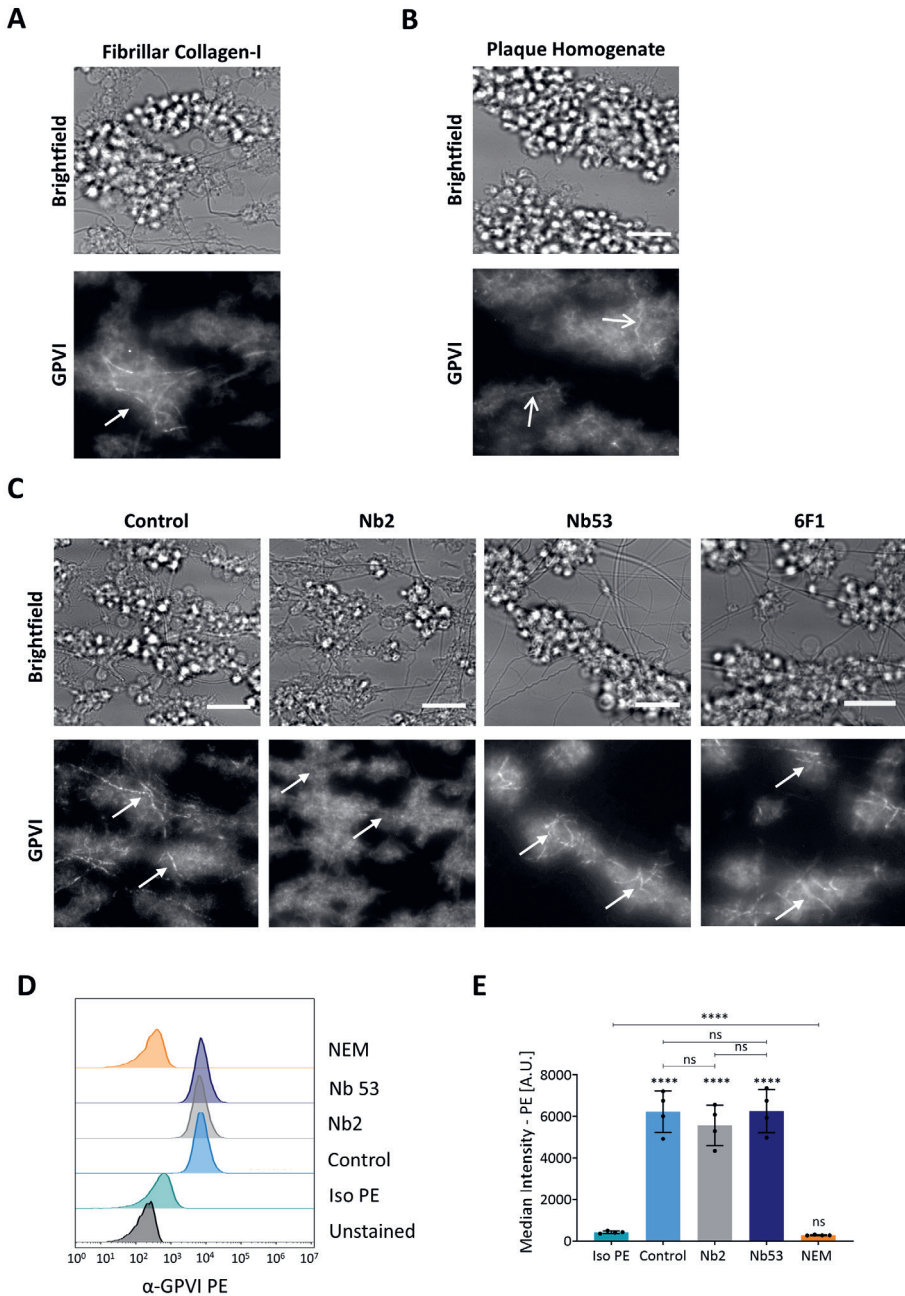




**Figure 6 (previous page) – Anti-GPVI Nb2 disrupts GPVI clustering along collagen fibers in flow.** (A) Clustering of Nb28 AF647 labeled GPVI along collagen-I fibers (arrows) in whole blood perfused over collagen-I (1000/s). Collagen fibers are visible in the brightfield image. (B) In flow over plaque, some fibrillar clusters of GPVI were seen (open arrows) but GPVI was mostly diffuse. (C) Preincubation of platelets with 500 nM Nb2 disrupted the clustering on collagen-I; negative control Nb53 or inhibition of  $\alpha 2\beta 1$  with 5  $\mu\text{g/ml}$  6F1 did not affect clustering of GPVI. Arrows indicate position of collagen fibers seen in brightfield images,  $n=5-7$ . Scale bars = 10  $\mu\text{m}$ . Washed platelets ( $2 \times 10^9/\text{ml}$ ) were incubated with 500 nM Nb2, Nb53 or 5 mM NEM (stimulator of GPVI shedding) for 2 hours before flow cytometry measurement of anti-GPVI (HY101)-PE binding (D). Representative histogram of median fluorescence intensity (MFI) of anti-GPVI-PE. (E) MFI of platelets with isotype-PE antibody or anti-GPVI-PE labeled control platelets, Nb2 and Nb53 treated platelets and NEM-treated platelets. Means  $\pm$  SD ( $n=4$ ), ns: not significant, \*\*\*\* $p < 0.0001$  (one-way ANOVA). Significance is shown compared to isotype control or between the treatments denoted by the bars.

## 4.4 Discussion

In the present study we used atherosclerotic plaque material as a physiologically relevant substrate to demonstrate that anti-GPVI Nbs can be used as effective inhibitors and imaging tools to study GPVI localization and function. Nb2 potently inhibited GPVI-mediated thrombus formation, disrupted GPVI clustering along collagen-I fibers, and blocked GPVI downstream signaling in response to collagen-I and plaque homogenate but did not induce receptor shedding. In addition, we showed non-inhibitory Nb28 can be used to provide mechanistic insight by visualizing GPVI localization in platelets in whole blood under flow, without interfering with the inhibitory activity of Nb2 on GPVI clustering. Furthermore, we demonstrate atherosclerotic plaque preparations exhibit strong thrombogenic potential, which is mediated through GPVI and is independent of individual integrins. Taken together the present work underlines the central role of GPVI in platelet activation via atherosclerotic plaque and supports the further development of Nb2 as a promising antithrombotic agent.

Human atherosclerotic plaque has previously been utilized as a physiological platelet agonist, however there is evidence for heterogeneity<sup>3,7,11,39</sup>. In order to limit this, we formed a pooled homogenate of 10 human atherosclerotic plaque samples. Collagen has been demonstrated to be the main platelet agonist present in plaque material, with evidence showing modification of plaque collagens results in their specificity for GPVI<sup>3,7-9,11</sup>. GPVI blockade or depletion in human and murine platelets has been shown to result in almost complete inhibition of plaque induced-thrombus formation, while integrin  $\alpha 2\beta 1$  inhibition had no effect<sup>7,8,11</sup>. Nb2 was able to block GPVI downstream signaling to both collagen-I and plaque, and effectively reduced total platelet tyrosine phosphorylation to plaque, but not to collagen-I – reflecting the activation of other receptors by this ligand. We have previously shown that Nb2 binds GPVI at a site adjacent to, but not overlapping with, the synthetic collagen related peptide (CRP) binding site and this causes a slight conformational change<sup>25</sup>. Nb2 can also outcompete GPVI for collagen-I binding in a solid-phase binding assay<sup>25</sup>. Addition of Nb2 to already spread platelets did not have a large effect, only reducing the percentage of  $\text{Ca}^{2+}$  spiking platelets on collagen-I, but not on plaque. As collagen has been proposed to be altered in plaque<sup>3,7,9</sup>, this could indicate that GPVI binds more tightly and cannot therefore be displaced by the addition of Nb2.

Under shear, Nb2 abolished thrombus formation on both plaque and collagen-I, yet adhesion was only affected on plaque. Platelet activation markers, particularly the highly GPVI-dependent PS exposure<sup>40-42</sup>, were also markedly decreased on both surfaces with Nb2 treatment. This is similar to that seen with the anti-GPVI Fab fragment of mAb 9O12<sup>8</sup>, the precursor antibody to the humanized form ACT017 (Glenzocimab)<sup>43</sup>. Combined inhibition of the two main platelet integrins  $\alpha 2\beta 1$  and  $\alpha \text{IIb}\beta 3$  was required to produce similarly strong inhibition of thrombus formation and platelet activation but lacked the effect on procoagulant platelet formation achieved by

Nb2. As eptifibatide treatment causes excessive bleeding <sup>44</sup>, combined inhibition of  $\alpha$ IIb $\beta$ 3 and  $\alpha$ 2 $\beta$ 1 would not be a viable treatment strategy to prevent thrombus formation. Inhibiting individual integrins did not result in any major effects on platelet adhesion and thrombus formation on plaque under flow. This lack of effect of integrin inhibition, together with the potent inhibition by Nb2, further illustrates the GPVI-dependence of platelet activation by plaque.

The small size, stability and high affinity of Nbs make them ideal reagents for imaging of receptors <sup>27, 29</sup>. Receptor clustering is important to sustain and amplify signaling in many different cell types, for example antigen receptors in lymphocytes <sup>45</sup>, and there are indications this is also the case for GPVI <sup>18-20</sup>. However, the GPVI studies were based on static spreading of washed platelets on collagen. Here we have shown for the first time, using fluorescently labeled Nb28, that GPVI clusters along exposed collagen-I fibers in whole blood under shear. In addition, using labeled Nb28 we also showed Nb2 disrupted this GPVI clustering. Inhibition of integrin  $\alpha$ 2 $\beta$ 1 under flow did not affect GPVI clustering or multilayer thrombus formation on collagen, although thrombus number and activation markers were still reduced, showing the combined activation of both receptors is required for full thrombus formation on collagen <sup>14</sup>. We have previously shown that platelets spread on fibrillar collagen-I, exhibited clustered GPVI and sustained GPVI-dependent signaling <sup>19, 20</sup>. We now show this clustering and sustained signaling is important for the build-up of platelet aggregates and PS exposure on collagen under flow, as Nb2 treatment does not affect platelet adhesion to collagen-I but abolishes multilayered thrombus formation and PS exposure.

More targeted approaches to manage atherothrombosis are needed as current treatments cause increased bleeding <sup>46</sup>. GPVI is a target for new therapies due to its platelet specificity <sup>12</sup>, major role in plaque activation <sup>7,8,10,11</sup>

and minimal involvement in hemostasis<sup>16, 22, 23, 40</sup>. The anti-GPVI Fab Glenzocimab (formerly ACT017) is already undergoing clinical trials for treatment of acute ischemic stroke<sup>47, 48</sup>. Nb2 has a high binding affinity for GPVI, with an equilibrium dissociation constant ( $K_D$ ) of 0.7 nM<sup>25</sup>, in comparison to ACT017 ( $K_D < 8$  nM)<sup>49</sup>. Nbs have been shown to have a relatively short half-life when used in vivo as they are quickly cleared from the system through the kidneys due to their small size. This can be counteracted by linkage to a larger inert molecule, such as serum albumin or by making multimeric forms of the Nb<sup>50</sup>. Yet their short half-life could provide a safety benefit in the acute setting of acute coronary syndromes or stroke, as any possible adverse effects on hemostasis would wear off more quickly in the event of bleeding. Several Nbs have already made the transition into the clinics by entering clinical trials<sup>50</sup>. The success of the bivalent Nb against VWF, Caplacizumab, which is used to treat the rare genetic disease, immune thrombotic thrombocytopenic purpura<sup>51, 52</sup> sets a good precedent for the use of Nbs to treat platelet-related disorders. Nbs are also very stable and resistant to extremes in pH and temperature and are therefore more amenable to different drug delivery methods. Indeed, Caplacizumab is delivered both intravenously and subcutaneously<sup>50, 52</sup>. In addition, the relative ease of Nb production in microbial expression systems has cost benefits in the large-scale production required for therapeutic uses<sup>53</sup>.

In summary, we demonstrate anti-GPVI Nbs are excellent new research tools which can be used to visualize or inhibit platelet GPVI. Nb2 effectively blocked GPVI-mediated platelet activation and thrombus formation by collagen and atherosclerotic plaque. Whilst fluorescent labeling of non-inhibitory Nb28 enabled visualization and interrogation of GPVI clustering in more physiological conditions of whole blood under shear. The potent inhibition of atherosclerotic plaque-induced thrombus formation by Nb2 advocates for its further investigation as a potential anti-thrombotic treatment.

**Author Contributions** NJJ designed and performed experiments, analyzed data, prepared figures and wrote the manuscript. CWS performed experiments and wrote the manuscript. AS and SJM performed experiments and revised the manuscript. YD generated nanobodies. COS wrote the MATLAB code for Ca<sup>2+</sup> mobilization analysis. MRT provided plaque material and revised the manuscript. YMCH, JWMH and SPW designed experiments, provided funding and supervision, and revised the manuscript. NSP designed and performed experiments, analyzed data, provided supervision and funding, and wrote the manuscript. All authors have read and approved the manuscript.

**Acknowledgments and Funding** This research was funded, in whole, or in part, by a Wellcome Trust Investigator Award (204951/B/16/Z). A Creative Commons (CC-BY) license is applied to the Author Accepted Manuscript arising from this submission, in accordance with the grant's open access conditions. NJJ is funded by a European Union's Horizon 2020 research and innovation program under Marie Skłodowska-Curie grant agreement No. 766118; NJJ is registered as a joint PhD student at the Universities of Maastricht (NL) and Birmingham (UK). SJM is supported by British Heart Foundation Accelerator Award (AA/18/2/34218). SPW is a British Heart Foundation Professor (CH 03/003), which also funds NSP. COS is funded by a Sir Henry Wellcome Postdoctoral Fellowship (221650/Z/20/Z). The authors kindly thank Barry Collier for supplying us with the  $\alpha 2\beta 1$  antibody 6F1, Killian Hughes for suggestions to improve the Ca<sup>2+</sup> mobilization analysis, Fawaz Alenazy for help with plaque homogenate preparation, Julie Rayes for help with FlowJo software, Chiara Pallini for preliminary imaging Nb characterization and Alice Pollitt for useful discussions.

**Conflicts of Interest** AS, MRT, SPW and NSP have a patent for the anti-GPVI nanobodies: WO2022/136457. The other authors have no conflicts of interest to declare.

## 4.5 References

1. World Health Organization. Cardiovascular diseases (CVDs): key facts. 2021; <https://www.who.int/en/news-room/fact-sheets/detail/cardiovascular-diseases>.
2. Kerrigan S, Moran N. The non-thrombotic role of platelets in health and disease. London, United Kingdom, Intech Open, 2015 [Online].
3. Van Zanten GH, de Graaf S, Slootweg PJ, *et al.* Increased platelet deposition on atherosclerotic coronary arteries. *J Clin Invest.* 1994; 93:615-632.
4. Hansson GK, Hermansson A. The immune system in atherosclerosis. *Nat Immunol.* 2011; 12:204-212.
5. Siess W, Zangl KJ, Essler M, *et al.* Lysophosphatidic acid mediates the rapid activation of platelets and endothelial cells by mildly oxidized low density lipoprotein and accumulates in human atherosclerotic lesions. *Proc Natl Acad Sci USA.* 1999; 96:6931-6936.
6. Siess W. Athero- and thrombogenic actions of lysophosphatidic acid and sphingosine-1-phosphate. *Biochim Biophys Acta.* 2002; 1582:204-215.
7. Penz S, Reininger AJ, Brandl R, *et al.* Human atheromatous plaques stimulate thrombus formation by activating platelet glycoprotein VI. *FASEB J.* 2005; 19:898-909.
8. Cosemans JM, Kuijpers MJ, Lecut C, *et al.* Contribution of platelet glycoprotein VI to the thrombogenic effect of collagens in fibrous atherosclerotic lesions. *Atherosclerosis.* 2005; 81:19-27.
9. Katsuda S, Kaji T. Atherosclerosis and extracellular matrix. *J Atheroscler Thromb.* 2003; 10:267-274.
10. Busygina K, Jamasbi J, Seiler T *et al.* Oral Bruton tyrosine kinase inhibitors selectively block atherosclerotic plaque-triggered thrombus formation in humans. *Blood.* 2018; 31:2605-2616.
11. Schulz C, Penz S, Hoffmann C, *et al.* Platelet GPVI binds to collagenous structures in the core region of human atheromatous plaque and is critical for atheroprogession in vivo. *Basic Res Cardiol.* 2008; 103:356-367.
12. Jandrot-Perrus M, Busfield S, Lagrue AH, *et al.* Cloning, characterization, and functional studies of human and mouse glycoprotein VI: a platelet-specific collagen receptor from the immunoglobulin superfamily. *Blood.* 2000; 96:1798-1807.
13. Miura Y, Ohnuma M, Jung SM, Moroi M. Cloning and expression of the platelet-specific collagen receptor glycoprotein VI. *Thromb Res.* 2000; 98:301-309.
14. Nieswandt B, Watson SP. Platelet-collagen interaction: is GPVI the central receptor? *Blood.* 2003; 102:449-461.

15. Rayes J, Watson SP, Nieswandt B. Functional significance of the platelet immune receptors GPVI and CLEC-2. *J Clin Invest*. 2019; 129:12-23.
16. Stegner D, Haining EJ, Nieswandt B. Targeting glycoprotein VI and the immunoreceptor tyrosine-based activation motif signaling pathway. *Arterioscler Thromb Vasc Biol*. 2014; 34:1615-1620.
17. Watson SP, Herbert JM, Pollitt AY. GPVI and CLEC-2 in hemostasis and vascular integrity. *J Thromb Haemost*. 2010; 8:1456-1467.
18. Ozaki Y, Suzuki-Inoue K, Inoue O. Platelet receptors activated via multimerization: glycoprotein VI, GPIb-IX-V, and CLEC-2. *J Thromb Haemost*. 2013;11:330-339.
19. Pallini C, Pike JA, O'Shea C, *et al*. Immobilized collagen prevents shedding and induces sustained GPVI clustering and signaling in platelets. *Platelets*. 2021; 32:59-73.
20. Poulter NS, Pollitt AY, Owen DM, *et al*. Clustering of glycoprotein VI (GPVI) dimers upon adhesion to collagen as a mechanism to regulate GPVI signaling in platelets. *J Thromb Haemost*. 2017; 15:549-564.
21. Tomlinson MG, Calaminus SD, Berlanga O, *et al*. Collagen promotes sustained glycoprotein VI signaling in platelets and cell lines. *J Thromb Haemost*. 2007;5:2274-2283.
22. Arai M, Yamamoto N, Moroi M, Akamatsu N, Fukutake K, Tanoue K. Platelets with 10% of the normal amount of glycoprotein VI have an impaired response to collagen that results in a mild bleeding tendency. *Br J Haematol*. 1995; 89:124-130.
23. Lockyer S, Okuyama K, Begum S, *et al*. GPVI-deficient mice lack collagen responses and are protected against experimentally induced pulmonary thromboembolism. *Thromb Res*. 2006; 118:371-380.
24. Harbi MH, Smith CW, Nicolson PLR, Watson SP, Thomas MR. Novel antiplatelet strategies targeting GPVI, CLEC-2 and tyrosine kinases. *Platelets*. 2021; 32:29-41.
25. Slater A, Di Y, Clark JC, *et al*. Structural characterization of a novel GPVI-nanobody complex reveals a biologically active domain-swapped GPVI dimer. *Blood*. 2021; 137:3443-3453.
26. Hamers-Casterman C, Atarhouch T, Muyldermans S, *et al*. Naturally occurring antibodies devoid of light chains. *Nature*. 1993; 363:446-448.
27. Erreni M, Schorn T, D'Autilia F, Doni A. Nanobodies as versatile tool for multiscale imaging modalities. *Biomolecules*. 2020; 10:1695.
28. Steeland S, Vandenbroucke RE, Libert C. Nanobodies as therapeutics: big opportunities for small antibodies. *Drug Discov Today*. 2016; 21:1076-1113.
29. Hassanzadeh-Ghassabeh G, Devoogdt N, De Pauw P, Vincke C, Muyldermans S. Nanobodies and their potential applications. *Nanomedicine (London)*. 2013;8:1013-1026.

30. Nicolson PLR, Nock SH, Hinds J, *et al.* Low-dose Btk inhibitors selectively block platelet activation by CLEC-2. *Haematologica*. 2021; 106:208-219.
31. Pike JA, Simms VA, Smith CW, *et al.* An adaptable analysis workflow for characterization of platelet spreading and morphology. *Platelets*. 2021; 32:54-58.
32. De Witt SM, Swieringa F, Cavill R, *et al.* Identification of platelet function defects by multi-parameter assessment of thrombus formation. *Nat Commun*. 2014; 5:4257.
33. Nurden AT, Rosa JP, Fournier D, *et al.* A variant of Glanzmann's thrombasthenia with abnormal glycoprotein IIb-IIIa complexes in the platelet membrane. *J Clin Invest*. 1987; 79:962-969.
34. Santoro SA, Walsh JJ, Staats WD, Baranski KJ. Distinct determinants on collagen support  $\alpha 2\beta 1$  integrin-mediated platelet adhesion and platelet activation. *Cell Regul*. 1991; 2:905-913.
35. Fernández DI, Provenzale I, Cheung HYF, *et al.* Ultra-high-throughput  $Ca^{2+}$  assay in platelets to distinguish ITAM-linked and G-protein-coupled receptor activation. *iScience*. 2022; 25:103718.
36. Lee D, Fong KP, King MR, Brass LF, Hammer DA. Differential dynamics of platelet contact and spreading. *Biophys J*. 2012; 102:472-482.
37. Gardiner EE, Arthur JF, Kahn ML, Berndt MC, Andrews RK. Regulation of platelet membrane levels of glycoprotein VI by a platelet-derived metalloproteinase. *Blood*. 2004; 104:3611-3617.
38. Gardiner EE, Karunakaran D, Shen Y, Arthur JF, Andrews RK, Berndt MC. Controlled shedding of platelet glycoprotein (GP)VI and GPIb-IX-V by ADAM family metalloproteinases. *J Thromb Haemost*. 2007; 5:1530-1537.
39. Shekhonin BV, Domogatsky SP, Idelson GL, Koteliansky VE, Rukosuev VS. Relative distribution of fibronectin and type I, III, IV, V collagens in normal and atherosclerotic intima of human arteries. *Atherosclerosis*. 1987; 67:9-16.
40. Nagy M, Perrella G, Dalby A, *et al.* Flow studies on human GPVI-deficient blood under coagulating and noncoagulating conditions. *Blood Adv*. 2020; 4:2953-2961.
41. Munnix IC, Strehl A, Kuijpers MJ, *et al.* The glycoprotein VI-phospholipase  $Cy2$  signaling pathway controls thrombus formation induced by collagen and tissue factor in vitro and in vivo. *Arterioscler Thromb Vasc Biol*. 2005; 25:2673-2678.
42. Lecut C, Schoolmeester A, Kuijpers MJ, *et al.* Principal role of glycoprotein VI in  $\alpha 2\beta 1$  and  $\alpha IIb\beta 3$  activation during collagen-induced thrombus formation. *Arterioscler Thromb Vasc Biol*. 2004; 24:1727-1733.
43. Alenazy FO, Harbi MH, Kavanagh DP, *et al.* GPVI inhibition by glenzocimab synergistically inhibits atherosclerotic plaque-induced platelet activation when combined with conventional dual antiplatelet therapy. *Eur Heart J*. 2021; 42



44. Saab F, Ionescu C, Schweiger MJ. Bleeding risk and safety profile related to the use of eptifibatide: a current review. *Expert Opin Drug Saf.* 2012; 11:315-324.
45. Liu W, Wang H, Xu C. Antigen receptor nanoclusters: small units with big functions. *Trends Immunol.* 2016; 37:680-689.
46. McFadyen JD, Schaff M, Peter K. Current and future antiplatelet therapies: emphasis on preserving haemostasis. *Nat Rev Cardiol.* 2018; 15:181-191.
47. ClinicalTrials.gov. Acute ischemic stroke interventional study (ACTIMIS). 2021.
48. ClinicalTrials.gov. Revacept in symptomatic carotid stenosis (Revacept CS02). 2021.
49. Lebozec K, Jandrot-Perrus M, Avenard G, Favre-Bulle O, Billiald P. Design, development and characterization of ACT017, a humanized Fab that blocks platelet's glycoprotein VI function without causing bleeding risks. *MAbs.* 2017; 9:945-958.
50. Jovčevska I, Muyldermans S. The therapeutic potential of nanobodies. *BioDrugs.* 2020; 34:11-26.
51. Peyvandi F, Cataland S, Scully M, *et al.* Caplacizumab prevents refractoriness and mortality in acquired thrombotic thrombocytopenic purpura: integrated analysis. *Blood Adv.* 2021; 5:2137-2141.
52. Scully M, Cataland SR, Peyvandi F, *et al.* Caplacizumab treatment for acquired thrombotic thrombocytopenic purpura. *N Engl J Med.* 2019; 380:335-346.
53. Kolkman J.A., D.A. L. Nanobodies: from llamas to therapeutic proteins. *Drug Discov Today Technol.* Summer 2010; 7:e95-e146.

## **4.6 Supplementary Methods**

### **Platelet spreading and imaging**

Glass coverslips were coated with 10 µg/ml fibrillar collagen-I or 500 µg/ml pooled plaque homogenate at 4°C overnight, then blocked with 5 mg/ml heat-denatured bovine serum albumin (BSA) for 60 minutes. Washed platelets ( $2 \times 10^7$ /ml) were allowed to spread for 45 minutes at 37°C, after preincubation with either PBS or 500 nM Nb2 for 10 minutes. Next, cells were fixed with 5% formalin (10 minutes), permeabilized with 0.1% Triton-X-100 (5 minutes) and labeled for 1 hour at RT with phalloidin- Alexa Fluor 488 in PBS with 3x PBS washes between each step. Coverslips were mounted onto microscope slides using Hydromount (National Diagnostics). Samples were imaged using a 63x

1.4 NA oil immersion objective lens on a Zeiss Axio Observer 7 epifluorescence microscope equipped with a Colibri 7 LED light source, Zeiss filter sets 38 for GFP/FITC and a Hamamatsu ORCA Flash 4 LT sCMOS camera for image acquisition. Image processing was done in FIJI 1.52a (NIH, Bethesda, USA). Platelet spreading analysis was carried out on all the platelets in 6 fields of view, per condition per experiment, as described in Pike *et al.* <sup>1</sup>.

### **Cytosolic Ca<sup>2+</sup> mobilization in live spread platelets**

Glass bottom dishes (MatTek Corp) were coated and blocked, as above. Freshly prepared washed platelets were loaded with 1  $\mu$ M Oregon Green-488 BAPTA-1-AM (ThermoFisher) at 37°C for 45 minutes. Excess dye was removed by addition of 25 ml modified Tyrode's-HEPES buffer, 3 ml ACD and 2.8  $\mu$ M prostacyclin, followed by 10 minutes of centrifugation at 1000 g, and resuspension in modified Tyrode's-HEPES buffer. Dye-loaded platelets ( $2 \times 10^7$ /ml) were allowed to spread in MatTek dishes for 45 minutes at 37°C. Two videos (1 frame per second for 2 minutes) were acquired both before and after addition of either 500 nM Nb2 or Nb53 using a Zeiss Axio Observer 7 epifluorescence microscope and 63 $\times$  1.4 N.A. objective and GFP filter set, as detailed above. Videos of Ca<sup>2+</sup> mobilization were analyzed by manually drawing of ~30 platelets per field of view, and generation of fluorescence intensity profiles for each platelet in ImageJ v1.52a. If there were more than 30 platelets in a FOV a grid pattern was applied to the image and platelets in the top left-hand corner of the image were selected first, with the area included increasing by one grid square to the right and below until 30 platelets were selected. The percentage of spiking platelets, as well as average duration and amplitude of the spikes were quantified using a MATLAB code adapted from Pallini *et al.* <sup>2</sup>, where a change in intensity was identified as a Ca<sup>2+</sup> spike if it increased >25% above baseline fluorescence intensity for each individual cell. A spike was defined to have ended once fluorescence intensity had decreased

by 80% of spike amplitude. Data were exported to Microsoft Excel for further analysis.

### **Western blotting**

Washed platelets ( $5 \times 10^8$ /ml) were preincubated with either PBS or 500 nM Nb2 or Nb53 for 10 minutes, before being stimulated with 10  $\mu$ g/ml fibrillar collagen-I or 500  $\mu$ g/ml pooled plaque homogenate at 1200 rpm and 37°C for 180 seconds on a shaking plate incubator (Eppendorf) in the presence of 9  $\mu$ M eptifibatide. As detailed by Nicolson *et al.*<sup>3</sup>, whole cell lysates were generated by addition of 5x SDS reducing sample buffer. Lysates were subjected to sodium dodecyl sulfate polyacrylamide gel electrophoresis (SDS-PAGE) and western blotting. PVDF membranes were blocked (5% BSA in TBST) and then incubated at 4°C overnight with antibodies (diluted in block) against phospho-tyrosine (1:1000, 4G10, Millipore, 05-321), phospho-PLC $\gamma$ 2 (1:250, Y1217, Cell Signalling, 3871S), phospho-LAT (1:500, Y200, Abcam, ab68139), phospho-Syk (1:500, Y525/526, Cell Signalling, 2710S) as well as total Syk (1:500, 4D10, St. Cruz, sc1240) or total LAT (1:500, Merck-Millipore, 06-807) as a loading control. Membranes were washed and incubated with HRP labeled secondary antibody at room temperature for 1 hour and developed using SuperSignal West Pico PLUS chemiluminescent substrate (Thermo-Scientific Pierce). Results were visualized on film, as well as imaged for quantification with an Odyssey Fc System (LI-COR Biosciences) in combination with image studio lite v5.2.

### **ELISA competition assay**

The binding of 100 nM Nb28 and Nb21 to immobilized GPVI-Fc (10 nM) in the presence of increasing concentrations of non-tagged Nb2 (0-2000 nM) was assessed using a competitive surface binding assay as previously described<sup>4</sup>. Binding of Nb28 and 21 was detected using HRP conjugated anti-His secondary antibody.

## Whole blood microfluidics

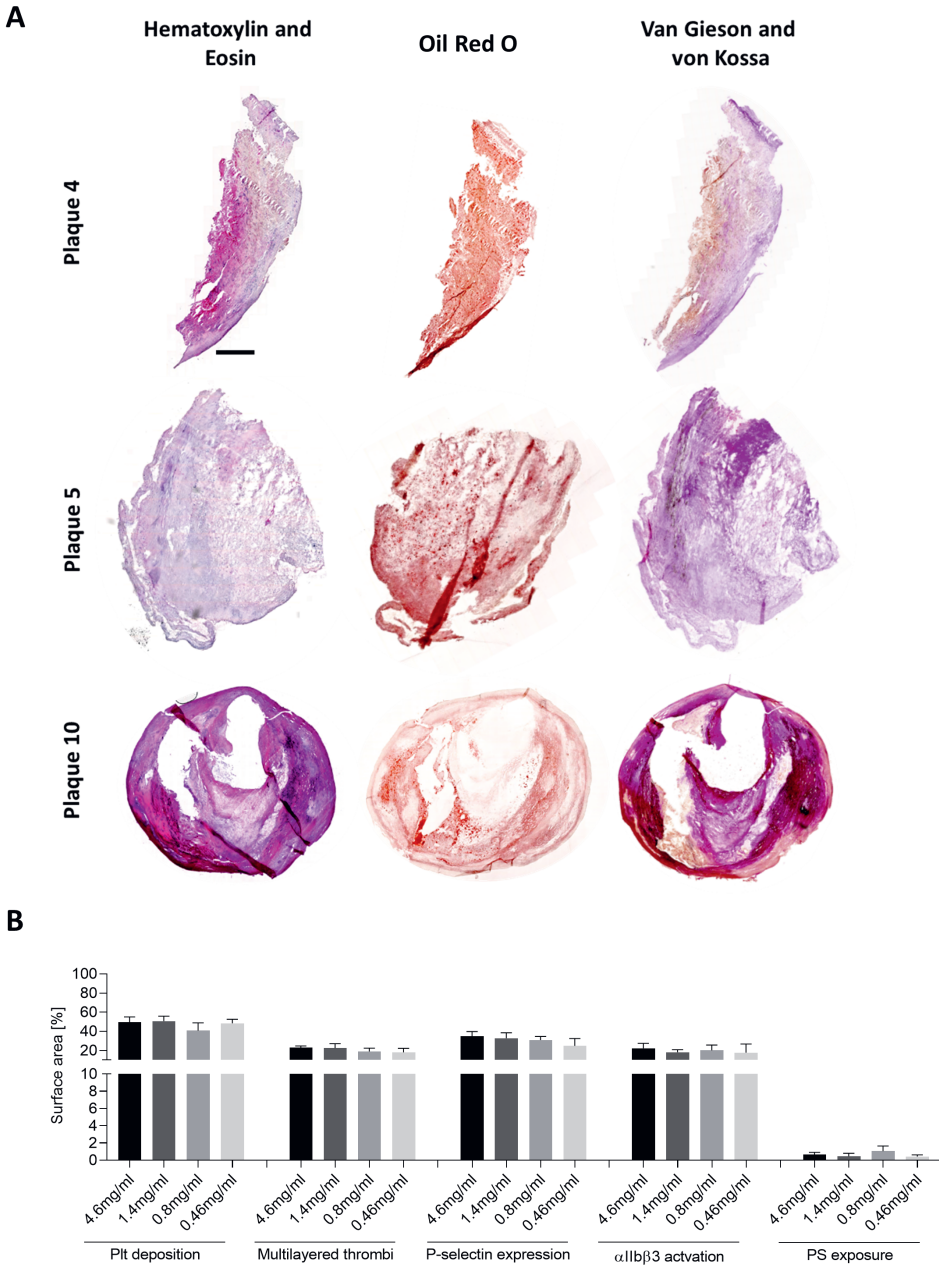
Whole blood samples (500  $\mu$ l) were perfused over 2 microspots through a Maastricht parallel flow chamber at a shear rate of 1000/s at room temperature, as described elsewhere <sup>5</sup>. In brief, degreased glass coverslips were coated with 0.5  $\mu$ l microspots of 100  $\mu$ g/ml fibrillar collagen-I and 500  $\mu$ g/ml pooled plaque homogenate overnight; and then blocked with 1% BSA in HEPES buffer (10 mM HEPES, 136 mM NaCl, 2.7 mM KCl, 2 mM MgCl<sub>2</sub>, pH 7.45) for 30 minutes. Citrated whole blood samples were thrombin inhibited (40  $\mu$ M PPACK) and recalcified (3.75 mM MgCl<sub>2</sub> and 7.5 mM CaCl<sub>2</sub>). The blood was preincubated for 10 minutes with either vehicle or 500 nM Nb2 or Nb53, prior to perfusion through the flow chamber for 3.5 minutes. Two endpoint brightfield images were taken, while flowing labeling buffer: HEPES buffer, 2 mM CaCl<sub>2</sub>, 1 unit/ml heparin, 5.5 mM glucose, 0.1% BSA and AF568 annexin A5 (for PS exposure, ThermoFisher), AF647 anti-CD62P mAb (for CD62P expression, BioLegend), and anti-fibrinogen FITC Ab (for integrin  $\alpha$ IIb $\beta$ 3 activation, DAKO) for 1.5 minutes. Unbound label was washed off, for 2 minutes, with rinse buffer (HEPES buffer, 2 mM CaCl<sub>2</sub>, 1 unit/ml heparin, 5.5 mM glucose and 0.1% BSA), and endpoint fluorescence images of three random fields of view were acquired with an EVOS AMF4300 microscope (Life Technologies). Brightfield images were quantified with two semi-automated ImageJ scripts generated in-house, to assess the percentage surface area covered by platelets (platelet deposition) as well as the surface area covered by thrombi (multilayered thrombi). For expression of the platelet activation markers (integrin activation, P-selectin expression and PS exposure) three more in-house generated semi-automated ImageJ scripts were employed to assess the percentage of the surface area covered by the fluorescent marker <sup>6</sup>. All raw values are averaged between images as well as runs, per donor. Next subtraction heatmaps were made using the program R. Average raw values over all donors and the two substrates, were univariate-normalized

at a scale of 0–10 for each parameter. Control values were then subtracted from the treatment values, and differences that were statistically significant ( $p < 0.05$ ) by a one-way ANOVA were then summarized in the heatmaps to only visualize relevant effects. Green represents inhibitory effects and red represents activation.

## References

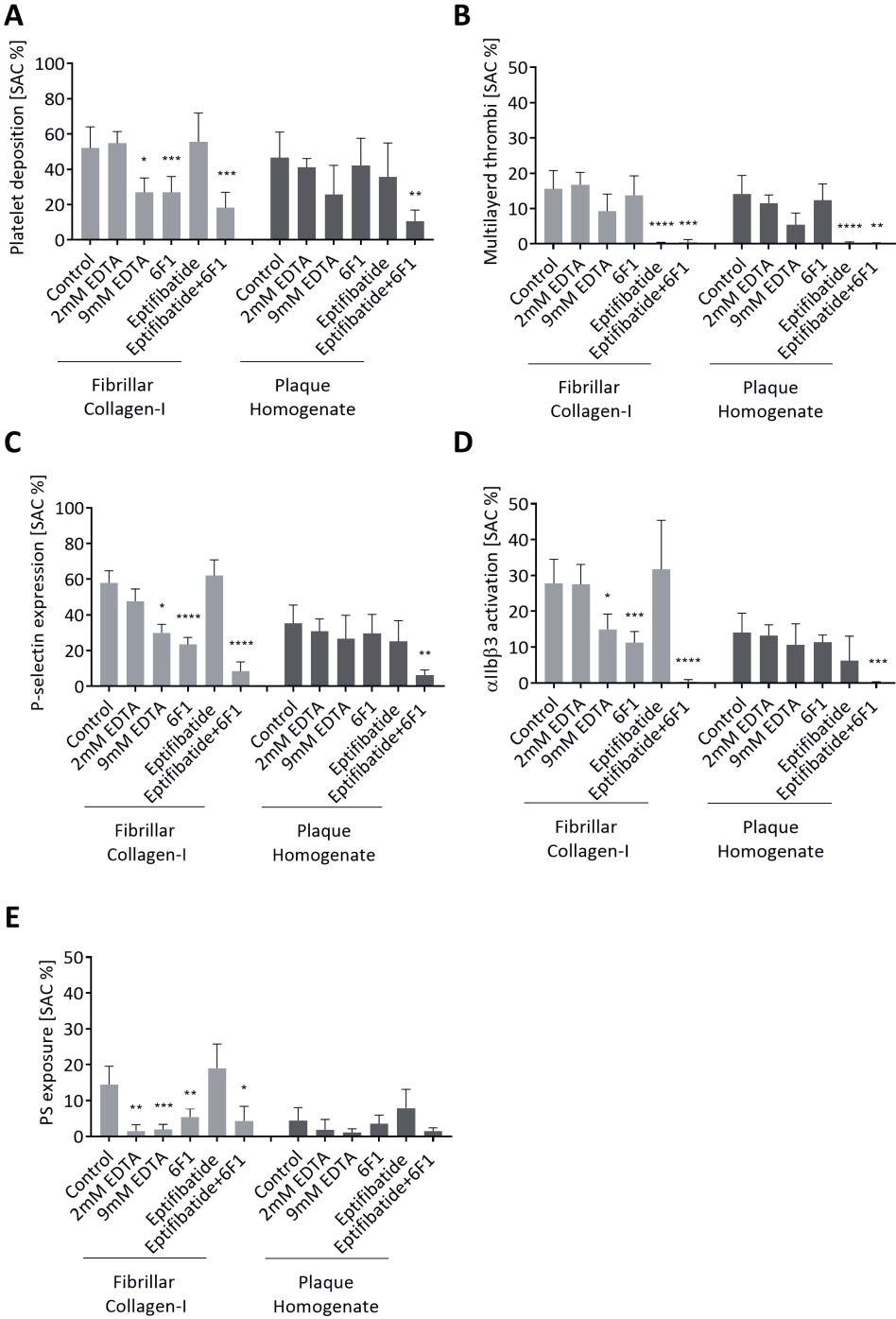
1. Pike JA, Simms VA, Smith CW, *et al.* An adaptable analysis workflow for characterization of platelet spreading and morphology. *Platelets*. 2021; 32:54-58.
2. Pallini C, Pike JA, O'Shea C, *et al.* Immobilized collagen prevents shedding and induces sustained GPVI clustering and signaling in platelets. *Platelets*. 2021; 32:59-73.
3. Nicolson PLR, Nock SH, Hinds J, *et al.* Low-dose Btk inhibitors selectively block platelet activation by CLEC-2. *Haematologica*. 2021; 106:208-219.
4. Slater A, Di Y, Clark JC, *et al.* Structural characterization of a novel GPVI-nanobody complex reveals a biologically active domain-swapped GPVI dimer. *Blood*. 2021; 137:3443-3453.
5. De Witt SM, Swieringa F, Cavill R, *et al.* Identification of platelet function defects by multi-parameter assessment of thrombus formation. *Nat Commun*. 2014; 5:4257.
6. Van Geffen JP, Brouns SLN, Batista J, *et al.* High-throughput elucidation of thrombus formation reveals sources of platelet function variability. *Haematologica*. 2019; 104:1256-1267.

## 4.7 Supplementary Figures

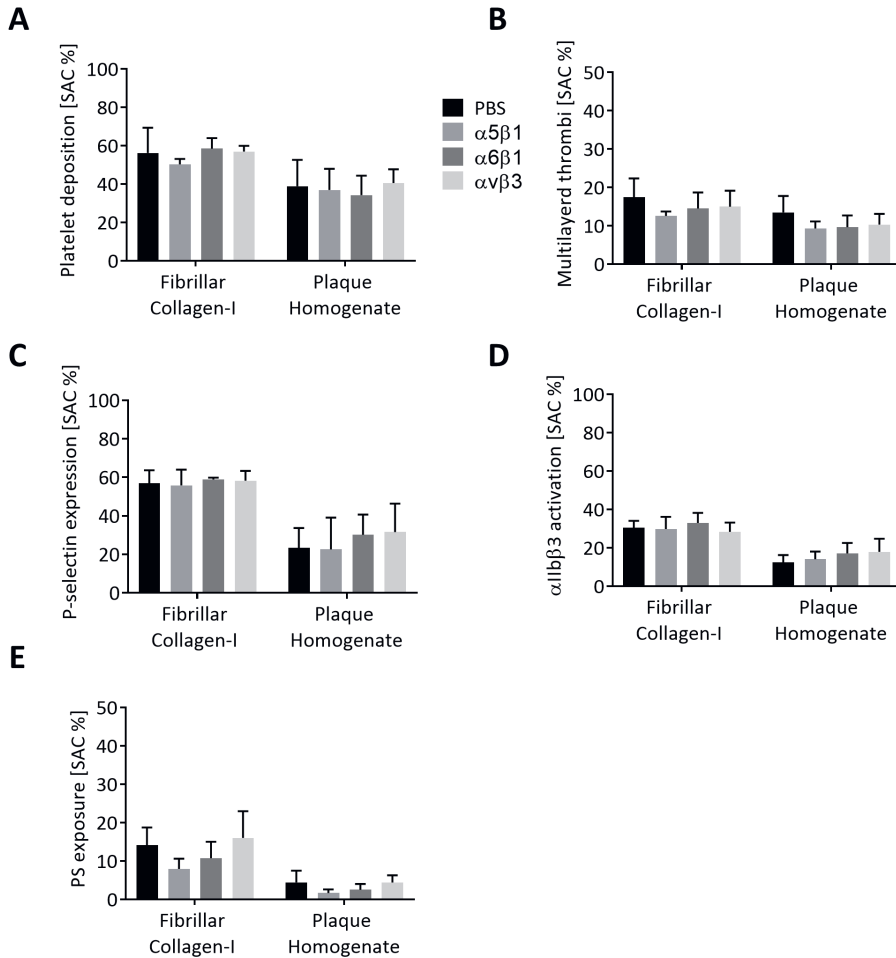


**Supplementary Figure 1 (previous page) – Atherosclerotic plaques exhibit heterogeneity in composition and plaque homogenate displayed no dose-dependent thrombus formation or platelet activation under flow.** (A) Half of all human plaques present in the pooled plaque homogenate were OCT imbedded, cryosectioned at 6  $\mu\text{m}$  and stained to assess general orientation of the plaque. Staining was with hematoxylin and eosin for nuclear and cellular compounds; with Oil Red O to visualize lipid deposition; as well as a double stained with van Gieson and von Kossa for global collagen content (in pink) and  $\text{Ca}^{2+}$  deposition (in black), respectively. Displayed are all stains of three representative plaques showing different distribution and overall presence of corresponding markers. Scale bar = 500  $\mu\text{m}$ . (B) Based on literature, four dilutions of pooled plaque homogenate were coated on glass coverslips and whole blood was perfused through parallel flow chamber at 1000/s. Thrombus parameters as well as expression of platelet activation markers were assessed (n=1). SAC = surface area coverage.

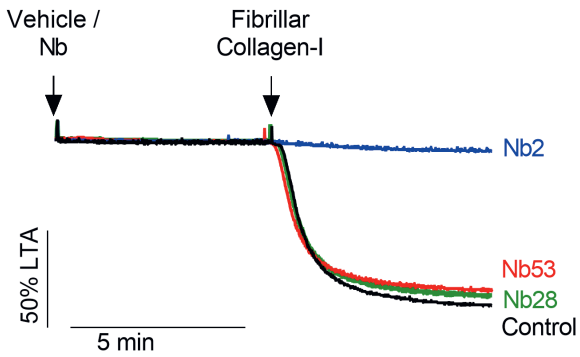
**Supplementary Figure 2 (following page) – Platelet activation induced by plaque homogenate is independent of individual integrin inhibition.** Whole blood was perfused over fibrillar collagen-I as well as plaque homogenate after preincubation for 10 minutes with 2 mM or 9 mM EDTA, 20  $\mu\text{g/ml}$  6F1, 9  $\mu\text{M}$  eptifibatide or 20  $\mu\text{g/ml}$  6F1 and 9  $\mu\text{M}$  eptifibatide. Surface area covered (SAC) by platelets (A), or multilayer thrombi (B) was extracted from brightfield images. Fluorescence images were quantified for P-selectin expression (C),  $\alpha\text{IIb}\beta\text{3}$  activation (D) and PS exposure (E) with semi-automated ImageJ scripts. N=3-5, \*p <0.05, \*\*p <0.005, \*\*\*p <0.0005, \*\*\*\*p <0.0001, one-way ANOVA.



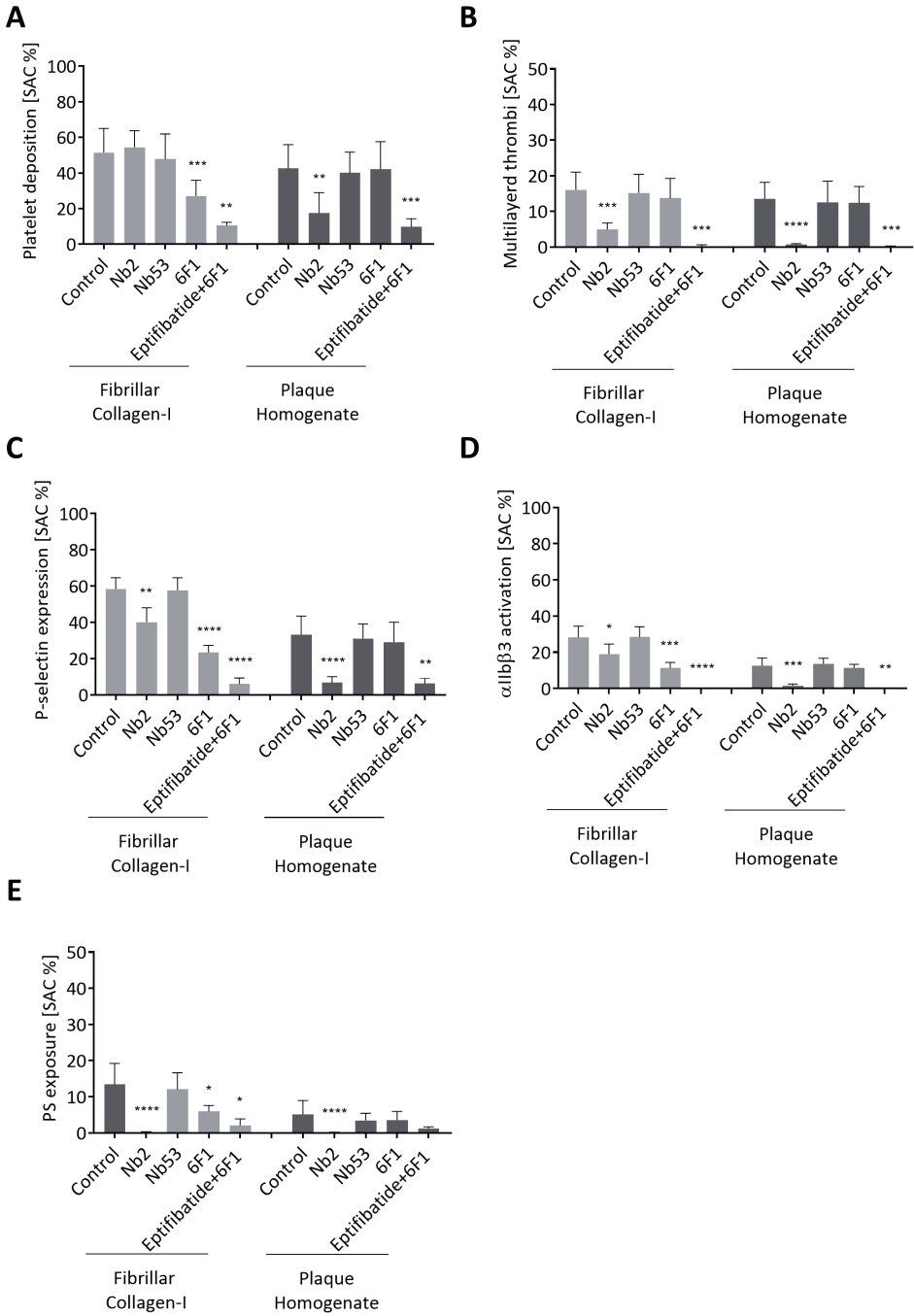




**Supplementary Figure 3 – Inhibiting integrins  $\alpha 5\beta 1$ ,  $\alpha 6\beta 1$  and  $\alpha \nu \beta 3$  individually does not affect thrombus formation.** Whole blood was perfused over fibrillar collagen-I as well as plaque homogenate after preincubation for 10 minutes with 20  $\mu\text{g/ml}$   $\alpha 5\beta 1$  or  $\alpha 6\beta 1$  or 100  $\mu\text{M}$   $\alpha \nu \beta 3$  inhibitors. Surface area covered (SAC) by platelets (A), or multilayer thrombi (B) was extracted from brightfield images. Fluorescence images were quantified for P-selectin expression (C),  $\alpha \text{IIb}\beta 3$  activation (D) and PS exposure (E) with semi-automated ImageJ scripts. N=3-5, one-way ANOVA, all changes shown were non-significant.



**Supplementary Figure 4 – Nb28 and Nb53 do not inhibit collagen-induced platelet aggregation.** Washed platelets were preincubated with 500 nM of either Nb2, Nb28 or Nb53 for 6 minutes prior to addition of 10  $\mu\text{g/ml}$  fibrillar collagen-I and platelet aggregation measured by light transmission aggregometry for 10 minutes.



**Supplementary Figure 5 (previous page) – Anti-GPVI Nb2 inhibits platelet activation at arterial shear rates.** Whole blood was perfused over fibrillar collagen-I as well as plaque homogenate after preincubation for 10 minutes with 500 nM Nb2 or negative control Nb53, 20 µg/ml 6F1 or 20 µg/ml 6F1 and 9 µM eptifibatide. Surface area covered (SAC) by platelets (A), or multilayer thrombi (B) was extracted from brightfield images. Fluorescence images were quantified for P-selectin expression (C),  $\alpha$ IIb $\beta$ 3 activation (D) and PS exposure (E) with semi-automated ImageJ scripts. N=3-5; \*p <0.05, \*\*p <0.005, \*\*\*p <0.0005, \*\*\*\*p <0.0001, one-way ANOVA.

**Supplemental Video 1 (online) – Plaque homogenate induces Ca<sup>2+</sup> mobilization in spread platelets.** Representative videos of Ca<sup>2+</sup> spiking in platelets loaded with 1 µM BAPTA-Oregon Green Ca<sup>2+</sup> indicator dye and spread on plaque homogenate (500 µg/ml) (left) and fibrillar collagen-I (10 µg/ml) (right) for 45 minutes prior to imaging. Images were taken every second for 2 minutes (n=7). Scale bar = 20 µm.





# Chapter 5

## **GPVI cluster size is related to thrombus formation and phosphatidylserine exposure in collagen-adherent platelets under shear stress**

Natalie J. Jooss, Christopher W. Smith, Jeremy A. Pike, Richard W. Famdale, Yvonne M. C. Henskens, Steve P. Watson, Johan W. M. Heemsker<sup>†</sup> and Natalie S. Poulter<sup>†</sup>

<sup>†</sup> Equal contribution

Contributions: NJJ designed and performed experiments, analyzed data, prepared figures and wrote the manuscript  
To be submitted as short report

**Abstract** Collagen-induced platelet activation is predominantly mediated by glycoprotein (GP)VI through formation of receptor clusters that coincide with the accumulation of signaling molecules and are hypothesized to drive a strong and sustained platelet activation. To determine the importance of GPVI clusters for thrombus formation, we used whole blood microfluidics and a nanobody (Nb), Nb28, labeled with AlexaFluor(AF) 488 to assess the surface distribution of GPVI on platelets adhering under shear to a range of collagen-like substrates with different platelet activation potentials. Automated analysis of GPVI surface distribution on platelets supported the notion that there is a relationship between GPVI cluster formation, thrombus size and phosphatidylserine exposure. Indeed, substrates that supported the formation of macro-clusters also induced significantly bigger aggregates with increased amounts of PS exposing platelets in comparison to substrates where no GPVI clusters were detected. Furthermore, we demonstrate that only direct inhibition of GPVI binding, but not of downstream signaling, is able to disrupt cluster formation. This work underlines the usefulness of labeled Nb28 as an imaging tool allowing novel experimental approaches and gives further insight into the significance of GPVI clustering under the more physiological condition of flow.

## 5.1 Introduction

Collagen mediated platelet activation is mediated by two main receptors, the glycoprotein receptor (GP) VI, which is the main signaling receptor for collagen on platelets <sup>1</sup>, and integrin  $\alpha 2\beta 1$  which mediates adhesion <sup>2</sup>. GPVI is associated with the immunoreceptor tyrosine-based activation motif (ITAM)-containing Fc receptor  $\gamma$  chain (FcR $\gamma$ ) at the platelet surface. Upon GPVI ligand binding, phosphorylation of the ITAM motif in FcR $\gamma$  induces a signaling cascade involving phosphorylation of several downstream proteins including Syk and LAT. This results in  $\text{Ca}^{2+}$  mobilization, cytoskeletal reorganization, granule secretion and thrombus formation <sup>3,4</sup>. Strong, sustained signals induce the formation of pro-coagulant platelets, characterized by exposure of phosphatidylserine (PS), a process linked to GPVI activation <sup>5</sup>. In platelet spreading assays, GPVI receptors were found to undergo varying levels of clustering depending on the type of collagenous substrate, with the large and multiligand collagen-I fibers inducing higher levels of clustering <sup>6,7</sup>. These large 'macro' GPVI clusters along collagen fibers can be seen using diffraction-limited microscopy and have been shown to be enriched in signaling molecules. The GPVI clusters, once formed, appear to be stable entities, even after downstream GPVI signaling is disrupted <sup>7,8</sup>. This suggests that the clustering of platelet GPVI is a prerequisite for sustained signaling in thrombus formation and thrombus stability under flow. However, this has not been investigated in detail.

Platelet GPVI is known to recognize and bind to consecutive glycine-proline-hydroxyproline (GPO) motifs which induce receptor engagement depending on their frequency and spacing, in conjunction with the fibrillar size of the triple helical collagens <sup>9</sup>. To proxy the GPVI-collagen interaction, GPO-enriched synthetic triple helical collagen-like peptides have been developed <sup>10</sup>. Repeated GPO sequences induce a strongly GPVI-dependent



platelet activation. Integrin  $\alpha 2\beta 1$  can bind to glycine-phenylalanine-hydroxyproline-glycine-glutamic acid-arginine (GFOGER) sequences. Accordingly, GFOGER-GPO peptides activate platelets by engagement of both collagen receptors, while the corresponding GFOGER-GPP peptides only act via integrin  $\alpha 2\beta 1$ <sup>11-13</sup>. For a shear-dependent platelet interaction with collagen peptides, von Willebrand factor (VWF) needs to be engaged. Therefore, in flow adhesion experiments using collagen-like peptides, a synthetic VWF-binding peptide (VWF-BP) is incorporated<sup>11-13</sup>.

We recently described the generation of a panel of cameloid nanobodies (Nb) against GPVI<sup>14</sup> and showed that Nb28 binds to GPVI without affecting collagen-binding<sup>15</sup>. This Nb can therefore be used to visualize the clustering of platelet GPVI under conditions of flow over a collagen-like surface. In the present study, we used whole blood microfluidics and Nb28 labeled with AlexaFluor(AF) 488 to assess the surface distribution of GPVI on platelets adhering under shear to a range of collagen-like substrates with different platelet activation potentials<sup>16</sup>. Our data support a relationship between GPVI cluster formation, thrombus size and PS exposure. Furthermore, we demonstrate that inhibition of GPVI binding, but not of downstream signaling, is able to disrupt the clustering.

## **5.2 Materials and Methods**

### **Antibodies and reagents**

Nanobodies were raised against the extracellular domain of GPVI by VIB Nanobody Service Facility, Brussels, <https://corefacilities.vib.be/nsf>) and expressed as described<sup>14</sup>. Collagen-related triple-helical peptides were obtained from CambCol Laboratories (Cambridge, UK) as C-terminal amides<sup>11,17</sup>: the following peptides were used H-GPC(GPP)<sub>5</sub>GFOGER(GPP)<sub>5</sub>GPC-NH<sub>2</sub> (GFOGER-GPP), GPC(GPO)<sub>3</sub>GFOGER(GPO)<sub>3</sub> GPC-NH<sub>2</sub> (GFOGER-GPO); VWF-binding peptide H-GPC(GPP)<sub>5</sub>GPRGQOGVMGFO (GPP)<sub>5</sub>GPC-

NH<sub>2</sub> (VWF-BP). Fibrillar collagen-I was from Nycomed, human placenta-derived collagen-III (1230-01S) from Southern Biotechnology; PRT-060318, a selective Syk inhibitor, from Bio-Connect; and the Rac-1 inhibitor EHT-1864 from AdooQ. The 6F1 mAb was a gift from Dr. Barry Coller (Rockefeller University, New York, USA).

### **Blood isolation**

Blood was collected into 4% sodium citrate from drug-free healthy volunteers, after informed consent, in accordance with the Declaration of Helsinki. Ethical approval was granted by the local medical ethics committees.

### **Platelet isolation and western blotting**

Washed platelets were isolated, as described <sup>18</sup> and stimulated (5x10<sup>8</sup>/ml) with 10 µg/ml fibrillar collagen or collagen-III under stirring conditions <sup>19</sup>. Cell lysates were resolved by gel electrophoresis and probed for total phosphotyrosine (4G10, Millipore); blots were developed with an Odyssey Fc System (LI-COR Biosciences).

### **Nb28 AF488 labeling**

In accordance with the manufacturer's instructions, the AF488 NHS ester (ThermoFisher Scientific) was used to label anti-GPVI Nb28 (1:40, dye:protein). Free dye was removed utilizing a Pierce dye removal column. Concentration of the labeled Nb was determined by a Nanodrop 2000/2000c apparatus (ThermoFisher).

### **Whole blood microfluidics**

Recalcified and thrombin inhibited whole blood was perfused over 3 microspots in a parallel flow chamber <sup>17,20</sup>. In brief, degreased glass coverslips were coated overnight at 4 °C with microspots containing either: 100 µg/ml fibrillar collagen, 250 µg/ml GFOGER-GPO + 100 µg/ml VWF-BP, 250 µg/ml GFOGER-GPP + 100 µg/ml VWF-BP or 100 µg/ml collagen-III. Blood samples

were preincubated for 10 minutes with either 500 nM Nb21, 20  $\mu$ M PRT-060318, 20  $\mu$ g/ml 6F1 mAb or 100  $\mu$ M EHT-1864, before addition of 40  $\mu$ M PPACK, 3.75 mM MgCl<sub>2</sub>, 7.5 mM CaCl<sub>2</sub> and 100 nM Nb28 AF488, following perfusion through a microfluidic chamber at wall-shear rate of 1000/s. After 3.5 minutes, two brightfield images were taken while flowing with label buffer <sup>16</sup>, to stain for PS exposure (AF568 annexin A5, ThermoFisher) and CD62P expression (AF647 anti-CD62P mAb, BioLegend). Fluorescence images of 3 fields of view were taken post-labeling and after perfusion of rinse buffer. Brightfield and fluorescence images of activation markers were quantified for surface area coverage by semi-automated ImageJ scripts <sup>20</sup>. Images of GPVI clustering were analyzed as detailed below. Microscopic recording during flow experiments was with an EVOS-FL microscope (ThermoFisher) equipped with an Olympus UPLSAPO 60x oil immersion objective <sup>20</sup>.

### **GPVI cluster quantification**

A random forest-based pixel classifier was trained within Ilastik (1.3.3post3) <sup>21</sup> to split the collected GPVI fluorescence images into three classes; background (no platelets), platelets (diffuse GPVI signal) and receptor clusters (brighter, localized GPVI signal). Training images were selected from across conditions and replicates and were annotated within the Ilastik user interface. The classifier was then run on the full dataset with a Fiji macro <sup>22</sup>, which also extracted the cluster and cell area parameters. For the calculation of mean cluster area, a minimum cluster size of 5 pixels was set.

### **Statistical analysis**

Data are shown as mean  $\pm$  SD. Statistical analyses were performed in GraphPad Prism V7, with tests detailed in figure legends.

### 5.3 Results and Discussion

Nanobodies, which consist of the variable region of cameloid heavy chain only antibodies, are stable and target-specific antibody fragments. Their small size (12-15kDa) high affinity renders them excellent imaging tools<sup>23</sup>. To assess the clustering of platelet GPVI in flow-dependent thrombus formation, whole blood supplemented with AF488-labeled Nb28 before perfusion over two substrates previously shown to have high GPVI activation potential (fibrillar collagen-I and collagen-like peptide GFOGER-GPO)<sup>16</sup>, and over two substrates with low GPVI activation potential (GFOGER-GPP and collagen-III)<sup>16</sup> (**Figure 1**). The collagen-like peptides were supplemented with von WVF-BP to allow shear-dependent platelet adhesion via GPIb-IX-V<sup>17</sup>. Fluorescence images of GPVI taken at the platelet-substrate focal-plane, revealed that high-intensity labeling, representing focused GPVI clusters, was only visible on the high activation substrates, in contrast to the more diffuse labeling patterns seen on the low GPVI activation substrates (**Figure 1A**). The Ilastik segmentation image shows detected GPVI clusters as white and non-clustered GPVI on platelets as green (**Figure 1A**, bottom row).

All of the four utilized substrates supported platelet adhesion and, to varying degrees, subsequent thrombus formation (**Figure 1A**). Quantification of platelet deposition in brightfield images revealed no difference between fibrillar collagen, GFOGER-GPO and GFOGER-GPP. However, there was an increase in platelet deposition on human collagen-III compared to fibrillar collagen-I and GFOGER-GPP (**Figure 1B**), but the thrombi formed on collagen III were also significantly less multi-layered than those on collagen-I. Formation of multi-layered thrombi was also significantly higher on fibrillar collagen-I in comparison to the integrin  $\alpha 2\beta 1$ -binding GFOGER-GPP peptide (**Figure 1C**). Although quantitation of the thrombi formed on GFOGER-GPO did not detect statistically significant differences in platelet deposition or

multilayer compared to the other collagens, the thrombi looked morphologically different in brightfield images in that they appeared tightly contracted (**Figure 1A**).

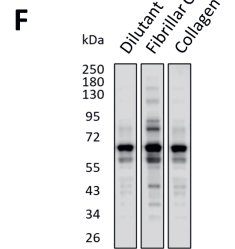
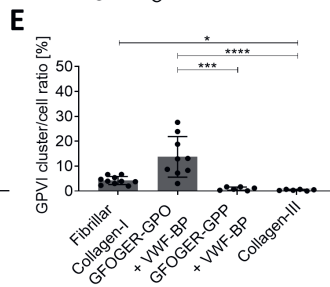
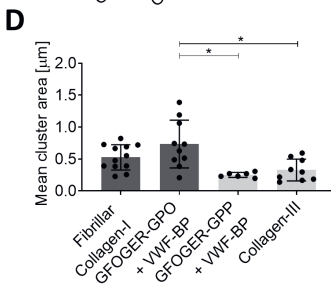
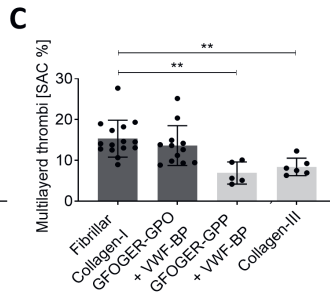
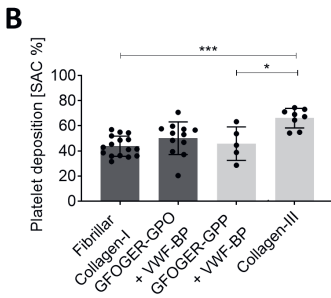
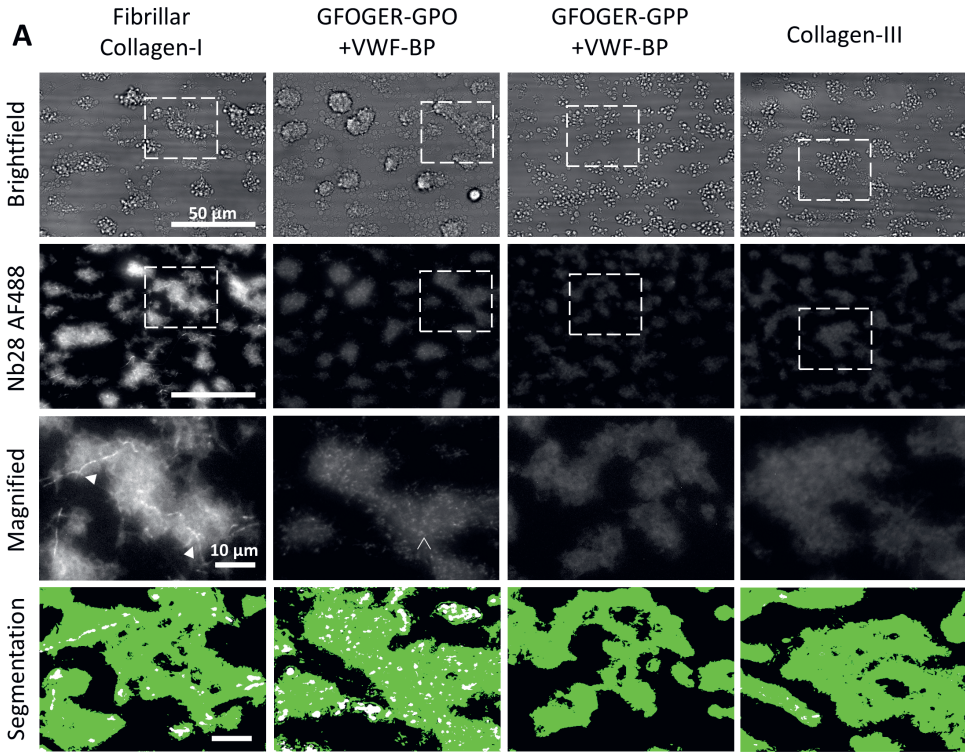
In immune cells, receptor clustering was found to be crucial for generating strong and sustained signaling signals <sup>24-26</sup>. Previous single molecule super-resolution microscopy of GPVI on platelets spreading on different collagenous substrates has shown that GPVI micro-clusters form on all substrates tested, including collagen-III, and there are differences in the sizes of these micro-clusters depending on the collagen type <sup>6</sup>. However, it is the macro-clusters, also visible under diffraction limited microscopy, that colocalize with the phosphorylated Syk and LAT proteins, therefore appear to be the hubs of sustained GPVI signaling <sup>7</sup>. The Nb28 AF488 labeling of GPVI in flow over fibrillar collagen- showed that macro-clusters of GPVI formed and aligned with the visible collagen fibers (**Figure 1A**, closed arrowhead), as we have shown recently <sup>15</sup>. The GFOGER-GPO peptide also induced visible, punctate, macro-clusters of GPVI (**Figure 1A**, open arrowhead), whereas GFOGER-GPP and collagen-III did not.

GPVI clusters could be segmented from the images using the machine learning, pixel classification software Ilastik <sup>21</sup>, which allowed cluster parameters to be quantified automatically (**Figure 1D,E**). We observed increased values for mean cluster area, as well as the proportion of the GPVI that was found in clusters (GPVI cluster: GPVI on platelet ratio) in platelets adhering to the high GPVI-dependent collagen types. The GPVI cluster size and proportion in clusters was significantly larger for GFOGER-GPO compared to GFOGER-GPP and collagen-III, whilst the proportion of receptor in clusters in platelets on fibrillar collagen-I was significantly greater than in platelets adhering to collagen-III (**Figure1 E**). In addition, western blot analysis of the tyrosine phosphorylation profile of platelets stimulated in suspension by

fibrillar collagen-I or collagen-III confirmed that fibrillar collagen-I induced increased signaling activity compared to collagen-III (**Figure 1F**). Taken together, these results indicate that there is a positive relationship between GPVI cluster size, downstream signaling activity and the formation of larger platelet aggregates.

Microfluidic assays allow measurements of multi-layered thrombus formation, as well as platelet activation by fluorescent labeling for P-selectin expression or PS exposure by annexin A5 binding <sup>17,20</sup>. Representative images of P-selectin and PS exposure induced by the different collagenous substrates are in **Figure 2A**. Quantitation of the surface area coverage of these markers demonstrated that there was no difference in the expression of P-selectin in platelets in contact with any of the four tested substrates (**Figure 2B**).

**Figure 1 (following page) – Nb28 AF488 assesses platelet GPVI cluster formation on collagenous substrates.** Recalcified and thrombin-inhibited whole blood supplemented with 100 nM Nb28 AF488 and at arterial shear rates (1000/s) perfused over fibrillar collagen-I, GFOGER-GPO + VWF-BP, GFOGER-GPP + VWF-BP or collagen-III. (A) Representative images of formed aggregates and GPVI clusters at focal plane of the substrates as well as output after cluster quantification (green=aggregates, white=clusters). Quantification of surface area covered (SAC) by (B) platelets and (C) thrombi. GPVI surface distribution expressed in the mean GPVI cluster size (D) as well as the pixel ratio between GPVI in clusters and GPVI on platelets (E) (n=5-16). (F) Western blot from platelets stimulated with 10 µg/ml fibrillar collagen-I or collagen-III for 180 seconds and blotted for total tyrosine kinase phosphorylation with 4G10 mAb (n=3). Scale bar = 50 µm and 10 µm full image and zoomed in, respectively. Mean ±SD, \*p <0.05, \*\*p <0.005, \*\*\*p <0.0005 (one-way ANOVA).



The ability of collagen-III to stimulate high P-selectin expression has been observed before <sup>17,20</sup>. This indicates that aggregate forming platelets, are active enough to secrete their  $\alpha$ -granules, regardless of the level of GPVI activation mediated by the substrate. However, platelet PS exposure is a well-established readout of overall GPVI activity <sup>5,27</sup> and we found highest PS exposure for platelets adhered on fibrillar collagen-I and GFOGER-GPO, with significant differences detected for both compared to collagen-III (**Figure 2C**). These data indicated that on collagen-like substrates with high GPVI activity (fibrillar collagen-I and GFOGER-GPO) GPVI forms large clusters and platelets exhibit a higher overall activation state under flow, as observed from the thrombus size and the PS exposure. In contrast, no macro-clusters of GPVI are seen in platelets adhering to substrates with low GPVI activity, *i.e.*, GFOGER-GPP and collagen-III, the thrombi are less multi-layered, and platelets are not so strongly activated.

In order to confirm this suggested relationship between GPVI clustering and overall platelet activation in whole blood flow, we studied whether the clustering, P-selectin and PS exposure observed on fibrillar collagen-I could be prevented by a panel of receptor or signaling inhibitors. For this purpose, we utilized the inhibitory anti-GPVI nanobody, Nb21 <sup>14</sup>; the selective, inhibitory anti- $\alpha 2\beta 1$  mAb 6F1 <sup>28</sup>; and small molecule drugs inhibiting the kinase downstream of GPVI, Syk (PRT-060318) <sup>16,29</sup> or the small GTPase Rac-1 (EHT-1864). Rac1 is known to affect phospholipase Cy2 activation in response to GPVI ligands, platelet spreading on collagen and platelet aggregate stability under flow <sup>30-33</sup>. Representative images of the effects by these treatments are in **Figure 3** with quantitation in **Figure 4**.



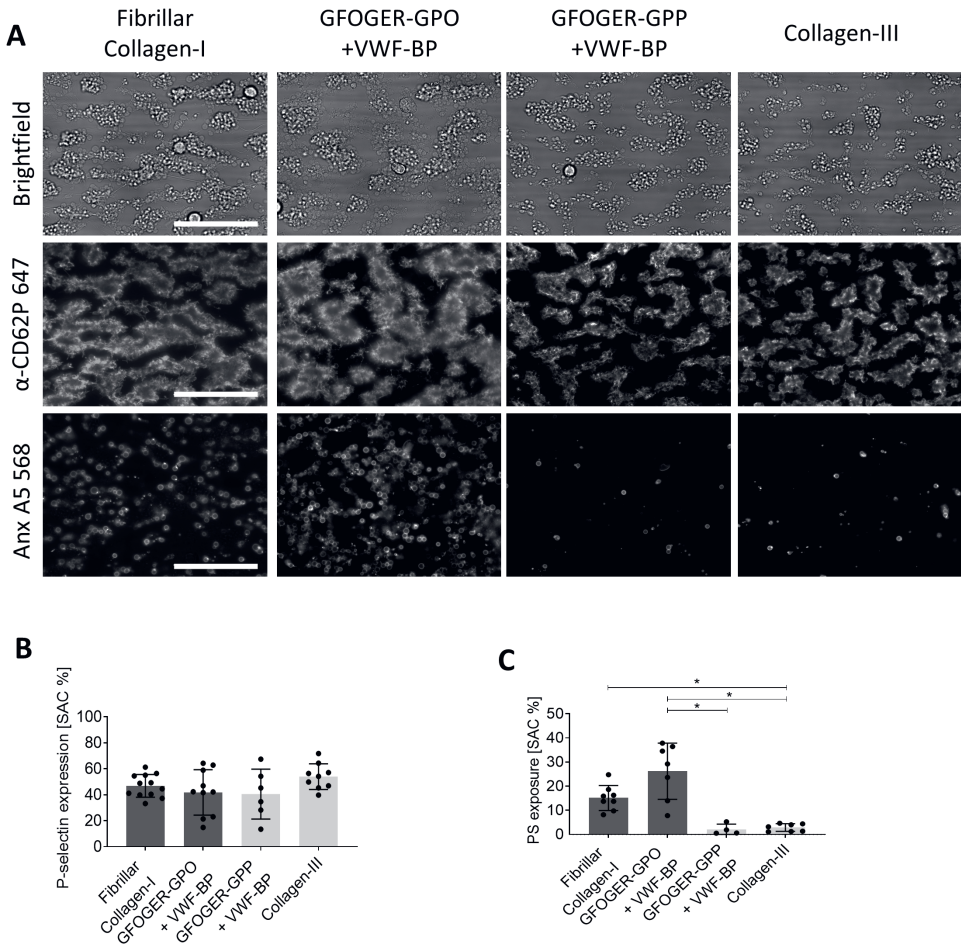


**Figure 2 – Relative presence of GPVI clusters correlates with number of phosphatidylserine exposing platelets.** Recalcified and thrombin-inhibited whole blood supplemented with Nb28 AF488 was perfused over indicated surfaces at 1000/s (see Figure 1); and at endpoint stained with AF647 anti-CD62P mAb (P-selectin) and AF 568 annexin A5 (PS exposure). (A) Representative images of thrombi and fluorescent staining. Quantification of surface area covered by P-selectin positive (B) and PS-exposing platelets (C). Further, quantification of mean GPVI cluster size (E) and pixel ratio of GPVI clusters/GPVI on platelets (F). Scale bar = 50  $\mu$ m. Means  $\pm$  SD (n=4-9), \*p <0.05, one-way ANOVA.

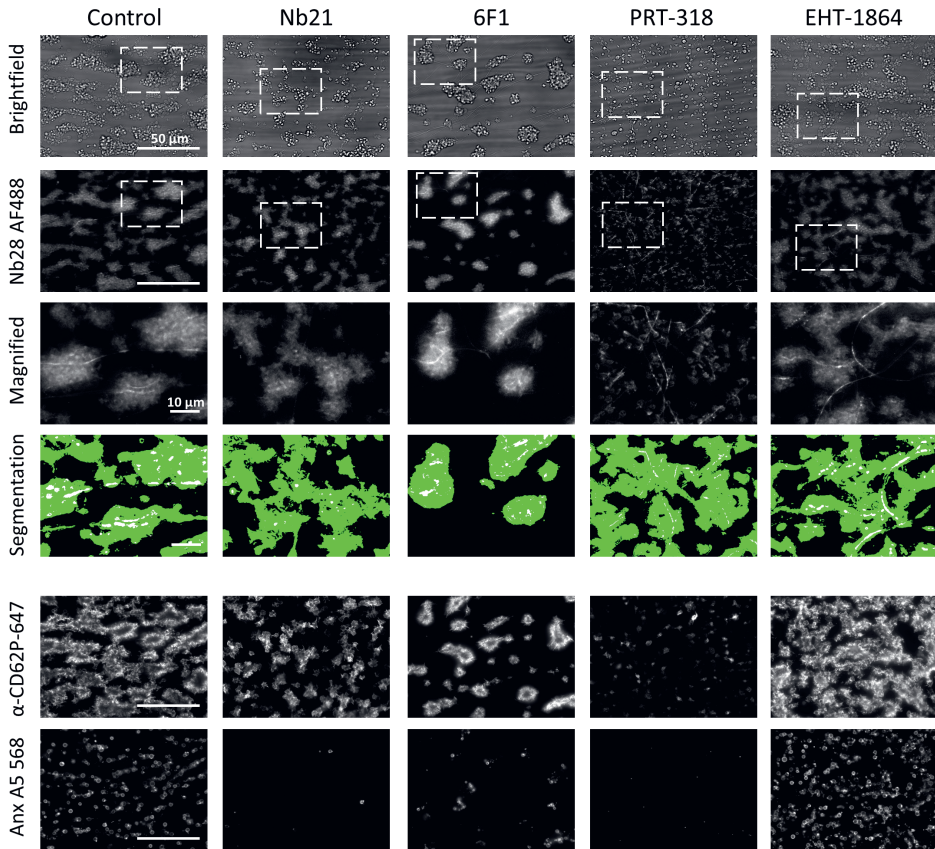


**Figure 3 – Inhibitor effects on parameters of thrombus formation on fibrillar collagen-I under flow.** Recalcified and thrombin-inhibited whole blood supplemented with 100 nM Nb28 AF488 was perfused over fibrillar collagen-I in the presence of vehicle control medium, 500 nM Nb21 (GPVI receptor inhibition), 20 μg/ml 6F1 ( $\alpha 2\beta 1$  inhibition), 20 μM PRT-060318 (Syk inhibition) or 500 μM EHT-1864 (Rac-1 inhibition). Representative images of (inhibited) thrombus formation and GPVI clusters. In addition, results of the segmentation analysis with GPVI clusters in white and platelets in green.  $\alpha$ -granule secretion was assessed by an antibody against P-selectin ( $\alpha$ -CD62P) and PS exposure was approximated from annexin A5 binding. Scale bar = 50 μm and 10 μm of full and zoomed-in images, respectively (n=4-8).

GPVI clustering was only disrupted by interfering with the GPVI-collagen interaction using Nb21 (**Figure 4A,B**). Whilst platelet deposition was unaffected (**Figure 4C**) as shown previously <sup>14</sup>, Nb21 caused a substantial and significant decrease in thrombus size (**Figure 4D**). P-selectin expression was unaffected (**Figure 4E**), but platelet PS exposure was significantly reduced (**Figure 4F**). Conversely, blockade of the other platelet collagen receptor, integrin  $\alpha 2\beta 1$ , did not affect GPVI clustering (**Figure 4A, B**) or PS exposure (**Figure 4F**) but decreased platelet deposition (**Figure 4C**), and multilayer thrombus formation (**Figure 4D**), which confirms previous data showing a role for integrin  $\alpha 2\beta 1$  in platelet adhesion to fibrillar collagen <sup>34,35</sup>. In addition, P-selectin expression was only reduced when integrin  $\alpha 2\beta 1$  was blocked, which has been shown before <sup>15</sup> and is likely due to the decreased platelet deposition, and thus fewer platelets to be P-selectin positive, when  $\alpha 2\beta 1$  is inhibited.

Pallini *et al.* <sup>7</sup> have shown that accumulation of signaling molecules is associated with GPVI clusters. Therefore, we utilized an inhibitor against Syk (PRT-060318) and one against Rac1 (EHT-1864) to interfere with the signaling pathway. Neither intervention affected GPVI clustering (**Figure 4A,B**). But inhibition of Syk by PRT-060318 almost completely abolished the formation of aggregates (**Figure 4D**). These findings are in accordance with previous data, showing a significant role of Syk in thrombus formation <sup>16</sup> and stability <sup>36</sup>. Moreover, GPVI clustering was maintained in the platelets adhered to the collagen under flow, which has also been observed in PRT-060318-treated spread platelets <sup>6,7</sup>. However, it did inhibit GPVI-mediated expression of platelet activation markers as PS exposure was completely lost (**Figure 4F**). Thus, PRT-060318, by inhibiting downstream Syk activity, has uncoupled GPVI clustering from thrombus formation and PS exposure. On the other hand, Rac1 inhibition led to a significant increase in platelet deposition, reflecting its role in platelet aggregate stability with inhibition resulting

embolism and a greater surface area coverage<sup>31</sup>. Further although depletion or inhibition of Rac1 has previously been shown to affect PLC $\gamma$ 2 activation in murine platelets<sup>30</sup> and phosphorylation of the protein in human platelets<sup>33</sup>, in this study, under flow, Rac1 inhibition was not sufficient to cause any significant effect on thrombus formation or clustering of GPVI.

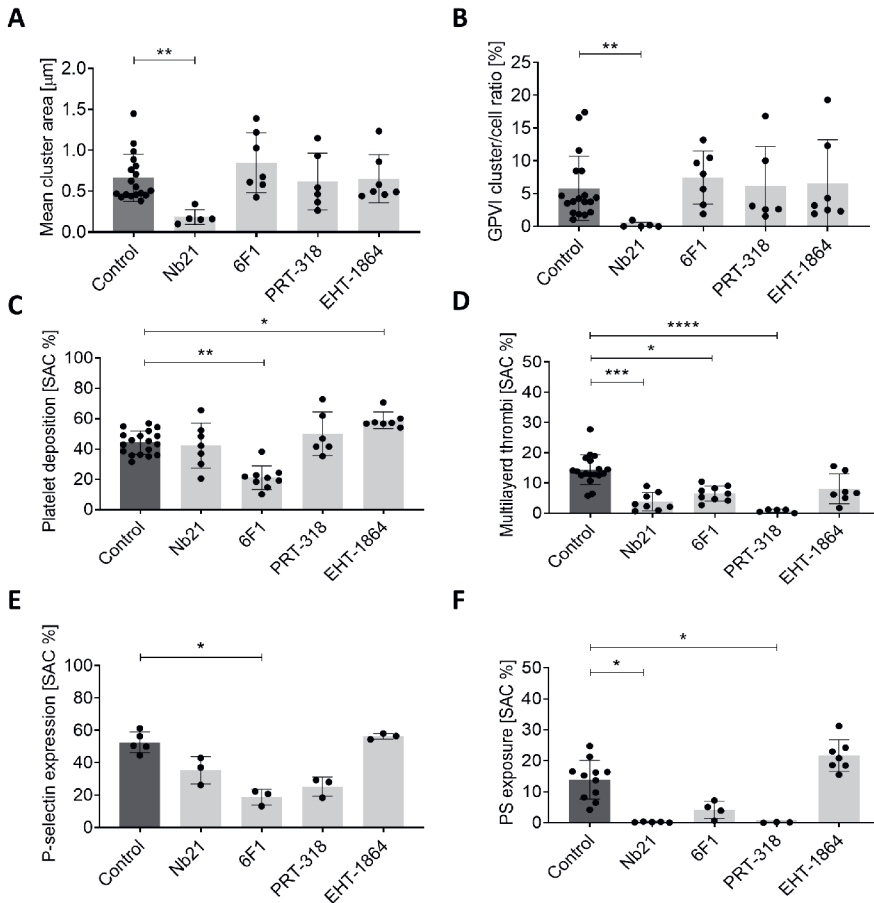


**Figure 4 – Inhibitor effects on GPVI clustering after blood perfusion over fibrillar collagen-I.** Quantification of data presented in Figure 3, namely quantification of GPVI cluster size (A) and GPVI cluster/platelet ratio (B). The surface area covered by platelets (C) and aggregates (D). Further. As well as expression of platelet activation markers P-selectin (E) or PS exposure (F). Means  $\pm$  SD (n=3-11), \*p < 0.05, \*\*p < 0.005, \*\*\*p < 0.0005 (one-way ANOVA).

The latter being in line with clustering studies on spread platelets<sup>33</sup>. Of note, in the present experimental set up, endpoint images are acquired and therefore alterations in thrombus built up over time are not reflected very well. This might explain less effects observed by EHT-1864 in comparison to alterations in aggregate formation in Rac1 knockout mice<sup>31</sup>.

Taken together, this study provides evidence for a relationship between the presence of GPVI macro-clusters in whole blood under flow and larger aggregates with more PS exposing platelets. In addition, the formation of GPVI clusters was independent of downstream signaling responses as it was only disrupted by GPVI receptor antagonism, and not by signaling inhibitors. These data give evidence that GPVI macro-cluster formation is needed to induce strong and sustained platelet activation, thrombus formation and platelet PS exposure. Accordingly, GPVI clustering is a prerequisite, but is not sufficient for full thrombus formation and platelet activation on highly GPVI-dependent collagen surfaces.

**Acknowledgements** NJJ is funded by a European Union's Horizon 2020 research and innovation program under Marie Skłodowska-Curie grant agreement No. 766118. NJJ is registered as a joint PhD student at the Universities of Maastricht (NL) and Birmingham (UK). SPW is a British Heart Foundation Professor (CH 03/003). The authors kindly thank Dr. Barry Coller for the  $\alpha 2\beta 1$  antibody 6F1.

**Authorship Contributions** NJJ designed and performed experiments, analyzed data, prepared figures and wrote the manuscript. CWS performed experiments and wrote the manuscript. JAP coded the clustering analysis pipeline. RWF supplied collagen-like peptides. YH, JWMH and SPW provided funding and supervision. NSP designed experiments, analyzed data, provided

supervision and funding, and wrote the manuscript. All authors have read and approved the manuscript.

**Conflicts of Interest** SPW and NSP have a patent for the anti-GPVI nanobodies: WO2022/136457.

## **5.4 References**

1. Nieswandt B, Watson SP. Platelet-collagen interaction: is GPVI the central receptor? *Blood*. 2003; 102:449-461.
2. Moroi M, Onitsuka I, Imaizumi T, Jung SM. Involvement of activated integrin  $\alpha 2\beta 1$  in the firm adhesion of platelets onto a surface of immobilized collagen under flow conditions. *Thromb Haemost*. 2000; 83:769-776.
3. Versteeg HH, Heemskerk JW, Levi M, Reitsma PH. New fundamentals in hemostasis. *Physiol Rev*. 2013; 93:327-358.
4. Stegner D, Haining EJ, Nieswandt B. Targeting glycoprotein VI and the immunoreceptor tyrosine-based activation motif signaling pathway. *Arterioscler Thromb Vasc Biol*. 2014; 34:1615-1620.
5. Nagy M, Perrella G, Dalby A, *et al*. Flow studies on human GPVI-deficient blood under coagulating and noncoagulating conditions. *Blood Adv*. 2020; 4:2953-2961.
6. Poulter NS, Pollitt AY, Owen DM, *et al*. Clustering of glycoprotein VI (GPVI) dimers upon adhesion to collagen as a mechanism to regulate GPVI signaling in platelets. *J Thromb Haemost*. 2017; 15:549-564.
7. Pallini C, Pike JA, O'Shea C, *et al*. Immobilized collagen prevents shedding and induces sustained GPVI clustering and signaling in platelets. *Platelets*. 2021; 32:59-73.
8. Onselaer MB, Nagy M, Pallini C, *et al*. Comparison of the GPVI inhibitors losartan and honokiol. *Platelets*. 2020; 31:187-197.
9. Jarvis GE, Raynal N, Langford JP, *et al*. Identification of a major GpVI-binding locus in human type III collagen. *Blood*. 2008; 111:4986-4996.
10. Farndale RW. Collagen-binding proteins: insights from the collagen toolkits. *Essays Biochem*. 2019; 63:337-348.
11. Smethurst PA, Joutsu-Korhonen L, O'Connor MN, *et al*. Identification of the primary collagen-binding surface on human glycoprotein VI by site-directed mutagenesis and by a blocking phage antibody. *Blood*. 2004; 103:903-911.
12. Munnix IC, Gilio K, Siljander PR, *et al*. Collagen-mimetic peptides mediate flow-dependent thrombus formation by high- or low-affinity binding of integrin  $\alpha 2\beta 1$  and glycoprotein VI. *J Thromb Haemost*. 2008; 6:2132-2142.

13. Pugh N, Simpson AM, Smethurst PA, de Groot PG, Raynal N, Farndale RW. Synergism between platelet collagen receptors defined using receptor-specific collagen-mimetic peptide substrata in flowing blood. *Blood*. 2010; 115:5069-5079.
14. Slater A, Di Y, Clark JC, *et al*. Structural characterization of a novel GPVI-nanobody complex reveals a biologically active domain-swapped GPVI dimer. *Blood*. 2021; 137:3443-3453.
15. Jooss NJ, Smith CW, Slater A, *et al*. Anti-GPVI nanobody blocks collagen- and atherosclerotic plaque-induced GPVI clustering, signaling and thrombus formation. *J Thromb Haemost*. 2022, in press.
16. Jooss NJ, De Simone I, Provenzale I, *et al*. Role of platelet glycoprotein VI and tyrosine kinase Syk in thrombus formation on collagen-like surfaces. *Int J Mol Sci*. 2019; 20:2788.
17. de Witt SM, Swieringa F, Cavill R, *et al*. Identification of platelet function defects by multi-parameter assessment of thrombus formation. *Nat Commun*. 2014; 5:4257.
18. Nicolson PLR, Nock SH, Hinds J, *et al*. Low-dose Btk inhibitors selectively block platelet activation by CLEC-2. *Haematologica*. 2021; 106:208-219.
19. Nicolson PLR, Hughes CE, Watson S, *et al*. Inhibition of Btk by Btk-specific concentrations of ibrutinib and acalabrutinib delays but does not block platelet aggregation mediated by glycoprotein VI. *Haematologica*. 2018;103:2097-2108.
20. Van Geffen JP, Brouns SL, Batista J, *et al*. High-throughput elucidation of thrombus formation reveals sources of platelet function variability. *Haematologica*. 2019; 104:1256-1267.
21. Berg S, Kutra D, Kroeger T, *et al*. Ilastik: interactive machine learning for (bio)image analysis. *Nat Methods*. 2019; 16:1226-1232.
22. Schindelin J, Arganda-Carreras I, Frise E, *et al*. Fiji: an open-source platform for biological-image analysis. *Nat Methods*. 2012; 9:676-682.
23. Erreni M, Schorn T, D'Autilia F, Doni A. Nanobodies as versatile tool for multiscale imaging modalities. *Biomolecules*. 2020; 10:1695.
24. Mbiribindi B, Mukherjee S, Wellington D, Das J, Khakoo SI. Spatial clustering of receptors and signaling molecules regulates NK cell response to peptide repertoire changes. *Front Immunol*. 2019; 10:605.
25. Minguet S, Swamy M, Alarcón B, Luescher IF, Schamel WW. Full activation of the T cell receptor requires both clustering and conformational changes at CD3. *Immunity*. 2007; 26:43-54.
26. Pigeon SV, Tabarin T, Yamamoto Y, *et al*. Functional role of T-cell receptor nanoclusters in signal initiation and antigen discrimination. *Proc Natl Acad Sci USA*. 2016; 113:e5454-5463.

27. Siljander PR, Munnix IC, Smethurst PA, *et al.* Platelet receptor interplay regulates collagen-induced thrombus formation in flowing human blood. *Blood*. 2004; 103:1333-1341.
28. Collier BS, Beer JH, Scudder LE, Steinberg MH. Collagen-platelet interactions: evidence for a direct interaction of collagen with platelet GPIa/IIa and an indirect interaction with platelet GPIIb/IIIa mediated by adhesive proteins. *Blood*. 1989; 74:182-192.
29. Hoellenriegel J, Coffey GP, Sinha U, *et al.* Selective, novel spleen tyrosine kinase (Syk) inhibitors suppress chronic lymphocytic leukemia B-cell activation and migration. *Leukemia*. 2012; 26:1576-1583.
30. Pleines I, Elvers M, Strehl A, *et al.* Rac1 is essential for phospholipase C $\gamma$ 2 activation in platelets. *Pflugers Arch*. 2009; 457:1173-1185.
31. McCarty OJ, Larson MK, Auger JM, *et al.* Rac1 is essential for platelet lamellipodia formation and aggregate stability under flow. *J Biol Chem*. 2005; 280:39474-39484.
32. Stefanini L, Boulaftali Y, Ouellette TD, *et al.* Rap1-Rac1 circuits potentiate platelet activation. *Arterioscler Thromb Vasc Biol*. 2012; 32:434-441.
33. Neagoe RAI, Gardiner EE, Stegner D, Nieswandt B, Watson SP, Poulter NS. Rac inhibition causes impaired GPVI signalling in human platelets through GPVI shedding and reduction in PLC $\gamma$ 2 phosphorylation. *Int J Mol Sci*. 2022; 23:3746.
34. Pugh N, Maddox BD, Bihan D, Taylor KA, Mahaut-Smith MP, Farndale RW. Differential integrin activity mediated by platelet collagen receptor engagement under flow conditions. *Thromb Haemost*. 2017; 117:1588-1600.
35. Auger JM, Kuijpers MJ, Senis YA, Watson SP, Heemskerk JW. Adhesion of human and mouse platelets to collagen under shear: a unifying model. *FASEB J*. 2005; 19:825-827.
36. Perrella G, Montague SJ, Brown HC, *et al.* Role of tyrosine kinase Syk in thrombus stabilisation at high shear. *Int J Mol Sci*. 2022; 23:493.







# Chapter 6

## Platelet glycoprotein VI and tyrosine kinase Syk in thrombus formation on collagen-like surfaces

Natalie J. Jooss<sup>†</sup>, Ilaria De Simone<sup>†</sup>, Isabella Provenzale<sup>†</sup>, Delia I. Fernandez<sup>†</sup>, Sanne L. N. Brouns, Richard W. Farndale, Yvonne M. C. Henskens, Marijke J. E. Kuijpers, Hugo ten Cate, Paola E. J. van der Meijden, Rachel Cavill and Johan W. M. Heemskerk

<sup>†</sup> Equal contribution

Contributions: NJJ designed and performed experiments, analyzed data, prepared figures and wrote the manuscript

Published: International Journal of Molecular Science, 2019, Vol 20, Pages 2788

**Abstract** Platelet interaction with collagens, facilitated by von Willebrand factor, is a potent trigger of shear-dependent thrombus formation mediated by subsequent engagement of collagen receptors, glycoprotein (GP)VI and integrin  $\alpha 2\beta 1$ . Protein tyrosine kinase Syk is central in the GPVI-induced platelet signaling pathway leading to elevated cytosolic  $Ca^{2+}$ . Here, we aimed to determine the Syk-mediated thrombogenic activity for several collagen peptides and (native) type I and III collagens. Whole blood was perfused over microspots of these substances, and thrombus formation was assessed using eight parameters, indicative of platelet adhesion, activation, aggregation and contraction, such as affected by the selective Syk inhibitor, PRT-060318. In platelet suspensions, only collagen peptides containing the consensus GPVI-activating sequence  $(GPO)_n$  and Horm collagen fibers caused Syk-dependent cytosolic  $Ca^{2+}$  rises. In microspots, these substances potently induced Syk-dependent thrombus formation. In contrast, integrin-binding collagen peptides without  $(GPO)_n$  sequence and other native fibrillar collagens stimulated platelets in a Syk-dependent way, only in whole blood under flow. Prediction models, based on regression analysis, indicated a mixed role of GPVI in thrombus formation on native collagen surfaces, which was abolished upon inhibition of Syk. Together, these findings indicate that GPVI-dependent signaling via the tyrosine kinase Syk supports platelets in thrombus formation on all fibrillar collagens and collagen peptides, even those lacking the  $(GPO)_n$  sequence.

## 6.1 Introduction

Platelet interaction with subendothelial collagens is a crucial step in hemostasis and arterial thrombosis after vascular injury and rupture of an atherosclerotic plaque, respectively <sup>1,2</sup>. In blood subjected to high shear rates, initial capture of platelets is mediated by von Willebrand factor (VWF), the latter of which is a ligand for the glycoprotein (GP) complex GPIb-V-IX <sup>3</sup> immobilized on exposed collagen. The two platelet collagen receptors, integrin  $\alpha 2\beta 1$  and GPVI, ensure stable platelet adhesion and mediate platelet activation <sup>4,5</sup>. For over twenty years, GPVI has been recognized as the central platelet-activating receptor for collagens <sup>6,7</sup>.

Studies using genetically modified mice have shown that the (patho)physiological process of arterial thrombus formation can be approximated by using microfluidics devices, in which whole blood is perfused over a collagen surface <sup>8</sup>. Collagen fibers immobilized in such devices, for instance in the form of microspots, bind plasma VWF, and then promote shear-dependent platelet adhesion, activation and aggregation <sup>3,9</sup>. Flow-dependent techniques have revealed a strong interplay of the receptors GPIb-V-IX, GPVI and  $\alpha 2\beta 1$  in the formation of large and stable multi-layered thrombi <sup>10,11</sup>. Markedly, the thrombi that are formed on collagen fibers are heterogeneous in structure with on the one hand, patches of aggregated platelets, expressing active  $\alpha \text{IIb}\beta 3$  integrins that bind fibrinogen and expressing CD62P following  $\alpha$ -granule secretion, and on the other hand, single procoagulant platelets, exposing phosphatidylserine (PS) that is, required for coagulation factor binding <sup>12</sup>. Particularly active in supporting thrombus formation is the standard collagen preparation Horm (collagen-H), which is a fibrillar type I collagen, prepared in a proprietary process, commonly used for diagnostics in the clinical laboratory. Still unexplained is why other

fibril-forming type I and III collagen preparations, also binding VWF, are less active in supporting thrombus formation under flow<sup>9, 13</sup>.

In the last two decades, synthetic collagen derived triple-helical peptides have been identified which, similarly to collagen-H, bind to GPVI and/or integrin  $\alpha 2\beta 1$ , and hence can induce platelet adhesion and activation *in vitro*<sup>10</sup>. Peptides containing the (GPO)<sub>n</sub> motif, in contrast to the supposedly inactive (GPP)<sub>n</sub> motif, bind to GPVI, whilst peptides with the GFOGER motif act as strong ligands for  $\alpha 2\beta 1$ <sup>14-16</sup>. Prototypes of such triple-helical peptides are the cross-linked collagen-related peptide (CRP-XL), with a (GPO)<sub>10</sub> sequence, acting as a potent GPVI agonist; and the combined GFOGER-(GPO)<sub>n</sub> sequence, binding to platelets via both receptors. Subtle changes in the GFOGER sequence were found to alter the affinity for  $\alpha 2\beta 1$ . For instance, substitution of phenylalanine in GFOGER with alanine in GAOGER resulted in lower affinity  $\alpha 2\beta 1$  binding, and to diminished platelet adhesion under static conditions<sup>17</sup>.

Platelet activation through GPVI<sup>18-20</sup>, but not through GPIb<sup>21</sup>, relies on a potent protein tyrosine kinase cascade, culminating in activation of the tyrosine kinase Syk. This GPVI signaling pathway involves phosphorylation of Fc receptor  $\gamma$ -chain via Src-family kinases, formation of a GPVI signalosome, after which Syk phosphorylates and activates phospholipase C (PLC) $\gamma 2$ , resulting in a rise of the central second messenger Ca<sup>2+</sup><sup>18, 22-24</sup>. However, the relative importance of this pathway was so far not investigated in platelets interacting under flow with surface-immobilized collagen peptides or native collagens – with differences in GPVI and  $\alpha 2\beta 1$  binding.

In the present paper, we aimed to investigate the role of GPVI, activating via Syk, in the establishment of thrombus formation under high shear induced by collagen like surfaces. Particular attention was given to the sub-processes of platelet adhesion, aggregation, and contraction as well as

to specific platelet activation processes. For this purpose, we used several collagen peptides and collagen-H, with an established GPVI dependency, and the selective Syk inhibitor PRT-060318 (Syk-IN). The latter compound has already been used to identify Syk-dependent pathways in mouse platelets <sup>21, 25</sup> and human T-cells <sup>26</sup>. As a direct readout of this signaling pathway, we assessed the Syk-dependent cytosolic Ca<sup>2+</sup> rises in platelets.

## **6.2 Materials and Methods**

### **Materials**

Collagen-related triple-helical peptides were synthesized as C-terminal amides and purified by reverse phase high performance liquid chromatography <sup>44, 45</sup>: H-GPC(GPO)<sub>3</sub>GFOGER(GPO)<sub>3</sub>GPC-NH<sub>2</sub> (GFOGER-GPO); H-GPC(GPP)<sub>5</sub>GFOGER(GPP)<sub>5</sub>GPC-NH<sub>2</sub> (GFOGER-GPP); cross-linked collagen-related (GPO)<sub>n</sub> peptide (CRP-XL); GPC(GPO)<sub>3</sub>GAOGER(GPO)<sub>3</sub>GPC-NH<sub>2</sub> (GAOGER-GPO); collagen type-III derived VWF-binding peptide VWF-III (VWF-BP), H-GPC(GPP)<sub>5</sub>GPRGQOGVMGFO (GPP)<sub>5</sub>GPC-NH<sub>2</sub> <sup>46</sup>. Collagen-I Horm derived from equine tendon (collagen-H) was obtained from Nycomed (Hoofddorp, The Netherlands); Human placenta-derived collagen-III (C4407) and fibrillar collagen-I (C7774) came from (Sigma-Aldrich (Zwijndrecht, The Netherlands). The latter was used to prepare monomeric collagen-I by pepsin treatment, as described <sup>47</sup>. The selective spleen tyrosine kinase (Syk) inhibitor PRT-060318 ((1R,2S)-2-aminocyclohexylamino)-4-(m-tolylamino)pyrimidine-5-carboxamide (Syk-IN) came from Bio-connect (Huissen, The Netherlands). Used for fluorescent staining were AlexaFluor(AF) 647 labeled anti-human CD62P mAb (304918, Biolegend, London, UK), FITC-labeled fibrinogen (F0111, Dako, Amstelveen, The Netherlands), and AF568-labeled annexin A5 (A13202, ThermoFisher, Eindhoven, The Netherlands). Fura-2 acetoxymethyl ester and pluronic were

from Invitrogen (Carlsbad CA, USA). Other materials were from sources described before <sup>48</sup>.

### **Blood isolation**

Blood was obtained by venepuncture from healthy volunteers, who had not received anti-platelet medication for at least two weeks. All subjects gave full informed consent according to the declaration of Helsinki. Studies were approved by the local Medical Ethics Committee. Blood samples were collected into 3.2% trisodium citrate (Vacurette tubes, Greiner Bio-One, Alphen a/d Rijn, The Netherlands). Subjects had platelet counts within the reference range, as measured with a Sysmex XN-9000 analyzer (Sysmex, Cho-ku, Kobe, Japan).

### **Platelet isolation and loading with Fura-2**

Platelet-rich plasma (PRP) was obtained from citrated blood by centrifugation at 870 g for 10 minutes. After addition of 1:10 vol./vol. acid citrate dextrose (ACD; 80 mM trisodium citrate, 183 mM glucose, 52 mM citric acid), the isolated PRP was centrifuged at 2,360 g for 2 minutes. Platelet pellets were resuspended into HEPES buffer pH 6.6 (10 mM HEPES, 136 mM NaCl, 2.7 mM KCl, 2 mM MgCl<sub>2</sub>, 5.5 mM glucose and 0.1 % bovine serum albumin). After addition of apyrase (1 U/ml) and 1:15 vol./vol. ACD, another centrifugation step was performed to obtain washed platelets <sup>48</sup>. The final pellet was resuspended in HEPES buffer pH 7.45.

### **Light transmission aggregometry**

Aggregation of washed platelets was measured by light transmission aggregometry, as described <sup>48</sup> using an automated Chronolog aggregometer (Havertown PA, USA). Platelet aggregation rate was determined from maximal curve slopes (% transmission change per minute).

## Whole blood microfluidic perfusion over microspots

Selected collagen-like peptides and collagens were microspotted on glass coverslips, essentially as described <sup>9</sup>. Table 1 displays the coding of nine microspots (M1-9).

**Table 1 – Overview of composition of microspots (M1-9), platelet receptors implicated in thrombus formation, and analyzed thrombus parameters (P1-8) from brightfield and fluorescence microscopic images, which were scaled as indicated for heatmap analysis. \*No GPVI-activating (GPP)<sub>n</sub> motif.**

<i>Microspot</i>		Platelet receptors		
		GPVI	$\alpha 2\beta 1$	GP1b
<i>M1</i>	GFOGER-GPO + VWF-BP	++	++	++
<i>M2</i>	CRP-XL + VWF-BP	++	o	++
<i>M3</i>	GAOGER-GPO + VWF-BP	++	+	++
<i>M4</i>	GFOGER-GPP + VWF-BP	(o) <sup>*</sup>	++	++
<i>M5</i>	VWF-BP	o	o	++
<i>M6</i>	Collagen-H (Horm type)	++	++	++
<i>M7</i>	Fibrillar collagen-I (human)	n.d.	n.d.	n.d.
<i>M8</i>	Monomeric collagen-I (human)	n.d.	n.d.	++
<i>M9</i>	Collagen-III (human)	n.d.	n.d.	++
<i>Parameter</i>		range	scaled	
<i>Brightfield</i>				
<i>P1</i>	Platelet deposition (% SAC)	0 - 51.52	0 - 10	
<i>P2</i>	Platelet aggregate coverage (% SAC)	0 - 21.09	0 - 10	
<i>P3</i>	Thrombus morphological score	0 - 4.10	0 - 10	
<i>P4</i>	Thrombus multilayer score	0 - 2.60	0 - 10	
<i>P5</i>	Thrombus contraction score	0 - 2.94	0 - 10	
<i>Fluorescence images</i>				
<i>P6</i>	PS exposure (% SAC)	0 - 13.91	0 - 10	
<i>P7</i>	CD62P expression (% SAC)	0 - 46.71	0 - 10	
<i>P8</i>	Fibrinogen binding (% SAC)	0 - 28.33	0 - 10	

N.d., not determined.

In brief, washed coverslips were coated with 3 different microspots, each containing a collagen (100  $\mu\text{g/ml}$ ) or a combination of collagen-like peptide (250  $\mu\text{g/ml}$ ) with VWF-BP (100  $\mu\text{g/ml}$ ). Coating doses were chosen to obtain maximal platelet adhesion in flow assays <sup>9</sup>. The most active microspots were



always located upstream, thereby preventing cross-activation of platelets between microspots<sup>9</sup>. Coated coverslips were incubated overnight in a humid chamber at 4°C, and then blocked with HEPES buffer pH 7.45 containing 1% bovine serum albumin for 30 minutes, before mounting into the Maastricht microfluidic chamber. For flow perfusion, 500 µl of citrated whole blood was preincubated for 10 minutes with either vehicle (0.5% DMSO and 0.4 µg/ml pluronic, f.c.) or inhibitor PRT-060318 (Syk-IN, 20 µM in vehicle solution, f.c.). After addition of 40 µM PPACK and recalcification (3.75 mM MgCl<sub>2</sub> and 7.5 mM CaCl<sub>2</sub>), blood samples were perfused through the microspot-containing flow chamber for 3.5 minutes at a wall shear rate of 1000/s. After 2 minutes of staining for PS exposure (AF568 annexin A5), CD62P expression (AF647 anti-CD62P mAb) and integrin αIIbβ3 activation (FITC-fibrinogen), residual label was removed by post-perfusion with HEPES buffer pH 7.45, containing 2 mM CaCl<sub>2</sub> and 1 U/ml heparin. Vehicle controls were performed in duplicates, while Syk-IN containing samples were repeated in triplicates, with blood from >5 healthy donors.

### **Brightfield and fluorescence microscopy**

From each microspot, two brightfield images (during labeling) and three 3-color fluorescence images (after removing label) were taken using an EVOS-FL microscope (Life Technologies, Bleiswijk, The Netherlands), equipped with Cy5, RFP and GFP LEDs, an Olympus UPLSAPO 60x oil-immersion objective, and a sensitive 1360×1024 pixel CCD camera<sup>49</sup>. Standardized image analysis was performed using semi-automated scripts operated in Fiji (ImageJ), as described<sup>49</sup>. Parameters extracted from brightfield images (P1-5), including thrombus signature scores (P3-5), and parameters from fluorescence images (P6-8) are indicated in Table 1.

## Cytosolic Ca<sup>2+</sup> measurements

Washed human platelets ( $2 \times 10^8$ /ml) were loaded with Fura-2 acetoxymethyl ester (3  $\mu$ M) and pluronic (0.4  $\mu$ g/ml) by 40 minutes incubation at room temperature. After another wash step and resuspension of platelets at the same concentration, changes in cytosolic [Ca<sup>2+</sup>]<sub>i</sub> were measured in 96-well plates using a Flex Station 3 (Molecular Devices, San Jose, CA, USA). In brief, 200  $\mu$ l of platelets were pre-treated with Syk-IN (PRT-060318, 5  $\mu$ M) or left untreated for 10 minutes. After addition of 1 mM CaCl<sub>2</sub>, the Fura-2-loaded cells were stimulated by automated pipetting with one of the following agonists (10  $\mu$ g/ml), for convenience indicated as M1-9 (see Table 1): GFOGER-GPO (M1), CRP-XL (M2), GAOGER-GPO (M3), GFOGER-GPP (M4), VWF-BP (M5), collagen-H (M6), fibrillar collagen-I (M7), monomeric collagen-I (M8) or collagen-III (M9).

Changes in Fura-2 fluorescence were measured over time at 37°C by ratio fluorometry, at dual excitation wavelengths of 340 and 380 nm, and emission wavelength of 510 nm. Agonist injection speed was set at 125  $\mu$ l/s, resulting in complete, diffusion-limited mixing. Separate wells contained Fura-2-loaded platelets that were lysed with 0.1% Triton-X-100 in the presence of 1 mM CaCl<sub>2</sub> or 9 mM EGTA/Tris, for determination of R<sub>max</sub> and R<sub>min</sub> values, respectively<sup>50</sup>. After correction for background fluorescence, ratio values were converted into nanomolar concentrations of [Ca<sup>2+</sup>]<sub>i</sub><sup>51</sup>. Measurements were performed in duplicate wells and completed within 2-3 hours of preparation of the cells.

## Data handling and statistics

GraphPad Prism 8 was employed for statistical analysis. Heatmaps were generated with the program R. For heatmap representation, parameter values were univariate normalized at a scale of 0-10<sup>46</sup>. Thrombus values of duplicate or triplicate flow runs from the same blood donor were averaged to obtain one

parameter set (vehicle plus Syk inhibited) per microspot and donor. Mean values of control and inhibitor runs were then compared per blood sample, using paired Student t-tests. P-values below 0.05 were considered to be significant. For subtraction heatmaps, a standard filter of  $p < 0.05$  was set to visualize relevant effects.

### **Modelling to predict GPVI activity**

Complete datasets (8 parameters, 9 surfaces) for flow runs of  $\geq 5$  donors were used to construct a partial-least square (PLS) model, to predict back for GPVI dependency. At first, range scaled data of the collagen peptide surfaces (M1-5) with known GPVI dependency were used to generate the PLS model, and collagen-H (M6) was predicted back to test the models reliability. Principal component analysis (PCA) in 1- and 2-component mode was used, while predictions were supported by cross-validated analysis of Q2, defined as  $1 - (\text{PRESS}/\text{TSS})$ <sup>52</sup>. Subsequently, parameter sets of M7-9 were predicted for GPVI dependency from the PLS model, as were parameters of M1-9 in the presence of Syk-IN. By default, prediction values of  $> 0.5$  were considered as positive for a GPVI dependency.

## **6.3 Results**

### **GPVI-dependent and Syk-dependent platelet activation by collagen-like peptides**

In order to validate the assumed potency of distinct collagen peptides to act as ligands for platelet GPVI, we first examined their ability to stimulate PLC $\gamma$ 2-mediated rises in cytosolic  $\text{Ca}^{2+}$ . As a discriminative inhibitor of this pathway, we used the compound PRT-060318 (Syk-IN), which has allowed to identify Syk-dependent activation pathways, evoked by GPVI<sup>21, 25</sup> or CLEC-2<sup>27</sup>. This compound furthermore phenocopied the consequences of Syk depletion in *Syk*<sup>-/-</sup> bone marrow chimeric mice on platelet responses<sup>28</sup>. Moreover, in

human platelets, Syk-IN selectively blocked GPVI/Syk-dependent tyrosine phosphorylation and aggregation responses of platelets in contact with fibrin<sup>29</sup>.

To obtain further information on the selectivity of Syk-IN as an inhibitor of GPVI-induced responses of human platelets, we monitored its effect (at common dose of 5  $\mu$ M) on platelet aggregation induced by CRP-XL, thrombin or stable ADP. Only with the GPVI agonist CRP-XL, Syk-IN caused complete inhibition, whereas with thrombin or ADP platelet aggregation remained unchanged in the presence of Syk-IN (**Supplementary Figure 1A**), in agreement with the studies reported for mouse platelets<sup>21, 25</sup>. Further control experiments with Fura-2-loaded human platelets indicated that Syk-IN did not suppress thrombin- or ADP-induced  $\text{Ca}^{2+}$  rises (**Supplementary Figure 1B**).

Using Syk-IN, we then evaluated the role of Syk in  $\text{Ca}^{2+}$  rises induced by the considered GPVI- dependent and –independent collagen peptides. Three peptides containing the consensus GPVI-activating motif  $(\text{GPO})_n$ , *i.e.* GFOGER-GPO (for convenience designated as M1, see Table 1), CRP-XL (M2) and GAOGER-GPO (M3), all caused a potent rise in  $[\text{Ca}^{2+}]_i$ , which was fully abolished by Syk-IN (**Figure 1**). Close examination of the  $\text{Ca}^{2+}$  traces showed differences between M1-3 in onset and maximum. The reason for this is unclear but may be linked to differences in conformation and/or GPVI clustering capacity of the various triple-helical peptides. On the other hand, two other collagen peptides, containing a  $(\text{GPP})_n$  motif but not  $(\text{GPO})_n$ , were unable to induce a  $[\text{Ca}^{2+}]_i$  rise; these were GFOGER-GPP (M4) and the VWF-binding peptide (M5). Addition of Syk-IN was here without effect. Overall, these results pointed to a complete Syk-dependent suppression of platelet  $\text{Ca}^{2+}$  rises, when induced by  $(\text{GPO})_n$ -containing collagen peptides, capable to activate GPVI.

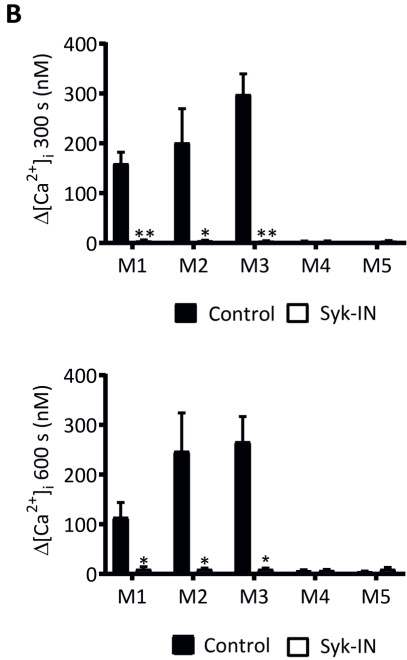
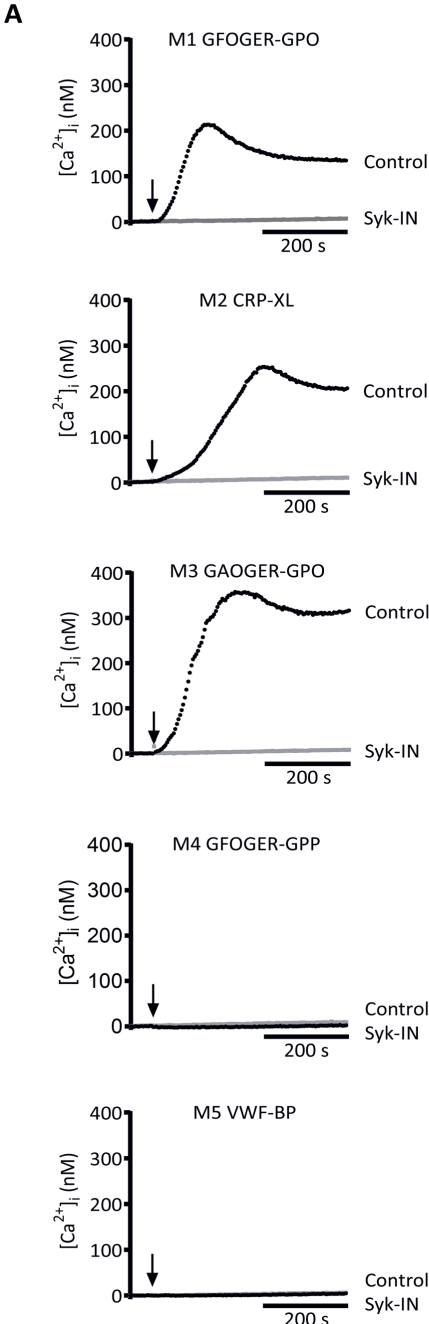


**Figure 1 (previous page) – Syk inhibition affecting platelet  $\text{Ca}^{2+}$  rises by collagen peptides with  $(\text{GPO})_n$  motif.** Fura-2-loaded platelets in 96-well plates were preincubated with Syk-IN (5  $\mu\text{M}$ ) or left untreated before stimulation with collagen peptide (M1-5, 10  $\mu\text{g}/\text{ml}$ ). Changes in  $[\text{Ca}^{2+}]_i$  were recorded over time per well-plate row by ratio fluorometry using a Flex Station 3. Peptides were injected into wells at 60 s (arrow) and reached platelets in a diffusion limited way. (A) Calibrated  $[\text{Ca}^{2+}]_i$  traces, recorded during 600 s in the absence (black, control) or presence (grey) of Syk inhibitor. Traces are representative of 3 experiments. (B) Quantification for M1-5 of increased  $[\text{Ca}^{2+}]_i$  at 300 s (top graph) or 600 s (bottom graph). Means  $\pm$  SE (n=3). Paired Student t-tests; \*p <0.05, \*\*p <0.01.

### **GPVI- and Syk-dependent parameters of thrombus formation on collagen- like peptides**

To assess how these five collagen peptides supported whole blood thrombus formation, we applied these as microspots (M1-5) in a microfluidic device, as described before <sup>9</sup>. All microspots were supplemented with VWF-BP (binding VWF from plasma) to allow GPIIb-mediated trapping of platelets at wall-shear rate of 1000/s. By end-stage multicolor microscopic imaging, it was possible to analyze up to eight thrombus and platelet characteristics: overall platelet deposition (parameter P1, see Table 1); platelet aggregation (P2); thrombus signature, *i.e.*, morphology, multilayer and contraction (P3-5); platelet procoagulant activity, measured as PS exposure (P6); and the platelet activation parameters CD62P expression (P7), and fibrinogen binding to activated integrin  $\alpha\text{IIb}\beta 3$  (P8).

Typically, the collagen peptides containing  $(\text{GPO})_n$  (M1-3) produced large thrombi with aggregated platelets, as well as high platelet PS exposure, CD62P expression and integrin activation (**Figure 2**). In contrast, the non-GPVI-stimulating  $(\text{GPP})_n$  peptide, GFOGER-GPP (M4) caused formation of smaller size thrombi, with residual CD62P expression and integrin activation, but essentially no PS exposure. Quantification of the raw image data

confirmed overall high parameter values for M1-3, indicating a strong support of thrombus formation (**Supplementary Figure 2**).

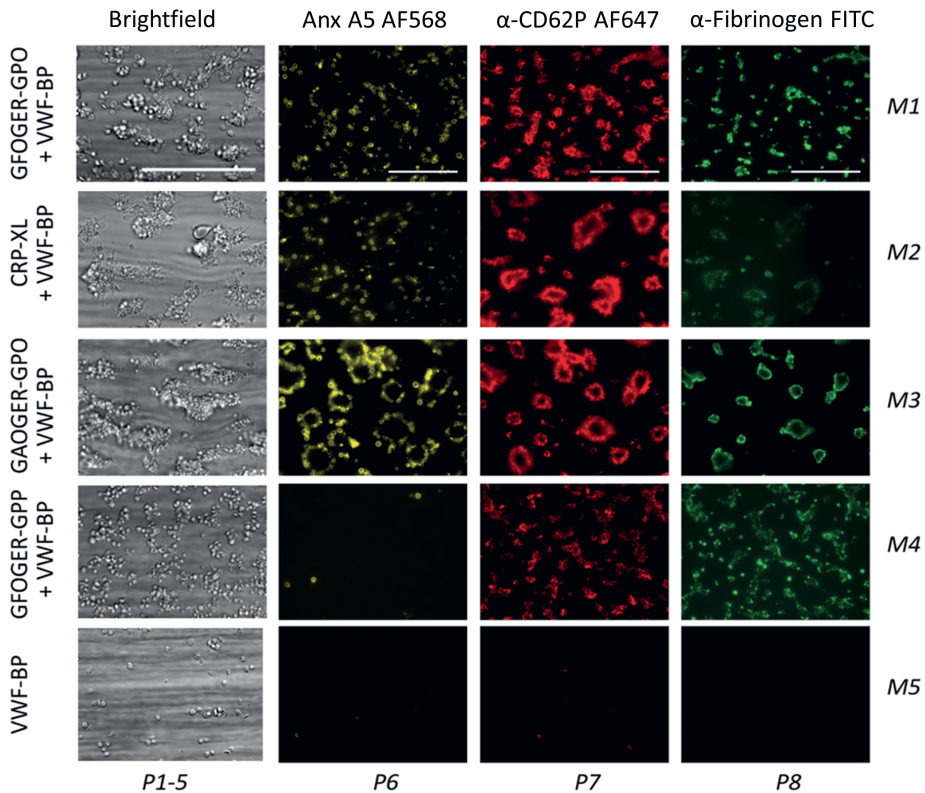


**Figure 2 – Thrombus formation on immobilized collagen peptides with or without (GPO)<sub>n</sub> motif.** Whole blood was perfused over microspots M1 (GFOGER-GPO + VWF-BP), M2 (CRP-XL + VWF-BP), M3 (GAOGER-GPO + VWF-BP), M4 (GFOGER-GPP + VWF-BP), and M5 (VWF-BP), with assumed platelet adhesion via GPIb, GPVI and/or integrin  $\alpha 2\beta 1$ , as in Table 1. Wall-shear rate was 1000/s at perfusion time of 3.5 minutes. Shown are representative brightfield microscopic images at end-stage, for analysis of platelet deposition (parameter P1) and thrombus characteristics (P2-5). In addition, end-stage 3-color fluorescence images for analysis of PS exposure (AF568 annexin A5, P6), CD62P expression (AF647  $\alpha$ -CD62P, P7), and fibrinogen binding (FITC, P8). Scale bars = 50  $\mu$ m, n = 5-7.

Interestingly, when comparing the two GFOGER peptides with GPVI-binding motif (M1) or without this motif (M4), the latter still induced residual platelet activation, in spite of lower thrombus signature scores (P4-5) and limited PS exposure (P6). Also of interest, M1 (GFOGER) with a supposedly higher affinity  $\alpha 2\beta 1$  binding site than M3 (GAOGER), performed less in almost all thrombus parameters (P1-2,3-5,7,8). These differences were made visible in a univariate scaled heatmap of all microspots and parameters (**Figure 3A**). Together, these data suggested that the clear distinction made between high- and low-affinity  $\alpha 2\beta 1$ -binding sites – established under static conditions<sup>11, 15</sup> –, becomes in part confused when immobilized collagen peptides are exposed to platelets in flowed whole blood. On the other hand, a lack of both GPVI- and  $\alpha 2\beta 1$ -binding sites, as in M5, resulted in almost no stable platelet adhesion and activation. Parallel flow runs on microspots M1-5 with blood samples that were pre-treated with Syk-IN (max effective dose of 20  $\mu\text{M}$ ), instead of the DMSO vehicle, resulted in marked reductions in the majority of thrombus parameters (**Figure 3A**). A subtraction heatmap, pinpointing only relevant changes ( $p < 0.05$ ), indicated that, for M1-4, essentially all parameters except for P1 (platelet deposition) were reduced by Syk inhibition (**Figure 3B**). Most drastic, complete reductions were seen for PS exposure (P6) on the 'active' (GPO)<sub>n</sub> surfaces M1-3. Surprisingly, Syk inhibition also affected platelet activation at the supposedly non-GPVI (GPP)<sub>n</sub> surface M4.

A summative plot was made indicating how individual (scaled) parameters were changed by Syk inhibition across microspots (**Figure 3C**). This revealed a complete reduction in P6 (PS exposure), along with strong reductions in P2 (aggregate coverage), P4 (thrombus multilayer), P5 (thrombus contraction) and P8 (fibrinogen binding). Less affected were P3 (thrombus morphology) and P7 (CD62P expression).



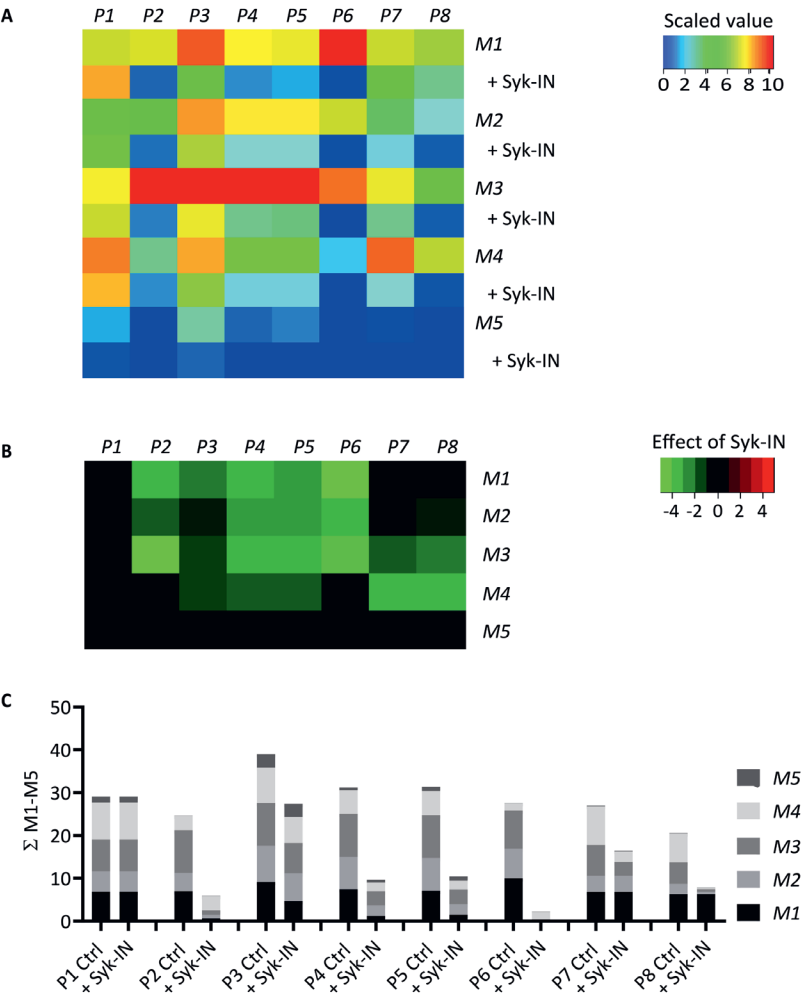


**Figure 3 – Effect of Syk inhibition on parameters of thrombus formation on immobilized collagen peptides.** Blood samples preincubated with vehicle (Ctrl) or Syk-IN (20 μM) were flowed over microspots M1-5, and thrombi formed were imaged to obtain parameters P1-8, as in **Figure 2**. Effects of Syk-IN were assessed per blood sample, surface and parameter. Mean values from individual blood samples (n=5-7) were univariate scaled to 0-10 per parameter across all surfaces M1-9. (A) Heatmap of scaled parameters, demonstrating mean effects of Syk-IN. Rainbow color code indicates scaled values between 0 (blue) and 10 (red). (B) Subtraction heatmap, representing scaled effects of Syk-IN, filtered for relevant changes (p <0.05, paired Student t-tests per surface and parameter). Color code represents decreases (green) or increases (red) in comparison to control runs. (C) Cumulative inhibitory effect per parameter over all microspots, indicating relevant changes.

## GPVI-induced and Syk-dependent platelet activation by different collagens

Subendothelial fibrillar collagen types I and III are considered to be the major platelet-activating collagens in the vessel wall, acting via GPVI and  $\alpha 2\beta 1$ <sup>30</sup>. The equine standard collagen (collagen-H), likely a modified type I collagen, is the most commonly used collagen type to study GPVI-induced platelet activation. This prompted us to compare four collagen preparations on their ability to support the GPVI-PLC $\gamma$ 2-Ca<sup>2+</sup> activation pathway: i.e., collagen-H (M6), human fibrillar collagen-I (M7), a degraded monomeric collagen-I (M8), and human collagen-III (M9). While realizing that the very high-molecular weight of fibrillar collagens results in a heterogeneous interaction with platelets in suspension, we evaluated the Ca<sup>2+</sup> rises induced by all four collagens. Markedly, the four collagens (M6-9) evoked a biphasic rise in [Ca<sup>2+</sup>]<sub>i</sub>, with an initial increase and a later second phase, which was highest for M7 and M9 (**Figure 4A,B**). In absolute levels, the increases in [Ca<sup>2+</sup>]<sub>i</sub> obtained with M6,7,9, at a late time point of 600 s, were 2-3 fold lower than those seen with the (GPO)<sub>n</sub>-containing collagen peptides (**Figure 4** vs. **Figure 1**). This difference is likely due to the large fibrillar structure of collagens, slowing down the rate and extent of diffusion-limited interactions with platelets. In addition, we found that Syk inhibition completely suppressed the [Ca<sup>2+</sup>]<sub>i</sub> transient induced by the standard collagen-H (M6) but did not alter the transients by other collagens **Figure 4**. Hence, this suggested the presence of a Syk-independent pathway of Ca<sup>2+</sup> mobilization of suspended natural collagens.

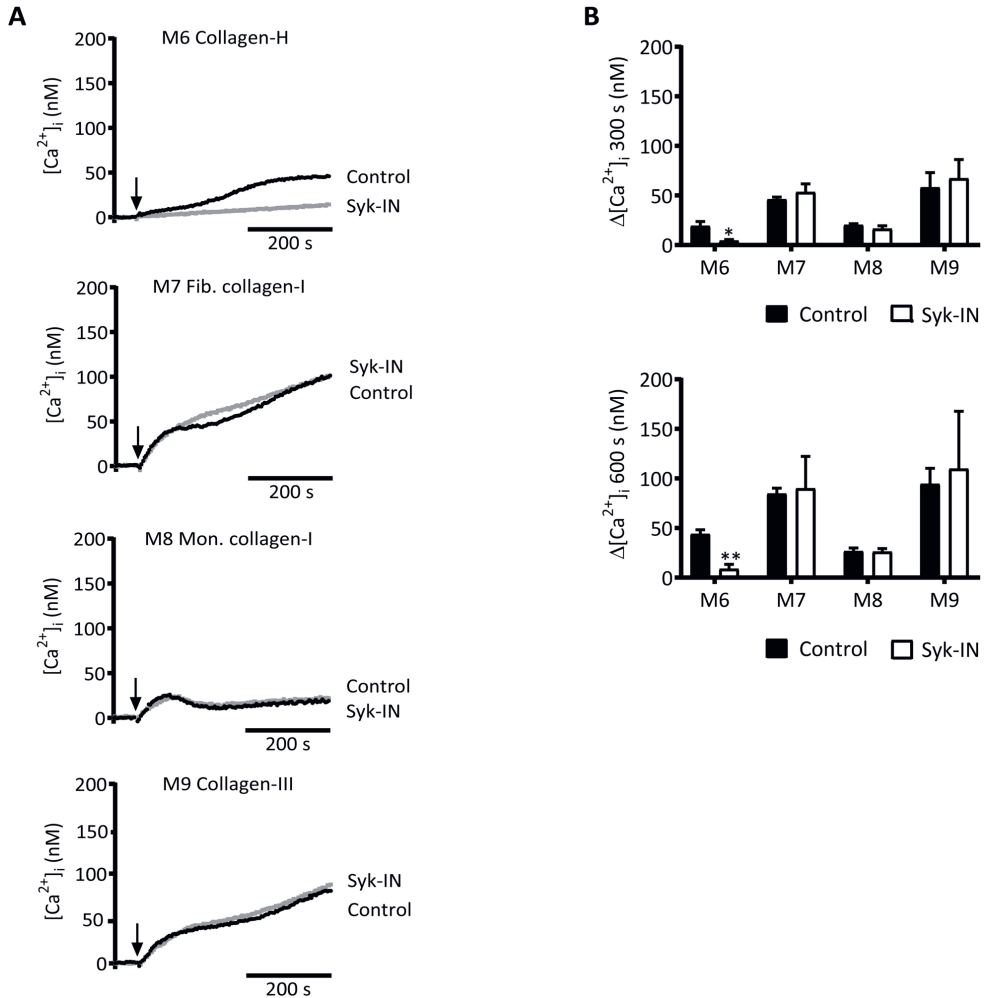


**Figure 4 – Syk inhibition differently affecting platelet Ca<sup>2+</sup> rises by collagens.** Fura-2-loaded platelets in 96-well plates were preincubated with Syk-IN (5 μM) or left untreated before stimulation with different collagens (M6-9, 10 μg/ml). Changes in [Ca<sup>2+</sup>]<sub>i</sub> were continuously monitored per well-plate row by ratio fluorometry using a Flex Station 3. Collagens were injected at 60 s (arrow) and reached platelets in a diffusion limited way. (A) Calibrated [Ca<sup>2+</sup>]<sub>i</sub> traces, recorded for 600 s in the absence (black, control) or presence (grey) of Syk inhibitor. Traces are representative of 3 experiments. (B) Quantification of [Ca<sup>2+</sup>]<sub>i</sub> rise after 300 s (top graph) and 600 s (bottom graph) for M1-5. Means ± SE (n=3). Paired Student t-test, \*p < 0.05, \*\*p < 0.01.

## GPVI- and Syk-dependent platelet responses in thrombus formation on collagens

The same collagen preparations (M6-9) were then applied as microspots to test their ability to support thrombus formation under flow. As indicated in **Figure 5**, collagen-H (M6) was most potent in provoking the formation of large-size aggregates of platelets with high PS exposure, granule secretion and fibrinogen binding, such in agreement with the known high GPVI- and  $\alpha 2\beta 1$ -activating potency of this collagen, when immobilized<sup>9, 11, 12</sup>. In comparison, the fibrillar type I (M7) and type III (M9) collagens formed only small aggregates of platelets with remaining secretion and fibrinogen binding, with only M9 causing residual PS exposure (**Figure 5**). The degraded monomeric collagen-I (M8) caused mostly single platelet adhesion with incidentally small-sized aggregates. The same conclusion was drawn from raw mean values of the individual parameters, obtained from these surfaces (**Supplementary Figure 3**).

Heatmapping of the eight scaled parameter values confirmed that the overall surface thrombogenicity decreased in the order of M6 > M7,9 > M8 (**Figure 6A**). Treatment of the blood with Syk-IN left platelet deposition (P1) unchanged but did decrease thrombus signature and platelet activation parameters (P2-5, P7-8) for the most active surfaces. A subtraction heatmap was built with a filter for relevant changes ( $p < 0.05$ ). This indicated for collagen-H (M6) as well as for native collagen-I and -III (M7,9) a reduction in almost all parameters, except for P1, in the presence of Syk-IN (**Figure 6B**). Most reduced were parameters of platelet aggregation and contraction (P2,4,5), and of platelet activation (P6 for M6, and P7-8 for M7,9).

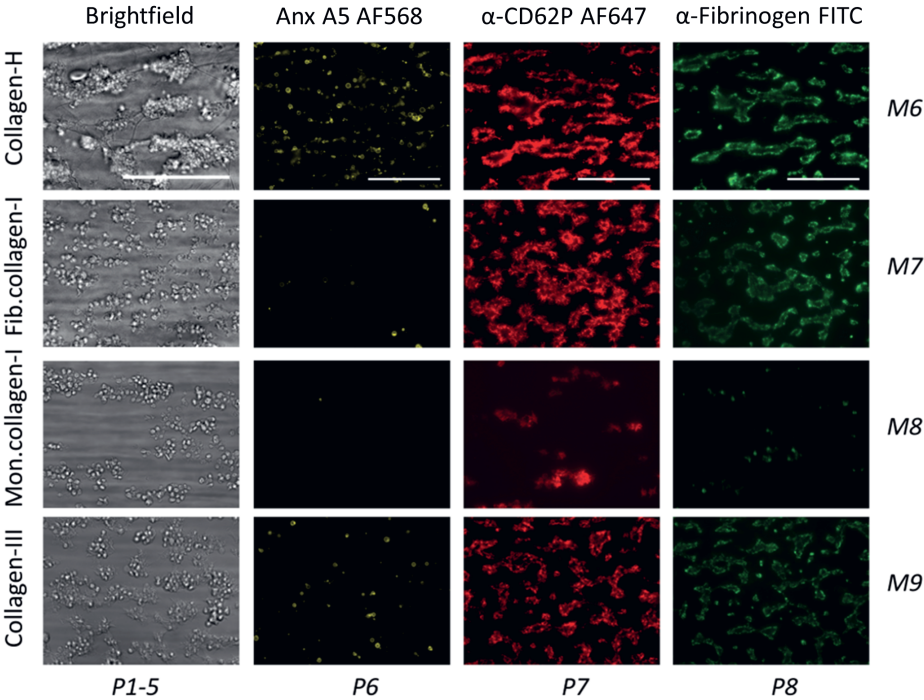


**Figure 5 – Thrombus formation on immobilized collagens.** Whole blood was perfused over microspots M6 (collagen-H), M7 (fibrillar collagen-I), M8 (monomeric collagen-I), M9 (collagen-III). Wall-shear rate was 1000/s and perfusion time 3.5 minutes. Shown are representative brightfield microscopic images at end-stage for analysis of platelet deposition (parameter P1) and thrombus characteristics (P2-5). In addition, end-stage 3-color fluorescence images for analysis of PS exposure (AF568 annexin A5, P6), CD62P expression (AF647  $\alpha$ -CD62P, P7), and fibrinogen binding (FITC, P8). Scale bars = 50  $\mu$ m, n = 5-7.

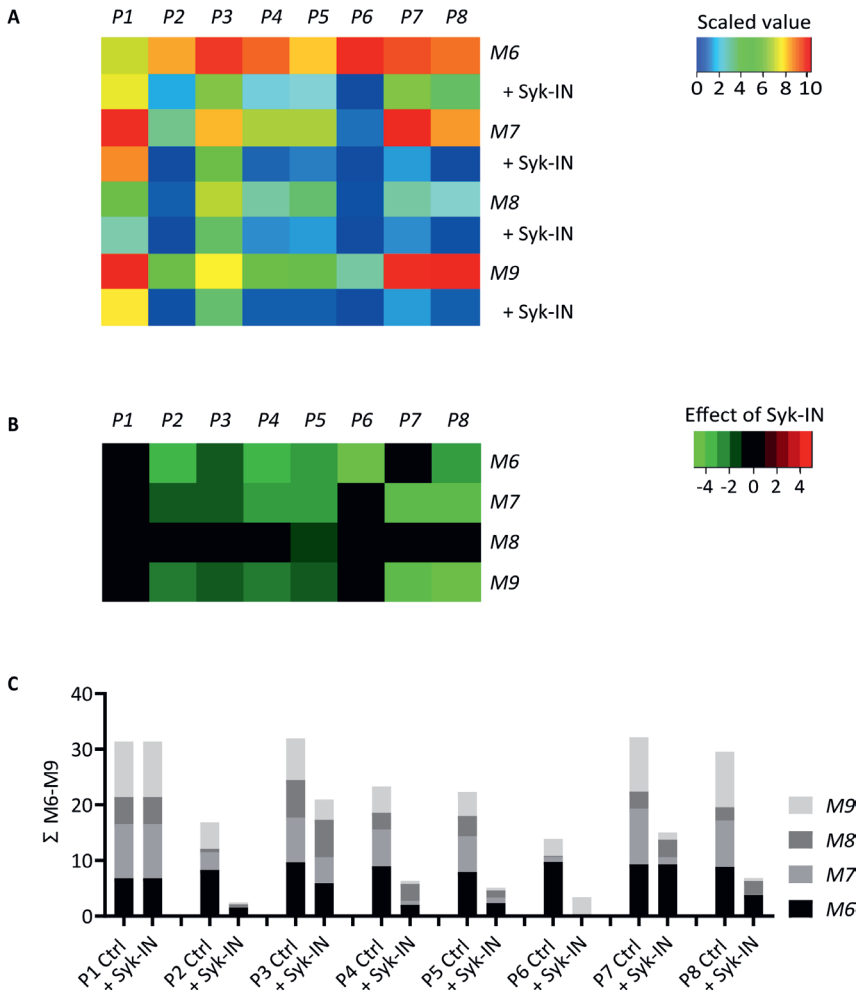


**Figure 6 – Effect of Syk inhibition on parameters of thrombus formation on immobilized collagen.** Whole blood preincubated with vehicle (Ctrl) or Syk-IN (20  $\mu$ M) was perfused over microspots M6-9, and thrombus formation was imaged to obtain parameters P1-8, as in **Figure 5**. Effects of Syk-IN were calculated per blood sample, surface and parameter. Mean values for all blood samples (n=5-7) were univariate scaled to 0-10 per parameter across all surfaces M1-9. (A) Heatmap of scaled parameters, showing mean effects of Syk-IN. Rainbow color code gives scaled values between 0 (blue) and 10 (red). (B) Subtraction heatmap representing scaled effects of Syk-IN, filtered for relevant changes ( $p < 0.05$ , paired Student t-tests per surface and parameter). Color code represents decreases (green) or increases (red) in comparison to control runs. (C) Cumulative inhibitory effect over all microspots per parameter, indicating relevant changes from control runs.

To obtain a better insight of the overall effect of Syk inhibition, again a summative plot was constructed per scaled parameter across all collagen microspots (**Figure 6C**). Importantly, this revealed a highly similar pattern of Syk inhibition, as previously seen for the collagen peptides. Thus, summing up the values for M6-9, we noticed a near complete reduction in P6 (M6, PS exposure), along with strong reductions in P2 (platelet aggregate coverage), P4 (thrombus multilayer), P5 (thrombus contraction) and P7 (CD62P expression), P8 (fibrinogen binding), as compared to vehicle-treated blood. Less affected by Syk inhibition was P3 (thrombus morphology), while platelet adhesion (P1) was unchanged.

### **Modelling of role of GPVI in thrombus formation on various collagens**

We used regression analysis to examine the generated dataset, consisting of 416 data points (52 mean control flow runs of 9 surfaces, 8 parameters) in a systematic manner regarding the assumed GPVI dependency per surface. First a partial least square (PLS) regression model was generated for the collagen peptides M1-3 with assumed high GPVI dependency plus for M4-5 with assumed no role of GPVI, after which the data from M6 (collagen-H) were predicted back into the model. This gave relevant components 1 and 2, explaining 68 and 15% of the variation, respectively (**Supplementary Figure 4**). This plot indicated a close cluster of flow runs of M1-3,6 with data of M5 (negative component 1) and data of M4 (negative component 2) laying further out in the model. This agrees with the large differences in (parameters of) thrombus formation on M4 and M5. The calculated beta matrix indicated that P2-6 similarly contributed to the modelled results. Because of this separation, the 1-component model was used for further analysis. Testing of the model showed near complete correct prediction for all surfaces, except for M4 (as no component 2) (**Table 2**).

**Table 2 – Modelled PLS analysis (based on 1 component PCA) of range-scaled data for collagen peptides (M1-5) plus collagen-H (M6), with assumed GPVI dependency.** Shown are means and ranges of prediction values. Predicted accuracy is given by numbers of mean flow runs per donor (control and Syk-IN); by default, correct prediction was set at >0.5. In addition, back-prediction of GPVI dependency of mean flow runs per donor for M7-9. Prediction outcomes are given in *italic*. Contribution of parameters to the prediction model was P2-6 >> P1,7,8.

Microspot	GPVI dependency	Prediction values		Correctly predicted	
		mean	range	ctrl	Syk-IN
<i>M1</i>	Positive	0.76	0.41-1.06	5/6	6/6
<i>M2</i>	Positive	0.59	0.27-0.76	4/5	5/5
<i>M3</i>	Positive	0.96	0.86-1.07	5/5	5/5
<i>M4</i>	Negative	0.76	0.57-0.97	0/6	6/6
<i>M5</i>	Negative	0.26	0.21-0.34	5/5	5/5
<i>M6</i>	Positive	0.81	0.68-1.11	7/7	6/7
<i>M7</i>	Mixed	n.d.	0.44-0.85	5/7	7/7
<i>M8</i>	Negative	n.d.	0.13-0.41	0/5	5/5
<i>M9</i>	Mixed	n.d.	0.49-0.67	3/5	5/5

N.d., not determined.

This model was further used to predict the role of GPVI on other collagen surfaces M7-9. For both native collagens (M7,9), the prediction for GPVI dependency was mixed, while for the monomeric collagen-I (M8) it was negative. Subsequently, we integrated into the model another set of 416 data points (52 mean flow runs with Syk-IN of 9 surfaces, 8 parameters) for prediction of the known absence of GPVI activity in Syk-inhibited blood samples. Markedly, across all surfaces tested, 51 out of all 52 samples predicted a negative GPVI dependency, wherein the only incorrectly predicted sample was just above the 0.5 threshold. Taken together, in addition to a complete GPVI independency of all Syk-inhibited samples, the constructed PLS model suggested no role of GPVI for surfaces M5 and M8.



## 6.4 Discussion

### Collagen peptides and GPVI-dependent platelet activation

The present data point to a clear separation between triple-helical collagen peptides that contain the established GPVI recognition motif, (GPO)<sub>n</sub><sup>15</sup>, and peptides that have a (GPP)<sub>n</sub> backbone instead. Collectively, we found that the (GPO)<sub>n</sub>-containing collagen peptides (M1-3): *i*) induced high platelet Ca<sup>2+</sup> rises under stasis; *ii*) accomplished a fast build-up of thrombi with aggregated and activated platelets under flow; and *iii*) caused platelet responses both under flow and stasis that were highly sensitive to inhibition of Syk. Accordingly, these peptides provided proof-of-principle evidence for a potent stimulation of the GPVI-Syk-PLCγ2-Ca<sup>2+</sup> pathway of platelet activation.

When immobilized, the (GPO)<sub>n</sub> peptide CRP-XL (M2), uniquely lacking an α2β1 interaction motif, produced smaller size thrombi (low parameter values P2-6) than the other peptides, which is in agreement with the known synergy between GPVI, α2β1 and GPIb-V-IX receptors in thrombus formation at high shear rate<sup>9-11</sup>. Synergy of GPVI and α2β1 can also explain why peptides containing the integrin-binding motif G(F/A)OGER evoked a faster Ca<sup>2+</sup> signal, when compared to CRP-XL. Seemingly in contrast with its lower binding affinity to platelets under stasis<sup>17</sup>, we observed higher parameters of thrombus formation with GAOGER-GPO (M3) than with GFOGER-GPO (M1). Explanation for this high activity may be increased interaction on the level of receptors with the (GPO)<sub>n</sub> motif.

On the other hand, the (GPP)<sub>n</sub>-containing peptides GFOGER-GPP (M4) and VWF-BP (M5) did not evoke detectable Ca<sup>2+</sup> rises under stasis. Yet, when immobilized, the integrin-binding peptide GFOGER-GPP evoked low-parameter thrombus formation in terms of platelet activation and aggregation under flow; and this activity was again suppressed by Syk inhibition.

## Collagens and GPVI-dependent platelet activation

Native fibrillar type I and type III collagens are among the vessel wall components that most strongly activate platelets <sup>7, 30</sup>. Due to the structural complexity of multiple adjacent triple helices in these collagens, little is known about how platelet receptors bind to the fibers, although there is evident that the co-presence of multiple binding sites in a fiber enforces platelet adhesion and activation <sup>31, 32</sup>. Recent high-resolution microscopy further indicates that copies of GPVI dimerize and cluster along the fibers of such collagen, a process that is considered to enforce GPVI-dependent platelet activation <sup>33, 34</sup>. Sequence analysis has shown that both collagens are made up for up to 10% of GPO triplets, with also  $\alpha 2\beta 1$ -binding sequences present, *e.g.*, GFOGER in collagen-I and GAOGER in collagen-III <sup>35</sup>.

This knowledge made us to compare the effects of human fibrillar collagen-I and collagen-III preparations with the standard collagen-H, *i.e.*, a commercial equine, type I-enriched preparation with unclear supramolecular characteristics <sup>36</sup>. Markedly, in suspended platelets, collagen-H (M6) was the only preparation that induced Syk-dependent  $Ca^{2+}$  rises, whereas the other collagens (M7,9) induced low  $Ca^{2+}$  rises that were insensitive to Syk inhibition. The microspotted collagen-H triggered the formation of large-size thrombi, with high parameters of platelet aggregation and activation, *i.e.*, responses that are known to be strongly GPVI-dependent <sup>9</sup>, and that in the present setting were consistently affected by Syk inhibition.

In comparison to collagen-H, the immobilized type I (M7) and type III (M9) collagens triggered formation of smaller thrombi with lower platelet activation parameters. Yet, for the native collagens, the summed suppressive effects on thrombus parameters of Syk inhibition were quite similar to those of Syk inhibition for collagen-H and (GPO)<sub>n</sub>-containing collagen peptides. Given the abundance of GPO triplets in both collagen-I and -III <sup>15</sup>, these findings

point to a GPVI-induced activation, which is limited in strength but relevant for the immobilized collagens subjected to flowed platelets. In agreement with a role for GPVI, others have shown that type I and III collagens cause GPVI dimer clustering when immobilized at a glass surface, with typically collagen-III being the most effective<sup>34</sup>. Of note, under flow conditions, VWF bound to both collagen types ensures GPIb-V-IX binding, thus allowing an enforcement of  $\alpha 2\beta 1$  and GPVI interactions<sup>13, 16</sup>.

In addition, we tested a protease-treated, monomeric collagen-I preparation (M8), which was inactive in supporting thrombus formation with no effects of Syk inhibition. These findings support the notion that the fibrillar structure of immobilized collagens helps to expose receptor (GPVI) binding sites upon stretching under flow conditions.

### **Comparative roles of GPVI and Syk in platelet activation**

As indicated above, a remarkable finding was that Syk inhibition also affected parameters of thrombus formation on surfaces that supposedly act independently of GPVI (GFOGER-GPP, M4) or have a low GPVI dependency (collagen-I, M7; collagen-III, M9). As another approach to examine the coherence in the multiparameter data set, a PLS model was constructed and used for principal component analysis. Plots indicated a narrow cluster for all high GPVI-activating surfaces (M1-3,6), with data of the other surfaces (M4,5) centering out. Using this model to predict the role of GPVI on other surfaces, results for the fibrillar collagens (M7,9) were mixed, whereas those for monomeric collagen-I (M8) were absent. Importantly, the prediction model revealed complete GPVI independency of the Syk-inhibited samples, regardless of the microspot. Accordingly, this strengthened the idea of low level GPVI and Syk activity on the low thrombogenic surfaces.

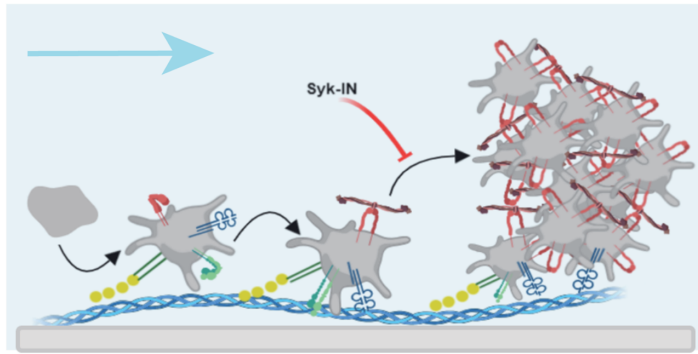
In recent years, evidence has been accumulated for a role of GPVI signaling in platelets contacting a variety of non-collagen surfaces. For

instance, GPVI dependency has been discovered for platelets interacting with laminin<sup>37</sup>, fibrin<sup>29,38</sup>, or fibrinogen<sup>39,40</sup>. In this perspective, it is likely that also for - (GPP)<sub>n</sub> containing - collagenous surfaces the Syk-dependent platelet activation can be traced back to residual GPVI activity. On the other hand, based on early studies, it cannot be excluded that (part of) the Syk-dependent platelet responses in thrombus formation at 'weaker' surfaces are mediated by signaling via integrin  $\alpha\text{IIb}\beta\text{3}$ <sup>41-43</sup>, thus bypassing GPVI. This will need to be studied by using specific GPVI-inhibitory tools.

## Conclusion

The present data reveal typical differences of preparations of collagens or collagen peptides when used in suspension with platelets or when immobilized as microspots and subjected to whole blood flow (**Figure 7**). Especially for the 'weaker' native fibrillar collagens, the latter situation appears to enhance the signaling capability of GPVI, thus stimulating platelet activation processes in thrombus formation. Apart from changes in the (immobilized) collagen structure, factors that are likely to contribute to the enhanced signaling events are the shear-dependent interaction of GPIb-V-IX with collagen-bound VWF and a priming platelet activation via integrin  $\alpha\text{2}\beta\text{1}$ . These and perhaps also other receptor interactions with the collagen fibers may ensure increased activation of the GPVI-PLC $\gamma\text{2}$ -Ca<sup>2+</sup> pathway, although we cannot rule out the presence of Syk-dependent signaling events bypassing GPVI, such as by direct triggering via the integrins  $\alpha\text{2}\beta\text{1}$  and  $\alpha\text{IIb}\beta\text{3}$ .

A



B

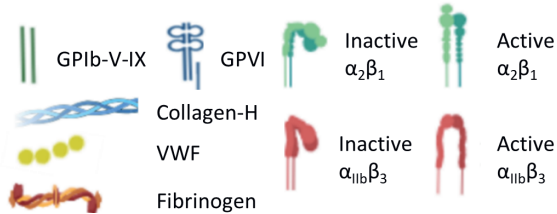
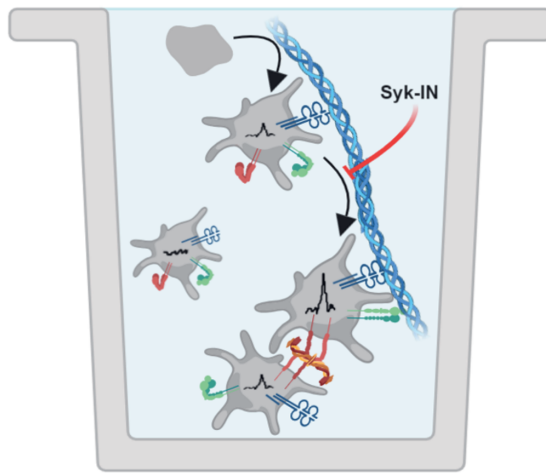


**Figure 7 – Schematic platelet adhesion and activation by collagen under flow or in suspension.** (A) Under flow conditions, immobilized collagen-H interacts with VWF to capture platelets via GPIb-V-IX and activate platelets via GPVI and integrin  $\alpha_2\beta_1$ . Thrombi build up by recruitment of flowing platelets interacting with collagen/VWF-adhered platelets. Syk inhibition suppresses initial platelet activation and platelet aggregate formation. (B) Collagen-H added to a suspension of platelets transiently interacts with GPVI, resulting in Syk-dependent cytosolic  $Ca^{2+}$  rises. Autocrine agonists will stimulate non-adhered platelets, responding by Syk-independent signals.

**Author Contributions** Conceptualization, JWMH, PEJvdM and MJEK; Method-ology, NJJ, IDS, IP and DIF; Formal Analysis, NJJ, IDS, IP DIF, SLNB and RC; Investigation, NJJ, IDS, IP and DIF; Resources, RWF and JWMH; Data Curation, NJJ; Writing – Original Draft Preparation, NJJ, IDS, IP and DIF; Writing – Review & Editing, JWMH; Visualization, NJJ, IDS, IP and DIF; Supervision, JWMH, YMCH, PEJvdM, MJEK and HtC; Funding Acquisition, JWMH, PEJvdM, MJEK and HtC.

**Acknowledgments and Funding** We acknowledge support from the Cardiovascular Centre (HVC), MUMC, Maastricht University. This work has received funding from the European Union's Horizon 2020 research and innovation program under the Marie Skłodowska-Curie grant agreement No. 766118.

**Conflicts of Interest** JH is a co-founder and shareholder of FlowChamber. The other authors declare no relevant conflict of interest.

## **6.5 References**

1. Versteeg HH, Heemskerk JW, Levi M, Reitsma PS. New fundamentals in hemostasis. *Physiol Rev.* 2013; 93:327-358.
2. Van der Meijden PE, Heemskerk JW. Platelet biology and functions: new concepts and future clinical perspectives *Nat Rev Cardiol.* 2019; 16:166-179.
3. Savage B, Almus-Jacobs F, Ruggeri ZM. Specific synergy of multiple substrate-receptor interactions in platelet thrombus formation under flow. *Cell.* 1998; 94:657-666.
4. Atkinson BT, Jarvis GE, Watson SP. Activation of GPVI by collagen is regulated by  $\alpha 2\beta 1$  and secondary mediators. *J Thromb Haemost.* 2003; 1:1278-87.
5. Auger JM, Kuijpers MJ, Senis YA, Watson SP, Heemskerk JW. Adhesion of human and mouse platelets to collagen under shear: a unifying model. *FASEB J.* 2005; 19:825-827.
6. Kehrel B, Wierwille S, Clemetson KJ, *et al.* Glycoprotein VI is a major collagen receptor for platelet activation: it recognizes the platelet-activating quaternary structure of collagen, whereas CD36, glycoprotein IIb/IIIa, and von Willebrand factor do not. *Blood.* 1998; 91:491-499.

7. Nieswandt B, Watson SP. Platelet-collagen interaction: is GPVI the central receptor? *Blood*. 2003; 102:449-461.
8. Baaten CC, Meacham S, de Witt SM, *et al*. A synthesis approach of mouse studies to identify genes and proteins in arterial thrombosis and bleeding. *Blood*. 2018; 132:e35-46.
9. De Witt SM, Swieringa F, Cavill R, *et al*. Identification of platelet function defects by multi-parameter assessment of thrombus formation. *Nat Commun*. 2014; 5:4257.
10. Pugh N, Simpson AM, Smethurst PA, *et al*. Synergism between platelet collagen receptors defined using receptor-specific collagen-mimetic peptide substrata in flowing blood. *Blood*. 2010; 115:5069-5079.
11. Siljander PR, Munnix IC, Smethurst PA, *et al*. Platelet receptor interplay regulates collagen-induced thrombus formation in flowing human blood. *Blood*. 2004; 103:1333-1341.
12. Munnix IC, Kuijpers MJ, Auger JM, *et al*. Segregation of platelet aggregatory and procoagulant microdomains in thrombus formation. Regulation by transient integrin activation. *Arterioscler Thromb Vasc Biol*. 2007; 27:2484-2490.
13. Fuchs B, de Witt S, Solecka BA, *et al*. Distinct role of von Willebrand factor triplet bands in glycoprotein Ib-dependent platelet adhesion and thrombus formation under flow. *Semin Thromb Hemost*. 2013; 39:306-314.
14. Knight CG, Morton LF, Onley DJ, *et al*. Collagen-platelet interaction: Gly-Pro-Hyp is uniquely specific for platelet GPVI and mediates platelet activation by collagen. *Cardiovasc Res*. 1999; 41:450-457.
15. Smethurst PA, Onley DJ, Jarvis GE, *et al*. Structural basis for the platelet-collagen interaction. The smallest motif within collagen that recognizes and activates platelet glycoprotein VI contains to glycine-proline-hydroxyproline triplets. *J Biol Chem*. 2007; 282:1296-1304.
16. Munnix IC, Gilio K, Siljander PR, *et al*. Collagen-mimetic peptides mediate flow-dependent thrombus formation by high- or low-affinity binding of integrin  $\alpha 2\beta 1$  and glycoprotein VI. *J Thromb Haemost*. 2008; 6:2132-2142.
17. Siljander PR, Hamaia S, Peachey AR, *et al*. Integrin activation state determines selectivity for novel recognition sites in fibrillar collagens. *J Biol Chem*. 2004; 279:47763-72.
18. Ichinohe T, Takayama H, Ezumi Y, *et al*. Collagen-stimulated activation of Syk but not c-Src is severely compromised in human platelets lacking membrane glycoprotein VI. *J Biol Chem*. 1997; 272:63-68.
19. Melford SK, Turner M, Briddon SJ, Tybulewicz VL, Watson PS. Syk and Fyn are required by mouse megakaryocytes for the rise in intracellular calcium induced by a collagen-related peptide. *J Biol Chem*. 1997; 272:27539-27542.
20. Watson SP, Herbert JMJ, Pollitt AY. GPVI and CLEC-2 in hemostasis and vascular integrity. *J Thromb Haemost*. 2010; 8:1457-1467.

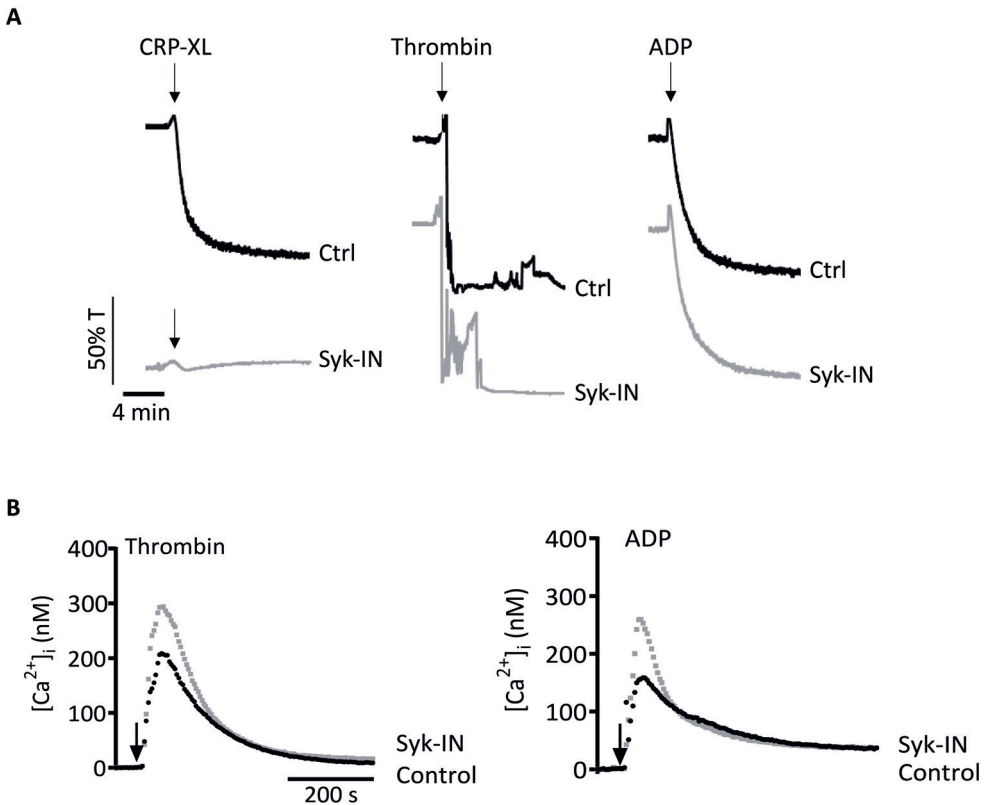
21. Badolia R, Kostyak JC, Dangelmaier C, Kunapuli SP. Syk activity is dispensable for platelet GPIb-IX-V signaling. *Int J Mol Sci.* 2017; 18:1238.
22. Yanaga F, Poole A, Asselin J, *et al.* Syk interacts with tyrosine-phosphorylated proteins in human platelets activated by collagen and cross-linking of the FcγIIA receptor. *Biochem J.* 1995; 311:471-478.
23. Munnix IC, Strehl A, Kuijpers MJ, *et al.* The glycoprotein VI-phospholipase Cγ2 signaling pathway controls thrombus formation induced by collagen and tissue factor in vitro and in vivo. *Arterioscler Thromb Vasc Biol.* 2005; 25:2673-2678.
24. Rayes J, Watson SP, Nieswandt B. Functional significance of the platelet immune receptors GPVI and CLEC-2. *J Clin Invest.* 2019; 129:12-23.
25. Reilly MP, Sinha U, André P, *et al.* PRT-060318, a novel Syk inhibitor, prevents heparin-induced thrombocytopenia and thrombosis in a transgenic mouse model. *Blood.* 2011; 117:2241-2246.
26. Ishikawa C, Senba M, Mori N. Anti-adult T-cell leukemia/lymphoma activity of cerdulatinib, a dual SYK/JAK kinase inhibitor. *Int J Oncol.* 2018; 53:1681-1690.
27. Pollitt AY, Poulter NS, Gitz E, *et al.* Syk and Src family kinases regulate C-type lectin receptor 2 (CLEC-2)-mediated clustering of podoplanin and platelet adhesion to lymphatic endothelial cells. *J Biol Chem.* 2014; 289:35695-35710.
28. Andre P, Morooka T, Sim D, *et al.* Critical role for Syk in responses to vascular injury. *Blood.* 2011; 118:5000-5010.
29. Onselaer MB, Hardy AT, Wilson C, *et al.* Fibrin and D-dimer bind to monomeric GPVI. *Blood Adv.* 2017; 1:1495-1504.
30. Farndale RW, Sixma JJ, Barnes MJ, de Groot PG. The role of collagen in thrombosis and haemostasis. *J Thromb Haemost.* 2004; 2:561-573.
31. Jung SM, Takemura Y, Imamura Y, Hayashi T, Adachi E, Moroi M. Collagen-type specificity of glycoprotein VI as a determinant of platelet adhesion. *Platelets.* 2008; 19:32-42.
32. Herr AB, Farndale RW. Structural insights into the interactions between platelet receptors and fibrillar collagen. *J Biol Chem.* 2009; 284:19781-19785.
33. Jung SM, Moroi M, Soejima K, *et al.* Constitutive dimerization of glycoprotein VI (GPVI) in resting platelets is essential for binding to collagen and activation in flowing blood. *J Biol Chem.* 2012; 287:30000-30013.
34. Poulter NS, Pollitt AY, Owen DM, *et al.* Clustering of glycoprotein VI (GPVI) dimers upon adhesion to collagen as a mechanism to regulate GPVI signaling in platelets. *J Thromb Haemost.* 2017; 15:549-564.
35. Farndale RW, Lisman T, Bihan D, *et al.* Cell-collagen interactions: the use of peptide Toolkits to investigate collagen-receptor interactions. *Biochem Soc Trans.* 2008; 36:241-50.



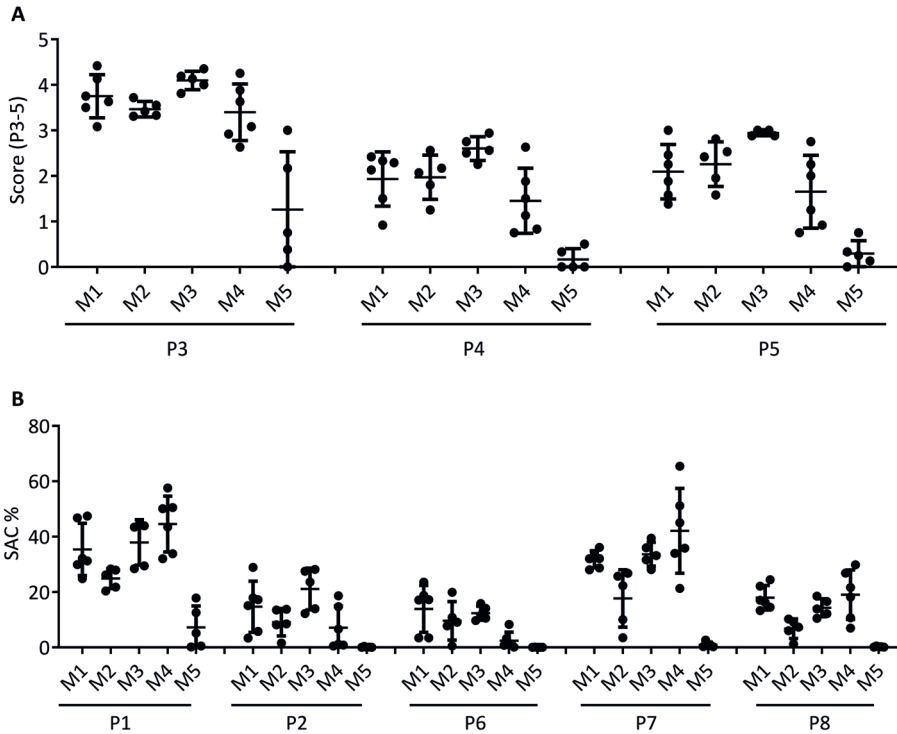
36. Heemskerk JWM, Sakariassen KS, Zwaginga JJ, *et al.* Collagen surfaces to measure thrombus formation under flow: possibilities for standardization. *J Thromb Haemost.* 2011; 9:856-858.
37. Ozaki Y, Suzuki-Inoue K, Inoue O. Novel interactions in platelet biology: CLEC-2/podoplanin and laminin/GPVI. *J Thromb Haemost.* 2009; Suppl. 1:191-194.
38. Mammadova-Bach E, Ollivier V, Loyau S, *et al.* Platelet glycoprotein VI binds to polymerized fibrin and promotes thrombin generation. *Blood.* 2015; 126:683-691.
39. Induruwa I, Moroi M, Bonna A, *et al.* Platelet collagen receptor glycoprotein VI-dimer recognizes fibrinogen and fibrin through their D-domains, contributing to platelet adhesion and activation during thrombus formation. *J Thromb Haemost.* 2018; 16:389-404.
40. Mangin PH, Onselaer MB, Receveur N, *et al.* Immobilized fibrinogen activates human platelets through glycoprotein VI. *Haematologica.* 2018; 103:898-907.
41. Gao J, Zoller KE, Ginsberg MH, Brugge JS, Shattil SJ. Regulation of the pp72syk protein tyrosine kinase by platelet integrin  $\alpha\text{IIb}\beta\text{3}$ . *EMBO J.* 1997; 16:6414-6425.
42. Oberfell A, Eto K, Mocsai A, *et al.* Coordinate interactions of Csk, Src, and Syk kinases with  $\alpha\text{IIb}\beta\text{3}$  initiate integrin signaling to the cytoskeleton. *J Cell Biol.* 2002; 157:265-275.
43. Van der Meijden PE, Feijge MA, Swieringa F, *et al.* Key role of integrin  $\alpha\text{IIb}\beta\text{3}$  signaling to Syk kinase in tissue factor-induced thrombin generation. *Cell Mol Life Sci.* 2012; 69:3481-3492.
44. Knight CG, Morton LF, Onley DJ, *et al.* Identification in collagen type I of an integrin  $\alpha\text{2}\beta\text{1}$ -binding site containing an essential GER sequence. *J Biol Chem.* 1998; 273:33287-33294.
45. Smethurst PA, Joutsu-Korhonen L, O'Connor MN, *et al.* Identification of the primary collagen-binding surface on human glycoprotein VI by site-directed mutagenesis and by a blocking phage antibody. *Blood.* 2004; 103:903-911.
46. De Witt S, Swieringa F, Cosemans JM, Heemskerk JW. Thrombus formation on microspotted arrays of thrombogenic surfaces. *Nat Protocol Exchange.* 2014; 2014:3309.
47. Siljander P, Lassila R. Studies of adhesion-dependent platelet activation: distinct roles for different participating receptors can be dissociated by proteolysis of collagen. *Arterioscler Thromb Vasc Biol.* 1999; 19:3033-3043.
48. Gilio K, Harper MT, Cosemans JM, *et al.* Functional divergence of platelet protein kinase C(PKC) isoforms in thrombus formation on collagen. *J Biol Chem.* 2010; 285:23410-23419.
49. Van Geffen JP, Brouns S, Batista J, *et al.* High-throughput elucidation of thrombus formation reveals sources of platelet function variability. *Haematologica.* 2019; 104:1256-1267.

50. Feijge MA, van Pampus EC, Lacabartz-Porret C, *et al.* Inter-individual variability in Ca<sup>2+</sup> signalling in platelets from healthy volunteers, relation with expression of endomembrane Ca<sup>2+</sup>-ATPases. *Br J Haematol.* 1998; 102:850-859.
51. Grynkiewicz G, Poenie M, Tsien RY. A new generation of Ca<sup>2+</sup> indicators with greatly improved fluorescence properties. *J Biol Chem.* 1985; 260:3440-3450.
52. Chin WW. Bootstrap cross-validation indices for PLS path model assessment. In: *Handbook of Partial Least Squares* (Eds. Vinci EV, *et al.*), 2010 Springer Berlin: pp. 83-92.

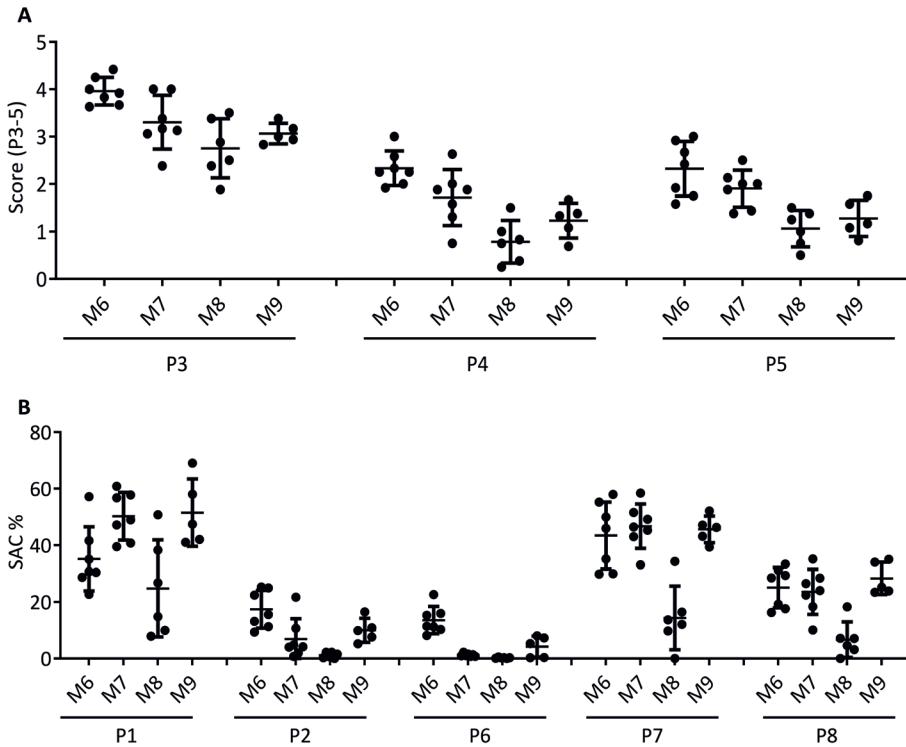
## 6.6 Supplementary Figures



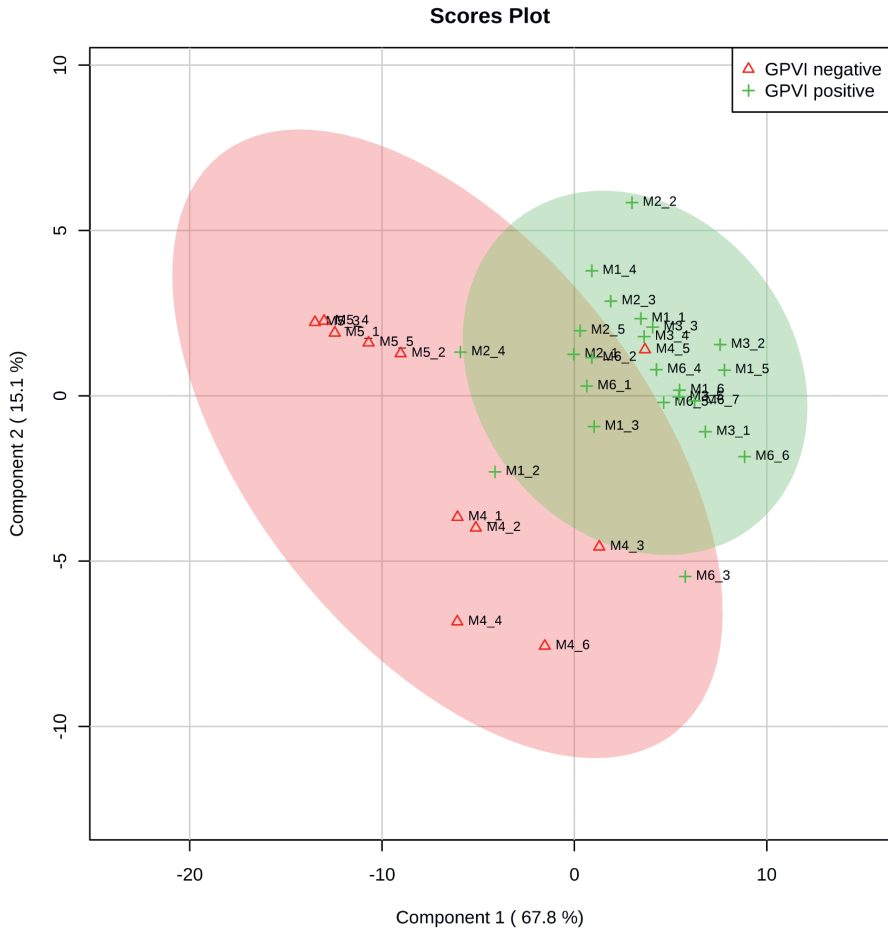
**Supplementary Figure 1 – Effect of Syk inhibitor PRT-060318 (Syk-IN) on agonist-induced platelet responses.** (A) Platelets in plasma ( $2.5 \times 10^8/\text{ml}$ ) were preincubated with vehicle (DMSO) or Syk-IN ( $5 \mu\text{M}$ ) for 10 minutes, and then activated with CRP-XL ( $10 \mu\text{g}/\text{ml}$ ), thrombin ( $8 \text{ nM}$ ) or stable ADP ( $5 \mu\text{M}$ ), as indicated. Shown are representative traces from light transmission aggregometry. (B) Fura-2-loaded platelets in 96-well plates were preincubated with Syk-IN ( $5 \mu\text{M}$ ) or left untreated before injection of thrombin ( $4 \text{ nM}$ ) or stable ADP ( $5 \mu\text{M}$ ), as in Figure 1. Shown are representative traces of changes in  $[\text{Ca}^{2+}]_i$  of control (black) and Syk-IN (grey) incubations. Arrows indicate addition indicated of agonists.



**Supplementary Figure 2 – Parameters of thrombus formation on immobilized collagen peptides: raw data.** Whole blood was perfused over microspots M1 (GFOGER-GPO + VWF-BP), M2 (CRP-XL + VWF-BP), M3 (GAOGER-GPO + VWF-BP), M4 (GFOGER-GPP + VWF-BP), and M5 (VWF-BP). Microscopic images were analyzed for parameters P1-8, as for Figure 2. Shown are raw mean outcome values from individual blood donors. (A) Parameters providing surface area coverage (SAC%) information: P1, platelet deposition; P2, platelet aggregate coverage; P6, PS exposure; P7, CD62P expression; P8, fibrinogen binding. (B) Score parameters: P3, thrombus morphological score (range 0-5); P4, thrombus multilayer score (range 0-3); P5, thrombus contraction score (range 0-3). Means  $\pm$  SD (n=5-7 donors).



**Supplementary Figure 3 – Parameters of thrombus formation on immobilized collagens: raw data.** Whole blood was perfused over microspots M6 (collagen-H), M7 (fibrillar collagen-I), M8 (monomeric collagen-I), M9 (collagen-III). Microscopic images were captured and analyzed for parameters P1-8, as for Figure 5. Shown are raw mean outcome values from individual blood donors. (A) Parameters providing surface area coverage (SAC%) information: P1, platelet deposition; P2, platelet aggregate coverage; P6, PS exposure; P7, CD62P expression; P8, fibrinogen binding. (B) Score parameters: P3, thrombus morphological score (range 0-5); P4, thrombus multilayer score (range 0-3); P5, thrombus contraction score (range 0-3). Means  $\pm$  SD (n=5-7 donors).



**Supplementary Figure 4 – Partial least squares with components 1 and 2, indicating distribution of thrombus formation parameters at microspots M1-6 for 5-7 individual blood samples per microspot. Note, the clustering (green area) of flow runs over (GPO)<sub>n</sub> containing surfaces M1-3 and M6, whereas flow runs with other surfaces M4 and M5 out-clustered with more negative contributions to component 2 or 1, respectively (red area). Red triangles indicate assumed negative GPVI contribution, green pluses indicate positive contribution.**

**Supplementary Table 1** – Scaled subtracted parameter values of thrombus formation (means), indicating effects of Syk-IN, for microspots M1-9 and parameters P1-8.

	P1	P2	P3	P4	P5	P6	P7	P8
<i>M1</i>	1.18±	0.10±	0.51±	0.15±	0.21±	0.03±	0.71±	0.62±
	0.46	0.14	0.17	0.16	0.20	0.05	0.49	0.66
<i>M2</i>	1.15±	0.16±	0.77±	0.30±	0.30±	0.04±	0.69±	0.31±
	0.24	0.13	0.15	0.20	0.15	0.06	0.39	0.28
<i>M3</i>	0.94±	0.10±	0.71±	0.37±	0.34±	0.01±	0.47±	0.11±
	0.24	0.07	0.17	0.23	0.12	0.00	0.27	0.08
<i>M4</i>	0.93±	0.17±	0.73±	0.34±	0.37±	0.13±	0.25±	0.04±
	0.29	0.29	0.09	0.34	0.40	0.16	0.18	0.03
<i>M5</i>	0.97±	1.27±	0.13±	0.00±	0.00±	0.63±	1.40±	0.36±
	1.18	2.13	0.12	0.00	0.00	0.79	2.65	0.43
<i>M6</i>	1.12±	0.19±	0.61±	0.22±	0.28±	0.02±	0.65±	0.42±
	0.33	0.10	0.15	0.17	0.18	0.02	0.35	0.44
<i>M7</i>	0.88±	0.03±	0.60±	0.10±	0.17±	0.03±	0.13±	0.02±
	0.21	0.06	0.20	0.11	0.12	0.02	0.08	0.02
<i>M8</i>	0.87±	2.91±	0.61±	0.64±	0.42±	0.16±	0.25±	0.12±
	0.56	6.23	0.35	0.74	0.28	0.15	0.16	0.17
<i>M9</i>	0.79±	0.07±	0.49±	0.13±	0.11±	0.03±	0.14±	0.05±
	0.20	0.07	0.06	0.23	0.13	0.03	0.12	0.05



# Chapter 7

## **Modulating roles of platelet PECAM1 and ITIM linked PTPN11 in collagen- and glycoprotein VI-induced thrombus formation**

Natalie J. Jooss\*, Marije G. Diender, Delia I. Fernández, Jingnan Huang, Floor C. J. Heubel-Moenen, Arian van der Veer, Marijke J. E. Kuijpers, Natalie S. Poulter, Yvonne M. C. Henskens\*, Maroeska te Loo\* and Johan W. M. Heemskerk\*

\* Equal contribution

Contributions: NJJ designed and performed experiments,  
analyzed data, prepared figures and wrote the manuscript  
To be submitted



**Abstract** The collagen receptors, glycoprotein VI (GPVI) and integrin  $\alpha 2\beta 1$ , jointly regulate collagen-induced platelet adhesion and thrombus formation under flow. Here we set out to determine how the ITIM (immunoreceptor tyrosine-based inhibitory motif) receptor PECAM1 and the protein tyrosine phosphatase PTPN11 can interfere with and modulate this collagen receptor dependent thrombus formation. Microspots of collagen-I,-III and -IV, with high and low GPVI dependency, served as surfaces for whole blood thrombus formation under flow. Integrin  $\alpha 2\beta 1$  and PECAM1 were inhibited with selective antibodies. Blood was used from healthy subjects and seven patients with Noonan syndrome with a confirmed gain of function mutation of *PTPN11* and a variable bleeding phenotype. Thrombus formation was measured in a multiparameter setting. With collagen types I, III and IV, inhibition of PECAM1 was without substantial effect on thrombus parameters after whole blood flow. However, with all collagens, PECAM1 inhibition fully restored the impaired thrombus formation caused by blockade of  $\alpha 2\beta 1$ . Flow studies with blood from seven Noonan patients with a gain of function mutation in *PTPN11* indicated a variable, but overall partial reduction in collagen-induced platelet activation that was even enforced by  $\alpha 2\beta 1$  blockage. However, the gain of PTPN11 activity did not enhance the rescuing effect caused by PECAM1 inhibition. Collectively, our results indicate that the PECAM1 and PTPN11 restraining mechanisms on collagen-induced thrombus formation are independent of the extent of GPVI activation, but dependent on other factors such as the PTPN11 activity and the engagement of  $\alpha 2\beta 1$ .

## 7.1 Introduction

Glycoprotein VI (GPVI) is a key signaling collagen receptor on human platelets, acting together with the adhesive receptor for collagen integrin  $\alpha 2\beta 1$ <sup>1-4</sup>. This set of receptors comes into action when subendothelial collagens are exposed to the blood stream as in vessel wall injury. Collagen-bound von Willebrand factor (VWF), in a shear dependent way, interacts with the platelet GPIb-V-IX complex to provide the first mechanism of platelet adhesion<sup>5,6</sup>. Subsequently, the two collagen receptors, GPVI and  $\alpha 2\beta 1$ , accomplish stable adhesion, signal transduction and functional platelet activation<sup>7-9</sup>. On the platelet membrane, GPVI is present in complex with the FcR  $\gamma$ -chain, carrying an immunoreceptor tyrosine-based activation motif (ITAM). Tyrosine phosphorylation of the ITAM via Src family kinases results in cascade of protein phosphorylation reactions, involving the tyrosine kinase Syk, the adapter protein LAT, and the effector proteins phosphatidylinositol 3 kinases (PI3K) and phospholipase C (PLC) $\gamma 2$ <sup>10-12</sup>. Activated PLC $\gamma 2$  generates inositol trisphosphate, mediating intracellular  $Ca^{2+}$  rises upon GPVI stimulation. Downstream functional events are platelet assembly to a thrombus via integrin  $\alpha IIb\beta 3$  activation (via PI3K), granule secretion and P-selectin expression (via PLC $\gamma 2$ ), platelet aggregation and surface exposure of the procoagulant phospholipid phosphatidylserine<sup>9,13</sup>. In this setting, the receptor type protein tyrosine phosphatase CD148 (PTPRJ) plays a positive role by accomplishing the initial SFK activation<sup>14</sup>.

Several platelet receptors bearing the immunoreceptor tyrosine-based inhibitory motif (ITIM) are known to antagonize the signaling by ITAM linked platelet receptors. This has been shown for the homotypic activating receptor PECAM1 (platelet endothelial cell adhesion molecule-1)<sup>15,16</sup>, and the heparin binding receptor G6b-B (MPIG6B)<sup>17-19</sup>. These two ITIM-linked receptors are highly expressed with 9,400 and 13,700 copies per platelet, respectively<sup>20</sup>.

'Negative' signaling via the ITIM receptors occurs through several protein tyrosine phosphatase non-receptor isoforms, in particular PTPN11 (Src homology region 2 domain-containing phosphatase-2, SHP2) and PTPN22<sup>21,22</sup>. However, some other PTPN isoforms enhance, rather than suppress, the ITAM dependent signaling, for example PTPN1 (protein tyrosine phosphatase 1B) and PTPN6 (SHP1)<sup>21,23</sup>. Overall, the conditions under which ITIM linked receptors and the associating tyrosine phosphatases can restrain the signaling responses of GPVI are still unclear.

In both human and mouse platelets, a gain of function mutation in the *PTPN11* gene led to an impaired platelet signaling upon GPVI stimulation<sup>24</sup>. Patients with such an autosomal dominant mutation are categorized as Noonan syndrome, and present with multiple symptoms such as a short stature, facial dysmorphism and developmental delay (OMIM: 163950). About half of the syndromic patients carries a gain of function *PMPN11* mutation, which is often but not always accompanied by a bleeding phenotype<sup>25</sup>. It is considered that the mutated PTPN11 (SHP2) protein shows constitutive tyrosine phosphatase activity, with a more favored active conformation in comparison to wildtype<sup>26,27</sup>. On the other hand, loss of function mutations in the *PTPN11* gene are also described, known as Noonan syndrome with multiple lentiginos (NSML) or formerly classified as Leopard syndrome (OMIM: 151100).

In the present report, we set out to further elucidate the cooperativity of the platelet collagen receptors GPVI and integrin  $\alpha 2\beta 1$  in flow dependent thrombus formation. We hypothesized that ITIM linked receptors and the connected tyrosine phosphatases become more prominent in restraining platelet activation upon: *i*) interaction of the cells with weaker activating collagen types, and *ii*) in the absence of  $\alpha 2\beta 1$  mediated adhesion stabilization. To investigate this, we studied the relatively abundant self-activating PECAM1

receptor, and we used blood from Noonan patients to investigate a modulating effect through altered PTPN11 activity.

## **7.2 Materials and Methods**

### **Materials**

Fibrillar Horn collagen-I was from Nycomed (Hoofddorp, The Netherlands); human collagen-IV (C7521) from Sigma-Aldrich (Zwijndrecht, The Netherlands); human collagen-III (1230-01S) from Southern Biotechnology (Birmingham, AL, USA). The blocking 6F1 mAb against integrin  $\alpha 2\beta 1$  was a kind gift from Dr. B. S. Coller (Rockefeller University, NY, USA). The inhibitory mouse anti-human PECAM1 mAb (303101, clone WM59, mouse IgG1) was purchased from BioLegend (London, UK). The control anti-PECAM1.2 mAb (MABF-2034, clone MBC 78.2, mouse IgG) came from Sigma-Aldrich (Merck, Amsterdam, The Netherlands) The polyclonal anti-G6b-B Ab (PA5-23300, rabbit IgG), the inhibitory anti-Fc $\gamma$ RIIA mAb (clone IV.3, mouse IgG2), and mouse IgG1 isotype control came from ThermoFisher Scientific (Eindhoven, The Netherlands). Anti-CD148 mAb (MABC-87, clone Ab1) and D-Phe-Pro-Arg chloromethyl ketone (PPACK) were from Sigma-Aldrich. Fluorescent stains came from the following sources: AlexaFluor(AF) 647 labeled anti-human CD62P mAb (304918, BioLegend); FITC-labeled anti-fibrinogen antibody (F0111, Dako, Amstelveen, The Netherlands); and AF568-labeled annexin A5 (A13202, ThermoFisher, Eindhoven, The Netherlands). Other materials were from sources described before <sup>28</sup>.

### **Subjects**

Blood samples were obtained by venipuncture from healthy volunteers who had not received anti-platelet medication for at least two weeks. Approval was obtained from the medical ethics committee from Maastricht University Medical Centre+ (MUMC+). Permission for blood drawing from Noonan

patients was obtained from medical ethics committees of Radboud University (Evaluation of Bleeding Disorders in Noonan Patients, non-WMO) and MUMC+ (ProBe-AHP: Predictors of Bleeding Evaluation in Adult Hematologic Patients with Bleeding Tendencies, METC 14-4-036, Dutch Trial Register, NL9643). All blood donors gave informed consent according to the declaration of Helsinki to participate in the study.

### **Collection and preparation of blood samples**

Blood was taken from healthy donors or patients into 3.2% trisodium citrate tubes (Vacuette tubes, Greiner Bio-One, Alphen a/d Rijn, The Netherlands). Almost all subjects had normal platelet counts within the reference range, such as established with a Sysmex XN-9000 analyzer (Sysmex, Cho-ku, Kobe, Japan). Platelets from one patient (NS3) were slightly below the normal range.

### **Microfluidics and thrombus formation**

Degreased coverslips were coated with 0.5  $\mu$ l microspots of 100  $\mu$ g/ml collagen-I, collagen-III or collagen-IV, as described before <sup>13</sup>. Per coverslip, coating was performed with two spots of the same collagen (humid chamber, overnight 4°C), and after a wash, the upstream microspot was post-coated for 1 hour with antibody solution (all 1  $\mu$ g/ml) and the downstream spot with saline. Subsequently, microspots were blocked with HEPES buffer pH 7.45 containing 1% BSA, before mounting into the flow chamber <sup>13</sup>.

For perfusion studies, whole blood samples preincubated with vehicle or inhibitor (10 minutes), were supplemented with PPACK (f.c., 40  $\mu$ M) and recalcified (f.c., 3.75 mM MgCl<sub>2</sub> and 7.5 mM CaCl<sub>2</sub>). The samples were then perfused through a parallel plate flow chamber at wall shear rate of 1000/s for 3.5 minutes. Two brightfield images were acquired per microspot, while perfusing the flow chamber with labeling buffer (HEPES buffer pH 7.45 containing 2 mM CaCl<sub>2</sub>, 1 U/ml heparin, and as stains AF647 anti-CD62P

mAb, FITC anti-fibrinogen mAb and AF568 annexin A5) <sup>13</sup>. After washing off non bound label with HEPES buffer, per microspot three random fields of view were images for multicolor fluorescence <sup>29</sup>. All raw data is given in Supplemental Datafile.

## Microscopy and image analysis

Images were acquired with an EVOS-FL microscope (Life Technologies, Bleiswijk, The Netherlands), equipped with three fluorescent LEDs combined with dichroic cubes (Cy5, RFP, GFP), an Olympus UPLSAPO 60x oil-immersion objective, and a sensitive 1360×1024-pixel CCD camera. As described before <sup>29</sup>, images were quantified for surface area coverage and scored for characteristic thrombus parameters utilizing established, semi-automated ImageJ scripts. Parameters 1-5 were generated from brightfield images, and parameters 6-8 from single color fluorescence images (**Table 1**).

**Table 1 – Annotations of microspots and parameters of thrombus formation.** Indicated per microspot are contributions of receptors to whole blood thrombus formation, adapted from Refs. <sup>31,49</sup>. Furthermore, listing of image analysis parameters (P1-8) from brightfield and fluorescence microscopy, and factor used for univariate scaled heatmaps. N.d., not determined.

Microspot		Platelet receptors		
		GPVI	$\alpha 2\beta 1$	GPIIb
M1	Collagen-I ( $\pm$ Ab post-coating)	++	+	+
M2	Collagen-III ( $\pm$ Ab post-coating)	+	+	+
M3	Collagen-IV ( $\pm$ Ab post-coating)	n.d.	n.d.	+
Parameter		range	scaled	
<i>Brightfield</i>				
P1	Platelet deposition (% SAC)	0 - 66	0 - 10	
P2	Platelet aggregate coverage (% SAC)	0 - 19	0 - 10	
P3	Thrombus morphological score	0 - 4	0 - 10	
P4	Thrombus multilayer score	0 - 3	0 - 10	
P5	Thrombus contraction score	0 - 3	0 - 10	
<i>Fluorescence images</i>				
P6	P-selectin expression (AF647 $\alpha$ -CD62P mAb, % SAC)	0 - 56	0 - 10	
P7	Integrin $\alpha$ IIb $\beta$ 3 activation (FITC $\alpha$ -fibrinogen Ab, % SAC)	0 - 24	0 - 10	
P8	PS exposure (AF568 annexin A5, % SAC)	0 - 10	0 - 10	

## Data handling and statistics

Data were tested for significance using GraphPad Prism V.8 software. Heatmaps were generated with the program R V.3.5.2. For the heatmap preparation, raw values per blood donor and condition were first averaged and then per parameter univariately scaled (0-10) across surfaces<sup>29</sup>. To visualize treatment effects, subtraction heatmaps were created from the scaled parameters relative to the relevant control values. One-way ANOVA was used to assess for statistical significance, set at  $p < 0.05$ .

## 7.3 Results

### **Blocking of PECAM1 activity restores the downregulated collagen-induced thrombus formation by integrin $\alpha 2\beta 1$ blockade**

Knowing the additive roles of GPVI and integrin  $\alpha 2\beta 1$  in thrombus formation on fibrillar collagen preparations<sup>8,30</sup>, we first set out to reexamine this for a range of vascular relevant collagens, *i.e.*, types I, III and IV. As indicated in Table 1, the two latter collagen types are relatively low in stimulating GPVI mediated platelet activation<sup>31</sup>. We furthermore investigated the contribution of the ITIM containing receptor PECAM1, using an anti-PECAM mAb (WM59, mouse IgG1), previously shown to inhibit PECAM1 dependent signaling. The WM59 antibody recognizes the first or second Ig domain of PECAM1, and thus prevents its homophilic ligation and ensuing signaling events<sup>16</sup>. Accordingly, we hypothesized attenuation of PECAM1 signaling mediated by the platelet inhibiting tyrosine phosphatase PTPN11 (SHP2) may be most effective under conditions where GPVI is lowly active, *i.e.*, not reinforced by integrin  $\alpha 2\beta 1$  dependent platelet contact with collagens.

To examine the consequences of PECAM inhibition, we perfused whole blood from healthy subjects over two collagen microspots, of which the upstream microspot was post-coated with the inhibitory anti-PECAM1

antibody WM59<sup>32</sup>. Perfusion experiments were all performed with recalcified citrated blood under high shear flow conditions<sup>13</sup>. For the blocking of platelet integrin  $\alpha 2\beta 1$ <sup>33</sup>, blood samples were preincubated with the 6F1 mAb or with a vehicle control (PBS). The platelet thrombi formed on collagens-I, -III or -IV were post-labeled with three fluorescent markers for platelet activation,  $\alpha$ -granule secretion (AF647 anti-CD62P mAb), integrin  $\alpha \text{IIb}\beta 3$  activation (FITC anti-fibrinogen mAb) and phosphatidyl-serine exposure (AF568 annexin A5). Representative microscopy images indicated for collagen-I the formation of large platelet aggregates, which stained highly for all activation markers (**Supplementary Figure 1A**). Typically, on collagen-I with 6F1 mAb present substantially smaller thrombi were formed, while the post-coating with inhibitory  $\alpha$ -PECAM1 mAb reversed this inhibition. When compared to collagen-I, collagen-III and collagen-IV induced the formation of smaller sized thrombi with lower platelet activation, while inhibitory effect of 6F1 mAb again were antagonized by the co-coated  $\alpha$ -PECAM1 mAb (**Supplementary Figure 1B,C**).

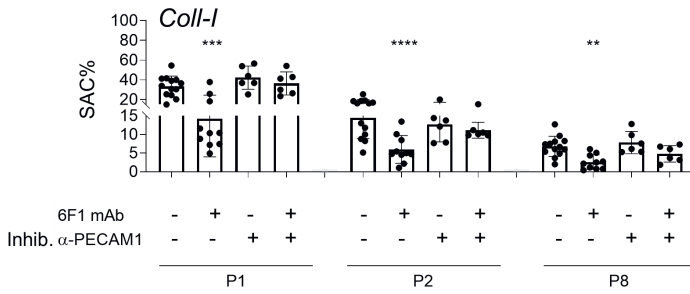
Quantification of the microscopy images resulted in eight parameters for: platelet adhesion (parameter P1), thrombus phenotypes (parameters P2-5), and platelet activation in three colors (parameters P6-8), as was validated before<sup>29</sup>. The analysis (based on surface area coverage) of platelet deposition (P1), thrombus multilayer size (P2) and phosphatidylserine exposure (P8) revealed that  $\alpha 2\beta 1$  blockade by 6F1 mAb significantly decreased all these parameters for each of the collagen surfaces (**Figure 1A i-iii**). When taking phosphatidylserine exposure as a marker for GPVI activity<sup>30</sup>, the data indicated that collagen-I most strongly stimulated the GPVI pathway. For all collagens, co-coating with the inhibitory  $\alpha$ -PECAM1 mAb – assumed to negatively modulate PECAM1 and ITIM signaling – do not affect platelet adhesion, thrombus size or platelet procoagulant activity. In sharp contrast, in the presence of  $\alpha 2\beta 1$  blocking 6F1 mAb, the co-coating with inhibitory  $\alpha$ -



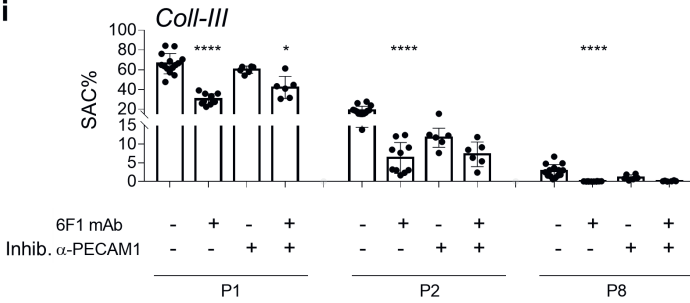
PECAM1 mAb resulted in a rescue of these parameters (P1, P2, P8), back to basal levels (**Figure 1A i-iii**). This rescue was greatest for the low GPVI and high  $\alpha 2\beta 1$  dependent surface, collagen-IV.

The generation of subtraction heatmaps for all parameters per microspot allowed a better visualization of the effects of co-coating with inhibitory anti-PECAM1 mAb under conditions where 6F1 mAb was absent or present. For these heatmaps, raw data were univariate scaled (0-10) across all surfaces, subtracted from the control values, and the scaled differences were filtered for relevant effects (arbitrarily set at  $p < 0.05$ ). The heatmaps pointed to a relevant lowering by 6F1 mAb of in total 5 (collagen-I), 7 (collagen-III) and 7 (collagen-IV) of the 8 parameters (**Figure 1B**). For all collagen surfaces, the  $\alpha 2\beta 1$  blockade most strongly affected thrombus multilayer size (P2), P-selectin expression (P6) and integrin  $\alpha IIb\beta 3$  activation (P7); and reduced to a lesser extent platelet deposition (P1) and phosphatidylserine exposure (P8). Importantly, with co-coated inhibitory anti-PECAM1 mAb, all parameter changed by  $\alpha 2\beta 1$  blockade were annulled for collagen-I and collagen-IV, whereas for collagen-III the platelet activation parameters P6 and P7 were still below control values. Taken together, these data point to a thrombus stimulating effect of the inhibitory anti-PECAM1 mAb – *i.e.*, compatible with the ITIM dependent signaling of PECAM1 – only under conditions of  $\alpha 2\beta 1$  blockade, regardless of the ‘platelet activating strength’ of the collagen type.

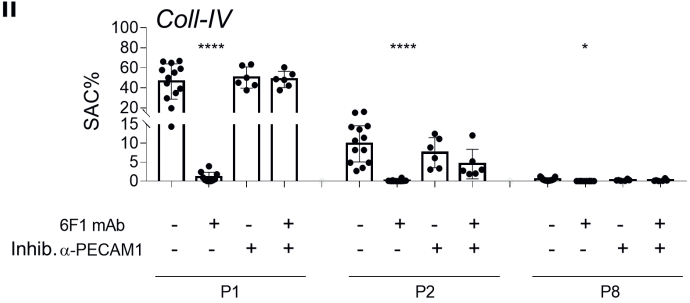
**A i**



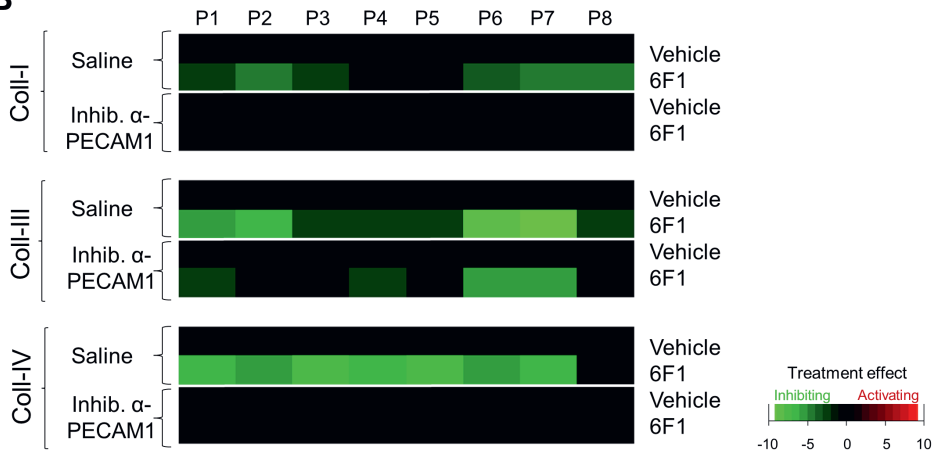
**ii**



**iii**



**B**



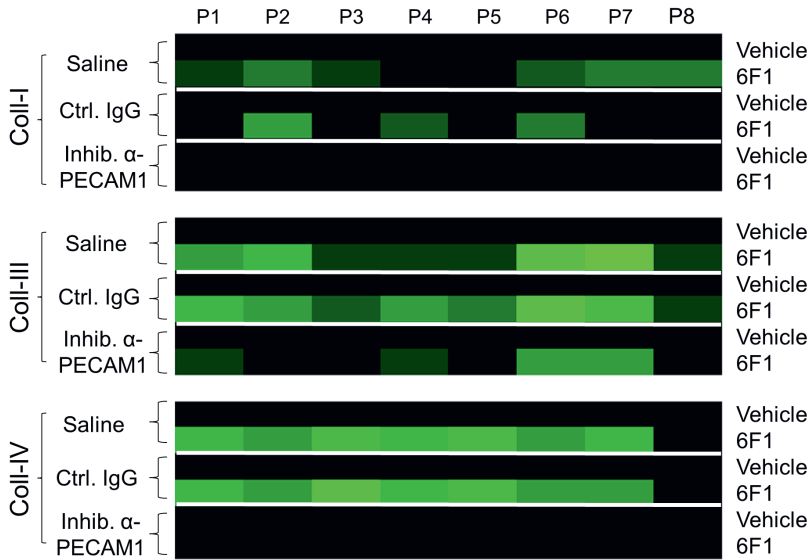
7

**Figure 1 (previous page) – Enhanced collagen-induced thrombus formation by inhibitory anti-PECAM1 antibody upon blockade of integrin  $\alpha 2\beta 1$ .** (A) Blood samples were preincubated with 6F1 mAb (20  $\mu\text{g}/\text{ml}$ ) or vehicle, and then perfused during 3.5 minutes at 1000/s over microspots of collagen-I (i), collagen-III (ii) or collagen-IV (iii); all microspots were post-coated with saline or inhibitory anti-PECAM1 mAb (clone WM59, mouse IgG1). Multicolor microscopic images were analyzed for platelet adhesion, thrombus phenotype and platelet activation parameters (Table 1). Shown are quantified data of platelet deposition (parameter P1), thrombus multilayer size (parameter P2), and phosphatidylserine exposure (parameter P8) in the presence or absence of 6F1 mAb and/or inhibitory anti-PECAM1 mAb. Representative images are shown in Supplemental. Figure 1. (B) Subtraction heatmap presentation of the eight univariately scaled (0-10) parameters across surfaces, showing values of treatment effect per microspot type relative to vehicle containing blood samples. For the color coding, a relevance filter was applied of  $p < 0.05$ . Means  $\pm$  SD ( $n=6-7$ ); one-way ANOVA \* $p < 0.05$ , \*\* $p < 0.005$ , \*\*\* $p < 0.001$ , \*\*\*\* $p < 0.0001$ . Raw data of P1-8 are given in Supplemental Datafile.

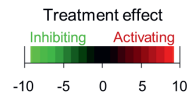
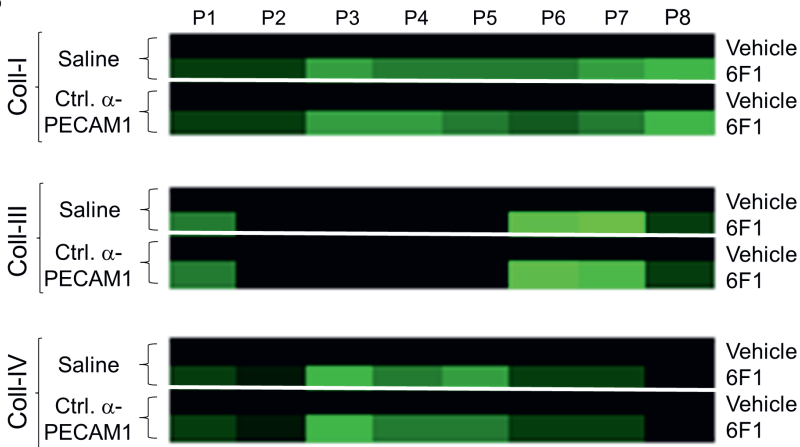
### **Effect of inhibitory anti-PECAM1 antibody in rescuing $\alpha 2\beta 1$ blocked thrombus formation**

To establish whether the co-coating effects were specific for the inhibitory anti-PECAM1 antibody, we repeated the flow experiments by co-coating collagen microspots with several other immunoglobulins or antibodies. As before, subtraction heatmaps were generated for the 3 collagens and 8 parameters. Upon co-coating of the collagens with mouse isotype control IgG1, heatmaps indicated that this did not alter the suppressive effects of  $\alpha 2\beta 1$  blockade by 6F1 mAb regarding the majority of parameters (**Figure 2A**). This was in clear contrast to the rescue effects by co-coated inhibitory anti-PECAM1 mAb. As another control, we co-coated the microspotted collagens with a control anti-PECAM mAb (clone MBC 78.2, mouse IgG) against the PECAM1 IgG domain 6, which has activating rather than inhibiting activity<sup>34</sup>. Subtraction heatmaps showed that this non inhibitory anti-PECAM1 antibody was unable to antagonize the effects of integrin  $\alpha 2\beta 1$  blockage with 6F1 mAb (**Figure 2B**).

**A**



**B**



7

**Figure 2 (previous page) – Selective effect of inhibitory anti-PECAM1 mAb in rescue of collagen-induced thrombus formation upon  $\alpha 2\beta 1$  inhibition.** Blood samples were preincubated with 6F1 mAb (20  $\mu\text{g}/\text{ml}$ ) or vehicle, and then perfused during 3.5 minutes at 1000/s over microspots of collagen-I, collagen-III or collagen-IV. Microspots were post-coated with saline, inhibitory anti-PECAM1 mAb (IgG1), mouse isotype control IgG1, or a control anti-PECAM mAb (clone MBC 78.2), as indicated. Multicolor microscopic images were analyzed for eight parameters (Table 1), which were univariate scaled. (A, B) Subtraction heatmaps for comparing per collagen type the effects of integrin  $\alpha 2\beta 1$  blockage (by 6F1 mAb) on parameters: P1, platelet deposition; P2, thrombus multilayer size; P3, thrombus morphological score; P4, thrombus multilayer score; P5, thrombus contraction score; P6, P-selectin expression; P7, integrin  $\alpha \text{IIb}\beta 3$  activation; P8, phosphatidylserine exposure. (A) Heatmapped effects of the 6F1 mAb on microspots of a collagen + inhibitory anti-PECAM1 mAb or the collagen + control IgG. (B) Heatmapped effects of 6F1 mAb on microspots of a collagen + control anti-PECAM1 mAb. Means  $\pm$  SD (n=3-7), tested for significance with one-way ANOVA. For color coding, a filter was applied of  $p < 0.05$ . Raw data are given in Supplemental Datafile.

To take this further, we also checked a co-coating of antibodies against the extracellular domains of two other ITIM linked receptors, G6b-B and CD148. For this purpose, we used microspots of collagen-IV, as this surface showed the largest effects of  $\alpha 2\beta 1$  blockade. The use of a polyclonal anti-G6bB antibody did not result in significant effects on the thrombus parameters P1, P2 and P8 with or without 6F1 mAb (**Figure 3A**). The use of anti-CD148 mAb (clone Ab1) – which is known to inhibit ITIM-mediated activity in bivalent form <sup>35</sup> – similarly was without effect on each parameter (**Figure 3B**). Subtraction heatmaps confirmed this for the all parameters P1-8, in that neither anti-G6b-B nor anti-CD148 antibody co-coating was able to antagonize the effects of  $\alpha 2\beta 1$  blockade (**Figure 3C**; raw data in Supplemental Datafile).

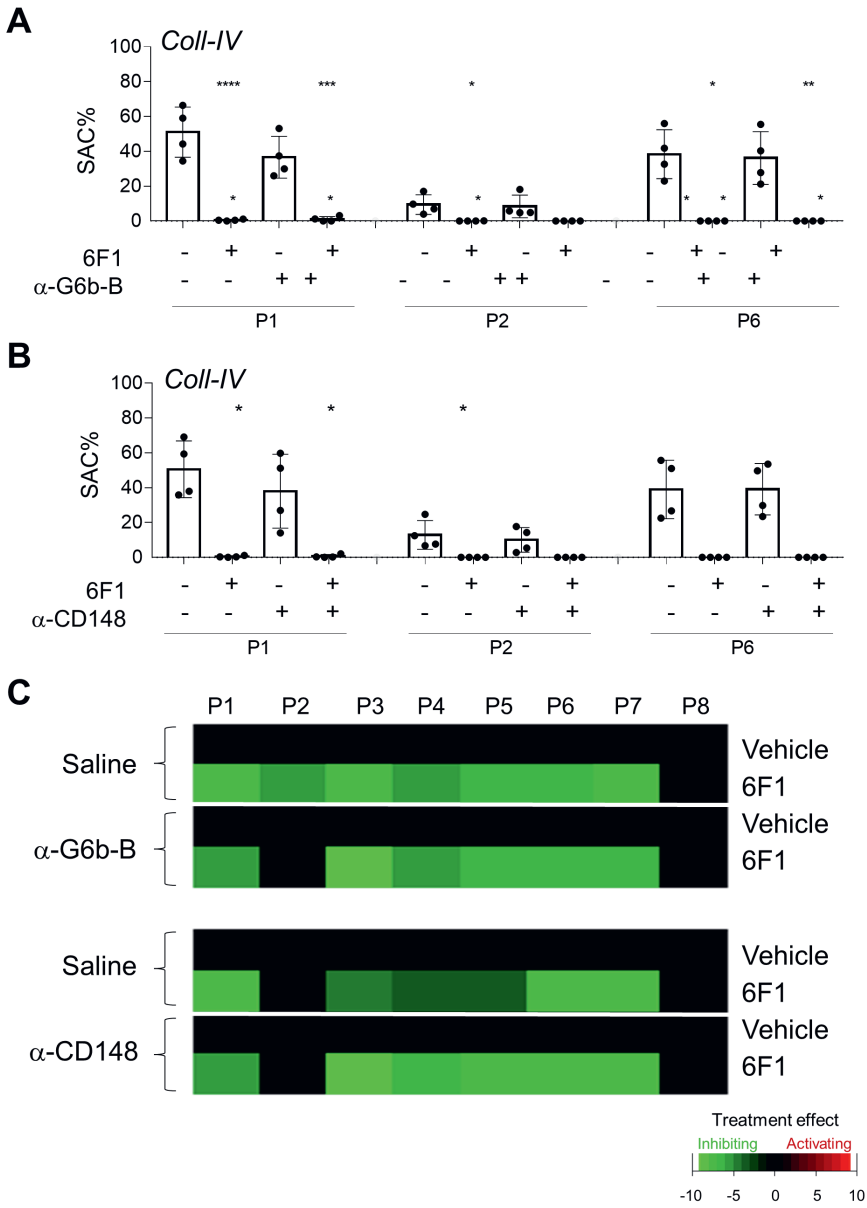


**Figure 3 (previous page) – Inability of other antibodies against ITIM containing receptors to rescue collagen-induced thrombus formation upon  $\alpha 2\beta 1$  inhibition.** Blood samples were preincubated with 6F1 mAb (20  $\mu\text{g}/\text{ml}$ ) or vehicle and perfused during 3.5 minutes at 1000/s over microspots of collagen-IV, as for Figure 1. Microspots were post-coated with saline, anti-G6bB Ab (rabbit polyclonal) or anti-CD148 mAb (clone Ab1). Multicolor microscopic images were analyzed for eight parameters (Table 1), which were univariate scaled. (A, B) Shown are quantified outcome data of collagen-induced platelet deposition (parameter P1), thrombus multilayer size (parameter P2), and phosphatidylserine exposure (parameter P8) in the presence or absence of 6F1 mAb (in blood) and/or anti-G6b-B Ab (A) or anti-CD148 mAb (B). In addition, subtraction heatmaps comparing the effects of integrin  $\alpha 2\beta 1$  blockage by 6F1 mAb on all 8 parameters (C). For color coding, a relevance filter was applied of  $p < 0.05$ . Means  $\pm$  SD (n=4), tested for significance with one-way ANOVA, \* $p < 0.05$ , \*\* $p < 0.005$ , \*\*\* $p < 0.001$  and \*\*\*\* $p < 0.0001$ . Raw data are given in Supplemental Datafile.

As another control, we checked if the inhibitory anti-PECAM1 mAb could act by platelet activation through the Fc $\gamma$ RIIA receptors<sup>36</sup>. To investigate this, blood samples were pretreated with the Fc $\gamma$ RIIA blocking mAb IV.3, and then perfused over microspots of collagen-I, collagen-III or collagen-IV with or without co-coated inhibitory anti-PECAM1 mAb. The results of this experiment with IV.3 present indicated that again that all thrombus parameters increased to normal in the combined presence of inhibitory anti-PECAM1 mAb and integrin  $\alpha 2\beta 1$  blockage (**Supplementary Figure 2**, compare with **Figure 2B**). This indicated that the rescue effect of inhibitory anti-PECAM1 mAb was independent of the Fc $\gamma$ RIIA activation pathway.

In summary, this experimental set indicated that the ability to restore the whole blood platelet activation and thrombus formation with blocked  $\alpha 2\beta 1$  back to normal was confined to the co-coating with inhibitory anti-PECAM1 mAb; and furthermore, that this rescue effect extended to all  $\alpha 2\beta 1$ -dependent collagen types. This suggested a mechanism of PECAM1 and ITIM mediated suppression of a collagen-induced thrombus formation that only becomes

functional under conditions where the  $\alpha 2\beta 1$  contribution to GPVI activity is absent.

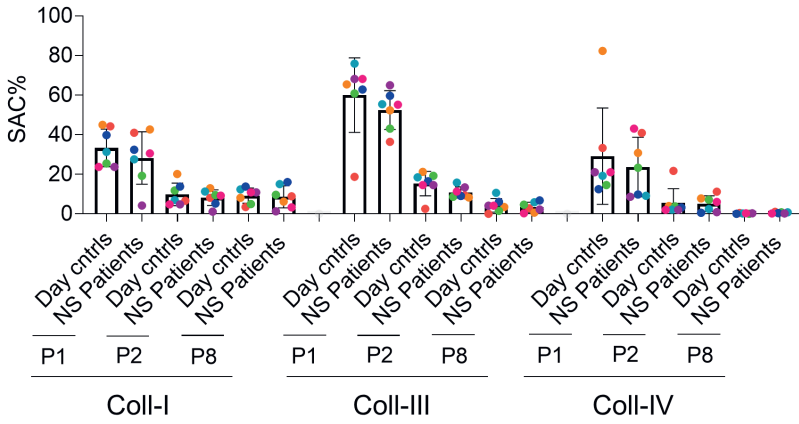
### **Changes in collagen-induced thrombus formation in Noonan patients with PTPN11 mutation**

To evaluate the role of PTPN11 signaling downstream of PECAM1 in the collagen-induced thrombus formation, we collected blood samples from seven Noonan syndrome patients with a gain of function mutation in the *PTPN11* gene. All patients had normal platelet and red blood cell counts, and five of the patients had a (mild) bleeding tendency (**Table 2**). After perfusion of blood samples, we noticed heterogeneity of the parameters between individual patients, which was somewhat higher than between the day control subjects; this held for the microspots of collagen-I (**Supplementary Figure 3A**), collagen-III (**Supplementary Figure 3B**) and collagen-IV (**Supplementary Figure 3C**). This agrees with the previously assessed intra-individual component of the various thrombus formation parameters<sup>29</sup>. When zooming in to the parameters P1, P2, P8, no major differences were seen for the whole cohort of patients, in comparison to the cohort of day control subjects (**Figure 4A**). However, when calculating the cumulative differences of univariate scaled parameters, we observed with 4 of the 7 patients (NS2, NS3, NS5, NS6) lower values for at least two collagen surfaces, in comparison to the control subjects (**Figure 4B**). In the subtraction heatmap versus means of controls, the relative impairments per patient could be ordered as NS6 > NS5, NS4 > NS2, NS3 (**Figure 4C**).

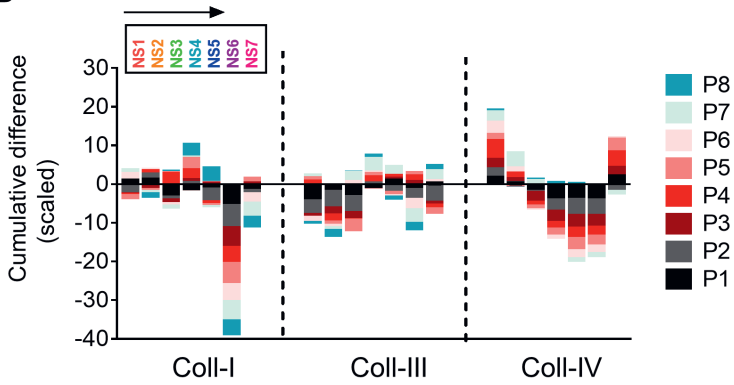
In general, the patient related changes were small on collagen-I (except for NS6), were clearest on collagen-VI for NS4-NS6 and limited on collagen-III surface for parameters P1-2 (NS1-NS3). Representative images of these differences are shown in **Supplementary Figure 4**.



**A**



**B**



**C**

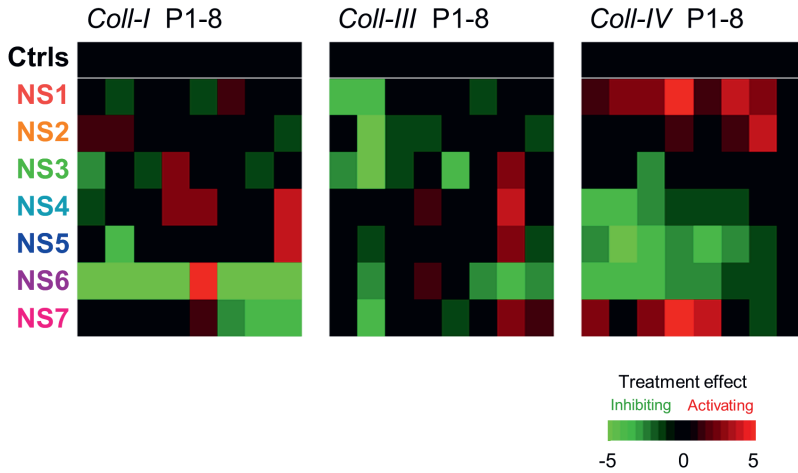


**Figure 4 (previous page) – Alterations in collagen-induced thrombus formation with Noonan syndrome patients.** Blood was taken from 6-day control subjects and 7 patients with Noonan syndrome (NS1-NS7), genotyped for a gain of function mutation in *PTPN11*. Blood samples were perfused over collagen-I, collagen-III or collagen-IV, after which images were analyzed, as in Figure 1. (A) Quantified raw outcome data per subject of collagen-induced platelet deposition (parameter P1), thrombus multilayer size (parameter P2), and phosphatidylserine exposure (parameter P8). (B) Cumulative plots of univariately scaled (0-10) parameters P1-8 per patient, in comparison to day control subjects. Indicated are relative increases and decreases versus mean values of all controls. Color code for patients as in panel A. (C) Heatmapped of differentially scaled parameter data per collagen type versus mean values of controls.

To determine the sensitivity of the patients' platelets for  $\alpha 2\beta 1$  blockage, similar flow runs were performed with blood samples preincubated with 6F1 mAb, while in addition microspots were co-coated with the inhibitory anti-PECAM1 mAb. Interestingly, the calculated cumulative decrease by 6F1 mAb for all parameters on collagen-I, -III or -IV only microspots ( $\geq 2$  surfaces) was higher for some of the patients (NS1-NS2, NS5-NS7) than for the day controls (**Figure 5A**).

**Table 2 – Overview of healthy subjects and genotyped patients hematological parameters.** NS, confirmed Noonan syndrome with (likely) pathogenic variants of *PTPN11*. \*Mean  $\pm$  SD.

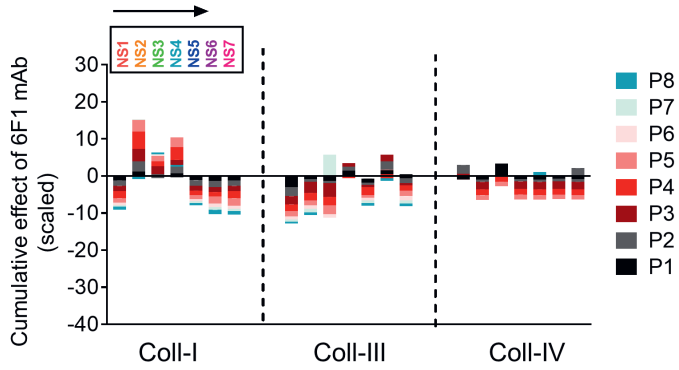
Subject	Age (years)	Red blood cells ( $10^{12}/L$ )	Platelets ( $\times 10^9/L$ )	Bleeding score	Genetics <i>PTPN11</i>
Day controls (6)*	>22	4.15 $\pm$ 0.33	272 $\pm$ 79	n.d.	n.d.
NS1	38	3.70	245	13	c.188A>G
NS2	13	4.78	212	1	c.1510A>G
NS3	12	4.79	148	1	c.205G>C
NS4	13	4.98	266	0	c.1510A>G
NS5	13	5.03	206	2	c.922A>G
NS6	5	4.93	254	0	c.1507G>A
NS7	4	4.37	283	1	c.1529A>G

N.d., not determined.

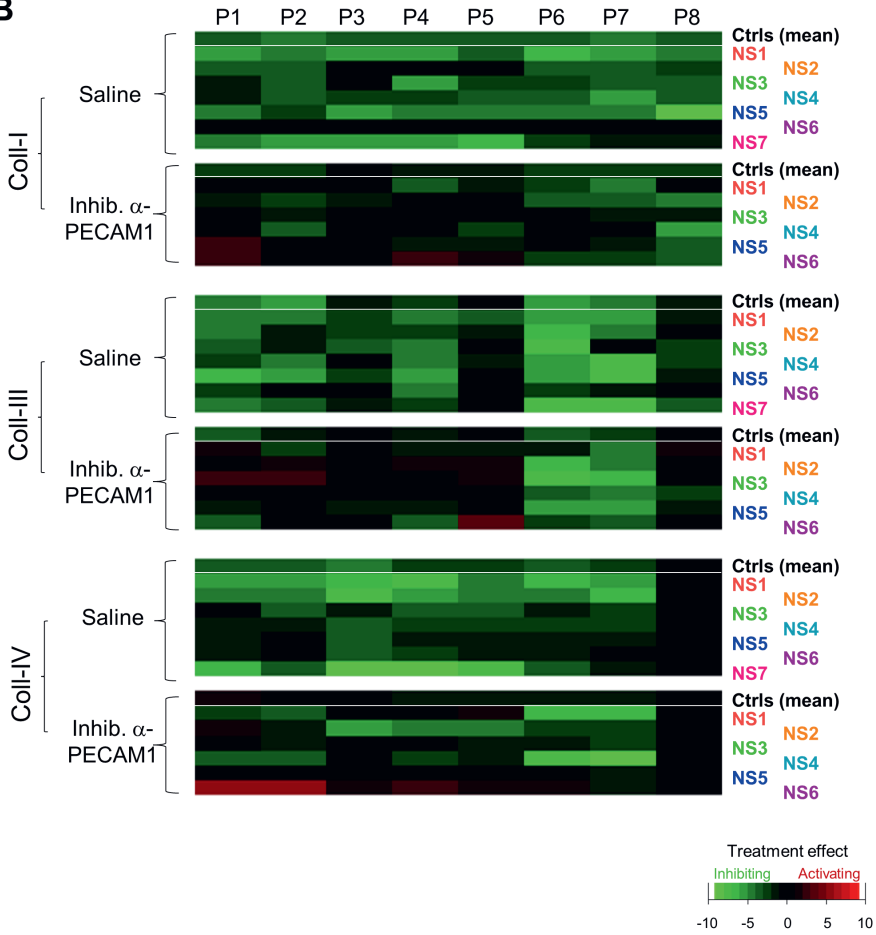
These decreases add to the lower thrombus formation parameters already seen under control conditions. Subtraction heatmaps were then made, to visualize the 6F1 mAb effects per patient and per collagen surface with or without inhibitory anti-PECAM1 mAb, in comparison to the day controls. In **Figure 5B**, the brighter green heatmap colors for many parameters (especially platelet activation markers P6-7) illustrate the overall larger effects of  $\alpha 2\beta 1$  blockage on spots not containing the antibody. Unexpectedly, with PECAM1 inhibition, the 6F1 effects reduced to a similar or even lower level (*i.e.*, remaining green colors) in the patients than (previously) seen in healthy control subjects (**Figure 5B**). Together, this indicated that the gain of PTPN11 function in these patients led to a variable, but overall lower collagen-induced platelet activation that was enforced by  $\alpha 2\beta 1$  blockage. However, the gain of PTPN11 activity did not enhance the rescuing effect by PECAM1 inhibition.

**Figure 5 (following page) – Increased responsiveness to  $\alpha 2\beta 1$  blockage with Noonan syndrome patients.** Blood was taken from 6-day control subjects and 7 patients with Noonan syndrome (NS1-NS7) was perfused over collagen surfaces, and thrombus parameters were scaled and analyzed, as for Figure 4. Collagen microspots were co-coated with saline or inhibitory anti-PECAM1 mAb. Blood samples contained blocking  $\alpha 2\beta 1$  6F1 mAb or vehicle. (A) Cumulative plots of scaled effects of 6F1 mAb per patient, parameter and collagen type. Indicated are relative increases and decreases versus mean values of all controls. Color code for patients as in Figure 4. (B) Subtraction heatmap of 6F1 mAb effects (scaled parameters P1-8) per patient for microspots of collagen-I, collagen-III and collagen-IV, co-coated with saline or inhibitory anti-PECAM1 mAb. Based on mean  $\pm$  SD (n=6 controls). For raw data, see Supplemental Datafile.

**A**



**B**



## 7.4 Discussion

In the present paper, we assessed if and how ITIM linked receptors and connected tyrosine phosphatases suppress GPVI dependent platelet responses under conditions of flow in which: *i*) platelets interact with more or less active collagens, and *ii*) integrin  $\alpha 2\beta 1$  is blocked and hence is unable to support GPVI activity. To investigate this, we perfused whole blood over collagen types I, III and IV, with a high or low GPVI activating potential, respectively <sup>31</sup>. Our results pointed to a specific thrombus modulating effect of the ITIM linked receptor PECAM1 which, however, was independent of the collagen type and became prominent under conditions of integrin  $\alpha 2\beta 1$  blockage.

For over two decades, it has been known that the PECAM1 receptors on human or mouse platelets serve to restrict and modulate platelet responses evoked by collagens <sup>37,38</sup>. One report has also shown that PECAM1 can act as a negative modulator of laminin induced platelet activation <sup>39</sup>. In addition, PECAM1 activity can also negatively regulate platelet responses to agonists of G protein-coupled receptors <sup>12,16</sup>. Yet, other reports using knockout mice pointed to only a weak role of PECAM1 in terms of activation via the collagen receptor GPVI <sup>40</sup>, but a larger role in megakaryocyte development <sup>41</sup>. In our hands, the negative regulatory contribution of PECAM1 to collagen dependent thrombus formation was strongest upon blockage of  $\alpha 2\beta 1$ , and it was surprisingly independent of the type of collagens, *i.e.*, of collagens inducing a higher or lower GPVI-induced platelet response. As a selective tool in the studies, we used the inhibitory anti-PECAM mAb WM59. This antibody recognizes the first or second Ig domain of PECAM1, and thereby prevents its homophilic ligation and consequently the signaling via PECAM1 <sup>16</sup>. By contrast, an antibody against the sixth Ig domain of PECAM1, which is considered to increase rather than inhibit PECAM1 activity <sup>15,42</sup>, appeared to

be without effect on the thrombus formation parameters. Jointly, our results thus support the idea of a weak role of PECAM1 in collagen dependent platelet activation, which can be boosted under particular conditions, *i.e.*, when platelet adhesion via  $\alpha 2\beta 1$  is suppressed. In other words, our findings indicate that, under flow, integrin  $\alpha 2\beta 1$  helps to prevent a PECAM1 and ITIM dependent negative regulation of platelet activation, likely through the involvement of protein tyrosine phosphatases.

Estimates for human platelets indicate that PECAM1 is expressed at a relatively high level (9,435 copies/platelet), when compared to GPVI (9,577 copies),  $\alpha 2\beta 1$  (4,588 copies) and PTPN11 (3,666 copies)<sup>20</sup>. In general, the receptor PECAM1 uses another PECAM molecule as a ligand, although also other ligands have been identified, such as integrin  $\alpha v\beta 3$  and the immune cell receptor CD38<sup>43,44</sup>. The dependency of PECAM1 effects on  $\alpha 2\beta 1$  dependent platelet adhesion can be considered as physiologically relevant, given the substantial variation in  $\alpha 2\beta 1$  expression on human platelets<sup>45,46</sup>, and the reports that subjects lacking  $\alpha 2\beta 1$  expression present with or without a bleeding phenotype<sup>47,48</sup>. For future research, it will be interesting to see how the (variable)  $\alpha 2\beta 1$  dependent modulation of PECAM1 signaling contributes to this phenotype.

As an approach to understand the signaling route involved, we used blood from patients with Noonan syndrome and an established gain of function mutation in the *PTPN11* gene, which encodes the corresponding protein tyrosine phosphatase non receptor (also known as SHP2). Noonan patients with such mutations present with a variable bleeding diathesis<sup>25</sup>, which has recently been linked to partial impairments in collagen-induced thrombus formation<sup>24</sup>. In our hands, using blood from five out of seven patients, we also observed reductions in thrombus parameters, which in particular concerned the less active collagens (types III and IV)<sup>31</sup>. We also observed additional

reductions in thrombus parameters upon  $\alpha 2\beta 1$  blockade, when compared to the blood from healthy control subjects. Together, this indicated that a gain of function of PTPN11 – via altered signaling or protein expression mechanisms in the patients' platelets – can negatively modulate the thrombus formation on collagens especially when  $\alpha 2\beta 1$  is blocked. However, with the patient blood, we did not observe a clearly enhanced recovery effect upon inhibition of PECAM1. This suggests that either the PECAM1 signaling through PTPN11 is already optimal with the wildtype phosphatase, or that other ITIM coupled signaling elements than PTPN11 steer the signaling process.

Taken together, our results indicate that the PECAM1 and PTPN11 restraining mechanisms on collagen-induced thrombus formation are independent of extent of GPVI activation, but dependent on other factors such as the engagement of  $\alpha 2\beta 1$ . Accordingly, the present work underlines the relevance for overlapping functions of the platelet collagen receptors and the potential of inhibitory signaling pathways to rescue defective phenotypes.

**Author Contributions** NJJ designed and performed experiments, analyzed data, prepared figures and wrote the manuscript. DF performed experiments and revised the manuscript. FCJHM, MGD, AvdV and MtL supplied patient samples and revised the manuscript. MJEK, YMCH, and NSP contributed to funding and supervision, and revised the manuscript. JWMH designed experiments, provided supervision and funding, and wrote the manuscript.

**Acknowledgments and Funding** We thank Dr. B. S. Coller, Rockefeller University, New York USA for the supplying of 6F1 antibody as well as Isabella Provenzale for help with plotting of some patient values. This work has received funding from the European Union's Horizon 2020 research and innovation program under the Marie Skłodowska-Curie grant agreement No. 766118 (TAPAS). NJJ is enrolled in a joint PhD program of the Universities of

Maastricht and Birmingham. DIF and JH are enrolled in a joint PhD program of the Universities of Maastricht and Santiago de Compostela (Spain).

**Conflicts of Interest** The authors declare no relevant conflict of interest.

## **7.5 References**

1. Nieswandt B, Watson SP. Platelet-collagen interaction: is GPVI the central receptor? *Blood*. 2003; 102: 449-461.
2. Lecut C, Schoolmeester A, Kuijpers MJ, *et al*. Principal role of glycoprotein VI in  $\alpha 2\beta 1$  and  $\alpha 11b\beta 3$  activation during collagen-induced thrombus formation. *Arterioscler Thromb Vasc Biol*. 2004; 24: 1727-1733.
3. Dumont B, Lasne D, Rothschild C, *et al*. Absence of collagen-induced platelet activation caused by compound heterozygous GPVI mutations. *Blood*. 2009; 114: 1900-1903.
4. Nagy M, van Geffen JP, Stegner D, *et al*. Comparative analysis of microfluidics thrombus formation in multiple genetically modified mice: link to thrombosis and hemostasis. *Front Cardiovasc Med*. 2019; 6: 99.
5. Clemetson KJ, Clemetson JM. Platelet GPIb-V-IX complex. Structure, function, physiology, and pathology. *Semin Thromb Hemost*. 1995; 21: 130-136.
6. Savage B, Almus-Jacobs F, Ruggeri ZM. Specific synergy of multiple substrate-receptor interactions in platelet thrombus formation under flow. *Cell*. 1998; 94: 657-666.
7. Kehrel B, Wierwille S, Clemetson KJ, *et al*. Glycoprotein VI is a major collagen receptor for platelet activation: it recognizes the platelet-activating quaternary structure of collagen, whereas CD36, glycoprotein IIb/IIIa, and von Willebrand factor do not. *Blood*. 1998;91:491-499.
8. Pugh N, Simpson AM, Smethurst PA, de Groot PG, Raynal N, Farndale RW. Synergism between platelet collagen receptors defined using receptor-specific collagen-mimetic peptide substrata in flowing blood. *Blood*. 2010; 115: 5069-5079.
9. Versteeg HH, Heemskerk JW, Levi M, Reitsma PH. New fundamentals in hemostasis. *Physiol Rev*. 2013; 93: 327-358.
10. Suzuki-Inoue K, Tulasne D, Shen Y, *et al*. Association of Fyn and Lyn with the proline-rich domain of glycoprotein VI regulates intracellular signaling. *J Biol Chem*. 2002;277:21561-21566.
11. Watson SP, Herbert JM, Pollitt AY. GPVI and CLEC-2 in hemostasis and vascular integrity. *J Thromb Haemost*. 2010; 8: 1456-1467.

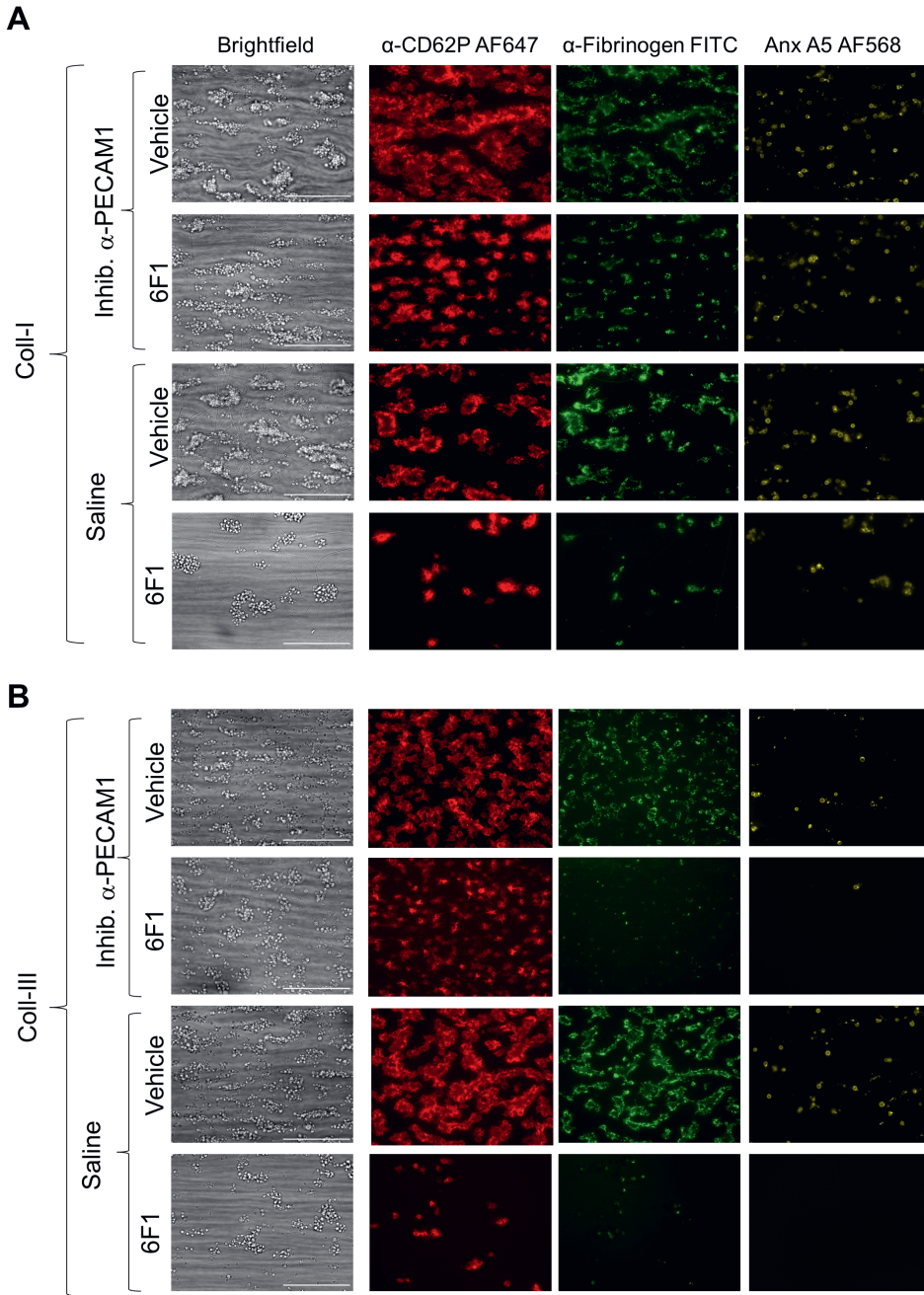


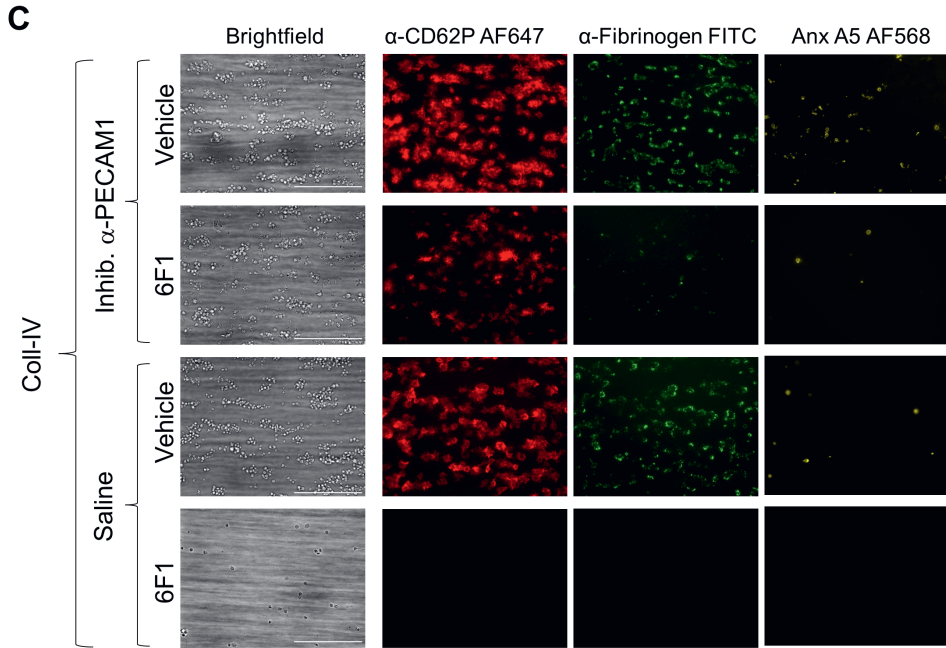
12. Bye AP, Unsworth AJ, Gibbins JM. Platelet signaling: a complex interplay between inhibitory and activatory networks. *J Thromb Haemost.* 2016; 14: 918-930.
13. De Witt SM, Swieringa F, Cavill R, *et al.* Identification of platelet function defects by multi-parameter assessment of thrombus formation. *Nat Commun.* 2014; 5: 4257.
14. Senis YA, Tomlinson MG, Ellison S, *et al.* The tyrosine phosphatase CD148 is an essential positive regulator of platelet activation and thrombosis. *Blood.* 2009; 113:4942-4954.
15. Cicmil M, Thomas JM, Leduc M, Bon C, Gibbins JM. Platelet endothelial cell adhesion molecule-1 signaling inhibits the activation of human platelets. *Blood.* 2002; 99: 137-144.
16. Jones CI, Garner SF, Moraes LA, *et al.* PECAM-1 expression and activity negatively regulate multiple platelet signaling pathways. *FEBS Lett.* 2009; 583: 3618-3624.
17. Newland SA, Macaulay IC, Floto AR, *et al.* The novel inhibitory receptor G6B is expressed on the surface of platelets and attenuates platelet function in vitro. *Blood.* 2007; 109: 4806-4809.
18. Mori J, Pearce AC, Spalton JC, *et al.* G6b-B inhibits constitutive and agonist-induced signaling by glycoprotein VI and CLEC-2. *J Biol Chem.* 2008; 283: 35419-35427.
19. Vögtle T, Sharma S, Mori J, *et al.* Heparan sulfates are critical regulators of the inhibitory megakaryocyte-platelet receptor G6b-B. *Elife.* 2019; 8: e46840.
20. Huang J, Swieringa F, Solari FA, *et al.* Assessment of a complete and classified platelet proteome from genome-wide transcripts of human platelets and megakaryocytes covering platelet functions. *Sci Rep.* 2021; 11: 12358.
21. Coxon CH, Geer MJ, Senis YA. ITIM receptors: more than just inhibitors of platelet activation. *Blood.* 2017; 129: 3407-3418.
22. Wang X, Wei G, Ding Y, *et al.* Protein tyrosine phosphatase PTPN22 negatively modulates platelet function and thrombus formation. *Blood.* 2022; 140: 1038-1051.
23. Heemskerk JW. More than reverting tyrosine kinases. *Blood.* 2022; 140: 939-941.
24. Bellio M, Garcia C, Edouard T, *et al.* Catalytic dysregulation of SHP2 leading to Noonan syndromes affects platelet signaling and functions. *Blood.* 2019; 134: 2304-2317.
25. Tartaglia M, Kalidas K, Shaw A, *et al.* PTPN11 mutations in Noonan syndrome: molecular spectrum, genotype-phenotype correlation, and phenotypic heterogeneity. *Am J Hum Genet.* 2002; 70: 1555-1563.
26. Tartaglia M, Mehler EL, Goldberg R *et al.* Mutations in PTPN11, encoding the protein tyrosine phosphatase SHP-2, cause Noonan syndrome. *Nat Genet.* 2001; 29: 465-468.

27. Tartaglia M, Martinelli S, Stella L *et al.* Diversity and functional consequences of germline and somatic PTPN11 mutations in human disease. *Am J Hum Genet.* 2006; 78: 279-290.
28. Gilio K, Munnix IC, Mangin P *et al.* Non-redundant roles of phosphoinositide 3-kinase isoforms  $\alpha$  and  $\beta$  in glycoprotein VI-induced platelet signaling and thrombus formation. *J Biol Chem.* 2009; 285: 33750-33762.
29. Van Geffen JP, Brouns SL, Batista J, *et al.* High-throughput elucidation of thrombus formation reveals sources of platelet function variability. *Haematologica.* 2019; 104:1256-1267.
30. Munnix IC, Gilio K, Siljander PR, *et al.* Collagen-mimetic peptides mediate flow-dependent thrombus formation by high- or low-affinity binding of integrin  $\alpha 2\beta 1$  and glycoprotein VI. *J Thromb Haemost.* 2008; 6: 2132-2142.
31. Jooss NJ, De Simone I, Provenzale I, Fernández DI, *et al.* Role of platelet glycoprotein VI and tyrosine kinase syk in thrombus formation on collagen-like surfaces. *Int J Mol Sci.* 2019; 20: 2788.
32. Wu XW, Lian EC. Binding properties and inhibition of platelet aggregation by a monoclonal antibody to CD31 (PECAM-1). *Arterioscler Thromb Vasc Biol.* 1997; 17: 3154-3158.
33. Penz S, Reininger AJ, Brandl R, *et al.* Human atheromatous plaques stimulate thrombus formation by activating platelet glycoprotein VI. *FASEB J.* 2005; 19: 898-909.
34. Sun QH, DeLisser HM, Zukowski MM, Paddock C, Albelda SM, Newman PJ. Individually distinct Ig homology domains in PECAM-1 regulate homophilic binding and modulate receptor affinity. *J Biol Chem.* 1996; 271: 11090-11908.
35. Takahashi T, Takahashi K, Mernaugh RL, Tsuboi N, Liu H, Daniel TO. A monoclonal antibody against CD148, a receptor-like tyrosine phosphatase, inhibits endothelial-cell growth and angiogenesis. *Blood.* 2006; 108: 1234-1242.
36. Bergmeier W, Stefanini L. Platelet ITAM signaling. *Curr Opin Hematol.* 2013;20: 445-450.
37. Patil S, Newman DK, Newman PJ. Platelet endothelial cell adhesion molecule-1 serves as an inhibitory receptor that modulates platelet responses to collagen. *Blood.* 2001; 97: 1727-1732.
38. Jones KL, Hughan SC, Dopheide SM, Farndale RW, Jackson SP, Jackson DE. Platelet endothelial cell adhesion molecule-1 is a negative regulator of platelet-collagen interactions. *Blood.* 2001; 98: 1456-1463.
39. Crockett J, Newman DK, Newman PJ. PECAM-1 functions as a negative regulator of laminin-induced platelet activation. *J Thromb Haemost.* 2010; 8: 1584-1593.
40. Dhanjal TS, Ross EA, Auger JM, *et al.* Minimal regulation of platelet activity by PECAM-1. *Platelets.* 2007; 18: 56-67.

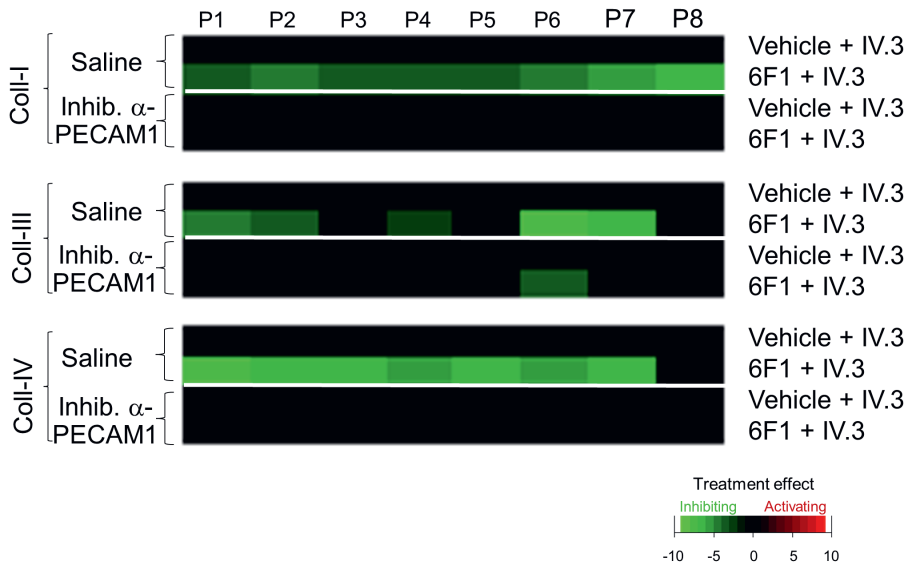
41. Dhanjal TS, Pendaries C, Ross EA, *et al.* A novel role for PECAM-1 in megakaryocytoikinesis and recovery of platelet counts in thrombocytopenic mice. *Blood*. 2007; 109: 4237-4244.
42. Yan HC, Pilewski JM, Zhang Q, DeLisser HM, Romer L, Albelda SM. Localization of multiple functional domains on human PECAM-1 (CD31) by monoclonal antibody epitope mapping. *Cell Adhes Commun*. 1995; 3: 45-66.
43. Jackson DE. The unfolding tale of PECAM-1. *FEBS Lett*. 2003; 540: 7-14.
44. Morandi F, Airoldi I, Marimpietri D, Bracci C, Faini AC, Gramignoli R. CD38, a receptor with multifunctional activities: from modulatory functions on regulatory cell subsets and extracellular vesicles, to a target for therapeutic strategies. *Cells*. 2019; 8: 1527.
45. Kunicki TJ, Kritzik M, Annis DS, Nugent DJ. Hereditary variation in platelet integrin  $\alpha 2\beta 1$  density is associated with two silent polymorphisms in the  $\alpha 2$  gene coding sequence. *Blood*. 1997; 89: 1939-1943.
46. Roest M, Sixma JJ, Wu YP, *et al.* Platelet adhesion to collagen in healthy volunteers is influenced by variation of both  $\alpha 2\beta 1$  density and von Willebrand factor. *Blood*. 2000; 96:1433-1437.
47. Deckmyn H, Chew SL, Vermynen J. Lack of platelet response to collagen associated with an autoantibody against glycoprotein Ia: a novel cause of acquired qualitative platelet dysfunction. *Thromb Haemost*. 1990; 64: 74-79.
48. Nieuwenhuis HK, Akkerman JW, Houdijk WP, Sixma JJ. Human blood platelets showing no response to collagen fail to express surface glycoprotein Ia. *Nature*. 1985; 318:470-472.
49. Van Zanten GH, de Graaf S, Slootweg PJ, *et al.* Increased platelet deposition on atherosclerotic coronary arteries. *J Clin Invest*. 1994; 93: 615-632.

## 7.6 Supplementary figures



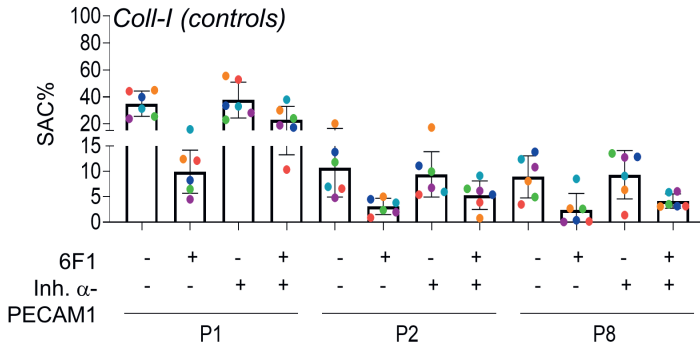


**Supplementary Figure 1 – Enhanced collagen-induced thrombus formation by PECAM1 blockage in the absence of integrin  $\alpha 2\beta 1$ :** representative microscopic images. Blood samples were preincubated with anti-  $\alpha 2\beta 1$  6F1 mAb (20  $\mu\text{g}/\text{ml}$ ) or vehicle, and then perfused during 3.5 minutes at 1000/s over microspots of collagen-I (A), collagen-III (B) and collagen-IV (C); all microspots were post-coated with saline or inhibitory anti-PECAM1 mAb (WM59). Brightfield and multicolor microscopic images were taken at end stage. Platelet labeling was with AF647 anti-CD62P mAb, FITC anti-fibrinogen mAb and AF568 annexin A5, as for Figure 1. Shown are representative images for per collagen surface with or without inhibitory anti-PECAM1 mAb (n=6-7). Scale bars = 50  $\mu\text{m}$ .

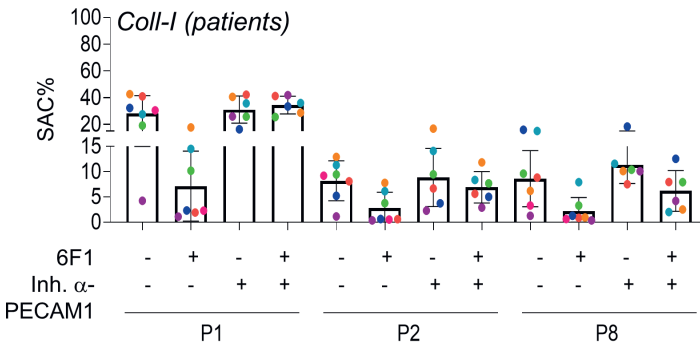


**Supplementary Figure 2 – Absence of Fc $\gamma$ RIIA role in anti-PECAM1 antibody effect on thrombus formation.** Blood samples were preincubated with inhibitory anti-Fc $\gamma$ RIIA mAb (20  $\mu$ g/ml) with or without anti  $\alpha$ 2 $\beta$ 1 6F1 mAb (20  $\mu$ g/ml) and vehicle, and then perfused during 3.5 minutes at 1000/s over microspots of collagen-I, collagen-III or collagen-IV, as for Figure 1. Microspots were post-coated with saline or inhibitory anti-PECAM1 mAb (WM59), as indicated. Multicolor microscopic images were analyzed for eight parameters (Table 1), which were univariate scaled. Shown is the subtraction heatmap, comparing per collagen type, the effects of combined integrin  $\alpha$ 2 $\beta$ 1 (6F1 mAb) and Fc $\gamma$ RIIA blockage (by IV.3 mAb) for parameters P1-8. Means  $\pm$  SD (n=3), tested for significance with one-way ANOVA. For color coding, a filter was applied of p < 0.05. Raw data for P1-8 are given in the Supplemental Datafile.

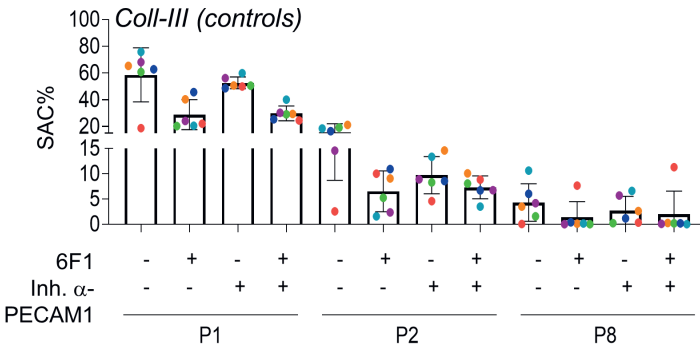
**A i**



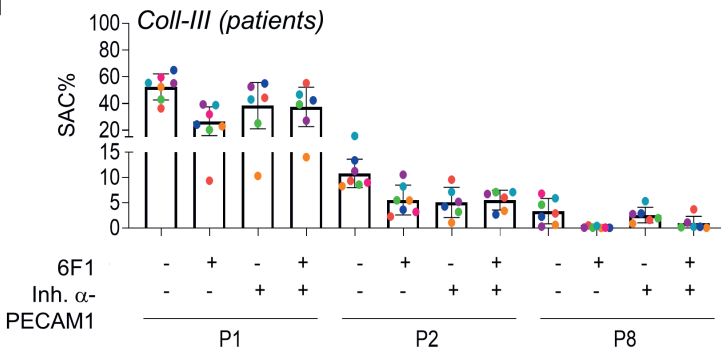
**ii**

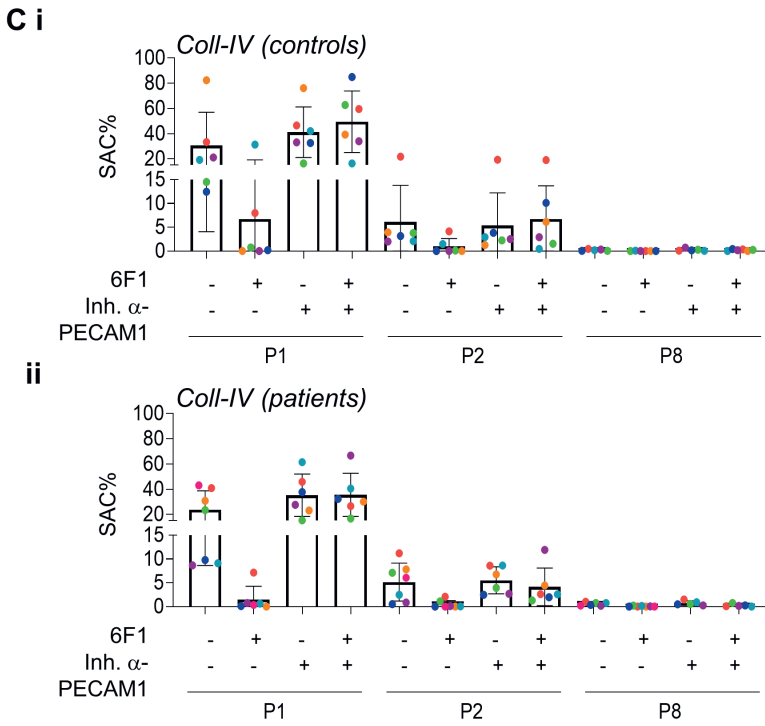


**B i**



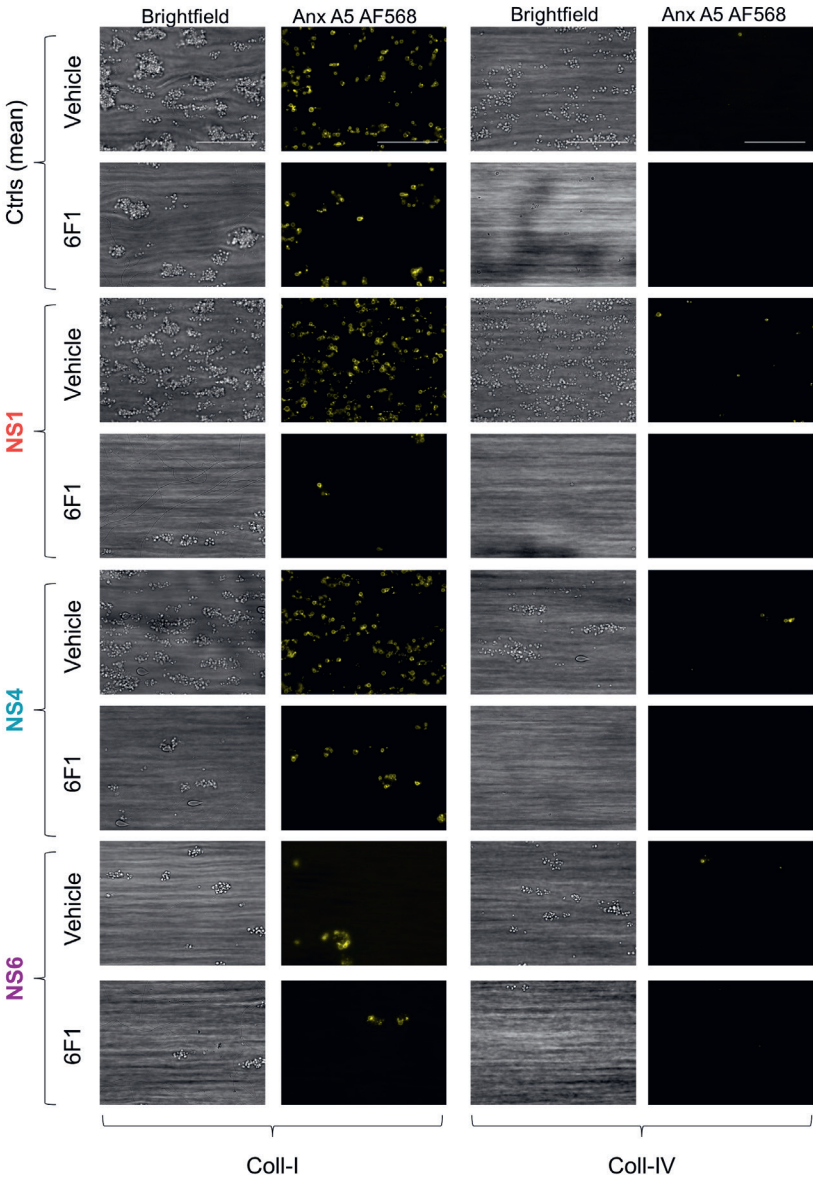
**ii**





**Supplementary Figure 3 – Raw data Noonan patients and day controls.** Blood samples from 6-day control subjects and 6 patients with confirmed Noonan syndrome and PTPN11 mutation were preincubated with anti-  $\alpha 2\beta 1$  6F1 mAb (20  $\mu\text{g}/\text{ml}$ ) or vehicle, and then perfused during 3.5 minutes at 1000/s over microspots of collagen-I (A), collagen-III (B) and collagen-IV (C); all microspots were post-coated with saline or inhibitory anti-PECAM1 mAb WM59. Multicolor microscopic images were analyzed for eight parameters of thrombus formation. Shown are quantified data per control subject (panels i) or per patient (panels ii) of platelet deposition (parameter P1), thrombus multilayer size (parameter P2), and phosphatidylserine exposure (parameter P8) in the presence or absence of 6F1 mAb and/or inhibitory anti-PECAM1 mAb.





**Supplementary Figure 4 – Alterations in collagen-induced thrombus formation for distinct Noonan syndrome patients.** Whole blood from control subjects and indicated patients was perfused over collagen surfaces, as described for Figure 4. Shown are endpoint brightfield (P1-5) and phosphatidylserine exposure (parameter P8) microscopic images obtained with blood from a representative day control subjects and from patients NS1, NS4 and NS6 perfused over collagen-I or collagen-IV. Where indicated, integrin  $\alpha 2\beta 1$  was blocked with 6F1 mAb. Scale bars = 50  $\mu$ m.

# 7.7 Supplementary data file

Supplementary Data for Figure 1 - Inhibitory anti-PECAM1

Donor	Condition	M1 P1	M1 P2	M1 P3	M1 P4	M1 P5	M1 P6	M1 P7	M1 P8	M1 PECAM1 P1	M1 PECAM1 P2	M1 PECAM1 P3	M1 PECAM1 P4	M1 PECAM1 P5	M1 PECAM1 P6	M1 PECAM1 P7	M1 PECAM1 P8
D1	PBS	31.74	13.48	3.16	1.81	1.66	26.27	14.70	6.72	36.84	13.76	3.63	2.50	1.88	44.02	23.01	5.37
D2	PBS	35.21	18.72	3.88	2.13	2.00	27.88	14.76	5.17	53.91	20.03	3.75	2.75	1.88	40.40	16.02	6.13
D3	PBS	20.19	10.03	2.81	1.69	1.56	20.10	5.31	2.83	25.24	7.68	2.75	2.25	1.88	35.23	9.68	5.30
D4	PBS	54.50	25.36	4.25	2.50	2.25	52.61	32.41	6.01	No data available	No data available	No data available	No data available	No data available	47.07	18.73	12.83
D5	PBS	35.83	13.74	4.00	2.50	2.31	32.37	14.00	10.13	36.90	12.13	3.75	3.00	2.38	49.77	12.01	9.85
D6	PBS	25.54	9.09	3.16	1.88	1.78	26.31	9.28	8.94	56.52	7.84	3.13	1.88	1.38	49.77	12.01	9.85
D7	PBS	40.81	16.20	3.81	2.31	45.67	24.89	7.38	7.38	43.85	14.40	3.50	3.00	2.50	48.25	24.84	7.60
D1	6F1	7.22	2.18	3.00	2.00	2.11	1.46	0.75	0.75	54.09	9.83	3.25	2.38	1.75	12.54	4.64	1.86
D2	6F1	7.46	4.54	1.75	1.06	1.07	3.73	1.14	0.80	41.25	11.17	3.63	2.38	2.00	37.02	7.85	3.68
D3	6F1	10.43	5.47	1.75	1.00	1.06	7.03	2.51	2.52	42.83	15.36	3.88	2.00	1.88	39.12	8.14	6.10
D4	6F1	4.90	1.06	1.63	1.00	0.88	2.35	1.41	0.42	No data available	No data available	No data available	No data available	No data available	46.56	18.14	7.33
D5	6F1	18.67	7.56	2.63	1.94	1.75	11.33	4.90	3.27	23.50	9.79	3.25	2.25	2.25	20.00	23.21	6.91
D6	6F1	14.34	6.64	2.63	1.50	1.56	12.16	3.92	4.39	30.02	10.51	3.50	2.25	2.00	23.21	6.91	6.75
D7	6F1	23.28	9.10	2.56	1.50	1.56	17.69	7.21	3.12	26.41	10.11	3.00	2.00	1.50	23.38	11.00	3.15

Donor	Condition	M2 P1	M2 P2	M2 P3	M2 P4	M2 P5	M2 P6	M2 P7	M2 P8	M2 PECAM1 P1	M2 PECAM1 P2	M2 PECAM1 P3	M2 PECAM1 P4	M2 PECAM1 P5	M2 PECAM1 P6	M2 PECAM1 P7	M2 PECAM1 P8
D1	PBS	65.82	17.59	3.69	2.13	2.25	50.49	26.49	5.71	54.13	11.81	3.50	2.13	1.50	54.01	18.63	1.86
D2	PBS	80.17	23.56	4.00	2.00	1.75	60.62	37.18	3.94	63.24	12.50	3.50	2.38	1.50	58.07	21.00	2.08
D3	PBS	86.65	28.66	3.88	1.91	1.91	51.73	48.76	3.97	62.68	15.41	3.75	2.38	1.88	48.53	10.66	0.78
D4	PBS	59.64	23.87	3.78	2.19	2.00	52.05	19.12	2.76	57.79	12.33	3.50	2.00	2.00	51.38	11.32	0.96
D5	PBS	59.64	16.84	3.56	2.06	1.75	45.46	12.98	2.13	62.87	10.62	3.13	1.75	1.50	41.95	6.91	0.61
D6	PBS	66.13	15.41	3.50	2.19	1.81	54.65	19.23	1.31	59.49	7.64	3.13	2.13	1.63	53.26	11.30	0.30
D1	6F1	39.10	7.67	3.00	1.00	1.25	8.75	3.08	0.12	44.71	6.36	3.25	2.00	1.50	23.35	3.93	0.21
D2	6F1	35.79	12.10	2.88	1.50	1.63	7.83	1.32	0.05	43.29	11.90	3.50	1.63	1.63	25.93	1.84	0.32
D3	6F1	28.69	8.53	3.25	1.25	1.25	5.18	0.80	0.10	31.57	5.42	3.13	1.25	1.13	7.87	0.35	0.01
D4	6F1	22.44	3.24	2.56	1.50	1.25	4.15	0.87	0.00	No data available	No data available	No data available	No data available	No data available	0.37	0.07	
D5	6F1	30.38	7.40	3.00	1.38	1.38	5.29	0.47	0.06	30.49	8.50	3.25	2.00	2.00	7.96	0.37	0.07
D6	6F1	29.59	6.09	1.75	0.94	0.88	3.77	0.62	0.03	40.82	9.18	3.25	2.00	1.75	21.70	2.60	0.12
D7	6F1	27.71	2.34	2.63	1.38	0.63	1.31	0.21	0.01	61.28	2.45	2.50	1.00	1.00	13.25	1.68	0.09

Donor	Condition	M3 P1	M3 P2	M3 P3	M3 P4	M3 P5	M3 P6	M3 P7	M3 P8	M3 PECAM1 P1	M3 PECAM1 P2	M3 PECAM1 P3	M3 PECAM1 P4	M3 PECAM1 P5	M3 PECAM1 P6	M3 PECAM1 P7	M3 PECAM1 P8
D1	PBS	27.26	4.19	3.00	1.17	0.96	26.73	13.35	1.04	45.18	3.06	2.75	1.50	0.83	52.98	21.55	0.64
D2	PBS	22.00	3.78	2.41	0.94	0.91	16.12	4.79	0.12	42.76	3.36	2.63	0.88	0.75	26.14	0.58	0.09
D3	PBS	62.67	14.76	3.83	2.17	1.85	39.66	20.24	0.50	63.44	11.18	3.42	1.83	1.25	40.53	12.36	0.20
D4	PBS	62.29	15.30	3.69	1.94	1.88	47.04	20.43	0.75	No data available	No data available	No data available	No data available	No data available	No data available	No data available	No data available
D5	PBS	47.27	10.93	3.06	1.25	1.19	28.81	9.03	0.28	62.47	12.52	3.00	1.75	1.75	50.12	10.83	0.15
D6	PBS	47.19	9.47	3.63	2.38	2.13	30.65	16.20	0.36	37.66	6.11	3.13	1.13	1.13	24.67	4.60	0.20
D7	PBS	64.99	11.47	3.38	2.00	1.88	42.96	21.71	0.17	50.15	8.91	3.25	2.00	1.63	31.23	8.24	0.24
D1	6F1	0.00	0.00	0.00	0.00	0.00	0.00	0.00	0.04	48.05	3.03	2.63	1.00	0.88	38.06	10.19	0.75
D2	6F1	0.11	0.00	0.00	0.00	0.00	0.03	0.00	0.00	60.51	2.77	2.25	0.50	0.25	17.23	0.40	0.20
D3	6F1	0.05	0.00	0.00	0.00	0.00	0.16	0.00	0.01	42.21	1.88	2.88	0.25	0.25	15.85	0.91	0.10
D4	6F1	0.04	0.00	0.00	0.00	0.00	0.00	0.00	0.00	37.63	5.23	2.88	0.88	0.88	10.78	0.35	0.04
D5	6F1	0.31	0.08	0.00	0.00	0.00	0.00	0.00	0.01	48.70	12.08	3.88	1.75	1.75	20.07	0.62	0.10
D6	6F1	1.68	0.13	0.88	0.13	0.13	0.02	0.01	0.01	53.63	2.01	2.50	1.00	1.00	11.30	0.95	0.21
D7	6F1	0.53	0.00	0.00	0.00	0.00	0.00	0.00	0.00	No data available	No data available	No data available	No data available	No data available	No data available	No data available	No data available



Supplementary Data for Figure 2 - IgG control Ab

Donor	Condition	M1 P1	M1 P2	M1 P3	M1 P4	M1 P5	M1 P6	M1 P7	M1 P8	M1 IgG P1	M1 IgG P2	M1 IgG P3	M1 IgG P4	M1 IgG P5	M1 IgG P6	M1 IgG P7	M1 IgG P8	
D1	PBS	31.74	13.48	3.44	2.00	1.88	26.27	14.70	6.72	29.68	13.86	3.75	2.50	2.50	17.16	7.54	2.38	
D2	PBS	35.21	18.72	3.88	2.13	2.00	27.88	14.76	5.17	29.75	13.56	3.63	2.13	1.88	32.99	15.82	5.79	
D3	PBS	20.19	10.03	3.06	1.94	1.75	20.10	5.31	2.83	18.24	9.38	1.88	1.00	1.13	19.59	4.52	3.89	
D4	PBS	54.50	25.36	4.25	2.50	2.25	52.61	32.41	6.01	31.84	18.83	4.00	2.50	2.25	42.82	26.95	7.45	
D5	PBS	35.83	13.74	4.00	2.50	2.31	32.37	14.00	10.13	23.75	11.10	3.88	2.75	2.38	32.53	13.28	10.19	
D6	PBS	25.54	9.09	3.50	1.88	1.81	26.31	8.28	8.94	31.23	12.30	3.75	2.50	2.50	28.36	9.19	7.74	
D7	PBS	40.81	16.20	3.81	2.38	2.31	45.67	24.89	7.38	42.88	13.51	3.50	3.00	2.13	48.99	20.13	9.47	
D1	6F1	No data available																
D2	6F1	No data available																
D3	6F1	No data available																
D4	6F1	4.90	1.06	3.25	1.75	1.75	2.35	1.41	0.42	3.65	1.11	1.63	0.75	0.75	0.92	0.78	0.11	
D5	6F1	18.67	7.56	3.50	2.50	2.13	11.33	4.90	3.27	13.67	7.04	1.88	1.25	1.25	9.80	3.60	3.89	
D6	6F1	14.34	6.64	3.38	2.00	2.00	12.16	3.92	4.39	19.70	4.00	2.88	1.17	1.88	8.17	3.42	3.29	
D7	6F1	23.28	9.10	3.25	2.00	2.00	17.69	7.21	3.12	11.55	3.89	3.00	1.75	1.50	11.05	4.11	0.65	

Donor	Condition	M2 P1	M2 P2	M2 P3	M2 P4	M2 P5	M2 P6	M2 P7	M2 P8	M2 IgG P1	M2 IgG P2	M2 IgG P3	M2 IgG P4	M2 IgG P5	M2 IgG P6	M2 IgG P7	M2 IgG P8	
D1	PBS	65.82	17.59	3.69	2.13	2.25	50.49	26.49	5.71	45.53	7.89	3.00	2.25	1.00	41.19	18.78	3.95	
D2	PBS	80.17	23.56	4.00	2.00	1.75	60.62	37.18	3.94	72.70	15.11	3.38	2.13	1.50	47.28	21.69	1.81	
D3	PBS	56.65	18.66	3.88	1.91	1.91	51.73	18.76	1.57	53.82	9.87	3.06	2.25	1.63	47.55	13.27	2.96	
D4	PBS	83.68	23.87	4.50	2.00	2.00	71.21	40.35	3.07	54.44	12.57	4.00	2.50	2.00	57.28	25.36	1.40	
D5	PBS	59.64	16.82	3.38	2.19	2.00	52.05	19.12	2.76	44.89	10.53	2.75	2.38	2.00	45.95	15.33	1.50	
D6	PBS	59.48	16.44	3.56	2.06	1.75	45.46	12.98	2.13	57.82	16.44	3.50	2.25	1.88	50.48	11.02	2.07	
D7	PBS	66.13	15.41	3.50	2.19	1.81	54.65	19.23	1.31	51.48	7.88	3.00	2.00	1.25	45.24	11.89	0.54	
D1	6F1	No data available																
D2	6F1	No data available																
D3	6F1	No data available																
D4	6F1	22.44	3.24	2.88	1.63	1.38	0.00	4.15	0.87	16.00	0.48	2.25	1.00	0.88	0.55	0.08	0.00	
D5	6F1	30.38	7.40	3.00	1.38	1.38	0.06	5.29	0.47	11.34	2.23	1.63	0.75	0.88	0.99	0.14	0.05	
D6	6F1	29.59	6.09	2.63	1.50	1.88	0.03	3.77	0.62	16.03	1.62	1.50	0.50	0.50	1.53	0.35	0.03	
D7	6F1	27.71	2.34	2.63	1.38	0.63	0.01	1.31	0.21	18.54	1.74	2.50	0.75	0.75	1.19	0.12	0.05	

Donor	Condition	M3 P1	M3 P2	M3 P3	M3 P4	M3 P5	M3 P6	M3 P7	M3 P8	M3 IgG P1	M3 IgG P2	M3 IgG P3	M3 IgG P4	M3 IgG P5	M3 IgG P6	M3 IgG P7	M3 IgG P8	
D1	PBS	27.26	4.19	3.00	1.17	0.96	26.73	13.35	1.04	45.53	8.58	3.75	1.75	1.50	30.93	13.21	1.53	
D2	PBS	22.00	3.78	3.06	0.94	0.75	16.12	4.79	0.12	19.74	3.98	2.38	0.94	0.81	21.25	7.58	0.13	
D3	PBS	62.67	14.76	3.83	2.17	1.85	39.66	20.24	0.50	54.08	12.89	3.88	2.38	2.00	31.06	11.58	0.26	
D4	PBS	62.29	15.30	3.69	1.94	1.88	47.04	20.43	0.75	57.34	18.09	3.63	1.88	1.88	48.09	21.22	0.39	
D5	PBS	47.27	10.93	3.06	1.25	1.19	28.81	9.03	0.28	31.49	5.88	3.38	1.50	1.25	28.08	7.44	0.17	
D6	PBS	47.19	9.47	3.63	2.38	2.13	30.65	16.20	0.26	41.18	9.94	3.75	2.38	2.13	20.96	4.05	0.19	
D7	PBS	64.99	11.47	3.38	2.00	1.88	42.96	21.71	0.17	52.84	10.12	3.63	2.00	1.75	53.51	19.97	0.15	
D1	6F1	No data available																
D2	6F1	No data available																
D3	6F1	No data available																
D4	6F1	0.11	0.00	0.00	0.00	0.00	0.03	0.00	0.00	0.38	0.17	0.00	0.00	0.00	0.00	0.00	0.00	
D5	6F1	2.88	0.50	0.63	0.13	0.13	0.07	0.01	0.01	1.34	0.03	0.00	0.00	0.00	0.00	0.00	0.00	
D6	6F1	1.68	0.13	0.88	0.13	0.13	0.02	0.01	0.01	3.25	0.18	1.00	0.00	0.00	0.00	0.00	0.00	
D7	6F1	0.53	0.00	0.00	0.00	0.00	0.00	0.00	0.00	0.30	0.00	0.00	0.00	0.00	0.00	0.00	0.00	

Supplementary Data for Figure 2 - Control anti-PECAM1

Donor	Condition	M1 P1	M1 P2	M1 P3	M1 P4	M1 P5	M1 P6	M1 P7	M1 P8	M1 cnpPECAM1	M1 cnpPECAM1	M1 cnpPECAM1	M1 cnpPECAM1	M1 cnpPECAM1	M1 cnpPECAM1	M1 cnpPECAM1	M1 cnpPECAM1	M1 cnpPECAM1
D1	PBS	34.36	10.13	3.88	2.25	2.00	34.74	18.50	10.30	25.13	3.63	2.50	2.00	2.00	2.52	13.66	10.61	10.61
D2	PBS	26.58	9.45	4.13	2.88	2.63	28.13	13.02	7.76	8.21	3.63	3.00	2.50	2.50	28.92	12.51	8.97	8.97
D3	PBS	22.03	9.09	4.00	2.25	2.45	24.17	12.56	3.71	25.61	10.46	2.88	2.25	2.88	24.13	11.65	4.18	4.18
D1	6F1	6.41	2.31	1.81	1.06	1.00	5.79	2.13	1.82	4.65	1.72	1.44	1.13	1.19	6.61	2.66	2.40	2.40
D2	6F1	17.82	5.92	1.88	1.19	1.31	18.44	6.97	4.44	13.42	4.66	1.81	1.50	1.50	17.13	4.32	1.72	1.72
D3	6F1	12.62	7.59	1.81	1.59	1.50	7.34	4.18	0.97	13.95	6.34	1.81	1.50	1.50	8.61	4.02	1.78	1.78

Donor	Condition	M2 P1	M2 P2	M2 P3	M2 P4	M2 P5	M2 P6	M2 P7	M2 P8	M2 cnpPECAM1	M2 cnpPECAM1	M2 cnpPECAM1	M2 cnpPECAM1	M2 cnpPECAM1	M2 cnpPECAM1	M2 cnpPECAM1	M2 cnpPECAM1	M2 cnpPECAM1
D1	PBS	66.07	15.00	4.00	2.50	1.50	57.93	25.73	4.55	54.32	8.27	3.75	2.38	1.75	51.66	23.29	3.36	3.36
D2	PBS	58.06	7.96	3.75	2.25	2.00	57.12	20.55	1.73	61.70	8.97	3.50	2.00	2.00	54.01	16.68	1.25	1.25
D3	PBS	55.24	4.39	4.00	2.75	2.25	53.51	25.74	1.47	48.51	5.75	3.50	2.75	2.25	51.96	15.92	1.67	1.67
D1	6F1	34.61	9.81	4.13	2.25	2.25	5.18	0.40	0.08	22.60	5.57	3.75	2.25	2.13	3.99	0.65	0.12	0.12
D2	6F1	33.81	4.36	3.63	1.63	1.50	6.02	0.92	0.08	26.56	3.58	3.25	1.88	1.88	5.07	0.75	0.04	0.04
D3	6F1	28.94	9.76	3.63	2.38	2.13	9.40	0.98	0.05	26.76	7.96	3.75	2.50	2.38	5.65	0.47	0.01	0.01

Donor	Condition	M3 P1	M3 P2	M3 P3	M3 P4	M3 P5	M3 P6	M3 P7	M3 P8	M3 cnpPECAM1	M3 cnpPECAM1	M3 cnpPECAM1	M3 cnpPECAM1	M3 cnpPECAM1	M3 cnpPECAM1	M3 cnpPECAM1	M3 cnpPECAM1	M3 cnpPECAM1
D1	PBS	19.64	5.07	2.63	1.38	1.31	15.34	7.59	0.14	18.42	4.30	2.25	1.25	1.13	12.96	5.97	0.17	0.17
D2	PBS	11.13	1.12	3.00	1.38	1.38	17.40	6.39	0.21	14.64	1.53	3.13	1.25	1.13	15.21	8.55	0.10	0.10
D3	PBS	14.19	3.43	2.38	1.25	1.25	9.83	4.81	0.04	11.44	2.18	2.25	1.25	1.13	12.11	5.30	0.06	0.06
D1	6F1	0.00	0.00	0.00	0.00	0.00	0.00	0.00	0.00	0.12	0.00	0.00	0.00	0.00	0.00	0.00	0.00	0.00
D2	6F1	0.01	0.00	0.00	0.00	0.00	0.00	0.00	0.00	0.03	0.00	0.00	0.00	0.00	3.93	0.00	0.00	0.00
D3	6F1	0.08	0.00	0.00	0.00	0.00	0.00	0.01	0.01	0.00	0.00	0.00	0.00	0.00	0.00	0.01	0.01	0.01

Donor	Condition	M1 P1	M1 P2	M1 P3	M1 P4	M1 P5	M1 P6	M1 P7	M1 P8	M1 cnpPECAM1	M1 cnpPECAM1	M1 cnpPECAM1	M1 cnpPECAM1	M1 cnpPECAM1	M1 cnpPECAM1	M1 cnpPECAM1	M1 cnpPECAM1	M1 cnpPECAM1
D1	PBS+IV3	32.52	12.72	4.00	2.38	2.00	35.43	17.29	11.57	33.21	10.88	2.50	2.00	2.00	51.15	18.49	10.37	10.37
D2	PBS+IV3	32.09	13.34	3.69	2.56	2.19	28.79	13.03	9.02	42.91	16.23	3.88	2.88	2.25	50.85	13.30	13.79	13.79
D3	PBS+IV3	43.70	16.96	3.81	2.38	2.50	48.56	22.29	6.88	36.57	11.62	3.38	2.63	2.00	43.92	25.72	7.10	7.10
D1	6F1+IV3	16.53	7.26	2.69	1.56	1.66	9.33	4.16	2.67	25.80	13.65	3.25	2.25	2.13	16.21	6.43	3.09	3.09
D2	6F1+IV3	16.78	4.46	1.73	1.44	1.44	12.60	6.61	1.98	22.33	7.58	2.81	1.91	1.69	14.76	5.74	2.97	2.97
D3	6F1+IV3	16.17	5.16	1.91	1.28	1.25	12.60	6.61	1.98	22.33	7.58	2.81	1.91	1.69	14.76	5.74	2.97	2.97

Donor	Condition	M2 P1	M2 P2	M2 P3	M2 P4	M2 P5	M2 P6	M2 P7	M2 P8	M2 cnpPECAM1	M2 cnpPECAM1	M2 cnpPECAM1	M2 cnpPECAM1	M2 cnpPECAM1	M2 cnpPECAM1	M2 cnpPECAM1	M2 cnpPECAM1	M2 cnpPECAM1
D1	PBS+IV3	53.02	12.68	3.44	2.19	1.88	50.31	20.28	3.05	35.50	6.12	3.00	2.13	1.88	26.19	1.60	0.35	0.35
D2	PBS+IV3	61.21	12.33	3.06	1.88	1.44	42.72	12.60	1.80	54.93	14.03	3.00	1.75	1.50	45.95	12.45	1.11	1.11
D3	PBS+IV3	57.96	10.56	3.38	1.88	1.31	40.93	12.00	1.05	57.78	6.84	2.75	1.63	1.25	39.10	7.06	0.44	0.44
D1	6F1+IV3	26.96	8.13	3.08	1.56	1.56	5.70	0.73	0.11	45.20	5.14	3.00	1.00	1.00	10.71	1.16	0.08	0.08
D2	6F1+IV3	25.20	3.61	2.34	0.94	0.97	2.11	0.32	0.07	37.84	5.56	3.13	1.50	1.13	17.30	2.47	0.33	0.33
D3	6F1+IV3	23.65	3.25	2.63	1.41	1.10	1.77	0.30	0.06	38.17	3.94	3.00	1.50	1.25	19.96	2.75	0.08	0.08

Donor	Condition	M3 P1	M3 P2	M3 P3	M3 P4	M3 P5	M3 P6	M3 P7	M3 P8	M3 cnpPECAM1	M3 cnpPECAM1	M3 cnpPECAM1	M3 cnpPECAM1	M3 cnpPECAM1	M3 cnpPECAM1	M3 cnpPECAM1	M3 cnpPECAM1	M3 cnpPECAM1
D1	PBS+IV3	28.79	4.62	2.03	0.88	0.94	13.79	3.22	0.12	48.16	4.95	2.88	1.00	0.88	35.54	0.66	0.12	0.12
D2	PBS+IV3	61.58	16.07	3.75	2.19	2.06	50.77	24.99	1.02	72.28	7.55	2.75	1.50	1.63	34.84	7.01	0.20	0.20
D3	PBS+IV3	54.88	12.79	3.69	1.94	1.75	34.40	16.47	0.46	58.54	7.03	3.13	1.75	1.63	31.96	5.74	0.16	0.16
D1	6F1+IV3	0.10	0.00	0.00	0.00	0.00	0.00	0.00	0.00	55.83	3.81	2.25	0.75	0.25	23.21	0.59	0.22	0.22
D2	6F1+IV3	2.89	0.06	0.00	0.00	0.00	0.05	0.01	0.00	41.90	4.34	2.63	0.88	0.88	11.84	2.63	0.17	0.17
D3	6F1+IV3	4.57	0.05	0.63	0.00	0.00	0.04	0.21	0.01	35.43	4.10	2.63	1.00	0.88	9.47	0.95	0.05	0.05

Supplementary Data for Figure 2 - Inhibitory anti-PECAM1 + IV.3



Supplementary Data for Figure 3 - Anti-G6B-b and anti-CD148

Donor	Condition	M3 P1	M3 P2	M3 P3	M3 P4	M3 P5	M3 P6	M3 P7	M3 P8	M3 G6Bb P1	M3 G6Bb P2	M3 G6Bb P3	M3 G6Bb P4	M3 G6Bb P5	M3 G6Bb P6	M3 G6Bb P7	M3 G6Bb P8
D1	PBS	34.49	3.93	2.63	0.75	0.63	22.95	8.95	0.49	35.93	4.85	3.00	1.00	0.75	21.22	6.97	0.39
D2	PBS	66.37	17.06	4.00	2.38	1.50	55.94	18.98	1.10	53.15	18.10	4.00	2.50	2.50	55.48	22.16	1.44
D3	PBS	59.03	6.96	3.50	1.50	1.50	41.83	22.89	0.52	37.34	4.81	3.38	1.13	1.38	40.26	18.00	1.31
D4	PBS	44.22	9.74	3.13	1.88	1.88	32.60	16.46	0.94	29.99	5.77	3.00	1.50	1.25	27.75	11.46	0.47
D1	6F1	0.00	0.00	0.00	0.00	0.00	0.00	0.00	0.00	0.02	0.00	0.00	0.00	0.00	0.00	0.00	0.00
D2	6F1	0.44	0.00	0.00	0.00	0.00	0.00	0.00	0.00	1.23	0.00	0.00	0.00	0.00	0.00	0.00	0.00
D3	6F1	1.09	0.00	0.25	0.00	0.00	0.00	0.01	0.00	3.10	0.00	0.50	0.00	0.00	0.00	0.00	0.00
D4	6F1	0.48	0.13	0.25	0.00	0.00	0.00	0.00	0.00	0.00	0.00	0.00	0.00	0.00	0.00	0.00	0.00

Donor	Condition	M3 P1	M3 P2	M3 P3	M3 P4	M3 P5	M3 P6	M3 P7	M3 P8	M3 CD148 P1	M3 CD148 P2	M3 CD148 P3	M3 CD148 P4	M3 CD148 P5	M3 CD148 P6	M3 CD148 P7	M3 CD148 P8
D1	PBS	37.96	7.66	3.25	1.38	1.13	35.66	12.38	0.41	41.06	2.91	3.13	1.88	0.75	23.84	10.04	0.31
D2	PBS	69.12	24.62	7.25	2.50	2.13	57.38	20.38	1.87	59.18	14.29	4.00	2.13	2.13	49.67	22.88	2.70
D3	PBS	59.34	12.47	0.50	0.00	0.00	51.08	26.51	1.48	51.23	14.29	4.00	2.13	1.25	29.79	14.65	0.51
D4	PBS	35.89	6.74	3.25	1.75	1.75	22.58	10.71	0.24	26.93	5.41	3.25	1.25	1.25	29.79	14.65	0.51
D1	6F1	0.33	0.00	0.00	0.00	0.00	0.00	0.00	0.00	0.29	0.00	0.00	0.00	0.00	0.00	0.00	0.00
D2	6F1	0.26	0.00	0.00	0.00	0.00	0.00	0.00	0.00	2.06	0.02	0.38	0.00	0.00	0.00	0.00	0.00
D3	6F1	1.15	0.00	0.00	0.00	0.00	0.08	0.03	0.04	0.23	0.00	0.00	0.00	0.00	0.00	0.00	0.00
D4	6F1	0.01	0.00	0.00	0.00	0.00	0.00	0.00	0.00	0.00	0.00	0.00	0.00	0.00	0.00	0.00	0.00

Donor	Condition	M1 P1	M1 P2	M1 P3	M1 P4	M1 P5	M1 P6	M1 P7	M1 P8	M1 PECAM1 P1	M1 PECAM1 P2	M1 PECAM1 P3	M1 PECAM1 P4	M1 PECAM1 P5	M1 PECAM1 P6	M1 PECAM1 P7	M1 PECAM1 P8
NS 1	PBS	40.97	8.09	3.63	2.13	1.75	46.45	24.68	8.84	42.19	6.68	3.38	2.38	1.75	47.88	29.57	7.52
NS 2	PBS	42.61	12.92	3.50	2.50	2.00	36.79	18.68	6.21	40.56	16.86	3.75	2.75	2.25	40.01	17.84	10.13
NS 3	PBS	19.21	9.44	3.25	3.00	2.25	30.43	16.57	9.61	25.73	9.46	3.25	2.50	2.00	22.18	15.01	10.39
NS 4	PBS	27.53	11.29	4.00	3.00	3.00	33.64	22.77	15.02	35.77	14.12	4.25	3.00	3.00	45.91	23.72	11.36
NS 5	PBS	32.35	7.23	3.75	1.00	1.00	35.33	18.61	1.35	46.68	3.72	3.25	1.25	2.00	44.21	19.19	16.44
NS 6	PBS	34.33	11.13	3.00	1.00	0.50	40.78	18.35	1.25	25.51	2.27	3.00	1.25	1.50	34.35	12.40	10.10
NS 7	PBS	30.51	9.21	3.75	2.25	2.50	17.71	6.76	3.28	No data available	No data available	No data available	No data available	No data available	No data available	No data available	No data available
NS 1	6F1	1.91	0.59	1.50	0.50	0.75	3.34	1.75	0.86	41.27	5.64	3.13	1.38	1.38	30.33	13.08	7.97
NS 2	6F1	17.79	7.78	3.50	2.00	0.92	9.45	3.72	0.92	28.72	11.85	3.00	2.25	2.25	16.40	5.80	2.53
NS 3	6F1	10.18	3.76	3.00	1.50	1.50	10.47	4.12	3.31	25.54	7.70	3.00	2.50	2.00	19.00	8.68	7.91
NS 4	6F1	14.50	6.12	2.88	2.13	1.88	7.84	3.04	7.91	35.98	8.36	4.00	3.00	2.25	48.22	20.81	2.00
NS 5	6F1	2.31	0.62	1.50	0.75	0.75	4.05	1.59	1.25	33.40	3.00	3.25	2.00	1.50	35.53	14.92	12.55
NS 6	6F1	1.09	0.36	1.50	0.75	0.50	1.41	0.30	0.37	41.84	2.88	3.00	2.00	1.50	19.26	3.61	4.21
NS 7	6F1	2.27	0.51	1.50	0.50	0.50	2.23	0.78	0.64	No data available	No data available	No data available	No data available	No data available	No data available	No data available	No data available
Day cent NS :	PBS	44.18	6.62	3.25	2.00	2.25	42.88	22.34	3.49	52.80	5.42	3.00	2.00	1.75	41.91	23.85	1.41
Day cent NS :	PBS	44.92	20.11	4.00	2.50	2.00	33.83	25.95	8.09	55.47	17.28	4.00	2.50	2.00	38.11	22.90	6.36
Day cent NS :	PBS	25.46	11.82	3.50	2.00	2.00	29.92	20.65	4.95	22.95	9.95	3.25	2.50	2.00	32.52	22.49	13.52
Day cent NS :	PBS	34.26	6.96	3.25	1.25	1.25	34.78	20.75	3.88	37.78	3.98	3.50	2.25	1.75	27.06	17.11	11.80
Day cent NS :	PBS	30.20	15.81	3.25	2.38	2.38	31.87	16.26	13.82	33.50	19.09	3.25	2.25	1.75	31.46	14.16	13.95
Day cent NS :	PBS	23.71	4.80	3.75	2.25	1.75	26.47	-	10.84	28.08	6.79	3.75	2.25	1.75	35.56	16.36	12.75
Day cent NS :	PBS	23.71	4.80	3.75	2.25	1.75	26.47	-	10.84	-	-	-	-	-	-	-	-
Day cent NS :	6F1	12.12	0.91	3.00	1.00	0.50	8.28	0.40	0.16	30.04	0.79	2.25	0.50	0.00	15.58	9.25	3.10
Day cent NS :	6F1	12.43	5.00	1.63	1.00	1.00	9.87	5.94	2.69	24.02	6.58	3.25	2.25	1.75	18.09	6.87	3.54
Day cent NS :	6F1	6.49	2.39	1.63	1.00	1.13	9.14	6.02	1.63	10.37	3.89	1.63	1.13	1.13	8.77	5.90	3.17
Day cent NS :	6F1	15.80	3.82	2.69	1.50	1.50	16.42	6.36	8.54	37.89	9.13	3.88	2.50	2.13	31.82	13.25	5.89
Day cent NS :	6F1	8.26	4.52	1.88	1.13	1.13	3.33	2.05	0.38	17.23	5.41	3.75	2.50	2.25	30.05	11.43	3.17
Day cent NS :	6F1	4.50	1.98	1.63	1.00	1.25	0.58	0.14	0.04	18.94	6.18	4.25	2.50	2.25	17.18	6.07	6.05
Day cent NS :	6F1	4.50	1.98	1.63	1.00	1.25	0.58	0.14	0.04	-	-	-	-	-	-	-	-

Supplementary Data for Figure 4 and 5 - Noonan Patients and day controls

Supplementary Data for Figure 4 and 5 - Noonan Patients and day controls

Donor	Condition	M2 P1	M2 P2	M2 P3	M2 P4	M2 P5	M2 P6	M2 P7	M2 P8	M2 PECAM1 P1	M2 PECAM1 P2	M2 PECAM1 P3	M2 PECAM1 P4	M2 PECAM1 P5	M2 PECAM1 P6	M2 PECAM1 P7	M2 PECAM1 P8
NS1	PBS	36.38	9.34	3.50	2.50	2.25	38.67	24.24	2.90	44.35	9.58	3.50	2.00	1.75	39.93	24.89	1.60
NS2	PBS	43.05	8.59	3.75	2.25	1.75	43.79	30.15	4.60	47.55	17.75	3.00	1.00	1.00	47.56	25.15	1.95
NS3	PBS	58.41	15.76	3.75	2.25	1.50	51.97	35.22	5.89	48.04	7.15	3.25	2.25	1.75	48.58	25.15	5.32
NS4	PBS	59.64	9.02	3.50	2.00	1.50	52.25	31.32	6.80	55.02	4.29	3.25	1.75	1.25	55.45	26.21	2.90
NS5	PBS	64.99	13.41	4.00	2.50	1.75	45.54	30.39	2.24	52.57	5.19	3.25	2.50	1.50	45.87	18.87	2.74
NS7	PBS	55.12	11.27	4.00	2.75	2.25	29.67	6.95	0.30				No data available				
NS1	6F1	9.38	2.29	2.25	1.17	1.25	3.58	1.33	0.52	55.32	6.02	3.08	1.42	1.33	28.13	7.38	3.69
NS2	6F1	21.96	5.44	1.94	1.06	1.32	2.23	0.04	0.01	14.05	3.39	1.63	0.81	0.88	3.64	0.37	0.05
NS3	6F1	20.36	5.49	1.63	1.00	1.00	39.31	26.57	0.07	39.31	7.12	3.25	1.50	1.50	2.83	0.55	0.14
NS4	6F1	31.85	7.45	1.88	1.06	1.00	33.76	18.78	0.05	42.38	3.56	2.75	1.00	1.00	1.85	0.75	0.18
NS5	6F1	24.24	3.63	3.00	1.00	1.50	4.24	0.87	0.05	42.38	2.70	2.75	1.15	1.00	14.59	2.71	0.25
NS6	6F1	39.29	10.56	4.00	1.50	2.50	11.66	1.68	0.08	27.20	6.74	3.50	1.50	2.50	31.12	4.43	1.10
NS7	6F1	31.93	3.20	3.00	1.25	1.25	1.24	0.41	0.07				No data available				
Day cnt NS1	PBS	18.73	2.54	3.00	1.25	1.00	4.25	0.87	0.05	49.90	4.58	3.00	1.50	1.50	21.59	2.33	0.31
Day cnt NS2	PBS	65.36	21.22	4.00	2.50	2.25	25.68	12.63	7.66	24.57	8.83	3.50	3.00	2.00	49.44	28.37	11.30
Day cnt NS3	PBS	60.81	19.18	3.75	2.50	2.00	58.32	19.09	3.48	50.65	14.60	3.00	2.50	1.50	48.33	17.86	2.61
Day cnt NS4	PBS	75.85	18.45	4.25	3.00	2.25	69.17	34.06	10.61	59.89	13.36	4.00	3.00	2.75	64.79	29.43	6.61
Day cnt NS5	PBS	62.83	16.49	3.75	2.50	2.50	51.47	21.03	6.03	48.38	8.56	3.75	2.50	2.50	47.28	15.45	1.18
Day cnt NS6	PBS	64.88	14.16	4.00	2.00	2.00	46.26	25.34	4.16	56.20	8.89	3.50	2.50	1.50	51.57	23.46	5.68
Day cnt NS7	PBS	68.10	14.58	4.00	2.00	2.00	46.26	25.34	4.16								
Day cnt NS1	6F1	22.12	10.00	4.00	3.00	2.50	25.68	12.63	7.66	24.57	8.83	3.50	3.00	2.00	49.44	28.37	11.30
Day cnt NS2	6F1	40.32	9.06	3.25	1.25	2.00	8.90	2.11	0.13	29.31	10.07	4.00	1.75	2.00	10.85	2.19	0.27
Day cnt NS3	6F1	20.31	5.24	1.88	1.00	1.00	3.12	-	0.02	29.11	8.07	4.00	1.00	2.00	16.96	2.96	0.18
Day cnt NS4	6F1	20.53	1.57	3.00	1.50	1.50	1.51	0.04	0.16	40.04	3.51	2.50	1.00	1.00	7.99	0.42	0.02
Day cnt NS5	6F1	45.70	10.92	4.25	2.25	2.25	13.48	3.97	0.38	25.38	6.71	3.25	2.00	2.00	13.70	4.81	0.17
Day cnt NS6	6F1	24.12	2.35	3.00	1.00	1.00	2.20	0.10	0.03	30.27	6.73	3.50	2.00	2.00	13.98	1.13	0.07
Day cnt NS7	6F1	24.12	2.35	3.00	1.00	1.00	2.20	0.10	0.03								
NS1	M3 P1	40.90	11.19	3.88	2.75	1.75	43.07	20.09	1.02	45.82	8.59	3.25	1.38	1.25	49.61	25.51	1.49
NS2	PBS	30.75	7.82	3.25	1.75	1.25	30.70	24.46	-	23.09	6.77	3.00	1.75	1.75	32.42	29.48	-
NS3	PBS	23.33	7.11	1.75	1.00	1.00	18.82	12.67	0.77	15.28	3.95	1.63	1.00	1.00	24.42	15.41	0.57
NS4	PBS	9.09	2.49	1.63	0.75	0.75	13.87	9.21	0.77	61.45	8.65	2.50	2.00	1.50	68.95	39.39	0.93
NS5	PBS	9.77	0.52	1.44	0.50	0.31	7.53	4.38	0.37	37.63	2.49	2.63	1.00	0.75	19.68	10.11	0.48
NS6	PBS	8.65	0.88	1.50	0.63	0.50	8.45	3.78	0.20	27.62	2.70	3.25	1.25	1.25	17.74	7.71	0.26
NS7	PBS	43.07	6.05	3.75	2.50	2.25	24.37	4.33	0.23				No data available				
NS1	6F1	7.15	2.06	1.06	0.63	0.50	0.00	0.00	0.00	26.58	2.62	3.25	1.63	1.63	7.33	0.65	0.07
NS2	6F1	10.65	0.63	0.63	0.00	0.00	0.00	0.00	0.00	16.68	1.31	2.00	1.00	0.50	15.60	1.98	0.77
NS3	6F1	28.48	1.09	1.25	0.00	0.00	9.66	2.51	0.22	16.68	1.31	2.00	1.00	0.50	15.60	1.98	0.77
NS4	6F1	0.64	0.07	0.06	0.00	0.00	0.06	0.02	0.14	40.47	2.59	2.63	1.13	1.00	18.90	4.08	0.00
NS5	6F1	0.12	0.00	0.00	0.00	0.00	0.00	0.06	0.00	32.26	1.98	3.00	1.00	0.75	16.26	3.12	0.26
NS6	6F1	0.76	0.11	0.00	0.00	0.00	0.18	0.01	0.06	66.63	11.91	4.00	2.00	1.75	25.97	1.41	0.14
NS7	6F1	0.34	0.00	0.00	0.00	0.00	0.00	0.00	0.00				No data available				
Day cnt NS1	PBS	33.30	21.68	4.50	2.50	2.50	28.92	17.30	0.45	46.52	19.27	4.00	3.00	2.25	22.34	8.78	0.09
Day cnt NS2	PBS	82.26	3.92	2.25	0.75	0.50	39.00	10.81	-	76.04	1.28	2.00	0.50	0.50	16.76	12.83	-
Day cnt NS3	PBS	14.51	3.81	3.00	1.00	1.00	10.40	2.92	0.86	16.33	2.24	2.25	1.00	1.00	18.07	0.80	0.28
Day cnt NS4	PBS	17.46	1.46	1.00	0.50	0.50	1.00	0.00	0.00	33.59	3.85	3.00	1.38	1.38	20.67	5.59	0.14
Day cnt NS5	PBS	12.46	3.17	3.50	1.50	1.38	9.63	4.06	0.07	32.59	3.85	3.00	1.38	1.38	20.67	5.59	0.14
Day cnt NS6	PBS	21.08	2.02	2.88	1.38	1.38	18.98	8.49	0.33	33.07	2.51	3.00	1.50	1.75	23.42	13.39	0.71
Day cnt NS7	PBS	21.08	2.02	2.88	1.38	1.38	18.98	8.49	0.33								
Day cnt NS1	6F1	0.00	0.00	0.00	0.00	0.00	0.00	0.00	0.00	59.53	19.06	4.50	3.00	2.50	9.49	0.01	0.34
Day cnt NS2	6F1	0.00	0.00	0.00	0.00	0.00	0.00	0.00	0.00	39.16	6.14	2.00	0.75	0.75	5.18	5.33	0.05
Day cnt NS3	6F1	0.76	0.12	0.00	0.00	0.00	0.00	-	0.00	62.62	1.52	1.00	0.00	0.00	17.55	5.05	0.25
Day cnt NS4	6F1	31.30	1.46	3.00	0.75	1.00	0.30	0.03	0.10	16.29	0.45	2.25	0.50	0.50	6.87	0.24	0.01
Day cnt NS5	6F1	0.18	0.00	0.00	0.00	0.00	0.00	0.00	0.01	84.84	10.11	3.50	2.00	1.50	28.99	7.52	0.41
Day cnt NS6	6F1	0.44	0.00	0.00	0.00	0.00	0.00	0.01	0.00	35.95	2.93	3.50	1.25	1.25	28.30	0.51	0.20
Day cnt NS7	6F1	0.04	0.00	0.00	0.00	0.00	0.00	0.00	0.00								







# Chapter 8

General discussion



This thesis investigates the effects of various approaches to assess and modulate glycoprotein VI (GPVI) receptor signaling and clustering as well as GPVI-dependent thrombus formation. In this chapter, I focus on the advantages and disadvantages of the approaches utilized, while taking into account modulators of the GPVI pathway described in the literature.

## **8.1 Microfluidics and platelet GPVI**

### **Different collagen sources, GPVI and thrombus formation**

The so-called Horm collagen, originally from Hormon Chemie, is routinely applied in clinical and research laboratories, and therefore considered as a gold standard collagen preparation for the evaluation of platelet aggregation. Although the exact chemical structure is unclear, it appears to be a modified and cross-linked, highly fibrillar collagen form obtained by the digestion of equine tendons and enriched in collagen type I triple helices with some collagen type III <sup>1,2</sup>. In microfluidic whole blood flow assays, Horm collagen mediates platelet adhesion via both collagen receptors, GPVI and integrin  $\alpha 2\beta 1$  <sup>3,4</sup>. Throughout this thesis, I have used this collagen type as a positive control agonist. Thus, in Chapters 3 and 6, Horm collagen acted as a strong, activating surface for flow-dependent thrombus formation and platelet phosphatidylserine exposure, in a similar way to the most active collagen-related peptide, GFOGER-(GPO)<sub>n</sub> <sup>5</sup>. However, collagen fibers with the thickness of Horm collagen are rarely seen in vascular tissues <sup>6</sup>, implying that such a thick fibrillar collagen is not the common adhesive protein for platelets in hemostasis and thrombosis.

In order to employ more native collagen forms as a surface for flow studies, we used several preparations derived from human placenta. However, these are purified by rather harsh isolation protocols, involving proteolytic degradation, aggressive acids and precipitation <sup>7,8</sup>. Therefore, as already pointed out in 1991 by Sixma, de Groot and colleagues <sup>9</sup>, these

collagen preparations should not be considered as naïve. In Chapters 3, 6 and 7, it was observed that the used preparations of collagen types I, III and IV (which were selected as representative for collagens in the arterial vessel wall) were overall less potent than Horm collagen in the support of thrombus formation and in platelet phosphatidylserine exposure. In agreement with earlier data from Siljander <sup>10</sup>, we found that the proteolytic digestion to produce ‘monomeric’ collagens weakened their ability to support thrombus formation and platelet procoagulant activity (Chapter 6). However, for the fibril-forming collagens (types I and III), my findings underline that a fibrillar structure promotes platelet activation <sup>1,11</sup>.

Whilst the synergistic role of the two platelet receptors GPVI and integrin  $\alpha 2\beta 1$  in flow-dependent platelet adhesion and activation by commonly used collagens is well accepted <sup>12,13</sup>, there is literature on the reduced role of  $\alpha 2\beta 1$  in plaque-collagen-induced thrombus formation <sup>14-16</sup>. Regarding GPVI, in mice, experimental atherothrombosis was found to rely on platelet GPVI signaling <sup>17</sup>. In the microfluidic studies of Chapter 4, we observed that the blockage of GPVI with an inhibitory nanobody had a strong thrombus-inhibiting effect using Horm collagen, which was even more pronounced on human atherosclerotic plaque homogenate. In contrast, the blockage of integrin  $\alpha 2\beta 1$  only affected thrombus formation with Horm collagen as a substrate.

The physiological relevance of  $\alpha 2\beta 1$  independency in plaque homogenate-induced thrombus formation is still unclear. One possibility is that the collagen fibers or collagenous substances present in plaque material have masked  $\alpha 2\beta 1$  binding sites <sup>14</sup>. Indeed, many matrix proteins are known to bind to collagens <sup>18</sup>. Alternatively, collagens in the plaque material may be subjected to chemical or structural changes, resulting in a breakdown of fibrils or in proteolytic cleavage by local matrix metalloproteinases <sup>1,19</sup>. This agrees with the observation that collagen digestion not so much reduces platelet

activation, but rather the  $\alpha 2\beta 1$  dependency<sup>10</sup>. Another relevant modifying factor for some collagens could be non-enzymatic glycation<sup>18</sup>.

In this thesis I have been utilizing different collagen types and different inhibiting agents for GPVI and integrin  $\alpha 2\beta 1$  and I have found a clear pattern of platelet-collagen receptor dependency. As schematized in **Figure 1**, collagens present in human plaque samples were exclusively GPVI-dependent. Human collagen type I and III preparations were susceptible to anti  $\alpha 2\beta 1$  interventions, whereas Horm collagen depended equally on the engagement of GPVI and  $\alpha 2\beta 1$ . On the opposite side of the spectrum was the human collagen type IV preparation, which showed complete abolishment of adhesion in the absence of  $\alpha 2\beta 1$  and only small effects when GPVI was inhibited.

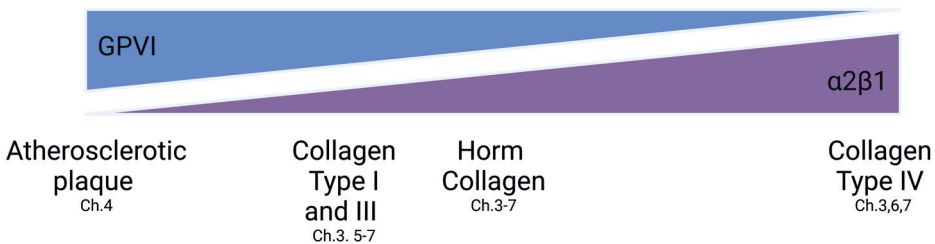


**Figure 1 – Different dependency on receptors GPVI and integrin  $\alpha 2\beta 1$  of flow-dependent platelet adhesion and activation by various collagens.** From left to right, in Chapter 4 we show high GPVI-dependency, but low  $\alpha 2\beta 1$ -dependency of atherosclerotic plaque-induced platelet activation. In other chapters, as indicated, the human-derived collagen types I and III were most sensitive towards GPVI inhibition. On the other hand, fibrillar Horm-type collagen relied on both GPVI and  $\alpha 2\beta 1$  interactions. Highest  $\alpha 2\beta 1$  dependency was found with human collagen type IV.

### GPVI receptor clustering and thrombus formation

The concept that clustering of ITAM-linked receptors increases the signaling strength has previously been developed for B-cell and T-cell receptors of

immune cells<sup>20-22</sup>. These studies demonstrated that resting cells already show a certain degree of nanoclustering<sup>23</sup>. For the T-cell receptors, antibody-induced cross-linking markedly enhanced the signaling outcome<sup>24</sup>, again by formed nanoclusters<sup>25</sup>.

Regarding platelets, until recently GPVI was only known as an ITAM-linked receptor that can form dimers and clusters, for instance when platelets adhere to collagen fibers<sup>26-28</sup>. In Chapters 4 and 5, I provide new evidence that microscopically visible GPVI clusters form in platelets adhering under flow, which suggests a higher extent of platelet activation, observed as increased thrombus formation and phosphatidylserine exposure. The macro-clusters of GPVI were visualized with the fluorescent-labeled non-inhibitory anti-GPVI nanobody Nb28. These findings complement the recent information that on a collagen surface the clustering of GPVI prevents it from shedding<sup>29</sup>. **Table 1** summarizes the ability of various collagens to induce GPVI clustering. In immune cells, it appeared that receptor clustering can increase the signaling amplitude up to 200 %<sup>30</sup>. For platelets, we calculated the difference in signaling between clustered GPVI (on Horn collagen) and non-clustered GPVI (on collagen type III) as a five-fold increase in phosphatidylserine exposure (**Table 1**). Interestingly, only the blockage of the GPVI receptor itself, *e.g.*, with an anti-GPVI nanobody, but not the inhibition of tyrosine kinases suppressed the GPVI cluster formation (Chapter 5). These findings are in accordance with previous work using platelets spread on collagen, where signaling inhibition (targeting Src, Syk or Rac1) also failed to affect the GPVI clustering<sup>28,29,31</sup>. Based on effects obtained with the GPVI-inhibitory Nb2, we concluded that cluster disruption diminished GPVI signaling (Chapter 4). Interestingly, only prior blockage of GPVI (Chapter 3), but not later blockage after 2 minutes of flow<sup>32</sup>, prevented the role of GPVI in thrombus formation. Together, this points to an immediate signal-enforcing role of collagen-formed GPVI clusters in the setting of thrombus formation.

**Table 1 – Summary of effects of (immobilized) collagens to support platelet activation and GPVI macro-clustering**, as visualized with the novel imaging tool, Alexa-Fluor labeled non-inhibitory anti-GPVI nanobody Nb28.

Type of collagen	Receptor engagement		Effect in platelet activation	GPVI macro-cluster formation	Chapter
	GPVI	$\alpha 2\beta 1$			
<i>Horm collagen (equine tendon)</i>	+++	+++	Potent activation in solution and when immobilized	++	3,4,5,6,7
<i>Collagen type I (human placenta)</i>	++	+	Medium activation only when immobilized	no*	3,6
<i>Collagen type III (human placental)</i>	++	+	Medium activation only when immobilized	no	3,5,6,7
<i>Monomeric collagen type III (monomeric)</i>	+	+	Low activation only when immobilized	n.d.	6
<i>Collagen type IV (human placental)</i>	+	++	Medium activation only when immobilized	no*	3,6,7
<i>Plaque-derived collagens</i>	+++	0	Activation in solution and when immobilized	+	4
<i>GFOGER-(GPO)<sub>n</sub></i>	+++	+++	Potent activation in solution and when immobilized	++	3,5,6
<i>GFOGER-(GPP)<sub>n</sub></i>	0	+++	Medium activation in solution and when immobilized	no	5,6

\*Clustering data (N. Jooss, 2021, data not shown); N.d., not determined

Previously, super-resolution microscopy demonstrated that platelets on collagen type III form small, oligomeric clusters of GPVI <sup>28</sup>. Using fluorescence microscopy, I observed macro-clusters on platelets adhered to Horm collagen, but not on platelets adhered to the vascular-derived collagens, in whole blood thrombus formation. Interestingly, however, there was macro-

clustering on platelets adhered under flow to plaque homogenate (Chapter 4) and on platelets adhered to the potent GPVI-activating collagen-like peptide GFOGER-(GPO)<sub>n</sub> (Chapter 5). For the latter surface, also very high phosphatidylserine exposure was noted, in contrast to the non-GPVI activating peptide GFOGER-(GPP)<sub>n</sub> which did not form GPVI clusters (**Table 1**). A certain degree of clustering is also described for the ITAM-linked CLEC2 receptor on platelets. Clusters were formed upon binding of its ligand podoplanin, this was accompanied by increased signaling and enhanced platelet adhesion<sup>33</sup>. In contrast to GPVI, the cluster formation of CLEC2 could be disrupted by inhibition of downstream tyrosine kinases. The reason for this difference between CLEC2 and GPVI is not clear, but it might be due to the repetitive GPO-rich binding sites for GPVI in the collagen triple-helices.

Taken together, the findings in various chapters support the idea that the presence and size of GPVI (macro)clusters enhance platelet activation, thrombus formation and the induction of procoagulant activity, thereby supporting the observations previously in washed platelets under stasis.

### **Microfluidic assays to proxy (patho)physiological blood flow**

Whole blood microfluidic assays allow us to investigate, in a high-throughput manner, multiple parameters of platelet activation and thrombus formation. Microfluidic testing of whole blood samples from many genetically modified mice provided information on thrombus formation that correlated well with the outcome of *in vivo* arterial thrombosis studies<sup>34</sup>. The Maastricht parallel-plate flow chamber thereby can provide important information on altered platelet phenotypes<sup>35</sup>. Regarding my own studies, it is difficult to say if the microfluidic flow settings recapitulate conditions of hemostasis, thrombosis or both. Yet, the use of human atherosclerotic plaque homogenate in flow assays may serve as a proxy measurement of atherothrombosis, but the microfluidic findings will clearly need validation from clinical and epidemiological studies.

This was already recognized in 2001, when the first whole blood flow methods were developed <sup>36</sup>.

In several chapters, using the multiparameter whole blood flow testing, I have examined the roles of human platelet collagen receptors, in particular GPVI and  $\alpha 2\beta 1$ , for different types of collagens (**Table 1**). For interpreting the microfluidic data, some limitations of the used setup need to be taken into account. First, before flow testing, the blood samples need to be citrated and then recalcified to mimic as closely as possible physiological  $\text{Ca}^{2+}$  and  $\text{Mg}^{2+}$  concentrations. Second, parallel-plate flow chambers lack the natural shear transients and stenotic wall-shear rates, which can go up to 10,000/s <sup>37</sup>, instead of the constant 1000/s commonly used in this thesis. This limitation can be overcome by using stenosis-type of microfluidic chambers, such as published by our and other groups <sup>38-40</sup>. Third, experimental choices, such as the addition of a thrombin inhibitor and the flow chamber temperature, greatly affect the extent of thrombus (and clot) formation <sup>41-43</sup>. Fourth, the absence of coagulation can be seen as a limitation, but here I note that working with isolated blood implies absence of the potent anticoagulant function of endothelial cells <sup>44</sup>. In spite of these limitations, the used flow chamber system has shown to be quite beneficial, for instance it is well established for the evaluation of the efficacy of antiplatelet drugs <sup>3,45,46</sup>, and to phenotype patients with platelet-related bleeding disorders <sup>43,47,48</sup>.

In Chapter 7 I investigated Noonan syndrome patients with a gain-of-function mutation in Shp2 (gene *PTPN11*), in which protein tyrosine phosphatase can provide negative feedback on ITAM signaling via GPVI <sup>49</sup>. Considering that Shp2 mediates part of the ITIM signaling responses of PECAM1, we observed that the PECAM1-dependent platelet inhibition via GPVI was most clearly effective upon  $\alpha 2\beta 1$  blockade. Interestingly, platelets from the various Noonan syndrome patients showed a variable impairment in GPVI-dependent thrombus formation, while usually the effect of  $\alpha 2\beta 1$

blockade in patients was higher than in control subjects. The latter finding may be explained by different expression levels of  $\alpha 2\beta 1$ <sup>50</sup>. However, it is unclear if this links to the heterogeneous bleeding phenotype observed in patients with such *PTPN11* mutations<sup>51</sup>. Recently, targeted stimulation of the ITIM-linked pathway has been proposed as a mode to suppress platelet function<sup>52</sup>, but the present findings suggest that such a treatment may be of limited effect.

## **8.2 Platelet collagen receptors as antithrombotic targets**

The clinically used antiplatelet therapies are directed toward inhibition of the P2Y<sub>12</sub> and PAR1 receptors, often in combination with aspirin (blocking the thromboxane synthase/cyclooxygenase complex)<sup>53</sup>. In a perioperative setting, integrin  $\alpha \text{IIb}\beta 3$ -inhibiting drugs can also be used<sup>54</sup>. Beyond the scope of this thesis fall the anticoagulants used for thrombosis treatment<sup>55</sup>. In spite of the overall efficacy of current antiplatelet drugs in the (secondary) prevention of arterial thrombosis, these drug therapies are accompanied with a risk of serious bleeding<sup>56,57</sup>. Hence, there is great interest in novel targets to suppress platelet activation.

One of the candidates in the hunt for new antiplatelet drugs is GPVI. There are several reasons for this: *i*) GPV is only expressed on platelets and megakaryocytes; *ii*) it is crucial in primary platelet activation; *iii*) absence of GPVI protects from arterial thrombosis with no more than small increases in bleeding times<sup>58,59</sup>; and *iv*) subjects lacking GPVI experience only limited bleeding diathesis<sup>41,60,61</sup>. In **Table 2**, current attempts to target GPVI and platelet-collagen interactions, as far as relevant for this thesis, are summarized in. Indicated are the strategy and the potential applications of candidate drugs.



**Table 2 – Overview of effects and application stage of platelet collagen receptor inhibitors.**

Reagent	What it does	How far in development	Chapter	Effects demonstrated in this thesis	Potential application
<i>Revacept</i>	Masks GPVI binding motif on collagen	Stage II clinical trial	3	Effective on highly GPVI dependent substrates	Inhibition of plaque-induced platelet activation
<i>9O12 Fab</i> ( <i>Glenzocimab</i> )	Fab fragment of anti-GPVI antibody	Stage II clinical trial	3	Partially effective but constant with all substrates	Inhibition of collagen- and plaque-induced platelet activation
<i>Nb2</i>	Blocking nanobody against GPVI	<i>In vitro</i> characterization	4	Potent with all tested GPVI-dependent substrates	Inhibition of collagen- and plaque-induced platelet activation
<i>6F1 mAb</i>	Blocking antibody against $\alpha 2\beta 1$	For scientific research	3,4	Potent with all vascular collagens	Inhibition of collagen-induced platelet activation
<i>PRT-060318</i> , <i>Btk inhibitors</i>	Small molecules targeting GPVI signaling	<i>In vitro</i> characterization	3,6	Potent with all GPVI-dependent substrates	Inhibition of GPVI-induced platelet activation

### Earlier developed GPVI-directed inhibitors

In Chapter 3, we used the multiparameter microfluidic method to compare two compounds interfering with the GPVI-collagen interaction, namely the GPVI-construct Revacept and the immune reagent 9O12 Fab (analog Glenzocimab). Our study revealed a difference in effect strength between Revacept and 9O12 Fab, depending on the type of collagen substrate. Whilst the 9O12 Fab generally inhibited the process of thrombus formation on all

collagen surfaces, Revacept was only effective with highly GPVI-dependent surfaces, when compared to the vascular collagen preparations. In Chapter 4, we showed that new anti-GPVI nanobody Nb2 was effective in suppressing thrombus formation on Horm collagen as well as on plaque homogenate. The latter effect is promising with regard to further development of the nanobody. Furthermore, in Chapters 3 and 6, I showed that the most potent antithrombotic reagent was the Syk inhibitor PRT-060318, being very effective on all types of collagen-like preparations. These results jointly illustrate that the type and the modus operandi of an anti-GPVI drug influence its expected antithrombotic effects.

Revacept, a construct of extracellular GPVI and FcR domains, was most potent in preventing platelet activation on collagen-like surfaces inducing high GPVI signaling. As a possible drawback, we speculated in Chapter 3 that circulating platelets may compete with the collagen bound Revacept in the *in vivo* situation. Partial replacement of Revacept-like constructs by platelets has indeed been demonstrated, but later cross-linking modifications in Revacept increased its binding efficacy<sup>62</sup>. Advantages of the use of Revacept are its long half-life time before elimination<sup>63</sup>, and its binding only to injured or diseased vessels with collagen exposure<sup>64</sup>. In addition, a reducing effect of Revacept was seen on atherosclerotic lesion progression in *ApoE*-deficient mice and rabbits<sup>65,66</sup>. Both Revacept and Glenzocimab (analogue of 9O12 Fab) are currently being tested in the clinic; the outcomes of phase-II trials are still unclear. It has already been shown that Glenzocimab is well tolerated, with a half-life extending to 10 hours<sup>67</sup>.

### **Potential of anti-GPVI nanobodies**

The cameloid-derived nanobodies are known to be target-specific with a high affinity and a low immunogenicity, due to the lack of an Fc region. Furthermore, the nanobodies are easy to produce<sup>68,69</sup>. Chapter 4 describes

potent platelet-inhibitory effects of a new anti-GPVI nanobody Nb2<sup>70</sup>, which suppressed the thrombus formation on all GPVI-dependent collagen-like surfaces. Recently, the molecular interactions of Nb2 and Glenzocimab with GPVI were resolved by crystallography<sup>70,71</sup>. It appeared that Nb2 binds close to the CRP-binding groove on GPVI,<sup>70</sup> which agrees with my findings that it suppresses platelet activation on GPO-rich collagen-related peptides. On the other hand, Glenzocimab was shown to bind at a different site of the GPVI extracellular region, agreeing with its wider range inhibition extending to collagen and fibrin, a property that can also be explained by the larger size of the antibody by causing steric hindrance<sup>71</sup>.

A drawback, though, of the small sized nanobodies is their rapid secretion after intravenous injection, often within minutes to hours<sup>72</sup>. This limitation can be overcome by linking the nanobody to larger molecules such as albumin<sup>69,73</sup>. Yet, it might be beneficial to utilize drugs that persist for a shorter time in the circulation after administration. GPVI antagonists could also be utilized only in acute conditions, act as a monotherapy<sup>74</sup>. Currently in the clinic used anti-platelet therapies are also administered for different periods, which vary dependent on the indication from life-long, 12 or 6 months<sup>53</sup>. Further GPVI inhibitors in combination with already approved antiplatelet therapies could also be advantageous. For example dual therapy with Revacept and aspirin, ticagrelor or abciximab, where additive effects for all 3 combinations were reported<sup>76</sup>.

### **Comparison with $\alpha 2\beta 1$ -directed inhibitors**

Chapters 3, 4 and 7 provide novel information on the other collagen receptor, integrin  $\alpha 2\beta 1$ , regarding collagen- and flow-dependent thrombus formation. As a selective tool, we used the blocking anti- $\alpha 2\beta 1$  antibody 6F1, which acts on platelets without side effects. In Chapter 4, we found that the antibody did not affect platelet adhesion and activation on atherosclerotic

plaque material, indicating absence of a role of  $\alpha 2\beta 1$  in this setting. In Chapter 7, the 6F1 antibody suppressed platelet adhesion to all vessel wall-types of collagens, even to a level that 6F1 completely blocked the adhesion on collagen type IV. As schematized in **Figure 1**, the 6F1 antibody suppressed platelet interactions with collagen types I and III more than with Horm collagen; this may also be linked to a lower GPVI activation potential of the former collagen types.

The overall robust inhibitory effect of collagen-induced thrombus formation by 6F1 antibody – with plaque material as an exception – may suggest that integrin  $\alpha 2\beta 1$  is an interesting target for platelet inhibition. However, some drawbacks are that: *i*) the integrin is also expressed on endothelial cells and T-cell populations <sup>77</sup>; and *ii*) patients as well as mice lacking  $\alpha 2\beta 1$  expression have been described with a bleeding phenotype <sup>78-80</sup>. On the other hand, a blocking peptide against  $\alpha 2\beta 1$  had promising, thrombus-reducing effects in a murine thrombosis model <sup>81</sup>.

A different factor taking into account, although not studied in my thesis, is the substantial inter-individual variety in platelet expression levels of  $\alpha 2\beta 1$  and GPVI. Common genetic variants have been identified for  $\alpha 2\beta 1$  (*ITGB1*, C807T) as well as GPVI (*GP6*, rs1613662) that associate with an altered receptor density on the platelet surface, and furthermore alter the collagen-induced thrombus formation under flow <sup>82,83</sup>. While the variants of *ITGB1* <sup>84,85</sup> and *GP6* <sup>86</sup> have also been linked to a different thrombosis risk, it is unclear how they influence the balance of combined GPVI and  $\alpha 2\beta 1$  involvement in thrombus formation per collagen type.

Chapter 7 explored how the combined roles of platelet GPVI and  $\alpha 2\beta 1$  are influenced by tyrosine phosphatase activity induced by the ITIM-linked PECAM1 receptor. For this purpose, we used an inhibitory anti-PECAM1 antibody, which had a platelet-stimulating effect that was absent from a range

of other control antibodies. We found that the sole inhibition of PECAM1 did not increase thrombus formation on any collagen surface tested. However, PECAM1 inhibition had a remarkable rescuing effect on thrombus formation under conditions where  $\alpha 2\beta 1$  was blocked with 6F1 antibody. These findings add to earlier evidence that the inhibitory effect of PECAM1 can be overruled, in case of increasing agonist concentrations <sup>87</sup>. Collectively our results suggest that especially the  $\alpha 2\beta 1$ -dependent enforcement of GPVI activity is sensitive to the PECAM1 inhibition.

### **Repurposing small-molecule tyrosine kinase inhibitors**

Another approach is to repurpose drugs, already approved for another indication, as anti-platelet compounds. Of particular interest, several tyrosine kinase inhibitors that are already in use for treatment of specific cancers. For instance, clinically effective drugs that block Syk or Btk were shown to inhibit GPVI-induced platelet activation <sup>88,89</sup>. Such compounds also affect other cell types <sup>90</sup>, but the most common off-target effects are already being examined in trials with cancer patients. For Btk inhibitors like ibrutinib, it was demonstrated that low doses can affect CLEC2-induced platelet activation <sup>91</sup>. Also, Syk inhibitors are promising, given the strong inhibitory effects on thrombus formation, as seen in Chapters 3 and 6. In addition, blood samples from patients taking a Syk inhibitor for cancer treatment showed a reduced thrombus formation <sup>46</sup>. In line with this, a dual therapy of Syk inhibitor (fostamatinib) with established anti-platelet drugs showed promising results in the treatment of coronary syndrome <sup>75</sup>.

### **8.3 Concluding remarks and future perspective**

The central molecule in this thesis is GPVI. I studied how to modulate its activity by platelet agonists including collagens and platelet inhibitors on the receptor and signaling levels. I could demonstrate the formation of GPVI macro-clusters upon collagen-induced thrombus formation, linked to the

extent of platelet activation. While weaker, vessel-wall derived types of collagens did not form these clusters, they were more dependent on integrin  $\alpha 2\beta 1$  activity to support thrombus formation. Altogether, the results add to the notion that GPVI is more relevant in atherothrombosis than in hemostasis. This underlines the suitability of GPVI as a target for atherothrombosis treatment.

While clinical trials with Revacept and Glenzocimab are so far promising, more *in vitro* experimental work is needed. In particular, the use of well-defined patient-derived plaque preparations with a stenotic-type flow chamber will gather even more pathophysiologically relevant data. Regarding the anti-GPVI Nb2, a limitation for *in vivo* use may be the usually short circulation time of such nanobodies, likely requiring modifications to prolong their physiological stability. Another unresolved question is why the collagen types I, III and IV have a reduced ability to support thrombus formation in comparison to the atherosclerotic plaque material. Further it would be interesting to express collagens in a more native state, for example collagens secreted from endothelial or smooth muscle cells, and probe them for their potential to induce platelet activation.

Current vessel-on-a-chip approaches are bringing in interesting new insights regarding these questions. This type of work is of value not only to generate physiologically relevant results when screening for antiplatelet drugs, but also to characterize patients with suspected platelet-related disorders, which are currently difficult to classify in the routine diagnostic testing.

Overall, the findings described in this thesis show good potential for further investigations into the following areas: *i*) importance of GPVI clustering in health and disease, *ii*) the use of more developed flow methods including vascular components, and *iii*) the antithrombotic potential of nanobody types

of GPVI inhibitors.

## 8.4 References

1. Farndale RW, Sixma JJ, Barnes MJ, de Groot PG. The role of collagen in thrombosis and hemostasis. *J Thromb Haemost.* 2004; 2:561-573.
2. Heemskerk JW, Sakariassen KS, Zwaginga JJ, Brass LF, Jackson SP, Farndale RW. Collagen surfaces to measure thrombus formation under flow: possibilities for standardization. *J Thromb Haemost.* 2011; 9:856-858.
3. De Witt SM, Swieringa F, Cavill R, *et al.* Identification of platelet function defects by multi-parameter assessment of thrombus formation. *Nat Commun.* 2014; 5:4257.
4. Pugh N, Maddox BD, Bihan D, Taylor KA, Mahaut-Smith MP, Farndale RW. Differential integrin activity mediated by platelet collagen receptor engagement under flow conditions. *Thromb Haemost.* 2017; 117:1588-1600.
5. Munnix IC, Gilio K, Siljander PR, *et al.* Collagen-mimetic peptides mediate flow-dependent thrombus formation by high- or low-affinity binding of integrin  $\alpha 2\beta 1$  and glycoprotein VI. *J Thromb Haemost.* 2008; 6:2132-2142.
6. Raspanti M, Reguzzoni M, Protasoni M, Basso P. Not only tendons: the other architecture of collagen fibrils. *Int J Biol Macromol.* 2018; 107:1668-1674.
7. Fitch SM, Harkness ML, Harkness RD. Extraction of collagen from tissues. *Nature.* 1955; 176:163.
8. Barnes MJ, Gordon JL, MacIntyre DE. Platelet-aggregating activity of type I and type III collagens from human aorta and chicken skin. *Biochem J.* 1976; 160:647-651.
9. Sixma JJ, Hindriks G, Van Breugel H, Hantgan R, de Groot PG. Vessel wall proteins adhesive for platelets. *J Biomater Sci Polym Ed.* 1991; 3:17-26.
10. Siljander P, Lassila R. Studies of adhesion-dependent platelet activation: distinct roles for different participating receptors can be dissociated by proteolysis of collagen. *Arterioscler Thromb Vasc Biol.* 1999; 19:3033-3043.
11. Herr AB, Farndale RW. Structural insights into the interactions between platelet receptors and fibrillar collagen. *J Biol Chem.* 2009; 284:19781-19785.
12. Nieswandt B, Watson SP. Platelet-collagen interaction: is GPVI the central receptor? *Blood.* 2003; 102:449-461.
13. Farndale RW, Lisman T, Bihan D, *et al.* Cell-collagen interactions: the use of peptide toolkits to investigate collagen-receptor interactions. *Biochem Soc Trans.* 2008; 36:241-250.
14. Cosemans JM, Kuijpers MJ, Lecut C, *et al.* Contribution of platelet glycoprotein VI to the thrombogenic effect of collagens in fibrous atherosclerotic lesions. *Atherosclerosis.* 2005; 181:19-27.

15. Penz S, Reininger AJ, Brandl R, *et al.* Human atheromatous plaques stimulate thrombus formation by activating platelet glycoprotein VI. *FASEB J.* 2005; 19:898-909.
16. Schulz C, Penz S, Hoffmann C, *et al.* Platelet GPVI binds to collagenous structures in the core region of human atheromatous plaque and is critical for atheroprogession in vivo. *Basic Res Cardiol.* 2008; 103:356-367.
17. Kuijpers MJ, Gilio K, Reitsma S, *et al.* Complementary roles of platelets and coagulation in thrombus formation on plaques acutely ruptured by targeted ultrasound treatment: a novel intravital model. *J Thromb Haemost.* 2009; 7:152-161.
18. Barnes MJ, Farndale RW. Collagens and atherosclerosis. *Exp Gerontol.* 1999;34:513-525.
19. Nadkarni SK, Bouma BE, de Boer J, Tearney GJ. Evaluation of collagen in atherosclerotic plaques: the use of two coherent laser-based imaging methods. *Lasers Med Sci.* 2009; 24:439-445.
20. Mbiribindi B, Mukherjee S, Wellington D, Das J, Khakoo SI. Spatial clustering of receptors and signaling molecules regulates NK cell response to peptide repertoire changes. *Front Immunol.* 2019; 10:605.
21. Minguet S, Swamy M, Alarcón B, Luescher IF, Schamel WW. Full activation of the T cell receptor requires both clustering and conformational changes at CD3. *Immunity.* 2007; 26:43-54.
22. Pigeon SV, Tabarin T, Yamamoto Y, *et al.* Functional role of T-cell receptor nanoclusters in signal initiation and antigen discrimination. *Proc Natl Acad Sci USA.* 2016;113:e5454-5463.
23. Garcia-Parajo MF, Cambi A, Torreno-Pina JA, Thompson N, Jacobson K. Nanoclustering as a dominant feature of plasma membrane organization. *J Cell Sci.* 2014;127:4995-5005.
24. Hartman NC, Groves JT. Signaling clusters in the cell membrane. *Curr Opin Cell Biol.* 2011; 23:370-376.
25. Pigeon SV, Tabarin T, Yamamoto Y, *et al.* Functional role of T-cell receptor nanoclusters in signal initiation and antigen discrimination. *Proc Natl Acad Sci USA.* 2016; 113:e5454-5463.
26. Miura Y, Takahashi T, Jung SM, Moroi M. Analysis of the interaction of platelet collagen receptor glycoprotein VI (GPVI) with collagen. A dimeric form of GPVI, but not the monomeric form, shows affinity to fibrous collagen. *J Biol Chem.* 2002; 277:46197-46204.
27. O'Connor MN, Smethurst PA, Davies LW, *et al.* Selective blockade of glycoprotein VI clustering on collagen helices. *J Biol Chem.* 2006; 281:33505-33510.
28. Poulter NS, Pollitt AY, Owen DM, *et al.* Clustering of glycoprotein VI (GPVI) dimers upon adhesion to collagen as a mechanism to regulate GPVI signaling in platelets. *J Thromb Haemost.* 2017; 15:549-564.



29. Pallini C, Pike JA, O'Shea C, *et al.* Immobilized collagen prevents shedding and induces sustained GPVI clustering and signaling in platelets. *Platelets*. 2021; 32:59-73.
30. Vanamee ES, Lippner G, Faustman DL. Signal amplification in highly ordered networks is driven by geometry. *Cells*. 2022; 11:272.
31. Neagoe RA, Gardiner EE, Stegner D, Nieswandt B, Watson SP, Poulter NS. Rac inhibition causes impaired GPVI signalling in human platelets through GPVI shedding and reduction in PLC $\gamma$ 2 phosphorylation. *Int J Mol Sci*. 2022; 23:3746.
32. Navarro S, Stegner D, Nieswandt B, Heemskerk JW, Kuijpers MJ. Temporal roles of platelet and coagulation pathways in collagen- and tissue factor-induced thrombus formation. *Int J Mol Sci*. 2021; 23:358.
33. Pollitt AY, Poulter NS, Gitz E, *et al.* Syk and Src family kinases regulate C-type lectin receptor 2 (CLEC-2)-mediated clustering of podoplanin and platelet adhesion to lymphatic endothelial cells. *J Biol Chem*. 2014; 289:35695-35710.
34. Baaten CC, Meacham S, de Witt SM, *et al.* A synthesis approach of mouse studies to identify genes and proteins in arterial thrombosis and bleeding. *Blood*. 2018;132:e35-e46.
35. Nagy M, van Geffen JP, Stegner D, *et al.* Comparative analysis of microfluidics thrombus formation in multiple genetically modified mice: link to thrombosis and hemostasis. *Front Cardiovasc Med*. 2019; 6:99.
36. Badimon L. Atherosclerosis and thrombosis: lessons from animal models. *Thromb Haemost*. 2001; 86:356-365.
37. Eskin SG, McIntire LV. Rheology of thrombosis. In: *Hemostasis and Thrombosis Vol 5* (Colman RW, Marder VJ, Clowes AW, George JN, Goldhaber SZ, eds.): Lippincott, Williams and Wilkins, New York, USA; 2006: pp. 738.
38. Westein E, van der Meer AD, Kuijpers MJ, Frimat JP, van den Berg A, Heemskerk JW. Atherosclerotic geometries exacerbate pathological thrombus formation poststenosis in a von Willebrand factor-dependent manner. *Proc Natl Acad Sci USA*. 2013;110:1357-1362.
39. Chan JM, Wong KH, Richards AM, Drum CL. Microengineering in cardiovascular research: new developments and translational applications. *Cardiovasc Res*. 2015; 106:9-18.
40. Zhao YC, Vatankhah P, Goh T, *et al.* Hemodynamic analysis for stenosis microfluidic model of thrombosis with refined computational fluid dynamics simulation. *Sci Rep*. 2021; 11:6875.
41. Nagy M, Perrella G, Dalby A, *et al.* Flow studies on human GPVI-deficient blood under coagulating and noncoagulating conditions. *Blood Adv*. 2020; 4:2953-2961.

42. Herfs L, Swieringa F, Jooss N, *et al.* Multiparameter microfluidics assay of thrombus formation reveals increased sensitivity to contraction and antiplatelet agents at physiological temperature. *Thromb Res.* 2021; 203:46-56.
43. Heubel-Moenen FC, Brouns SL, Herfs L, *et al.* Multiparameter platelet function analysis of bleeding patients with a prolonged platelet function analyser closure time. *Br J Haematol.* 2022; 196:1388-1400.
44. Versteeg HH, Heemskerk JW, Levi M, Reitsma PH. New fundamentals in hemostasis. *Physiol Rev.* 2013; 93:327-358.
45. Baaten CC, Veenstra LF, Wetzels R, *et al.* Gradual increase in thrombogenicity of juvenile platelets formed upon offset of prasugrel medication. *Haematologica.* 2015;100:1131-1138.
46. Tullemans BM, Veninga A, Fernandez DI, *et al.* Multiparameter evaluation of the platelet-inhibitory effects of tyrosine kinase inhibitors used for cancer treatment. *Int J Mol Sci.* 2021; 22:11199.
47. Van Geffen JP, Swieringa F, Heemskerk JW. Platelets and coagulation in thrombus formation: aberrations in the Scott syndrome. *Thromb Res.* 2016; 141:S12-16.
48. Brouns SL, Tullemans BM, Bulato C, *et al.* Protein C or protein S deficiency associates with paradoxically impaired platelet-dependent thrombus and fibrin formation under flow. *Res Pract Thromb Haemost.* 2022; 6:e12678.
49. Coxon CH, Geer MJ, Senis YA. ITIM receptors: more than just inhibitors of platelet activation. *Blood.* 2017; 129:3407-3418.
50. Samaha FF, Kahn ML. Novel platelet and vascular roles for immunoreceptor signaling. *Arterioscler Thromb Vasc Biol.* 2006; 26:2588-2593.
51. Tartaglia M, Kalidas K, Shaw A, *et al.* PTPN11 mutations in Noonan syndrome: molecular spectrum, genotype-phenotype correlation, and phenotypic heterogeneity. *Am J Hum Genet.* 2002; 70:1555-1563.
52. Soriano Jerez EM, Gibbins JM, Hughes CE. Targeting platelet inhibition receptors for novel therapies: PECAM1 and G6b-B. *Platelets.* 2021; 32:761-769.
53. Gremmel T, Michelson AD, Frelinger AL, Bhatt DL. Novel aspects of antiplatelet therapy in cardiovascular disease. *Res Pract Thromb Haemost.* 2018; 2:439-449.
54. Bledzka K, Smyth SS, Plow EF. Integrin  $\alpha\text{IIb}\beta\text{3}$ : from discovery to efficacious therapeutic target. *Circ Res.* 2013; 112:1189-1200.
55. Siegal DM, Anand SS. Considerations for use of direct oral anticoagulants in arterial disease. *Res Pract Thromb Haemost.* 2021; 5:10.1002.
56. Lamberts M, Olesen JB, Ruwald MH, *et al.* Bleeding after initiation of multiple antithrombotic drugs, including triple therapy, in atrial fibrillation patients following myocardial infarction and coronary intervention: a nationwide cohort study. *Circulation.* 2012; 126:1185-1193.

57. Vries MJ, van der Meijden PE, Henskens YM, ten Cate-Hoek AJ, ten Cate H. Assessment of bleeding risk in patients with coronary artery disease on dual antiplatelet therapy. A systematic review. *Thromb Haemost.* 2016; 115:7-24.
58. Nieswandt B, Schulte V, Bergmeier W, *et al.* Long-term antithrombotic protection by in vivo depletion of platelet glycoprotein VI in mice. *J Exp Med.* 2001; 193:459-469.
59. Kato K, Kanaji T, Russell S, *et al.* The contribution of glycoprotein VI to stable platelet adhesion and thrombus formation illustrated by targeted gene deletion. *Blood.* 2003; 102:1701-1707.
60. Dumont B, Lasne D, Rothschild C, *et al.* Absence of collagen-induced platelet activation caused by compound heterozygous GPVI mutations. *Blood.* 2009; 114:1900-1903.
61. Hermans C, Wittevrongel C, Thys C, Smethurst PA, Van Geet C, Freson K. A compound heterozygous mutation in glycoprotein VI in a patient with a bleeding disorder. *J Thromb Haemost.* 2009; 7:1356-1363.
62. Jamasbi J, Megens RT, Bianchini M, *et al.* Cross-linking GPVI-Fc by anti-Fc antibodies potentiates its inhibition of atherosclerotic plaque- and collagen-induced platelet activation. *JACC Basic Transl Sci.* 2016; 1:131-142.
63. Schüpke S, Hein-Rothweiler R, Mayer K, *et al.* Revacept, a novel inhibitor of platelet adhesion, in patients undergoing elective PCI: design and rationale of the randomized ISAR-PLASTER trial. *Thromb Haemost.* 2019; 119:1539-1545.
64. Borst O, Gawaz M. Glycoprotein VI: novel target in antiplatelet medication. *Pharmacol Ther.* 2021; 217:107630.
65. Bültmann A, Herdeg C, Li Z, *et al.* Local delivery of soluble platelet collagen receptor glycoproteinVI inhibits thrombus formation invivo. *ThrombHaemost.* 2006; 95:763-766.
66. Ungerer M, Rosport K, Bültmann A, *et al.* Novel antiplatelet drug revacept (dimeric glycoprotein VI-Fc) specifically and efficiently inhibited collagen-induced platelet aggregation without affecting general hemostasis in humans. *Circulation.* 2011; 123:1891-1899.
67. Renaud L, Lebozec K, Voors-Pette C, *et al.* Population pharmacokinetic /pharmacodynamic modeling of glenzocimab (ACT017) a glycoprotein VI inhibitor of collagen-induced platelet aggregation. *J Clin Pharmacol.* 2020; 60:1198-1208.
68. Steeland S, Vandenbroucke RE, Libert C. Nanobodies as therapeutics: big opportunities for small antibodies. *Drug Discov Today.* 2016; 21:1076-1113.
69. Shen Z, Xiang Y, Vergara S, *et al.* A resource of high-quality and versatile nanobodies for drug delivery. *iScience.* 2021; 24:103014.
70. Slater A, Di Y, Clark JC, *et al.* Structural characterization of a novel GPVI-nanobody complex reveals a biologically active domain-swapped GPVI dimer. *Blood.* 2021; 137:3443-3453.

71. Billiald P, Slater A, Pugnère M, *et al.* Targeting platelet glycoprotein VI with glenzocimab: a novel mechanism of inhibition. Proc of ISTH Congress 2022; London, UK.
72. Kontermann RE. Half-life extended biotherapeutics. *Expert Opin Bio I Ther.* 2016; 16:903-915.
73. Adams R, Griffin L, Compson JE, *et al.* Extending the half-life of a Fab fragment through generation of a humanized anti-human serum albumin Fv domain: an investigation into the correlation between affinity and serum half-life. *MAbs.* 2016; 8:1336-1346.
74. Andrews RK, Arthur JF, Gardiner EE. Targeting GPVI as a novel antithrombotic strategy. *J Blood Med.* 2014; 5:59-68.
75. Harbi MH, Smith CW, Alenazy FO, *et al.* Antithrombotic effects of fostamatinib in combination with conventional antiplatelet drugs. *Int J Mol Sci.* 2022; 23:6982.
76. Mojica Muñoz AK, Jamasbi J, Uhland K, *et al.* Recombinant GPVI-Fc added to single or dual antiplatelet therapy in vitro prevents plaque-induced platelet thrombus formation. *Thromb Haemost.* 2017; 117:1651-1659.
77. Ghatak S, Niland S, Schulz JN, *et al.* Role of integrins  $\alpha 1\beta 1$  and  $\alpha 2\beta 1$  in wound and tumor angiogenesis in mice. *Am J Pathol.* 2016; 186:3011-3027.
78. Nieuwenhuis HK, Akkerman JW, Houdijk WP, Sixma JJ. Human blood platelets showing no response to collagen fail to express surface glycoprotein Ia. *Nature.* 1985; 318:470-472.
79. Deckmyn H, Chew SL, Vermynen J. Lack of platelet response to collagen associated with an autoantibody against glycoprotein Ia: a novel cause of acquired qualitative platelet dysfunction. *Thromb Haemost.* 1990; 64:74-79.
80. Holtkötter O, Nieswandt B, Smyth N, *et al.* Integrin  $\alpha 2$ -deficient mice develop normally, are fertile, but display partially defective platelet interaction with collagen. *J Biol Chem.* 2002; 277:10789-10794.
81. Zhang C, Zhang L, Zhang Y, *et al.* Development of antithrombotic nanoconjugate blocking integrin  $\alpha 2\beta 1$ -collagen interactions. *Sci Rep.* 2016; 6:26292.
82. Roest M, Sixma JJ, Wu YP, *et al.* Platelet adhesion to collagen in healthy volunteers is influenced by variation of both  $\alpha 2\beta 1$  density and von Willebrand factor. *Blood.* 2000; 96:1433-1437.
83. Van Geffen JP, Brouns S, Batista J, *et al.* High-throughput elucidation of thrombus formation reveals sources of platelet function variability. *Haematologica.* 2019; 104:1256-1267.
84. Leone AM, De Stefano V, Burzotta F, *et al.* Glycoprotein Ia C807T gene polymorphism and increased risk of recurrent acute coronary syndromes: a five year follow up. *Heart.* 2004; 90:567-569.

85. Kazemi A, Fatemi A, Givtaj N, Peighambari MM. Association of platelet collagen receptor polymorphisms with premature acute myocardial infarction. *Blood Coagul Fibrinolysis*. 2012; 23:527-531.
86. Perrella G, Nagy M, Watson SP, Heemskerk JW. Platelet GPVI (glycoprotein VI) and thrombotic complications in the venous system. *Arterioscler Thromb Vasc Biol*. 2021; 41:2681-2692.
87. Patil S, Newman DK, Newman PJ. Platelet endothelial cell adhesion molecule-1 serves as an inhibitory receptor that modulates platelet responses to collagen. *Blood*. 2001; 97:1727-1732.
88. Van Eeuwijk JM, Stegner D, Lamb DJ, *et al*. The novel oral Syk inhibitor, BI1002494, protects mice from arterial thrombosis and thromboinflammatory brain infarction. *Arterioscler Thromb Vasc Biol*. 2016; 36:1247-1253.
89. Zheng TJ, Lofurno ER, Melrose AR, *et al*. Assessment of the effects of Syk and BTK inhibitors on GPVI-mediated platelet signaling and function. *Am J Physiol*. 2021; 320:c902-915.
90. Bye AP, Unsworth AJ, Gibbins JM. Platelet signaling: a complex interplay between inhibitory and activatory networks. *J Thromb Haemost*. 2016; 14:918-930.
91. Nicolson PL, Nock SH, Hinds J, *et al*. Low-dose Btk inhibitors selectively block platelet activation by CLEC-2. *Haematologica*. 2021; 106:208-219.



# **Chapter 9**

**Samenvatting**

**Summary**

**Zusammenfassung**

**Impact**

**Curriculum Vitae**

**Publications**

**Acknowledgements**

## **Samenvatting**

Bloedplaatjes zijn cruciaal bij het in stand houden van de hemostase en het voorkomen van bloedverlies bij vaatletsel. De plaatjes sturen echter ook pathologische processen aan, met name de arteriële trombose. Wereldwijd vormen arterieel trombotische aandoeningen, leidend tot beroerte, hartinfarct en trombo-embolie, nog steeds een van de belangrijkste doodsoorzaken. Risicopatiënten krijgen plaatjesremmers voor-geschreven, die weliswaar effectief zijn, maar ook als bijwerking bloedingen kunnen hebben. Om deze laatste tegen te gaan zijn er meer gerichte vormen van antiplaatjesmedicatie nodig. Hiervoor lijkt de plaatjes specifieke collageenreceptor glycoproteïne VI (GPVI) een veelbelovende kandidaat.

**Hoofdstuk 1** geeft een algemeen overzicht van de processen van plaatjesactivering en de daaropvolgende trombusvorming, zoals deze optreedt bij arteriële stromingscondities. Hierna volgt een meer uitvoerige beschrijving van de voor dit proefschrift meest relevante plaatjesagonist collageen; en verder van de twee collageenreceptoren die tot expressie worden gebracht op plaatjes, namelijk GPVI en  $\alpha 2\beta 1$ . Het daaropvolgende deel introduceert de huidige mogelijkheden om in te grijpen in de interacties van plaatjes met collagenen. Deze zijn in het bijzonder: i) het recombinante GPVI-fusie-eiwit Revaccept, dat GPVI bindingsmotieven op de collageenvezels afschermt; ii) het Fab-fragment 9O12 gericht tegen humaan GPVI, dat de receptorinteractie voorkomt; iii) antilichamen van kameelachtigen, genaamd nanobodies (Nb), die geselecteerd zijn op anti-GPVI werking. Aangezien mijn onderzoek uitgebreid gebruik maakt van microfluidic-apparaten voor het testen van plaatjesactivering en trombusvorming in volbloed onder stromingscondities, is het laatste deel van het hoofdstuk gewijd aan de vele mogelijkheden van deze techniek.



**Hoofdstuk 2** betreft commentaar op een artikel van Staessens & De Meyer (*Platelets, 2021; 32:331*), waarin 177 trombi van patiënten met een beroerte werden bestudeerd en samenstelling van die trombi werd geëvalueerd middels histologische kleuring. De trombussamenstelling bleek verband te houden met de efficiëntie van chirurgische verwijdering na de beroerte. Voor deze verzamelde trombi beschrijven de auteurs zones met rode bloedcellen en daarnaast zones rijk aan plaatjes, die respectievelijk een lossere of een dichtere structuur vertoonden. Het hoofdstuk plaatst deze bevindingen in de context met andere literatuur en bespreekt enkele tekortkomingen van het onderzoek. Dit zijn bijvoorbeeld de afwezigheid van kwantificering van de immunohistochemische gegevens en de het niet beschikbaar zijn van patiënt-gerelateerde parameters en klinische interventie-uitkomsten. Dergelijke gegevens kunnen belangrijk zijn voor een patiëntafhankelijke vergelijking met de samenstelling van de trombi. Afgezien daarvan is deze studie op dit moment de enige, die een indrukwekkend aantal monsters van ex vivo trombi combineert met een breed panel van histologische kleuringen. De publicatie valideert de kennis uit handboeken en laat verder mogelijkheden zien om de behandeling van patiënten met ischemische beroerte te verbeteren.

**Hoofdstuk 3** vergelijkt de effecten van vier klinisch relevante verbindingen, gericht op het blokkeren van de interactie van plaatjes met diverse collagenen. Als centraal testsysteem werden microfluidic-kamers gebruikt, waarin volbloed over verschillende collageenpreparaten of collageenachtige substraten werd geleid. Microscopische beelden werden opgenomen om de mate van remming op verschillende parameters van trombusvorming te kunnen bepalen. Als GPVI-remmers werden gebruikt het recombinante GPVI-construct Revacept, het anti-humaan GPVI Fab-fragment 9O12 (lijkend op Glenzocimab) en de Syk-eiwitremmer PRT-060318; verder werd als integrine  $\alpha 2\beta 1$ -antagonist het antilichaam 6F1 gebruikt. Het

hoofdstuk toont aan dat al deze interventies leidden tot remming van de trombusvorming op de meeste collageen-gerelateerde oppervlakken, alhoewel de mate van remming sterk varieerde tussen de interventies en de collageensubstraten. De gevonden verschillen tussen Revacept en 9O12 Fab hadden vooral betrekking op het GPVI-activerende vermogen van het collageen, waarbij Revacept actiever was bij meer actieve, met GPO-peptide verrijkte substraten. Dit verschil kan als relevant worden beschouwd voor de lopende klinische onderzoeken met Revacept en Glenzocimab. Van alle interventies bleek verreweg de krachtigste remmer de Syk-antagonist PRT-060318, gevolgd door de wat mildere effecten van het 6F1 antilichaam, vooral wat betreft humane vasculaire collageenpreparaten. Daarnaast presteerde 6F1 ook beter dan Revacept. Onze resultaten impliceren dat voorzichtigheid geboden is bij het selecteren van een bepaald collageensubstraat voor het testen van antiplaatjesgeneesmiddelen op effecten in stroomafhankelijke trombusvorming.

**Hoofdstuk 4** beschrijft mogelijkheden om te interveniëren in de interactie van plaatjes-GPVI met collagenen middels een nieuw anti-humaan GPVI nanobody (Nb) 2. De gegevens in dit hoofdstuk laten zien dat Nb2 een remmend effect heeft op de collageenafhankelijke trombusvorming, alsmede op de GPVI signalering in de plaatjes. Deze effecten werden waargenomen met zowel gezuiverd fibrillair collageen als collageenbevattend atherosclerotisch plaque-homogenaat, afkomstig van patiënten. Verder bleek dat deze twee substraten verschilden wat betreft de rol van integrine  $\alpha 2\beta 1$ , die hoog was bij het fibrillaire collageen en laag was bij het plaque-homogenaat. Bij plaque-homogenaat remde alleen een gecombineerde blokkade van  $\alpha 11\beta 3$  en  $\alpha 2\beta 1$  de plaatjesadhesie en trombusvorming in dezelfde mate als Nb2 alleen. Daarnaast reduceerde Nb2 de signaaloverdracht door GPVI voor wat betreft de fosforylering van de eiwitten Syk, Lat en PLC $\gamma$ 2, vooral na plaque-stimulering. Aanvullend werk in dit

hoofdstuk is gericht op het vinden van het werkingsmechanisme van Nb2, waarbij bleek de Nb een verstorend effect had op de clustervorming van GPVI-moleculen, resulterend in een beperkte receptorsignalering. Concluderend is er een gemeenschappelijke rol van GPVI bij de activering van plaatjes door atherosclerotische plaques en geïsoleerde collagenen. Verder relateerde de clustering van GPVI met de mate van signaaloverdracht in plaatjes en de mate van trombusvorming op het collageen-substraat. Alles bij elkaar genomen motiveert dit werk voor nader onderzoek naar Nb2 als een potentieel antitrombotisch middel

Als een vervolg beschrijft **Hoofdstuk 5** hoe nanobodies ook gebruikt kunnen worden om de clustering van GPVI op geactiveerde plaatjes in kaart te brengen. Voor dit doel werd een nieuwe, niet-remmend anti-GPVI Nb, namelijk Nb28, fluorescent gelabeld en dan gebruikt bij bloedperfusie-experimenten over collagenen. Bij vier verschillende collageentypen werd de verdeling van GPVI over het plaatjesoppervlak onderzocht met Nb28 AF488, daarbij gebruik makend van geautomatiseerde beeldanalyse. Het gelabelde Nb28 liet de vorming van macroclusters van GPVI zien in plaatjes die het collageen hechtten. De clustervorming viel samen met een verhoogde procoagulante activiteit van de plaatjes en een versterkte trombusvorming. Sterke kleuring en plaatjesactivering werden alleen waargenomen bij fibrillair collageen en bij collageen-gerelateerd peptide met een GPVI-bindingsmotief. Typisch was de clustervorming van GPVI afwezig in plaatjes gehecht aan de minder actieve substraten collageen-III of collageen-gerelateerd peptide zonder GPVI-bindingsmotief. Verder bleek dat clustering alleen kon worden verstoord door directe receptorremming, maar niet door een blokkade van de signaaloverdracht middels GPVI, alhoewel een dergelijke blokkade wel de trombusvorming gedeeltelijk verminderde. Concluderend daarmee is dat de clustering van GPVI een proces is dat niet alleen plaatsvindt in geïsoleerde

plaatjes, maar ook in plaatjes die betrokken zijn bij de trombusvorming onder stromingscondities.

**Hoofdstuk 6** betreft de rol van het proteïnekinase Syk op de trombusvorming onder stromingscondities en op de  $\text{Ca}^{2+}$ -mobilisatie in plaatjes. Daarbij zijn wederom verschillende vasculaire collagenen gebruikt alsmede collageen-gerelateerde peptiden. Aangetoond kon worden dat de remming van Syk met PRT-060318 een sterk onderdrukkend effect had op de trombusvorming bij alle collageenachtige substraten. De stof PRT-060318 blokkeerde bovendien de  $\text{Ca}^{2+}$ -reacties van de plaatjes voor zover die opgewekt konden worden door een collageen of collageen-gerelateerde peptide. De uitkomsten van de trombusvorming zijn tevens gebruikt om op basis van regressieanalyse een voorspellingsmodel te maken voor de GPVI-afhankelijkheid van collageenpreparaten. Het ontwikkelde model laat een gemengde rol zien van GPVI bij de trombusvorming op diverse collageenoppervlakken, die echter afwezig was na de remming van Syk. Dit hoofdstuk toont verder aan dat de Syk-route in plaatjes essentieel is voor de trombusvorming op collagenen, en dat dit geldt voor alle collageenpreparaten zelfs als die de GPVI-specifieke herkenningsequentie GPO missen.

In **Hoofdstuk 7** is nagegaan in welke mate tyrosine-fosfatasen in staat zijn om de GPVI-afhankelijke trombusvorming te onderdrukken, in het bijzonder onder omstandigheden waarbij integrine  $\alpha 2\beta 1$  geblokkeerd is. Hiertoe zijn de modulerende effecten op trombusvorming onderzocht van de ITIM-gekoppelde receptor PECAM1, die het tyrosinefosfatase non-receptor type PTPN11 aanstuurt. Experimenten met collagenen met een hoge of lage GPVI-afhankelijkheid toonden aan dat de verminderde trombusvorming door blokkade van  $\alpha 2\beta 1$  kon worden hersteld, wanneer ook PECAM1 werd geremd met behulp van een selectief antilichaam. De negatieve regulatie door PECAM1 werd verder onderzocht met behulp van bloedmonsters van

patiënten met een gain-of-function mutatie in PTPN11 - die behept zijn met het Noonan-syndroom, dat gepaard gaat met een milde bloedingsziekte. Flowkamer-studies met bloed van zeven Noonan-patiënten toonden een variabele, maar gedeeltelijke vermindering van collageen-geïnduceerde plaatjesactivering, die werd versterkt door  $\alpha 2\beta 1$ -blokkering. Echter de gain-of-function van PTPN11 gaf geen versterking van het trombus-herstellend effect door PECAM1-remming. Tezamen geven de resultaten van dit hoofdstuk aan dat de PECAM1- en PTPN11-onderdrukkende mechanismen van de collageen-geïnduceerde trombusvorming onafhankelijk zijn van de mate van GPVI-activering, maar afhankelijk zijn van andere factoren zoals de PTPN11-activiteit en de betrokkenheid van integrine  $\alpha 2\beta 1$

De algemene discussie in **Hoofdstuk 8** bespreekt de bevindingen gepresenteerd in dit proefschrift in relatie tot de huidige literatuur. Besproken worden de verschillende plaatjeseffecten van collageenpreparaten, mede in vergelijking met atherosclerotisch plaquemateriaal. De relatieve rol van GPVI is groter bij plaque-geïnduceerde trombusvorming dan bij vasculair collageen-geïnduceerde trombusvorming, waarin integrine  $\alpha 2\beta 1$  actiever is. Ook beschrijf ik de relevantie van GPVI-clustering voor plaatjesactivering, en beargumenteer ik of microfluidic volbloedtesten een goede benadering zijn van de (patho)fysiologische stromingscondities bij trombose en hemostase. In het laatste deel van hoofdstuk 8 vergelijk ik de eerder ontwikkelde en de nieuw opgekomen GPVI-remmers wat betreft hun werkzaamheid en mechanisme. Samengevat biedt dit proefschrift een aanzienlijk verdiept inzicht in de variabiliteit van de rol van GPVI als collageenreceptor, en in de vele mogelijkheden om de plaatjes-activerende functie van GPVI te veranderen.

## **Summary**

Platelets are crucial in maintaining hemostasis and therefore preventing blood loss upon vessel injury. However, platelets also drive pathological processes, most importantly arterial thrombosis, which are worldwide still a leading cause of death, due to stroke, myocardial infarction, and thromboembolism. Patients at recurrent risk of these diseases receive antiplatelet agents, in many cases they are effective, but can also cause bleeding side effects. More targeted approaches of antiplatelet medication are needed, for which the platelet-specific collagen receptor glycoprotein VI (GPVI) is a promising candidate.

**Chapter 1** introduces basic principles of the multi-step processes of platelet activation in arterial thrombus formation as it occurs under flow conditions. The chapter follows with a more in-depth description of the for this thesis most relevant platelet agonist collagen and of the two main collagen receptors expressed on platelets, GPVI and integrin  $\alpha 2\beta 1$ . The next part introduces the current options to intervene with platelet-collagen interactions. These are in particular: *i*) the recombinant GPVI fusion protein, Revacept, which masks GPVI-binding motifs on exposed collagen fibers; *ii*) the Fab fragment, 9O12, directed against human GPVI to directly prevent receptor agonist interaction; *iii*) camelid heavy chain antibodies, called nanobodies (Nb), which have been selected to target GPVI on the platelet receptor level. Since this thesis extensively describes the use of whole blood microfluidics for the assaying of platelet activation and thrombus formation under flow, the last part of the chapter is dedicated to reported capabilities of this technique.

**Chapter 2** provides a commentary on a paper by Staessens & De Meyer (*Platelets*, 2021; 32:331), in which 177 thrombi from stroke patients were collected and their structure was evaluated by histological staining. The detailed thrombus composition appeared to be linked to the efficiency of surgical removal after the stroke. For the analyzed thrombi, the authors described red blood cell zones and platelet-rich zones, which were linked to a

looser or a denser structure, respectively. The chapter brings these findings in context with other literature and discusses some shortcomings of the study. For instance, the absence of quantification of the immunohistochemistry data and the unavailability of patient-related parameters or clinical intervention outcomes, which would have been important for comparison with the composition of the thrombi. Nevertheless, at present this is the only study marrying an impressive *ex vivo* thrombus sample size with a broad panel of histological stains. It does validate textbook knowledge and gives better incentives to improve the treatment of patients with ischemic stroke.

**Chapter 3** describes an effort to investigate and compare the inhibition patterns of four clinically relevant interventions, aimed to block the interactions of platelets with collagens. As a central test system, microfluidic chambers were used, in which whole blood was flowed over a series of collagens or collagen-like substrates. Microscopic images were taken to assess the level of inhibition on thrombus formation parameters. As GPVI inhibitors were used the recombinant GPVI construct Revaccept, the anti-human GPVI Fab fragment 9O12 (resembling Glenzocimab), and the Syk protein tyrosine kinase inhibitor PRT-060318; furthermore, as an integrin  $\alpha 2\beta 1$  antagonist the antibody 6F1 was utilized. In the chapter, it is revealed that all interventions led to an overall downregulation of the thrombus formation on most collagen-like surfaces, although the precise patterns of inhibition varied greatly between the individual treatments and the collagen substrates. Differences seen between Revaccept and 9O12 Fab related to the GPVI-activating potential of the specific collagen, with Revaccept being more active on GPO-enriched substrates. This finding may be relevant for the ongoing clinical trials with Revaccept and the 9O12-based antibody Glenzocimab. Among all antagonists, universally and most potent was the Syk inhibitor PRT-060318, followed by moderate effects of the 6F1 antibody. This especially was the case for human vascular-type of collagen preparations, in which cases 6F1 outperformed



Revacept. Our results imply that caution is needed when selecting a certain collagen substrate for the testing of antiplatelet drugs for effects in flow-dependent thrombus formation.

**Chapter 4** examines the approach to prevent GPVI-collagen interactions with a novel anti-human GPVI nanobody Nb2. The data presented in this chapter show that Nb2 impairs collagen-dependent thrombus formation as well as the GPVI-dependent signaling. This nanobody effect was observed with a fibrillar collagen and with collagen-containing patient derived atherosclerotic plaque homogenate. The chapter also points out that the two substrates were different concerning the degree of  $\alpha 2\beta 1$  engagement, which was high for the fibrillar collagen and was low with the plaque homogenate. For plaque homogenate, only the combined blockage of  $\alpha 11\beta 3$  and  $\alpha 2\beta 1$  was able to inhibit platelet adhesion and thrombus formation to the same extent as Nb2 alone. Furthermore, Nb2 prevented GPVI signaling, observed as a loss of Syk, Lat and PLC $\gamma$ 2 phosphorylation, especially upon plaque stimulation. Additional work was directed to find the mode of action of Nb2, which likely is through the disruption of GPVI clustering and a consequently restricted receptor signaling. Overall, this work emphasizes the critical difference in GPVI-mediated platelet activation by atherosclerotic plaque or by isolated collagen. Collectively, the data warrant further investigation of Nb2 as a potential anti-thrombotic agent.

As a continuation of the Nb work, **Chapter 5** describes how nanobodies can be used as novel tools to investigate the clustering of GPVI on activated platelets. For this purpose, the non-inhibitory anti-GPVI Nb28 was fluorescently labeled, and then used in whole blood flow studies over collagens. For four different collagen types, the distribution of GPVI on the platelet surface was examined with Nb28 AF488 using an automated image analysis. Labeled Nb28 appeared to indicate the formation of macro-clusters

of GPVI on platelets that adhered to various substrates. This cluster formation corresponded with the extent of thrombus formation and the platelet procoagulant activity (phosphatidylserine exposure). High staining and high platelet responses were only observed on the most active fibrillar collagen and on the collagen-related peptide with a GPVI binding motif. No GPVI cluster formation was observed of platelets that adhered to less active substrates, such as collagen III and collagen-related peptide without GPVI binding motif. Interestingly, the clustering could be disrupted by direct receptor inhibition, but not by pharmacological inhibition of downstream signaling molecules, although this partly reduced the thrombus formation. In general, the work shows that GPVI (macro-) clustering is a process that occurs not only in static but also in flow conditions and is then linked to increased platelet activation.

**Chapter 6** investigates the role of platelet Syk on thrombus formation under flow as well as on platelet signaling via cytosolic  $\text{Ca}^{2+}$  mobilization, in response to various vascular-type of collagens and collagen-related peptides. It is demonstrated that the selective inhibition of Syk with PRT-060318 suppressed parameters of thrombus formation for all collagen-like substrates. The compound furthermore reduced platelet  $\text{Ca}^{2+}$  responses with those collagens or collagen-related peptides that were able to activate the platelets in suspension. The obtained thrombus formation data was also used to build a prediction model, based on regression analysis, for the GPVI dependency of collagen preparations. The model indicated a mixed role of GPVI in thrombus formation on vascular-derived collagen surfaces, which was abolished upon inhibition of Syk. This gave further proof that the Syk pathway in platelets is essential for the thrombus formation with all platelet-activating collagens, even with those lacking the GPVI-specific recognition sequence GPO.

In **Chapter 7**, investigates to what extent protein tyrosine phosphatases are able to downregulate GPVI-dependent thrombus formation, also under conditions where integrin  $\alpha 2\beta 1$  is blocked. For this purpose, modulatory effects were examined on thrombus formation of the ITIM-linked receptor PECAM1, which couples to the protein tyrosine phosphatase non-receptor type PTPN11. Experiments using collagens with high or low GPVI dependency showed that the impairment of thrombus formation upon blockage of  $\alpha 2\beta 1$  could be restored when also PECAM1 was inhibited using a selective antibody. The supposedly negative regulation by PECAM1 was further examined using blood samples from patients with a gain-of-function mutation in PTPN11 - presenting with the Noonan syndrome, which includes a small to moderate bleeding phenotype. Flow studies with blood from seven Noonan patients showed a variable, but overall partial reduction of the collagen-induced platelet activation that became enforced upon  $\alpha 2\beta 1$  blockage. However, the gain of PTPN11 activity did not enhance the rescuing effect caused by PECAM1 inhibition. Taken together, the results of this chapter indicate that the PECAM1 and PTPN11 restraining mechanisms on collagen-induced thrombus formation are independent of the extent of GPVI activation, but dependent on other factors such as the PTPN11 activity and the engagement of integrin  $\alpha 2\beta 1$ .

The general discussion **Chapter 8** places the findings presented in this thesis in context with the current literature. Discussed are the different platelet-activating effects of collagen preparations, also in comparison to atherosclerotic plaque material. The relative role of GPVI appears to be higher in plaque-induced thrombus formation than in vascular collagen-induced thrombus formation, where integrin  $\alpha 2\beta 1$  is more active. Furthermore, I discuss the relevance of GPVI clustering for platelet activation, and debate to which extent microfluidic whole blood assays can approximate (patho)-physiological flow conditions in thrombosis and hemostasis. In the final part of

Chapter 8, I compare the earlier developed and the newly arising GPVI inhibitors in terms of action and mechanism. Conclusively, this thesis has deepened the insight into the variable role of GPVI as a collagen receptor and into the many ways to interfere with its platelet-activating function.

# **Zusammenfassung**

Blutplättchen oder Thrombozyten sind entscheidend für die Aufrechterhaltung der Hämostase und verhindern daher den Blutverlust bei Gefäßverletzungen. Thrombozyten fördern jedoch auch pathologische Prozesse, vor allem arterielle Thrombose, welche weltweit immer noch eine Hauptursache für Schlaganfälle, Myokardinfarkt und Thromboembolie ist. Patienten mit einem anhaltenden Risiko für diese Erkrankungen erhalten Thrombozyten-funktionshemmer (TAH), die in den meisten Fällen wirksam sind, aber auch Blutungen verursachen können. Deshalb besteht ein Bedarf an gezielteren Angriffspunkten, der Thrombozyten spezifische Kollagenrezeptor Glycoprotein VI (GPVI) ist hierfür ein vielversprechender Kandidat.

**Kapitel 1** führt grundlegende Prinzipien des mehrstufigen Prozesses von Thrombozytenaktivierung in der arteriellen Thrombusbildung ein, wie sie unter Flussbedingungen auftritt. Darauf folgt eine eingehendere Beschreibung der für diese Dissertation relevantesten Thrombozyten-Agonisten Kollagen und der beiden Hauptkollagenrezeptoren, die auf Thrombozyten exprimiert werden, GPVI und Integrin  $\alpha 2\beta 1$ . Danach werden präklinische Wirkstoffe vorgestellt, welche in die Wechselwirkung von Thrombozyten und Kollagen eingreifen. Dies sind insbesondere: *i)* das rekombinante GPVI-Fusionsprotein Revacept, welches GPVI Motive auf exponierten Kollagenfasern maskiert; *ii)* das Antikörper Fragment, 9O12, welches gegen das menschliches GPVI gerichtet ist, um Interaktion zwischen GPVI und seinen Bindungspartner zu verhindern; also auch *iii)* Kamelid Antikörper Fragmente aus der schweren Kette, sogenannt Nanobodies (NB), welche gegen GPVI selektiert wurden. Da diese Dissertation die Verwendung von Vollblutflusskammern zur Prüfung der Thrombozytenaktivierung und der Thrombusbildung unter atrialen Bedingungen umfassend beschreibt, ist der letzte Teil des Kapitels dieser Technik gewidmet.

**Kapitel 2** enthält einen Kommentar zu einem Artikel von Staessens & de Meyer (*Platelets*, 2021; 32: 331), bei dem 177 Thromben von Schlaganfallpatienten gesammelt und ihre Struktur durch histologische Färbung bewertet wurde. Die Effizienz der chirurgischen Entfernung nach dem Schlaganfall schien mit der genauen Thrombuszusammensetzung in Verbindung zu stehen. Für die untersuchten Thromben beschrieben die Autoren eine Zone reich an roten Blutkörperchen sowie thrombozytenreiche Zonen, die im ersten Fall mit einer lockeren oder im zweiten Fall mit einer dichteren Struktur auftraten. Das Kapitel bringt diese Erkenntnisse in einen Kontext mit anderer Literatur und erörtert einige Mängel der Studie. Beispiele sind dies das Fehlen einer Quantifizierung der Immunhistochemie-Daten und die Nichtverfügbarkeit von patientenbezogenen Parametern oder klinischen Interventionsergebnissen, die für den Vergleich mit der Zusammensetzung der Thromben von Interesse gewesen wären. Trotzdem ist diese Studie derzeit die Einzige, die eine beeindruckende *ex-vivo* Thrombus Probengröße mit einer breiten Palette an histologischen Färbungen vereint. Es bestätigt das Lehrbuchwissen und bietet bessere Anreize, um die Behandlung von Patienten mit einem ischämischen Schlaganfall zu verbessern.

**Kapitel 3** beschreibt eine Untersuchung, welche Hemmmuster von vier klinisch relevanten Interventionen beschreibt und vergleicht wie Wechselwirkungen von Thrombozyten und Kollagenen blockiert werden können. Als zentrales Testsystem wurde die Flusskammer verwendet, bei der Vollblut über eine Reihe von verschiedenen Kollagenen oder kollagenähnliche Substraten perfundiert wurde. Mikroskopische Bilder wurden aufgenommen, um den Grad der Reduktion von Thrombusparametern zu bewerten. Als GPVI-Inhibitoren wurden das rekombinante GPVI-Konstrukt-Revacept, das Anti-Human-GPVI-Fab-Fragment 9O12 (Proxy für Glencocimab) und der Syk-Protein-Tyrosinkinase-Inhibitor PRT-060318. Darüber hinaus wurde als Integrin  $\alpha 2\beta 1$ -Antagonist der

Antikörper 6F1 verwendet. In diesem Kapitel wird gezeigt, dass alle Interventionen zu einer allgemeinen Verringerung der Thrombusbildung auf den meisten kollagenähnlichen Substraten führten, obwohl die genauen Hemmungsmuster zwischen den einzelnen Antagonisten und den Kollagenantagonisten stark variierten. Wie zum Beispiel Unterschiede zwischen Revacept und 9O12 Fab im Zusammenhang mit dem GPVI-aktivierenden Potenzial des jeweiligen Kollagens, wobei Revacept auf GPO-reichen Substraten wirksamer ist. Dieses Ergebnis könnte von Relevanz für die laufenden klinischen Studien mit Revacept und dem 9O12-basierten Antikörper Glencocimab sein. Bei allen Antagonisten war der SYK-Inhibitor PRT-060318 am wirksamsten, gefolgt von moderaten Wirkungen des 6F1-Antikörpers. Dies war besonders für die menschlichen Kollagenpräparate der Fall, bei denen 6F1 Revacept übertraf. Unsere Ergebnisse deuten darauf hin, dass bei der Auswahl eines bestimmten Kollagensubstrats für die Evaluation von Thrombozytenfunktionshemmer auf Effekte bei der Thrombusbildung elementar ist.

**Kapitel 4** untersucht die Möglichkeiten, GPVI-Kollagen-Wechselwirkungen mit einem neuartigen Anti-Human-GPVI-Nanobody(Nb) 2 zu verhindern. Die in diesem Kapitel dargelegten Daten zeigen, dass Nb2 die kollagenabhängige Thrombusbildung sowie die GPVI-abhängige Signalkaskade vermindert. Dieser Nanobody-Effekt wurde mit einem fibrillären Kollagen und mit von Patienten isolierten kollagenhaltigen atherosklerotischem Plaque-Homogenat untersucht. Das Kapitel weist auch darauf hin, dass die beiden Substrate hinsichtlich des Grades der  $\alpha 2\beta 1$ -Beteiligung unterschiedlich waren, welcher für das fibrilläre Kollagen hoch war und mit Plaque-Homogenat niedrig. Für das Plaque-Homogenat war nur die kombinierte Blockierung von  $\alpha 11\beta 3$  und  $\alpha 2\beta 1$  in der Lage, die Thrombozytenadhäsion und die Thrombusbildung in gleichem Maße wie Nb2 allein zu hemmen. Darüber hinaus verhinderte Nb2 die GPVI-



Signalübertragung, das als Verlust von Syk-, LAT- und Plc $\gamma$ 2 - Phosphorylierung beobachtet wurde, insbesondere bei Plaque-Stimulation. Zusätzliche Experimente deuten darauf hin, dass die Verminderung von Thrombusbildung als auch GPVI Signalübertragung wahrscheinlich auf eine Unterbindung des GPVI-Clusterings zurück zu führen ist. Insgesamt betont diese Studie den kritischen Unterschied in der GPVI-vermittelten Thrombozytenaktivierung durch atherosklerotische Plaques und durch isoliertes Kollagen. Des Weiteren rechtfertigen die Daten eine weitere Untersuchung von Nb2 als potenzielles anti-thrombotisches Therapeutikum. Als Fortsetzung der Nanobody Arbeit beschreibt **Kapitel 5**, wie Nanobodies auch als neuartige Tools verwendet werden können, um die Clusterbildung von GPVI auf aktivierten Thrombozyten zu untersuchen. Zu diesem Zweck wurde der nicht hemmende Anti-GPVI-Nb28 mit einem Fluorochrome markiert und dann in der Vollblut Flusskammer über Kollagenen angewendet. Für vier verschiedene Kollagentypen wurde die Verteilung von GPVI auf der Thrombozyten-oberfläche mit Nb28 AF488 unter Verwendung einer automatisierten Bildanalyse untersucht. Die Bildung von Makro-Klustern wurde quantifiziert und korrespondierte mit dem Ausmaß der Thrombusbildung und der prokoagulatorischen Aktivität von Thrombozyten (Phosphatidylserin-Exposition). Ein erhöhtes Nb28 AF488 Signal und eine hohe Thrombozytenreaktion wurden nur mit dem aktivsten fibrillären Kollagen und auf dem kollagenartigen Peptid mit einem GPVI-Bindungsmotiv beobachtet. Es wurde keine GPVI-Klusterbildung auf Thrombozyten beobachtet, die an weniger aktiven Substraten wie Kollagen III und dem kollagenartigen Peptid ohne GPVI-Bindungsmotiv adhärirten. Interessanterweise konnte die Clusterbildung durch direkte Rezeptorhemmung verhindert werden, jedoch nicht durch pharmakologische Hemmung von nachgeschalteten Signalmolekülen, obwohl dies die Thrombusbildung teilweise reduzierte. Im Allgemeinen zeigt die Studie, dass

GPVI (Makro-) Klustering ein Prozess ist, der nicht nur bei statischen, sondern auch unter Flussbedingungen auftritt und dann mit einer erhöhten Thrombozytenaktivierung verbunden ist.

**Kapitel 6** untersucht die Rolle des Signalmoleküls Syk in Thrombozyten bei der Thrombusbildung in der Flusskammer sowie bei der Thrombozytensignalkaskade durch zytosolische  $\text{Ca}^{2+}$ -Mobilisierung ausgelöst durch verschiedene Kollagen Typen und kollagenartige Peptide. Diese Studie zeigt, dass die selektive Hemmung von Syk mit PRT-060318 alle Parameter der Thrombusbildung für alle kollagenähnlichen Substrate unterdrückte. Des Weiteren reduzierte PRT-060318 die Thrombozyten- $\text{Ca}^{2+}$ -Antwort mit diesen Kollagenen oder kollagenbedingten Peptiden, welche die Thrombozyten in Suspension aktivieren konnten. Die erhaltenen Daten bezogen auf Thrombusbildung in der Flusskammer wurden auch verwendet, um ein Vorhersagemodell auf der Grundlage einer Regressionsanalyse für die GPVI-Abhängigkeit von Kollagenpräparaten zu erstellen. Das Modell zeigte eine gemischte Rolle von GPVI bei der Thrombusbildung auf vaskulären Kollagenoberflächen, die bei der Hemmung von Syk aufgehoben wurde. Dies lieferte einen weiteren Beweis dafür, dass die Signalkaskade um Syk in Thrombozyten für die Thrombusbildung mit allen aktivierenden Kollagenen unerlässlich ist, selbst wenn GPO, die GPVI-spezifischen Erkennungssequenz, fehlt.

In **Kapitel 7** wird untersucht, in welchem Ausmaß Protein-Tyrosine Phosphatasen in der Lage sind, die GPVI-abhängige Thrombusbildung herunter zu regulieren, im Besonderen wenn Integrin  $\alpha 2\beta 1$  blockiert ist. Zu diesem Zweck wurden modulatorische Effekte auf die Thrombusbildung des ITIM-verknüpften Rezeptors PECAM1 untersucht, welcher mit dem „protein tyrosine phosphatase non-receptor type“ PTPN11 interagiert. Experimente mit Kollagenen, welche hohe oder niedrige GPVI-Abhängigkeit haben,

zeigten, dass die Reduktion der Thrombusbildung bei Blockierung von  $\alpha 2\beta 1$  wiederhergestellt werden konnte, wenn PECAM1 unter Verwendung eines selektiven Antikörpers inhibiert wurde. Die in der Literatur postulierte negative Regulation durch PECAM1 wurde weiter unter Verwendung von Blutproben von Patienten mit einer „gain-of-function“ Mutation in PTPN11 untersucht, welche auch als Noonan-Syndrom bezeichnet wird und einen schwache bis mittelstarke Blutungsphänotyp aufweist. Flusskammer Studien mit Blut von sieben Noonan Patienten zeigten eine variable, aber partielle Reduktion der kollageninduzierten Thrombozytenaktivierung, die bei  $\alpha 2\beta 1$ -Blockade verstärkt wurde. Die Erhöhung der PTPN11-Aktivität wurde jedoch nicht durch PECAM1-Hemmung aufgehoben. Zusammengefasst zeigen die Ergebnisse dieses Kapitels, dass die Mechanismen welche die PECAM1- und PTPN11 auf die kollageninduzierte Thrombusbildung haben unabhängig der GPVI-Aktivierung sind, jedoch von anderen Faktoren wie der PTPN11-Aktivität und der Einbeziehung von Integrin  $\alpha 2\beta 1$  abhängig sind.

In der allgemeinen Diskussion in **Kapitel 8** werden die in dieser Dissertation vorgestellten Ergebnisse in Zusammenhang mit der aktuellen Literatur gebracht. Diskutiert werden die unterschiedlichen Thrombozyten aktivierende Wirkungen von Kollagenpräparaten, auch im Vergleich zu atherosklerotischem Plaque Material. Da die relative Rolle von GPVI in der Plaque-induzierten Thrombusbildung höher zu sein scheint als bei vaskulärer Kollagen-induzierter Thrombusbildung, wobei im letzteren Fall Integrin  $\alpha 2\beta 1$  aktiver ist. Darüber hinaus wird die Relevanz der GPVI-Klusterbildung für die Thrombozytenaktivierung und in welchem Umfang Vollblut Flusskammern (patho)-physiologische Bedingungen in Thrombose und Hämostase darstellen können diskutiert. Im letzten Teil von Kapitel 8 vergleiche ich bereits entwickelte als auch neu entstehende GPVI-Inhibitoren in Bezug auf ihre Wirkungsmechanismen. Zusammenfassend hat diese Dissertation dazu

beigetragen einen tieferen Einblick in die variable Rolle von GPVI als Kollagenrezeptor und die diversen Ansätze GPVI zu inhibieren zu erlangen.

**Impact**

Platelets are blood cells that prevent the loss of extensive blood volumes however also contribute to arterial thrombosis. After a vessel is injured, platelets become activated by the exposed collagen and aggregate together, forming a platelet-fibrin thrombus. Whilst this is a crucial process in hemostasis, platelets also become activated due to rupture or erosion of an atherosclerotic plaque in atherothrombosis. Herein, occlusive platelet thrombi are formed, mediated by collagen that is present in the atherosclerotic plaque, leading to for example, myocardial infarction, stroke or transient ischemic attacks. These events are still leading causes of death world-wide, and patients are usually prescribed anti-platelet drugs to prevent a second thrombosis. Whilst the currently used drugs are effective in preventing the thrombosis, they are prone to causing unwanted bleeding events in some of the patients. Therefore, other treatment options are currently investigated. A promising approach is to prevent platelet-collagen interactions via inhibition of the collagen receptor, glycoprotein VI (GPVI).

In this thesis, we compared the various approaches used to interfere in the GPVI-dependent interaction of platelets with collagens. This was done by a whole blood flow chamber set up with collagen coatings, assessing the effects on thrombus formation. In Chapter 3, we investigated the effects of direct inhibition of GPVI on the receptor level with the antibody fragment 9O12, as well as by a recombinant GPVI fusion protein intended to mask GPVI motifs on the collagen fibers. These reagents are already being tested in clinical trials. In Chapters 3-7, we also studied a signaling blocker, PRT-060318, downstream of GPVI; novel anti-GPVI nanobodies (cameloid antibody fragments), and the antibody 6F1 inhibiting the  $\alpha 2\beta 1$  integrin, which is another collagen receptor on platelets. Chapters 3-4 in particular show strong effects on thrombus formation of the GPVI or signaling inhibition, which is a very promising finding.

The GPVI-directed nanobodies, are not only excellent tools to inhibit GPVI, but can also be used as imaging tools. In Chapters 4-5 we show how a fluorescently labeled non-inhibitory anti-GPVI nanobody can be utilized to investigate the clustering of GPVI on platelets. This process had never previously been shown in connection with thrombus formation. We also show that the GPVI clustering coincides with a higher degree of platelet activation and an increased thrombus size. These data can help the field to better understand the role of (clustered) GPVI, possibly also to find improved GPVI interventions.

Still additional work will need to be done, in the lab and in clinical trials, to define which approaches to inhibit platelet GPVI will prove to be most effective. In comparison to conventional antibodies, the use of small-sized nanobodies has advantages, but a modification will be needed to improve their half-life in the circulation, given that unmodified nanobodies are quickly excreted.

In Chapter 7 we investigated rare patients with the complex Noonan syndrome, which is sometimes associated with a bleeding phenotype. Platelet defects in these patients stem from a gain of function mutation in the *PTPN11* gene, which interferes in the GPVI signaling activity. We include additional data to the already existing work, using the Maastricht flow chamber to phenotype patient blood samples, in order to gain insight into the underlying mechanism of the platelet defect. In particular we showed that the mutation in these patients only partially affected the capability of their platelets to form thrombi. Based on extensive experiments, we concluded that platelets from patients showed a rescuing effect of the interaction between GPVI and integrin  $\alpha 2\beta 1$ .

Chapters 3-6 furthermore illustrate the differences between various collagen preparations on the induction of platelet activation and thrombus

formation, as well as the effects on these processes of the tested inhibitors. It is concluded that the preparation of more physiological collagen types is needed for optimal point-of-care testing of blood samples. As well as that a move forward is needed towards more advanced vessel-on-a-chip models.

The studies presented in this thesis are of use to the scientific community as well as the general public, as the microfluidics set up bridges the gap between *in vitro* studies with isolated platelets or blood and *in vivo* animal models as well as clinical trials. Flow chambers provide a well-established micro-technique, where different platelet agonists and flow rates can be applied, thus making it possible to probe for overall effects and drawing additional conclusions about an outcome *in vivo*. This is of importance, as results from mouse studies in atherosclerosis, which process is fairly different between mouse and man, cannot always be translated into effects seen in human disease.

Taken together, with this thesis I come to two major conclusions: *i)* GPVI is indeed a promising target for a next generation of effective and safe anti-platelet drugs; *ii)* the flow chamber is a valuable tool to bridge *in vitro* and *in vivo* scientific studies, and to assist in the diagnosis of platelet-related dysfunctions.



# **Curriculum Vitae**

Natalie J. Jooss was born on October 20<sup>th</sup> 1989 in Heidenheim a.d. Brenz (Germany). In 2011, she received a Bachelor of Science from the Rheinische Friedrich-Wilhelms-Universität Bonn (Germany) in Molecular Biomedicine. Next, she moved to Stockholm (Sweden) to pursue a Master of Science within the Biomedicine Program at the Karolinska Institutet. Subsequently, she became an European early-stage researcher within the Horizon-2020 program TAPAS, a Marie Skłodowska-Curie innovative training network (ITN), where she worked on a project shared between Maastricht University (The Netherlands) and the University of Birmingham (United Kingdom). In this project, she was supervised by JWM Heemskerk and YMC Henskens as well as SP Watson and NS Poulter, respectively. As a PhD student, she spent 4 years to elucidate the roles of platelet collagen receptors in the context of platelet-platelet interactions and thrombus formation, by utilizing the Maastricht flow chamber. This work is already partially published in peer reviewed journals and is presented on national and international conferences. After being engulfed in collagen-mediated platelet activation, as demonstrated in this thesis, Natalie Jooss moves on to obtain a postdoc position in the B. Psaila laboratory at the University of Oxford (United Kingdom). Here, she will work on organoid models and single cell RNA sequencing in order to investigate malignant megakaryocyte and platelet biology.

## **Publications**

1. **Jooss NJ**, HENSKENS YMC, WATSON SP, FARNDALE RW, GAWAZ MP, JANDROT-PERRUS M, POULTER NS, HEEMSKERK JWM. *Comparative analysis of pharmacological drugs interfering with collagen induced thrombus formation*. **Thromb Haemost**, 2022, under revision.
2. **Jooss NJ**, SMITH CW, SLATER A, MONTAGUE SJ, DI Y, O'SHEA C, THOMAS MR, HENSKENS YMC, HEEMSKERK JWM, WATSON SP, POULTER NS. *Anti-GPVI nanobody blocks collagen- and atherosclerotic plaque-induced GPVI clustering, signaling and thrombus formation*. **J Thromb Haemost**, 2022 Jul 27. doi: 10.1111/jth.15836.
3. **Jooss NJ** AND POULTER NS. *A large-scale histological investigation gives insight into the structure of ischemic stroke thrombi*. **Platelets**, 2021. doi: 10.1080/09537104.2020.1869713.
4. **Jooss NJ**, DE SIMONE I, PROVENZALE I, FERNANDEZ DI, BROUNS SL, FARNDALE RW, HENSKENS YM, KUIJPERS MJ, TEN CATE H, VAN DER MEIJDEN PE, CAVILL R, HEEMSKERK JW. *Role of platelet glycoprotein VI and tyrosine kinase Syk in thrombus formation on collagen-like surfaces*. **Int J Mol Sci**, 2019. doi: 10.3390/ijms20112788.
5. HUANG J, **Jooss NJ**, FERNÁNDEZ DI, SICKMANN A, GARCÍA Á, WICHAPONG K, DIJKGRAAF I, HEEMSKERK JWM. *Roles of focal adhesion kinase PTK2 and integrin  $\alpha$ IIb $\beta$ 3 signaling in collagen- and GPVI-dependent thrombus formation under shear*. **Int J Mol Sci**, 2022 Aug 4;23(15):8688. doi: 10.3390/ijms23158688.
6. BOURNE J, SMITH C, **Jooss N**, DI Y, BROWN H, MONTAGUE S, THOMAS M, POULTER N, RAYES J, WATSON SP. *CLEC-2 supports platelet aggregation in mouse but not human blood at arterial shear*. **Thromb Haemost**, 2022 Jul 11. doi: 10.1055/a-1896-6992.
7. PETERS LJ, BAATEN CC, MAAS SL, LU C, NAGY M, **Jooss NJ**, BIDZHEKOV K, MORENO-ANDRES D, JANKOWSKI J, BIESSEN EA, DÖRING Y, HEEMSKERK JW, KUIJPERS MJ AND VAN DER VORST EP. *MicroRNA-26b attenuates platelet adhesion and aggregation in mice*. **Biomedicines**, 2022 Apr 23;10(5):983. doi: 10.3390/biomedicines10050983.

8. MIN Y, HAO L, LIU X, TAN S, SONG H, NI H, SHENG Z, **Jooss N**, LIU X, MALMSTRÖM RE, SUN Y, LIU J, TANG H, ZHANG H, MA C, PENG J, HOU M, LI N. *Platelets fine-tune effector responses of naïve CD4<sup>+</sup> T cells via platelet factor 4-regulated transforming growth factor  $\beta$  signaling.* **Cell Mol Life Sci**, 2022 Apr 18;79(5):247. doi:10.1007/s00018-022-042791.
  
9. LEBERZAMMER J, AGTEN SM, BLANCHET X, DUAN R, IPPEL H, MEGENS RT, SCHULZ C, ASLANI M, DUCHENE J, DÖRING Y, **Jooss NJ**, ZHANG P, BRANDL R, STARK K, SIESS W, JURK K, HEEMSKERK JW, HACKENG TM, MAYO KH, WEBER C, VON HUNDELSHAUSEN P. *Targeting platelet-derived  $\mu$  CXCL12 impedes arterial thrombosis.* **Blood**, 2022; doi: 10.1182/blood.2020010140.
  
10. HEUBEL-MOENEN FCJI, BROUNS SLN, HERFS L, BOERENKAMP LS, **Jooss NJ**, WETZELS RJH, VERHEZEN PWM, MACHIELS P, MEGY K, DOWNES K, HEEMSKERK JWM, BECKERS EAM, HENSKENS YMC. *Multiparameter platelet function analysis of bleeding patients with a prolonged platelet function analyser closure time.* **Br J Haematol**, 2022. doi: 10.1111/bjh.18003.
  
11. ZHI Z, **Jooss NJ**, SUN Y, COLICCHIA M, SLATER A, MORAN LA, FUNG CHEUNG HJ, DI Y , RAYES J , POULTER NS, WATSON SP, IQBAL AJ. *Galectin-9 activates platelet ITAM receptors glycoprotein VI and C-type lectin-like receptor-2.* **J Thromb Haemost**, 2021. Doi: 10.1111/jth.15625.
  
12. SLATER A, DI Y, CLARK JC, **Jooss NJ**, MARTIN EM, ALENAZY FO, THOMAS MR , ARIËNS RA, HERR AB, POULTER NS, EMSLEY J, WATSON SP. *Structural characterisation of a novel GPVI nanobody-complex reveals a biologically active domain-swapped GPVI dimer.* **Blood**, 2021. doi: 10.1182/blood.2020009440.
  
13. HERFS L, SWIERINGA F, **Jooss NJ**, KOZLOWSKI M, HEUBEL-MOENEN FCJ, VAN OERLE R, MACHIELS P, HENSKENS Y, HEEMSKERK JWM. *Multiparameter microfluidics assay of thrombus formation reveals increased sensitivity to contraction and antiplatelet agents at physiological temperature.* **Thromb Res**, 2021. doi: 10.1016/j.thromres.2021.04.014.

14. D'ALESSANDRO E, BECKER C, BERGMEIER W, BODE C, BOURNE JH, BROWN H, BÜLLER HR, TEN CATE-HOEK A, TEN CATE V, VAN CAUTEREN YJ, CHEUNG YF, CLEUREN A, COENEN D, CRIJNS HJ, DE SIMONE I, DOLLEMAN SC, KLEIN CE, FERNANDEZ DI, GRANNEMAN L, VAN 'T HOF A, HENKE P, HENSKENS YM, HUANG J, JENNINGS LK, **Jooss NJ**, KAREL M, VAN DEN KERKHOF D, KLOK FA, KREMERS B, LÄMMLE B, LEADER A, LUNDSTROM A, MACKMAN N, MANNUCCI PM, MAQSOOD Z, VAN DER MEIJDEN PE, VAN MOORSEL M, MORAN LA, MORSER J, VAN MOURIK M, NAVARRO S, NEAGOE RA, OLIE RH, VAN PARIDON P, POSMA J, PROVENZALE I, REITSMA PH, SCAF B, SCHURGERS L, SEELIG J, SIEGBAHN A, SIEGERINK B, SOEHNLEIN O, SORIANO EM, SOWA MA, SPRONK HM, STOREY RF, TANTIWONG C, VENINGA A, WANG X, WATSON SP, WEITZ J, ZEERLEDER SS, TEN CATE, H, Scientific Reviewer Committee. *Thrombo-inflammation in cardio-vascular disease: an expert consensus document from the Third Maastricht Consensus Conference on Thrombosis*. **Thromb Haemost**, 2020. doi: 10.1055/s-0040-1708035.

## **Acknowledgements**

Doing a PhD was an experience, of which I would not want to miss a single moment. All the ups, the downs as well as the Eureka and what the heck moments. The realization that it requires not only hard work and determination but also a pinch of luck. Yet most importantly that there are people to share this wonderful adventure with.

To have four supervisors makes it quite a task to schedule meetings, but besides this I am deeply grateful to all of you; for your advice and engagement as well as all the time you spend on me and my various projects. **Johan**, you are incredibly supportive and a brilliant scientist. Further, I greatly appreciate your sense of humor. **Natalie** (a.k.a. the Boss), you are a wizard in integrating seemingly random bits of data, and your extraordinary resilience is impressive. **Steve**, you taught me a lot about science etiquette, and never failed to give me a chance to develop. **Yvonne**, your drive to improve patient care and diagnostics has been infatuating.

A PhD is a massive task, that nobody can take on by themselves. Therefore, I would like to thank the **Marie Skłodowska-Curie Actions - ITN of the European Union** for funding the infamous TAPAS consortium. Further, all the **fellow ESRs** and **respective supervisors** alike, for interesting meetings and constructive feedback. In addition, I would like to recognize scientists I was fortunate enough to collaborate with, for example the **von Hundelshausen** and **van der Vorst** groups, the **Igbal** group as well as many thought-provoking and very helpful mails with **Prof. Barry Coller**, **Prof. Richard Farndale** and **Prof. Martine Jandrot-Perrus**.

When moving between labs the great advantage is, that one gets to meet twice as many amazing people. Yet, at the same time this makes it impossible to name each and every one of you here, so first and foremost, I want to give a general and very heartfelt – thank you – to the **groups in**



**Birmingham as well as Maastricht** for being equally welcoming, kind and supportive in every step of the way.

Nevertheless, special thanks go to: my Dutch “roomies”: **Bibian, Giorgia, Mieke** and **Sanne**, for many “koffietjes” and everything that goes with them. **Constance** and **Magdi** the cool, calm and collect veterans of the flow chamber. A prime example for cynical British sense of humor: **Abs** the self-proclaimed delight. KitKat enthusiast, **Chris**, for being Chris. As well as the “the clique” **Caroline, Joana** and **Martina**, for many hours spent in great company.

Blood, sweat and tears; the present thesis is based on blood. Hence, it is very important to me to acknowledge the countless healthy, now slightly anemic, **donors** as well as all the **phlebotomists**. Without you this thesis would not exist, I hope you feel your contribution to my science was worth it.

And lastly, I would like to mention all the people that accompanied me through my PhD, regardless of the fact that they did not choose this challenge, I did. To my **family**, you have been nothing but supportive and patient with me, in particular when being entirely engulfed in my own little world. Ihr habt mir, so lange ich mich erinnern kann, den Rücken gestärkt und hattet immer ein unbeirrbares Vertrauen in meinen Weg. Further, my dear **non-platelet friends, Christina, Jella, Kathrin, Lena, Petra** and **Tabea**, you never failed to remember my current place of residence, made me aware of how fast time passes and that we really should meet up. Thank you so very much.

I am humbled by how many people spent time and resources supporting me, therefore making this thesis possible. I do not think I am in touch with my emotions enough to put into words how deeply and truly grateful I am.

All that is left to say is, Dankeschön.



